Synthesis and Characterization of 5-Hydroxymethylfurfural Derivative Based Materials

Daihui Zhang

Department of Bioresource Engineering

Faculty of Agricultural and Environmental Science

Macdonald Campus of McGill University

Ste-Anne-de-Bellevue, Québec, Canada

February 2018

A thesis submitted to McGill University

In partial fulfillment of the requirements of the degree of

Doctor of Philosophy

Abstract

The production of polymers from petroleum-based chemicals has caused serious sustainability concerns, therefore stimulating the development of bio-based polymers. 5-hydroxymethylfurfural (HMF) is a promising platform chemical that has been widely utilized in various fields, such as biofuels precursors, fine chemicals synthesis, and monomers to polymers. The synthesis of HMF derivative based polymers offers a wide range of possibilities which has been explored in Chapter 2. Therefore, the main objective of this research was to synthesize and characterize HMF derivative based linear polymers or networks with tunable structures and properties using the thiol-Michael addition reaction. Furthermore, the potential applications were explored as well.

The thiol-Michael addition reaction offers high conversion, mild reaction conditions, and rapid reaction rate. However, there are few research works reporting on the synthesis of linear polymers using this reaction, probably due to the occurrence of side reactions. Therefore, the potential side reactions which occur when performing the thiol-Michael addition reaction were elucidated using a model reaction between furfural acrylate and 1-propanethiol (**Chapter 3**). Moreover, linear poly(β-thioether esters) were successfully synthesized from HMF derivative (2,5-furan diacrylate) and 1,6-hexanedithiol using a catalytic amount of dimethylphenylphosphine (DMPP) under mild reaction conditions (M_n=20000 g/mol). The occurrence of the Diels-Alder (DA) reaction between the furan rings in the polymeric chains and bismaleimide was preliminarily confirmed due to the formation of organogels.

Since the properties of polymers are related to their compositions and structures, three commercial dithiol monomers, including 1,4-benzenedithiol, 1,3-propanedithiol, and dithiothreitol, were used to synthesize 2,5-furan diacrylate (2,5-FDA) based polymers with varied structures and properties (**Chapter 4**). The synthesis of copolymers was investigated as well using 1,6-hexanedithiol and 1,4-benzendithiol as monomers. ^{1}H NMR analysis of the synthesized copolymers revealed that the ratios of these two dithiol monomers present in the copolymers matched well the theoretical ratios. In addition, the synthesized linear polymers with hydroxyl groups as side groups were investigated as hot melt adhesives, showing an adhesive strength of 1.5 MPa on wood substrates. Several interesting phenomena, including multiple melting peaks and two-stage degradation behaviour observed by DSC and TGA, were elucidated by different techniques. Additionally, 2,5-FDA based linear polymers were dynamically

crosslinked by the DA reaction using bismaleimide as the crosslinker to improve the thermal and mechanical properties. As the weight ratio of crosslinker to polymer increased from 1:10 to 1:2, the storage modulus at room temperature was significantly enhanced from 1.5 MPa to 1691 MPa. The presence of flexible thioether linkages in the polymer allowed the synthesis of thermoplastic elastomers (TPEs) using 2,5-FDA, 1,3-propanedithiol and dithiothreitol. The maximum elongation at break of TPEs could reach above 450 %.

Despite the successful synthesis of TPEs reported in **Chapter 4**, their relatively poor solvent resistance and unsatisfactory elasticity could limit their applications. Hence, a thermoset elastomer was synthesized by the combination of the thiol-Michael addition reaction and the DA reaction (**Chapter 5**). When the weight ratio of polymer to crosslinker was 5:1, the Young's modulus, ultimate strength, and elongation at break were 4.3±0.6 MPa, 5.7±1.1 MPa, and 205.3±20.1%, respectively. Moreover, a high elastic recovery (98.9 %) and low residual strain (0.7 %) were observed after the third cycle during the cyclic tensile test. Additionally, the structure and functionality of elastomers were varied by the synthesis of linear copoly(β-thioether ester). The mechanical properties of the elastomers were adjusted by the incorporation of flexible polymeric chains. Although covalent bonds were formed to generate the networks, the reprocessability of thermosets elastomers was demonstrated due to the reversibility of the DA reaction.

Due to the renewability, non-toxicity, biodegradability, and tunable crystallization behavior of polylactic acid (PLA), PLA was used as hard blocks in the synthesis of TPEs. Therefore, the last chapter reported the use of soft segments having thioether groups to synthesize PLA based elastomers (**Chapter 6**). The reaction was carried out in a one-pot reaction under mild reaction conditions due to the efficient macromolecular coupling between the thiol and the acrylate groups of polymers catalyzed by DMPP. Moreover, the properties of PLA based elastomers were adjusted by either varying the molecular weights of the soft segments or crosslinking the soft segments by the DA reaction due to the presence of furan rings. The tensile strength of a PLA based TPEs sample was significantly improved from 0.4 MPa to 3.3 MPa after crosslinking the soft segments. Importantly, due to the reversibility of the DA reaction, crosslinked TPEs could be still potentially melt-processed.

In conclusion, this work has demonstrated the use of the thiol-Michael addition reaction to synthesize 2,5-FDA based linear polymers with varied structures and properties. The occurrence of the DA reaction between furan rings in the polymeric chains and maleimide groups provided an efficient approach to further adjust the thermal and mechanical properties. Due to the reversibility of the DA reaction, networks synthesized by the combination of the thiol-Michael addition and the DA reaction may be used as reversible adhesive, self-healing or recycled materials, and coating applications. The work presented here, therefore, provides an insight to explore HMF and its derivative based high-performance materials.

Résumé

La pollution causée par les polymères synthétisés à partir d'hydrocarbures a grandement stimulé la production de polymères biosourcés. Le 5-hydroxyméthylfurfural (HMF) est un produit chimique prometteur qui a été largement utilisé dans divers domaines, tels que précurseurs de biocarburants, la synthèse de produits chimiques, et la synthèse de monomères. L'objectif de cette thèse était de synthétiser des polymères à partir de monomères dérivés du HMF. Les monomères dérivés du HMF peuvent mener à la synthèse d'une vaste gamme de polymères. Ces polymères furent l'objet d'une revue de la littérature (Chapitre 2).

La réaction d'addition de thiol-Michael offre des taux de conversion élevés, des conditions de réactions légères, et la vitesse de réaction est rapide. Cependant, seulement quelques études sur la synthèse de polymères linéaires à l'aide de cette réaction sont disponibles dans la littérature, probablement en raison des réactions secondaires découlant de la réaction d'addition de thiol-Michael. Par conséquent, les réactions secondaires possibles qui se produisent lors de l'exécution de la réaction d'addition de thiol-Michael ont été élucidées en utilisant un modèle de réaction entre l'acrylate de furfural et le 1-propanethiol (Chapitre 3). De plus, des poly(esters de β-thioéthers) linéaires furent synthétisés avec succès à partir d'un dérivé de HMF (diacrylate de 2,5-furane), du 1,6-hexanedithiol, ainsi qu'une quantité catalytique de diméthylphénylphosphine (DMPP). Le polymère avait une masse moleculaire moyenne de 20000 g/mol. De plus, la réaction de Diels-Alder (DA) entre le furane des chaînes polymériques et le bismaléimide a été confirmée due à la formation d'organogels.

Puisque les propriétés des polymères sont dépendantes de leurs compositions et structures, trois monomères dithiol dont le 1,4-benzenedithiol, le 1,3-propanedithiol, et le dithiothréitol, ont été utilisés pour synthétiser du 2,5-furane diacrylate (2,5-FDA) afin de varier les structures et propriétés des polymères (Chapitre 4). De plus, la synthèse de copolymères a été étudiée à l'aide de monomères de 1,6-hexanedithiol et 1,4-benzendithiol. L'analyse par RMN des copolymères a révélé que les ratios entre les deux monomères dithiol présents dans les copolymères correspondent avec les ratios théoriques. Les polymères linéaires synthétisés avec des groupes hydroxyles comme groupements latéraux ont été étudiés comme adhésifs, montrant une force d'adhérence de 1,5 MPa sur des substrats de bois. Les propriétés thermiques et mécaniques des polymères linéaires à base de 2,5-FDA furent modifiées en les réticulant de façon dynamique par

la réaction DA en utilisant du bismaléimide. Comme le ratio agent de réticulation: polymère a varié de 1:10 à 1:2, le module d'élasticité a augmenté de 1,5 MPa à 1691 MPa. La présence de liens thioéther flexibles dans le polymère a permis la synthèse d'élastomères thermoplastiques (TPE) à partir de 2,5-FDA, 1,3-propanedithiol et de dithiothréitol. L'allongement maximum à la rupture des TPE à atteind plus de 450%.

Malgré la synthèse réussie de TPE présentée au chapitre 3, leur faible résistance aux solvants et leur faible élasticité peuvent limiter leurs applications. Par conséquent, un élastomère thermodurcissable fut synthétisé par la combinaison de la réaction d'addition de thiol-Michael et la réaction DA (chapitre 5). Lorsque le ratio massique polymère: agent de réticulation était de 5:1, le module de Young, la force maximale, et l'allongement étaient de 4.3±0.6 MPa, 5.7±1.1 MPa et 205.3±20.1%, de façon respective. De plus, une forte reprise élastique (98,9 %) et une faible déformation résiduelle (0,7 %) ont été observées. La structure et les fonctionnalités des élastomères ont été modifiées par la synthèse de copoly(β-thioéther esters) linéaires. Les propriétés mécaniques des élastomères ont été ajustées par l'incorporation de chaînes polymères flexibles. Bien que les liaisons covalentes aient été formées pour générer le réseau polymère, le reconditionnement des élastomères thermodurcissables a été démontré grâce à la réversibilité de la réaction de DA.

En raison de son caractère renouvelable, non-toxique, biodégradable, ainsi que l'ajustement du taux de cristallisation, l'acide polylactique (PLA) a été utilisé dans la synthèse des TPE. Par conséquent, le dernier chapitre de cette thèse a porté sur l'utilisation de segments souples ayant des groupements thioéthers afin de synthétiser des élastomères à base de PLA (chapitre 6). Les propriétés des élastomères à base de PLA ont été ajustées en soit faisant varier le poids moléculaire des segments souples ou en réticulant les segments souples par la réaction DA due à la présence de furane. La résistance à la traction des polymères a été considérablement améliorée, passant de 0,4 MPa à 3,3 MPa, à la suite de la réticulation des segments souples.

En conclusion, ce travail a démontré l'utilisation de la réaction d'addition de thiol-Michael afin de synthétiser des polymères à base de 2,5-FDA. De plus, la réaction de DA entre le furane des chaînes polymériques et les groupes maléimides est une approche efficace pour ajuster les propriétés thermiques et mécaniques des polymères. En raison de la réversibilité de la réaction DA, les réseaux polymères synthétisés par la combinaison de la réaction d'addition de thiol-

Michael et la réaction DA peuvent être utilisés comme adhésifs réversibles, matériaux intelligents ou être recyclés.

Table of Contents

List of Figures

List of Tables

List of Schemes

List of Abbreviations

Abbreviation	
HMF	5-hydroxymethylfurfural
FDCA	2,5-furandicarboxylic acid
BHF	2,5-bis(hydroxymethyl) furan
PEF	poly (ethylene-2,5-furandicarboxylate)
PET	polyethylene terephthalate
PBT	polybutylene terephthalate
PPF	poly (propylene-2,5-furandicarboxylate)
PBF	poly (butylene-2,5-furandicarboxylate)
PPT	poly(propylene-2,5-terephthalate)
2,5-FDA	2,5-furan diacrylate
PLA	polylactic acid
DMPP	dimethylphenylphosphine
DFF	2,5-diformylfuran
TBT	tetrabutyl titanate
DABCO	1,4 diazabicyclo[2.2.2]octane
DHMF	5,5'-dihydroxymethyl furoin
EG	ethylene glycol
DMFD	2,5-furandicarboxylate
BOF	2,5-bis[(oxiranylmethoxy)methyl]-furan
BOB	2,5-bis[(2-oxiranylmethoxy)methyl]-benzene
DBU	1,8-diazabicycloundec-7-ene
TEA	triethylamine
Bismaleimide	1,1'-(Methylenedi-4,1-phenylene)bismaleimide
DMAP	4-dimethylaminopyridine
DFDA	5,5'-methylenedifurfurylamine
CH_3DFDA	5,5'-ethylidenedifurfirylamine
TBD	1,5,7-triazabicyclo[4.4.0]dec-5-ene
BD	1,4-butanediol
DA	Diels-Alder
TPEs	thermoplastic elastomers
BET	Brunauer-Emmett-Teller
DPOF	DFF-based porous organic frameworks
T_g	glass transition temperature
T_m	melting point temperature
T_{cc}	cold crystallization temperature
EA	activation energy
DI	dispersity index
G'	storage modulus
M_w	weight average molecular weight
M_n	number average molecular weight
DSC	differential scanning calorimetry
TGA	thermogravimetric analysis

GPC	gel permeation chromatography
GC-MS	gas chromatography mass spectrometry
WAXS	wide-angle X-ray scattering
DMTA	dynamic mechanical thermal analysis
Py-GC-MS	pyrolysis- GC-MS
DMA	dynamic mechanical analyzer
POM	polarized optical microscopy
ATR-FTIR	attenuated total reflection (ATR) Fourier-transform infrared spectroscopy
NMR	nuclear magnetic resonance
COSY	correlation spectroscopy
HSQC	heteronuclear single quantum coherence spectroscopy
^{13}C CP/MAS	^{13}C cross-polarization magic angle spinning
^{13}C DP/MAS	^{13}C direct polarization magic angle spinning
MTDSC	modulated temperature DSC
XRD	X-ray diffraction

Acknowledgements

After over three years, I finally reached this stage to write my thesis. It has been a journey with joy, excitement, disappointment, and frustration. I will remember this journey, which is one of the greatest treasures of my life.

First and foremost, I would thank my supervisor, Dr. Marie-Josée Dumont, for her guidance and encouragement throughout my graduate school career. I appreciated the fact that she gave me the freedom to carry out the experiments, and allowed me to work with different research groups. Without her support, I would not have accomplished this work. Moreover, I really appreciated her efforts to provide a research assistantship to support me during the study, which gave me the opportunity to completely focus on the research work. I felt fortunate to have worked with her.

I would like to thank Dr. Yaylayan, Dr. Lefsrud, Dr. Shafaroudi and Dr. Qi for their invaluable suggestions during my comprehensive examination, which helped me to shape the thesis work. I would also like to thank Mr. Yvan Gariépy for his help in my work. Without him, it was impossible to finish the research work within three years. Furthermore, I want to thank Dr. Chao-Jun Li, Dr. Milan Maric, Dr. Orsat and Dr. Raghavan to allow me to access the instruments in their labs. Dr. Robin Stein is thanked for the NMR experiment training, his kindness and patience to help me to setup the experiment. Mr. Petr Fiurasek is also thanked for the DSC training, his helps to find the instruments I needed, and his suggestions about the results. Finally, I would thank Dr. Luis Fernando Del Rio and Dr. Otman Oulanti from FPInnovations to have given me access to the press for compression molding.

My labmates, Meng, Bryan, Na, Shrestha, Zhanghu, Agneev, Karolin, Daniel and Guillermo, are thanked for making my days so pleasant. I have been so lucky to have had them as my colleagues and friends. I remember the times we spent together to play games, to talk about the funny things, to complain about the experiments, and to exercise at the gym. Hopefully, we will have the chance to gather together in the future.

Last but not least, I would like to thank all my relatives and friends in China. Without their helps to take care of my mother, I would not have been able to continue my studies. I feel sorry to have left my mother alone for the past several years. Luckily, she has recovered well, and I am

glad to tell her that I will go back to China soon. Finally, I would like to thank my girlfriend, Chenhuan. Without her encouragement and support, I cannot imagine how hard it would have been to go through all these things. I am very happy that we finally made it. I want to thank her for her understanding and to have waited for almost four years.

Contribution of Authors

This thesis is submitted in the form of original papers published, accepted or to be submitted for publication in the peer-reviewed scientific journals. The candidate, Daihui Zhang, was responsible for designing and carrying out the experiments, as well as performing the data analysis and writing the manuscript and the thesis. Dr. Marie-Josée Dumont, as the supervisor of the candidate, contributed to all aspects of the research work, including planning and guiding the research, reviewing and correcting the manuscript and thesis. Dr. Alice Cherestes provided partial suggestions for the first research paper and co-edited the manuscript. The details of the papers are provided as follows:

1-Zhang, D., Dumont, M.J., (2016), Advances in polymer precursors and bio-based polymers synthesized from 5-hydroxymethylfurfual, ***Journal of Polymer Science Part A: Polymer Chemistry***, **55**, 1478-1492.

2-Zhang, D., Dumont, M.J., Cherestes, A., (2016), An efficient strategy for the synthesis of 5-hydroxymethylfurfural derivative based poly (β-thioether ester) *via* thiol-Michael addition polymerization, ***RSC Advances***, **6**, 83466-83470.

3-Zhang, D., Dumont, M.J., (2018), Synthesis, characterization and potential applications of 5-hydroxymethylfurfural derivative based poly (β-thioether ester) synthesized *via* thiol-Michael addition polymerization, ***Polymer Chemistry***, **9**, 743-756.

4-Zhang, D., Dumont, M.J., (2018), Reprocessable 5-hydroxymethylfurfural derivative-based thermoset elastomers synthesized through the thiol-Michael and Diels-Alder reactions, Submitted for Publication.

5-Zhang, D., Dumont, M.J., (2018), 5-hydroxymethylfurfural derivative based thermoplastic elastomers synthesized *via* thiol-Michael addition reaction utilizing poly(lactic acid) as hard end blocks, ***Macromolecular Chemistry and Physics***, DOI: 10.1002/macp.201800039.

Chapter 1: Introduction

1.1 General Introduction

The interest in polymers synthesized from renewable resources has been growing due to the issues related to the environment, as well as the concerns about the potential depletion of petroleum resources. Therefore, a variety of natural macromolecules and renewable monomers, such as polysaccharides, lignin, succinic acid, vegetable oils, terpenes, and furan-based derivatives, have emerged in the synthesis of various polymers.[1] 5-hydroxymethylfurfural (HMF) is a promising platform chemical owing to its sustainability and functional groups available for further reactions. Due to the importance of HMF, research works have focused on several key aspects such as: (1) biological properties, such as the metabolism of HMF and its toxicological effects[2]; (2) synthesis of HMF including the catalysts used[3], the feedstocks used[4], and the solvent systems used[3f, 5]; (3) derivatives of HMF as biofuels precursors[6], fine chemicals[7], monomers for polymers[1f, 7-8]; and (4) industrial production of HMF and its derivatives[4b, 8b, 9].

One of the important applications of HMF is its use in the synthesis of derivatives for the production of polymers. Examples of these derivatives include 2,5-furandicarboxylic acid (FDCA) and 2,5-bis(hydroxymethyl)furan (BHF).[10] For example, FDCA and ethylene glycol were used to synthesize poly(ethylene-2,5-furandicarboxylate) (PEF).[11] It was observed that the thermal and barrier properties of PEF were comparable to its fossil-fuel analogue polyethylene terephthalate (PET). Currently, the polymerization techniques which have been used to synthesize polymers from HMF and its derivatives include esterification, transesterification, enzymatic polymerization, ring opening polymerization, and free radical polymerization.[11-12] However, these techniques are often performed under rigorous conditions where high temperature, vacuum and long reaction times are generally needed. These reaction conditions do lead to the decarboxylation of FDCA, and therefore milder reaction conditions are required.

The thiol-Michael addition reaction offers high conversion yield, mild reaction conditions, and rapid reaction rates.[13] This reaction can be performed for the synthesis of small molecules, the surface functionalization of materials and polymer modification, and the formation of networks.[14] However, this reaction is rarely used for the synthesis of linear polymers.[16] This could be due to side reactions occurring when phosphines and amine catalysts are used.[16c, 17] The presence of side-reactions is an issue when designing polymers through the step-growth

polymerization technique since they can prevent the formation of the desired structure. The side-reactions also influence the molecular weight of linear polymers. Therefore, the elucidation of side-reactions in the thiol-Michael addition polymerization is of importance. Additionally, to illustrate the versatility of this polymerization technique, it is necessary to synthesize polymers with tunable structures and properties using dithiol monomers with different structures, especially those containing functional groups.[18-19] Furthermore, the synthesis of copolymers has been suggested to be a useful approach to adjust the thermal, mechanical, and barrier properties of polymers, depending on the ratio and the structure of the (co)monomers used.[20] However, few information is available on the synthesis of copolymers *via* the thiol-Michael addition reaction, particularly from the renewable resources.[16g]

The incorporation of sulfur into polymers can enhance several properties of polymers, including the flexibility of polymer chains and the refractive index of materials.[14a] Sulfur-containing materials have been used in applications such as optical lenses and automobile windshields.[21] A large number of research studies have reported the use of thiol-yne, thiol-epoxy and thiol-ene reactions to synthesize sulfur-containing polymers and networks.[22] For example, isosorbide based polycarbonate elastomers have been synthesized *via* the thiol-ene reaction.[23] Plant-derived phenolic acids have also been investigated to synthesize elastomers.[24] However, research studies on the characterization of networks synthesized *via* the thiol-Michael addition are limited,[14a,25] especially when bio-based monomers are used.[26] Furthermore, the lack of reprocessability due to the formation of covalent bonds caused other environmental concerns. Because of the reversibility of the Diels-Alder (DA) reaction between furan rings and the maleimide moieties, materials synthesized through this reaction can display several interesting properties, such as self-healing, recyclability and reprocessing capacity. Therefore, the presence of furan rings in the polymeric chains is expected to provide reactive sites for the occurrence of the DA reaction, which can generate a variety of dynamically crosslinked networks with controlled crosslinking densities. This can potentially improve the thermal and mechanical properties of the materials, and also enable the materials to be reprocessed after use.

Polylactic acid (PLA) has been used for food packaging and biomedical applications due to its renewability, non-toxicity, biodegradability, and tunable crystallization behavior. PLA has also been used as hard segments in the synthesis of thermoplastic elastomers (TPEs). Various types of

polymers with low T_g have been evaluated as the soft segments in PLA based TPEs. Despite the fact that highly flexible thioether groups are generated after the thiol-Michael addition reaction, no information is available on the use of poly(β-thioether ester) as soft segments for PLA based TPEs. Therefore, it is of interest to synthesize PLA based TPEs using thioether groups as soft segments due to the flexibility of the thioether groups, the potential biodegradability of thioether ester groups, as well as the presence of furan rings for further modification.

1.2 Hypotheses

The following hypotheses have been evaluated:

1. Using a suitable catalyst, the thiol-Michael addition reaction can be utilized to efficiently synthesize linear polyesters from 2,5-FDA and aliphatic dithiol monomer with relatively high molecular weights.

2. The thiol-Michael addition reaction can be used to synthesize 2,5-FDA based (co)polymers with varied structures and properties by using different dithiol monomers.

3. The utilization of the DA reaction between the furan rings in the polymeric chains and bismaleimide (as crosslinker) can dynamically tailor the thermal and mechanical properties of the synthesized linear polymers.

4. Reprocessable 2,5-FDA based thermoset elastomers can be synthesized *via* the combination of thiol-Michael addition reaction and Diels-Alder reaction.

5. The Thiol-Michael addition reaction can be used to efficiently initiate the macromolecular coupling reaction between the thiol and acrylate groups of polymers to triblock copolymers to synthesize TPEs.

1.3 Study Objectives

The objective of this work was to investigate the potential of thiol-Michael addition reaction to synthesize HMF derivative based linear polymers. Additionally, the use of the furan rings in the polymers was evaluated to tune the thermal and mechanical properties of polymers *via* the DA reaction. The specific study objectives are described as follows:

1. To review the current research work on the synthesis and characterization of HMF and its derivatives based polymers, and thereby selecting the research avenues meriting further investigation (**Chapter 2**).

2. a) To examine the catalyst efficiency and side reactions occurring during the thiol-Michael addition reaction using a model reaction. b) To synthesize a HMF derivative (2,5-FDA) from HMF ready for the thiol-Michael addition reaction. c) To synthesize and characterize linear polymers using the catalysts screened from the model reaction. d) To preliminarily evaluate the occurrence of DA reaction by observing the formation of a reversible organogel (**Chapter 3**).

3. a) To synthesize and characterize linear polymers prepared by the thiol-Michael addition reaction using different dithiol monomers in order to obtain polymers with tunable structures and properties. b) To synthesize and characterize copolymers from 2,5-FDA, 1,4-benzendithiol and 1,6-hexanedithiol. c) To evaluate the potential application of poly(β-thioether ester)s as an adhesive. d) To determine the kinetics of the DA and retro-DA reaction, and then improve the thermal and mechanical properties of poly(β-thioether ester)s *via* the DA reaction. e) To synthesize and characterize TPEs *via* the combination of different dithiol monomers (**Chapter 4**).

4. a) To utilize the combination of thiol-Michael and DA reactions to synthesize reprocessable thermoset elastomers. b) To impart the functionalities to the synthesized elastomers by the synthesis of functional linear copolymers. c) To tune the mechanical properties of thermoset elastomers (**Chapter 5**).

5. a) To incorporate poly(β-thioether ester) as the soft segments in PLA based TPEs. b) To adjust the mechanical properties of TPEs *via* the DA reaction between the furan rings in the soft segments and the crosslinkers (**Chapter 6**).

Chapter 2: Literature Review-Advances in Polymer Precursors and Bio-based Polymers Synthesized from 5-hydroxymethylfurfural

2.1 Abstract

In recent years, considerable efforts have been made regarding the synthesis of renewable chemicals from natural resources. 5-hydroxymethylfurfural (HMF) is an interesting platform chemical which has been widely exploited due to its rich chemistry and potential availability. The versatility of HMF has been demonstrated in several areas such as fine chemicals, biofuel precursors and polymers. In particular, the potential to replace petroleum-based analogues in the preparation of polymers associated with high performance has been observed owing to the structural rigidity of furan rings. This review aims at critically discuss the current research studies related to the derivatives of HMF, alongside with the synthesis and characterization of (co) polymers derived from HMF and its derivatives.

2.2 Introduction

The interest in polymers synthesized from renewable resources has been growing due to issues related to the environment, as well as the concerns about the potential depletion of petroleum resources. Therefore, a variety of natural macromolecules and renewable monomers, such as polysaccharides, lignin, succinic acid, vegetable oils, terpenes, and furan-based derivatives, have emerged in the preparation of various polymers.[27] 5-hydroxymethylfurfural (HMF) is a promising platform chemical owing to its sustainability and functional groups available for further reactions. Due to the importance of HMF, research works have focused on several key aspects: (1) biological properties, such as the metabolism of HMF and toxicological effects;[28] (2) synthesis of HMF including the catalysts used,[31] the feedstocks used,[30] and the solvent systems;[29f, 31] (3) derivatives of HMF as biofuels precursors,[32] fine chemicals,[33] monomers for polymers;[27f, 33-34] and (4) industrial production of HMF and its derivatives.[30b,34b,35]

One of the most important applications of HMF is to synthesize monomers for polymers, such as 2,5-furandicarboxylic acid (FDCA) and 2,5-bis(hydroxymethyl) furan (BHF). In addition to the synthesis of FDCA-based polyesters, their physical properties (i.e. crystallinity, thermal and mechanical properties, thermal degradation, structural properties and permeability) have been investigated as well.[36] The thermal and barrier properties of polyethylene 2,5-furandicarboxylate

(PEF) were highly comparable to their analogue polyethylene terephthalate (PET). More recently, catalytic production of FDCA from lignocellulosic biomass,[37] and FDCA-based polyesters and polyamides have been reviewed.[38] However, other HMF derivatives, such as BHF and 2,5-diformylfuran (DFF) should be emphasized as well,[28a] especially in combination with Diels-Alder reactions to prepare cross-linked or functional polymers.[26d,39] Therefore, the aim of this review is to combine and condense the body of researches performed on the synthesis of HMF derivatives, the synthesis and the characterization of (co)- polymers from HMF and derivatives. Furthermore, future work to this field has also been suggested.[40]

2.3 Bio-based furans monomers and derivatives

The chemical structure of HMF comprises of a furan ring, a hydroxyl group and a formyl group, which are available for reduction, oxidation, esterification, or other reactions leading to useful target molecules. In this section, a variety of derivatives which may be or have been utilized in the areas of polymer science and engineering are presented. Note that details related to their synthesis can be found in other reviews and scientific publications.[28a,28b,30b,33,39c]

2.3.1 Symmetrically functional derivatives of HMF

Due to the presence of functional groups on opposite sides of the heterocyclic ring of HMF, the preparation of symmetrically functional monomers is possible. **Figure 2.1** summarizes a number of versatile monomers obtained by oxidation, reduction and derivatization of HMF. The following paragraphs will discuss these monomers which have been used in the synthesis of polyesters, polyurethanes and thermoset resins.[39c]

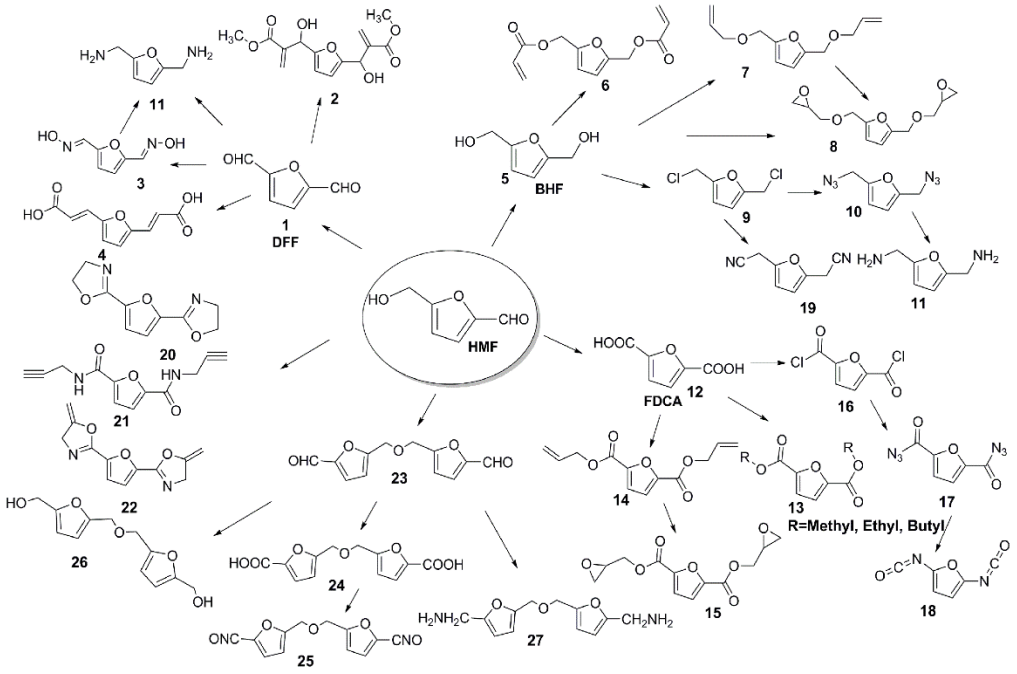

Figure 2.1 Symmetrically functional derivative of HMF

The oxidation of hydroxyl and formyl groups of HMF to FDCA (12) can be performed *via* aerobic oxidation with Pt catalysts supported on TiO_2 and ZrO_2,[41] RuO_2 catalysts with Mg-based supports,[42] magnetic Pd catalysts,[43] Ru/C catalyst,[44] as well as Au catalysts with a variety of supports.[45] Enzyme-catalyzed oxidation and a whole-cell biotransformation of HMF to (12) have also been performed.[46] Diesters (13) have been synthesized *via* the esterification of (12) with corresponding alcohols.[47] Direct oxidative esterification of HMF to dimethyl 2,5-furandicarboxylate (13, R=methyl) was achieved using Au-ZrO_2 and Au-CeO_2 catalysts, respectively.[48] These monomers are valuable polyester precursors. Reaction of (12) and $SOCl_2$ in DMF afforded 2,5-furandiarbonyl chloride (16),[49] which was used in the synthesis of polyesters and polyamides.[50] Moreover, the addition of sodium azide in a solution of (16) yielded 2,5-dicarbazidofuran (17), which was further converted to diisocyanatofuran (18). Like other diisocyanates, (18) must be stored in an inert atmosphere due to its susceptibility to moisture.[51] Other derivatives of (12), such as diglycidyl ester of 2,5-furandicarboxylic acid (15) and bis(prop-2-enyl)furan-2,5-dicarborxylate (14) have been synthesized.[52] The use of (15) for the synthesis of bio-based epoxy resins showed promising results in terms of higher curing activity, elevated glass transition temperature (T_g), as well as similar mechanical properties as compared to diglycidyl ester of terephthalic acid.[52]

BHF (5) is another valuable building block chemical. The acylation of the hydroxyl groups of (5) with acryloyl chloride using trimethylamine as catalyst yielded 2,5-furan diacrylate (6). The addition of (6) as a difunctional cross-linker through photo-polymerization increased the tensile strength of acrylated epoxidized vegetable oils based polymer networks by up to 4.2 times as compared with those without addition of (6).[53] Moreover, (6) has been used as a monomer for the synthesis of side-chain functional polyesters *via* the Baylis-Hillman reaction.[54] Reaction of (5) with ally bromide produced 2,5-bis-allyloxymethyl-furan (7), which was utilized to prepare heteromacrocycles by ring-closing metathesis.[55] The synthesis of 2,5-bis[(2-oxrianylmethoxy)methyl]-furan (8) was performed by reaction of (5) with epichlorohydrin using tetrabutylammonium hydrogen sulfate as the catalyst. (8) has been utilized to prepare high-performance epoxies.[56] 2,5-bis(chloromethyl)furan (9) was synthesized by reacting (5) with $SOCl_2$ and pyridine in $CHCl_3$ at -10 ^oC.[57] Furthermore, (9) has been used to obtain 2,5-bis(azidomethyl)furan (10) and 2,5-bis(cyanomethyl)furan (19).[57b,58] 2,5-bis(aminomethyl)furan (11), a building block for polyamides, can be synthesized by several approaches. Using Raney nickel as a catalyst, (11) was obtained by stirring a solution of (10) at 1 atm of H_2 at room temperature for 40 h.[57b] It can also be synthesized from DFF (1) with furan-2,5-dicarbaldehyde dioximes (3) as the intermediate.[59] Recently, (11) was prepared by the direct reductive amination of (1) with ammonia in one step. The use of acid treated Raney-Ni catalysts in combination with a THF-water medium was of importance because of its ability to suppress side reactions, leading to a relatively high yield (46 %).[60]

Additionally, 2,5-furandiacrylic acid (4), a photo-responsive monomer, was synthesized from (1) using an excess of malonic acid and pyridine.[61] The photocyclodimerization of (4) was a reversible process. Irradiation with a tungsten bulb led to the formation of dimers. The thermal decomposition of dimers to (4) occurred at 220 ^oC.[61] Dialdehyde groups of (1) were also available for the Baylis-Hillman reaction. Therefore, reaction of (1) with methyl acrylate using 1,4 diazabicyclo[2.2.2]octane (DABCO) as a catalyst generated (2).[62]

Li *et al.* described a facile and efficient method to synthesize 2,5-bis(4,5-dihydrooxazol-2-yl)furan (20) *via* reaction of (12) with β-amino alcohols in toluene for 24 h.[63] Recently, bio-based thermosets obtained through the polymerization of (20) with sebacic acid were prepared and characterized.[64] Other derivatives, such as N,N-di(prop-2-ynyl)furan-2,5-dicarboxamide (21)

and 2,2'-furan-2,5-diylbis(5-methylene-4,5-dihydro-1,3-oxazole) (22), have been prepared as well.[65] They might be employed to synthesize polymers *via* radical polymerization or azide-alkyne reactions.[66] 5,5'-(oxydimethylene)-di-2-furaldehyde (23) used for the synthesis of polyurethane foams was obtained *via* etherification of HMF catalyzed by several different catalysts, such as graphene oxide, homogeneous organic acids, and molecular sieves with Brönsted and Lewis acid sites.[67] Other approaches, such as the thermal dehydration of HMF in the presence of dimethyl-sulfoxide,[68] and the Williamson reactions between HMF and 5-chloro-methyl-2-furfural with an excess of base, have been used for the synthesis of (23) as well.[69] Dialdehyde groups of (23) can be further oxidized to dicarboxylic acids (24) using silver oxide in basic condition.[67c] The conversion of (24) to diisocyanates (25) was accomplished in two steps using diazides as the intermediates.[67a] Derivatives from (23), such as diols (26)[70] and diamines (27) have also been prepared.[71]

In addition to the derivatives mentioned above, continuous efforts are being put into upgrading HMF. Recently, Chen *et al.* have prepared a monomer, 5,5'-dihydroxymethyl furoin (DHMF) from the HMF in 95% yield *via* organocatalysis. Selective oxidation and reduction of DHMF afforded diol and tetraol monomers which were utilized in the synthesis of linear or cross-linked polyurethanes.[72] The synthesis of bis(hydroxylmethylfurfural)amine from HMF has also recently been reported by reacting HMF with primary amines in the presence of homogeneous catalysts. These new monomers offer great potentials to form functional biopolymers with tunable properties.[73]

2.3.2 Unsymmetrically Functional Derivatives of HMF

Figure 2.2 shows the derivatives of HMF prepared by selectively reacting hydroxyl or formyl groups of HMF. HMF can be efficiently converted to 5-hydroxymethyl-2-vinylfuran (28) by the Wittig reaction. This derivative is a good candidate for radical polymerization initiated by azobisisobutyronitrile.[74] The conversion of HMF to 5-(hydroxymethyl)furan-2-carbonitrile (29) can be accomplished using iodine in an aqueous ammonia solution.[75] 5-hydroxymethyl-2-furancarboxylic acid (30) has been prepared *via* the selective oxidation of aldehyde group to carboxylic acid through a whole-cell biotransformation (*Serratia liquefaciens* strain),[76] or a heterogeneous catalyst prepared by immobilization of $[MoO_2(acac)_2]$ on montmorillonite K-10 clays.[77] In addition, HMF has been selectively carbonylated to 5-formylfuran-2-acetic acid (31)

in an acidic aqueous medium using Pd complex of trisulfonated triphenylphosphine as the catalyst.[78] The transformation of HMF to 1,3-dioxolane-4-methanol, 2-[5-(hydroxymethyl)-2-furanyl] (32) can be catalyzed by molybdenum and tungsten promoted SnO_2 solid acids.[79] Bio-based acrylate (33) has been synthesized by the Baylis-Hillman reaction of methyl acrylate with HMF.[54,80] The reaction of the hydroxyl group with acryloyl chloride gave 5-hydroxymethylfurfuryl acrylate (34).[54]

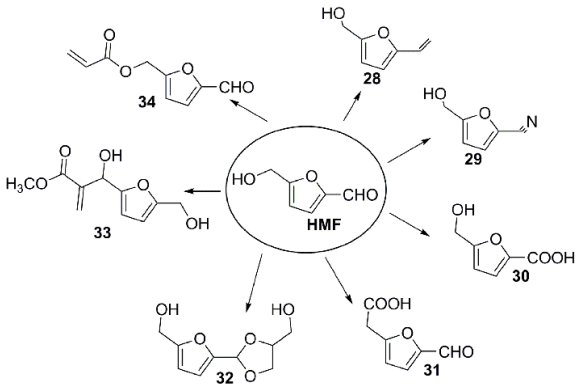

Figure 2.2 Unsymmetrically functional derivatives of HMF

2.3.3 Derivatives of HMF from furan ring reactions

Most chemicals derived from the reaction of furan rings can be considered as potential biofuels candidates or precursors.[81] However, some derivatives have been utilized for the synthesis of polymers (**Figure 2.3**). For the furan rings, a variety of reactions have been observed, such as reactions with electrophiles, nucleophiles, oxidants, reductants, cycloaddition, as well as metals and metallic derivatives.[82] Oxidation of the furan ring of HMF to (35) was performed in two steps using meta-chloroperoxybezoic acid as the oxidant.[83] Maleic anhydride (36), a versatile chemical intermediate, has been produced from HMF *via* oxidation with molecular oxygen using $VO(acac)_2$ as a catalyst.[84] Acid catalyzed decomposition of HMF generated levulinic acid (37). The properties and potential applications of levulinic acid have been reviewed.[85] Catalytic hydrogenation of HMF gave 2,5-tetrahydrofuran dimethanol (38) in a quantitative yield using a Ra-Ni catalyst at 100 ^{o}C.[86] 1,6-hexanediol (39) can be prepared *via* different routes, such as direct hydrogenation of HMF with a mixture of copper chromite and Pd/C as catalysts, and a two-step approach *via* (38) using Rh-Re/SiO_2 as a catalyst.[87] Recently, the direct production of (39) from HMF was achieved over a reusable Pd/zirconium phosphate

catalyst at 140 ºC using formic acid as a hydrogen source.[88] Further preparation of caprolactone (40) was successful in methyl isobutyl ketone at the reflux temperature for 30 mins, using the catalyst made *in situ*.[87] Conversion of (40) into caprolactam (41) by the reaction with ammonia was straightforward and has been well-established.[89] Last but not least, the Diels-Alder reaction between furan rings and maleimides, particularly for furfural and its derivatives, has been recognized as a versatile "click tool" in the macromolecular synthesis.[90] In the case of HMF and its derivatives, the effect of substitutions connected to the furan ring should be considered in the design of monomers through Diels-Alder reactions, since those substitutions significantly influenced the reactivity between the furan derivatives and the maleimide derivatives.[91] For example, FDCA, an oxidation product of HMF, has been utilized to synthesize furan polyesters. However, the electron-withdrawing effect of the carbonyl groups connected to the furan ring prevented the Diels-Alder reaction of furan rings with maleimide.

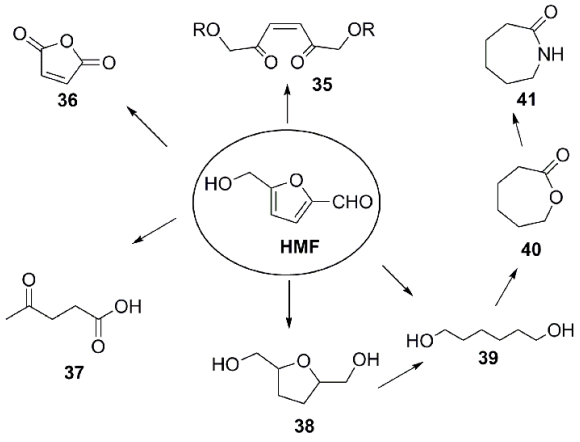

Figure 2.3 Derivatives of HMF *via* furan ring reactions

In summary, a variety of HMF derivatives have been presented in the literatures. However, the problems in the synthesis of HMF derivatives still exist, such as low yield, high cost and high energy input. Thus, efforts to synthesize these derivatives in an economically feasible and environmentally friendly way are still needed. In addition, information about some of the HMF derivatives which can potentially be used in the synthesis of polymers is still missing. It deserves to be further investigated due to the renewability of HMF and unique properties of furan rings (diene). Moreover, the synthesis of new HMF derivatives could increase the utilization of HMF in the polymer field.[72]

2.4 Polymers derived from HMF and its derivatives

The interest in polymers derived from HMF and its derivatives has been rapidly increasing not only due to the sustainability and rich chemistry of HMF, but also due to the unique properties of these polymers. Currently, the preparation of HMF derivatives based polymers are mainly performed *via* chemical approaches.[34c,92] Enzymatic catalysis routes have been recently evaluated as well.[40] Therefore, in this section, the synthesis and characterization of polymers *via* chemical methods will be reviewed, starting from three key monomers (FDCA, BHF and DFF).

2.4.1 Chemical polymerization

2.4.1.1 Polymers from FDCA and its derivatives

Due to the presence of two carboxylic acid groups, FDCA and its derivatives have been utilized in the synthesis of (co)polyesters, polyamides and other interesting polymers. Researches on (co)polyesters have been growing quickly in terms of synthesis, structural analysis, determination of the physical properties, as well as the sorption behavior with water, oxygen and carbon dioxide. Among FDCA based polyesters, poly (ethylene-2,5-furandicarboxylate) (PEF) and poly (butylene-2,5-furandicarboxylate) (PBF) are the most comprehensively studied due to their resemblance to the engineering plastic polyethylene terephthalate (PET) and polybutylene terephthalate (PBT). Poly (propylene-2,5-furandicarboxylate) (PPF) as the replacement of poly(propylene-2,5-terephthalate) (PPT) has also been investigated in terms of thermal behavior, solid state structure and barrier properties.[93] Besides these, varieties of other monomers, such as longer aliphatic linear diols, aromatic diols and renewable aliphatic acids, have been used to prepare (co)polyesters.[94-95]

Poly(ethylene-2,5-furandicarboxylate)

Being entirely prepared from renewable FDCA and ethylene glycol (EG), PEF has been proposed as an important alternative for PET.[38a,96] More importantly, it presents high performance in terms of thermal stability, mechanical and barrier properties. Recently, a detailed description of PEF synthesis *via* two stage melting polymerization has been presented (**Scheme 2.1**).[64] The starting materials, reaction temperatures and catalysts have been suggested to influence the polymerization process and the polymer properties. The preferable starting monomer used for the polymerization reactions was dimethyl ester 2,5-furandicarboxylate

(DMFD), rather than FDCA, in order to prevent the decarboxylation of FDCA. A high polymerization temperature (over 250 °C) was not recommended due to the color issue and a lower yield. In addition, tin (IV)/tin (II) catalyst system contributed to the increase in molecular weights. This approach seems to be effective, and has been widely adopted. However, issues still exist, such as a long reaction time (hours to days) required to attain high reaction extents, and poor mass and heat transfer when the melt viscosity was high. Other synthesis routes, such as direct esterification using tetrabutyl titanate as a catalyst,[97] ring opening polymerization of cyclic FDCA based monomers,[98] and the combination of melting polymerization and subsequent solid state post condensation,[99] have also been presented. For the ring opening polymerization, although PEF with weight-average molecular weight between 50,000 and 60,000 g/mol has been synthesized,[98] the complicated process for the preparation of cyclic monomer and relatively low yield might limit its application.

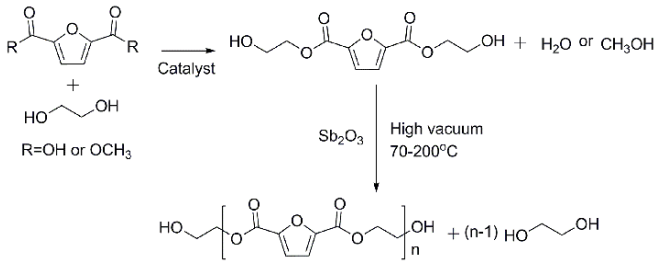

Scheme 2.1 Synthesis of poly(ethylene 2,5-furandicarboxylate)[96]

The structure of PEF prepared *via* two stage melting polymerization was found to be semi-crystalline. The T_g and melting point (T_m) were in the range of 75-80 °C and 210-215 °C, respectively.[96] PEF was thermally stable up to 300 °C. These behaviors were similar to those of PET, although PEF showed a relatively lower thermal stability. The density of amorphous PEF (1.43 g/cc) was higher than the density of amorphous PET (1.33 g/cc).[36a] On the other hand, the differential scanning calorimetry (DSC) curves showed the absence of cold-crystallization and subsequent melting peak for amorphous PEF during the first heat cycle as compared to a significant cold-crystallization and melting peak for PET. This observation indicated a long time-scale for the crystallization process in PEF, probably due to the structural rigidity and the nonlinear axis of rotation around the furan ring.[36a] However, Bikiaris *et al.* observed a cold-crystallization peak and subsequent melting peak of melt-quenched PEF in the non-isothermal cold-crystallization experiment.[36b] Furthermore, it showed that the cold crystallization

temperature (T_{cc}) increased with the increase of heating rates in the DSC analysis. The melting points were higher at slower rates due to the increased crystal stability. For PET, melting points were less affected by the different heating rates, and cold crystallization peaks were always located in about the middle of the range between T_g and T_m. From cold-crystallization studies and T_{cc}-T_g differences, it was suggested that PEF chains were much less flexible than those of PET. Additionally, isothermal crystallization from the melt revealed multiple melting peaks for each PEF samples crystallized at different temperatures. The intensity and position of the peaks also varied in each PEF sample. It was suggested that two populations of lamellae of different stabilities, rather than recrystallization, might have contributed to these multiple melting behaviors of PEF. Furthermore, wide-angle X-ray scattering (WAXS) study of each PEF samples showed similar peak patterns. It indicated that melting of crystals of different forms generated during the process of isothermal crystallization failed to explain the different melting behavior in each PEF samples.[36b] Es *et al.* also observed multiple melting transitions for a high M_w PEF from DSC analysis obtained after isothermal crystallization at various temperatures (150 to 200 ^oC), but they believed that the multiple melting behavior was the result of melting and recrystallization of imperfect crystals.[73]

More recently, the Avrami equation was used to describe the isothermal crystallization kinetics of PEF. The Avrami exponent (n) values were in the range of 2.2-2.6.[36b] In addition, the maximum growth rate calculated with obtained Hoffman-Lauritzen parameters was $T_{c,max}$ = 167 ^oC.[100] It was also observed that the catalyst content and the polymerization conditions somehow influenced the rate of melt crystallization at T_c= 170 ^oC. Sbirrazzuoli *et al.* investigated the non-isothermal crystallization kinetics of PEF obtained *via* the direct esterification process. Similar structures of PEF crystals either formed from the glassy state or from the melt were observed *via* WAXS, but the growth dynamics were different. The Hoffman-Lauritzen theory described well the crystallization of PEF from the glassy state, but showed some deviations for PEF crystallized from the melt. A faster crystallization rate of crystals from the glassy state was found, which might be beneficial for PEF industrial production and processing.[101]

The mechanical analysis revealed that the Young's modulus and the maximum stress of PEF were 2070-2450 MPa and 35-67 MPa, respectively, which were comparable to those of PET (2000 MPa and 45 MPa, respectively).[97] Es *et al.* observed that PEF showed a brittle fracture

behavior during the stress-strain test.[99] The elongation at break was 2.81 %, and much lower than that of PET (90-250 %). It might be the result of relatively lower molecular weight of PEF than PET. Dynamic mechanical thermal analysis (DMTA) performed on amorphous PEF showed that the storage modulus values (E') was in the range of 1.74 GPa to 2.28 GPa. When the temperature was above T_g, an obvious decrease in E' indicated the relatively poor mechanical properties. However, annealing was able to improve the mechanical properties above the T_g.[99]

Recently, a frequency dependent Arrhenius relationship was utilized to analyze the β relaxation of PEF and PET in order to investigate the macroscopic properties of the polymers.[36a] From the tan δ curves, it was seen that the peak maximum of PEF pertaining to the β relaxation shifted to a higher temperature in comparison with PET, and the value decreased from 0.05 to 0.03. The shift was attributed to an increase in chain rigidity of PEF. Furthermore, the activation energy (EA) of the β relaxation of PEF and PET were 68 ± 2 and 72 ± 1 kJ/mol, respectively. Both phenyl ring-flipping and carbonyl motions were believed to contribute to the relaxation behavior in PET, but ring-flipping motion in PEF was inhibited due to the nonlinear axis of the furan ring rotation and the ring polarity (**Figure 2.4**). Therefore, Koros *et al.* suggested that the carbonyl motions in PEF were more complex, and it might undergo some concerted motions with small scale furan ring oscillations.[36a]

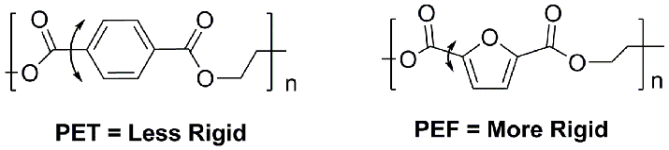

Figure 2.4 Polyester performance versus ring-flipping[36a]

Studies on the thermal degradation kinetic and decomposition mechanism of PEF *via* pyrolysis- GC-MS (Py-GC/MS) showed that its decomposition occurred in two steps. The β-hydrogen bond scission dominated the decomposition process, producing vinyl compounds and carboxyl derivatives.[102] Moreover, a low amount of aldehydes and carbonyl compounds were detected as the products of α-hydrogen bond scission and radical chain scission. This mechanism was similar to other FDCA based polyesters with longer diols.[103]

For the packaging applications, Koros *et al.* systematically investigated the sorption and the transport of carbon dioxide, water and oxygen in amorphous PEF.[36d,104] The O_2 sorption behavior

of PEF was similar to PET at 35 °C, but it showed a significant reduction (~11×) in oxygen permeability as compared to PET. The difference in oxygen permeability was mainly a result of a reduction in the chain mobility in PEF. In the case of CO_2, there were drastic reductions in permeability (19×) and diffusivity (31×) in PEF at 1 atm as compared to PET.[104a] Kinetic and equilibrium sorption properties of PEF were also examined at 35 °C over the entire water activity range. PEF showed a higher equilibrium water uptake (~1.8×) as compared to PET due to the higher affinity between water and polar furan ring. In addition, a significant reduction of the water diffusion coefficient for PEF was observed because of decreased segmental mobility of non-symmetrical furan ring. Finally, PEF exhibited an average permeability reduction of ~2.8× for water as compared to PET at 35 °C.[104b,104c]

Taking recycling into consideration, both mechanical (re-extrusion) and chemical recycling (decomposition) are possible. An assessment of depolymerization products of FDCA based polyesters showed that hydrolysis or methanolysis catalyzed by a base, such as sodium methoxide and 1,5,7-triazabicyclo[4.4.0]dec-5-ene (TBD), can recover dimethyl 2,5-furandicarboxylate and FDCA.[105] The methanolysis rate for PEF was much faster than that of PET. About 52 % of an initial PEF bar-shaped sample dissolved into methanol, while only 2 % of an original PET bar-shaped sample dissolved after a 90-minute test. In addition, when recycle streams of PET and PEF were mixed, the addition of up to 5 % (w/w) PEF showed no significant effect on the mechanical and physical properties of PET.[36c]

Poly(butylene-2,5-furandicarboxylate)

Poly (butylene 2,5-furandicarboxylate) (PBF) prepared from FDCA and 1,4-butanediol has been widely investigated as well.[106] Gross *et al.* examined the effect of catalyst amounts, reaction time and temperature on the molecular weight and dispersity index (DI) of PBF. The polymerization process was a two-stage melt-polycondensation.[107] An increase in catalyst concentration (within a certain range) increased the molecular weight, and decreased the DI of PBF. Nevertheless, when the catalyst concentration reached 200 ppm, further increase in catalyst concentration showed less effect on them. In addition, the second-stage polymerization temperature was of importance for the final molecular weight of PBF. When the second-stage temperature was 200 °C, the M_w of PBF gradually increased during the extension of the reaction time from 2 to 8 h. However, a decrease in the M_w of PBF was observed when the second-stage

reaction temperature was set to 220, 240 and 260 °C. Zhou *et al.* have utilized a direct esterification method to prepare PBF. T_g, T_m and T_d of PBF were 31 °C, 172.2 °C and 373 °C, respectively, which were lower than those of PBT.[97] The stress-strain curves revealed that Young's modulus, tensile strength and elongation at break were 1.1 GPa, 19.8 MPa and 2.8 %, respectively. The hydrophilicity of the polymeric matrix was confirmed by the result of the water contact angle test (84°).[97] Recently, Dubois *et al.* suggested that FDCA with high purity (99.9 %) facilitated the preparation of PBF with high M_w.[98] As a result, tensile modulus, strength and elongation at break were 1.9 GPa, 56 MPa and 256 %, respectively. In contrast to only one transition at 172 °C (T_m) mentioned above,[97] Ma *et al.* observed two different transitions of PBF using DSC at about 130 °C and 170 °C, respectively. The observation was similar to that of PBT (strained β-crystal, unstrained α-crystal), indicating the possible presence of different crystallinities.[106a] X-ray diffraction (XRD) analysis at different temperatures also revealed two transitions which occurred at 120 °C and 180 °C, respectively, which were consistent with the DSC results. Bikiaris *et al.* observed multiple melting behavior of PBF after isothermal crystallization from the melt in the DSC analysis.[109] However, only peaks of α-crystal modification without β-crystal were observed in the WAXS results, and no crystal transition occurred on heating. Therefore, it was suggested that these multiple peaks in DSC might be the result of a recrystallization process.[109]

The effect of M_w on the thermal and mechanical properties of PBF was studied (**Table 2.1**).[107] T_g values of sample 3-6 were similar to that of PBT (40 °C). The presence of lower M_w species as plasticizers might have resulted in the relatively lower T_g for sample 1 and 2. Furthermore, the value of ΔH_m decreased from 46 to 34 J/g when increasing M_w from 16×10^3 to 65×10^3 g/mol. The mobility of chains in PBF with low M_w increased, which was beneficial to the crystallization of polymers during cooling from melt. Furthermore, PBF samples with different M_w possessed similar spectra in the DMTA analysis. There were two relaxation peaks in the tan δ plot at -74 °C and +39 °C, respectively. The micro-Brownian motion of polymer chains in the amorphous regions was responsible for the higher temperature peak, while another relaxation peak was mainly associated with the motion of butanediol groups and carbonyl residues in the non-crystalline phase. Results of the mechanical properties of PBF showed that the elongation at break and stress at break significantly increased when comparing sample 2-6 with sample 1. With a further increase in the M_w for samples 3 to 6, the values of the Young's modulus,

elongation at break and stress at break were similar. When the M_w of the samples was too low, the lack of sufficient entanglements might have failed to provide satisfactory mechanical properties. Furthermore, samples with different percent crystallinity (from 8 to 44 %) were prepared by varying the annealing conditions for sample 6. The elongation at break significantly decreased from over 1000 to 7 % with the increase in the crystallinity, but it showed less effect on the Young's modulus and stress at break. It was suggested that when the amorphous phase was in the glassy state (below T_g), the presence of crystallinity regions slightly influenced the variation of the modulus.

Table 2.1 Thermal and Mechanical Parameters for PBF Determined by DSC and Tensile Testing as a Function of PBF Molecular Weight[107]

	GPC Results		First heating	Second heating				
Sample no.	$M_w \times 10^3$ (g/mol)	DI[a]	T_g(°C)[b]	ΔH_m(J/g)[c]	T_m(°C)[c]	Young's Modulus (MPa)	Elongation at break (%)	Stress at break (MPa)
1	16	2.2	34	46	173	742±23	2.5±0.6	5.5±1.1
2	27	2.6	37	40	173	847±43	506±82	12.1±4.2
3	38	2.4	38	39	173	919±48	1184±28	29.3±1.5
4	49	2.3	39	38	172	969±64	1105±24	28.5±1.7
5	61	2.7	40	35	171	964±37	1108±108	32.9±5.2
6	65	2.8	39	34	172	959±58	1055±56	31.8±2.9

[a] DI equals to M_w/M_n. [b] Glass transition temperature determined from the first heating scan at 20 °C/min after quenching melted samples from liquid nitrogen. [c] Heat of fusion and melting temperatures determined from the second heating at 10 °C/min after cooling at 10 °C/min from the melt.

Solid-state ^{13}C NMR was used to study the structure of PBF.[106a] Five signals were shown in ^{13}C cross-polarization magic angle spinning (^{13}C CP/MAS) NMR at 24.9, 65.8, 122.2, 147.8 and 159.0 ppm, respectively. However, the furan carbon signal at 122.2 ppm was split into two in ^{13}C direct polarization magic angle spinning (^{13}C DP/MAS) NMR at 122.2 and 112.7 ppm, respectively. It was suggested that a carbon signal from the amorphous phase of polymers was able to be significantly augmented in ^{13}C DP/MAS. Therefore, the results demonstrated the presence of furan rings in the crystalline and amorphous phases. In addition, it indicated that local phase changes could influence the chemicals shifts of the furan carbon, instead of the

carbons from butylene and ester. On the other hand, observations by polarized microscope showed that PBF retained the feature of PBT with fast crystallization, which is important for future commercial application. WAXS analysis revealed the crystal structure of PBF as triclinic crystal system.[110] The thermal stability and decomposition kinetic of PBF were investigated *via* thermogravimetric analysis (TGA) together with Py-GC/MS.[102] The decomposition occurred in one step as compared to two steps for the PEF, and mainly *via* β-hydrogen bond scission. Furthermore, a low amount of aldehydes and radicals of 2-furancarbonyl and OH groups were detected, indicating the presence of α-hydrogen bond and radical scission. The decomposition mechanism was quite similar to that of PBT.

Copolyesters

Copolyesters from FDCA can be prepared by either incorporating more than one aliphatic diols or introducing other diacids monomers. Therefore, the properties of polymers, such as biodegradability, thermal, mechanical and barrier properties, are tunable, depending on the ratio and the structure of comonomer.[111] Preliminary results from the work of Gandini *et al.* showed that the thermal properties of poly (ethylene 2,5-furandicarboxylate-co-1,3-propylene-2,5-furandicarboxylate) (PEF-PPF) were similar to PEF rather than PPF, even though there were 76 % of propylene moieties.[49b] Additionally, Nie *et al.* studied the reactivity of ethylene glycol (EG) and 1,4-butanediol (BD) with FDCA, as well as the solubility of the corresponding copolyesters. ^{1}H NMR of PEF-PBF showed that the content of EG and BD was adjustable *via* changing the initial feed ratios. Moreover, BD showed a higher reactivity than EG in the polymerization process. PEF-PBF was difficult to dissolve in THF, toluene and chloroform but soluble in TFA, as well as slightly soluble in hot DMSO.[112]

Dubois *et al.* have prepared poly (butylene succinate-co-butylene furandicarboxylate) (PBS-PBF) *via* direct esterification and polycondensation.[113] The effect of mole percentage of FDCA (δF) on the polymer yield, solubility, color, thermal and mechanical properties were studied. δF in the reaction system was able to influence the yield of polymer. When δF was less than 50 mol%, the reaction occurred following a two-step melt polycondensation procedure. However, when δF was in the range of 60-90 mol%, low M_w copolyesters were obtained under the same conditions. Both FDCA and succinic acid were able to catalyze the side reactions, such as the formation of THF. FDCA has a stronger acidity than succinic acid. Therefore, the increase of δF

could accelerate the side reactions leading to an incomplete esterification reaction. Several approaches have been proposed to resolve the issue, such as adding a tetrabutyl titanate (TBT) catalyst at the first stage together with an increase in diols/diacids ratio, lowering the esterification reaction temperature to suppress the side reactions, as well as using a TBT-$La(acac)_3$ mixture at the second stage to catalyze the polycondensation.[113] The solubility analysis indicated that the composition of PBS-PBF influenced the solubility of polymers in organic solvents. PBS-PBF with high δF (over 80 mol %) showed poor solubility in chloroform, heptane and methanol, but it was soluble in hot 1,1,2,2-tetrachloroethane at 50 ^{o}C. Fenouillot *et al.* exploited the biodegradation ability of PBS-PBF.[114] It showed that 90 % of copolyester could biodegrade within 180 days.

Ji *et al.* utilized adipic acid as a substitute for succinic acid to synthesize poly (butylene adipate-co-butylene furandicarboxylate) (PBA-PBF).[115] $T_{d,5}$ and $T_{d,max}$ of PBA-PBF were 342-388 ^{o}C and 417-430 ^{o}C, respectively. The effects of mole percentage of FDCA on T_g, T_m and the mechanical properties are shown in **Table 2.2**. The T_g of copolyesters gradually increased with the increase in the mole percentage of FDCA, due to the stiffer chain conformation. The structure of PBA-PBF changed from semi-crystalline to amorphous, then to semi-crystalline according to the DSC and XRD results. It was suggested that the presence of adipate and furandicarboxylate units in a random way interrupted the crystallization of the chains (PBA-PBF30 to PBA-PBF50). The mechanical properties of PBA-PBF showed that the Young's modulus and tensile strength first decreased, and then increased, whereas the elongation at break followed the opposite trend. These properties were highly related to the variation in crystallinity of the copolymers. From the results of enzymatic degradation, it was observed that the introduction of small amounts of FDCA (below 10 mol%) was beneficial to the degradation of PBA-PBF by lipase. The presence of FDCA decreased the crystallinity of PBA. However, furan units were eventually able to prevent the biodegradation of copolymers because of the rigidity of furan rings, as well as the overall high crystallinity.[115] Furthermore, Dubois *et al.* observed that the solubility of PBA-PBF was also composition-dependent.[108]

Table 2.2 Glass Transition Temperature (T_g), Melting Temperature (T_m), Young's Modulus (E), Tensile Strength (σ_{max}) and Elongation at Break (ε_{max}) of PBA, PBF and PBA-PBF Copolyesters[115]

Samples	T_g (°C)	T_m (°C)	E(MPa)	σ_{max}(MPa)	ε_{max}(%)
PBA	-[a]	55	168 ± 3.0	15 ± 1.2	463 ± 37
PBA-PBF10	-[a]	49	110 ± 10	12 ± 1.0	755 ± 64
PBA-PBF20	-44	30	55 ± 5.1	11 ± 1.1	976 ± 53
PBA-PBF30	-37	-[c]	0.14 ± 0.03	2.6 ± 0.08	1850 ± 183
PBA-PBF40	-28	-[c]	1.5 ± 0.4	19 ± 1.3	1521 ± 93
PBA-PBF50	-19.7	-[c]	10 ± 0.7	20 ± 0.9	1040 ± 56
PBA-PBF75	0[b]	134	76 ± 4.2	30 ± 1.6	425 ± 23
PBF	36	171	875 ± 18	35 ± 2.6	55 ± 10

[a] Not measured due to instrumental limitation. [b] Estimated from DSC analysis of PBA-PBF75 during second heating at 10 °C/min. [c] No T_m was observed.

Poly (lactic acid) (PLA) has been widely utilized in the packaging and biomedical fields due to its biodegradability and biocompatibility.[116] Recently, PEF-PLA copolymers were obtained using Sb_2O_3 as catalyst.[117] The M_w of copolyesters varied between 6900 and 9000 g/mol. Degradation experiments showed that PEF-PLA had an improved degradability in comparison with PEF. Moreover, high T_g and $T_{d,5\%}$ values (76 and 324 °C, respectively) were observed after the incorporation of 8 mol% of lactyl units in PEF-PLA.[117] Cao *et al.* have synthesized PEF-PLA with higher M_w (68000 to 130000 g/mol) by two-stage condensation polymerization.[118] The T_g and $T_{d,5\%}$ of PEF-PLA were adjustable depending on the molar ratio of PEF to PLA. Moreover, PEF-PLA were biodegradable in PBS solution and soil, which was evaluated by weight loss, molecular weight and structural changes, as well as SEM observation.

Copolyesters derived from terephthalic acid and FDCA have been synthesized in order to increase the bio-based content of PET.[119] The solubility of the copolyesters was poor. PET-PEF-4/1 (20 mol % furan) was semi-crystalline, and displayed similar thermal properties to PET in terms of T_g (62.4 °C), T_c (125 °C) and T_m (220 °C). The DMA analysis showed that the β and α transition temperatures of PET-PEF-4/1 were -40.9 and 67.5 °C, respectively, as compared to those of PET (-58.3 and 103.2 °C, respectively). **Table 2.3** summarizes the molecular weights and partial thermal properties of FDCA-based (co)polyesters. Generally, the T_g and T_m of FDCA-based polyesters gradually decreased with the increase in the methylene units of aliphatic linear diols (from 2 to 18). Polyesters were thermally stable up to 300 °C. Additionally, the

incorporation of methyl groups as the side chain of polymers increased the T_g, such as the T_g of polymer synthesized from 2,3-butanediol (71-113 °C) and ethylene glycol (75-80 °C).

Table 2.3 Molecular Weight (M_n), Glass Transition Temperature (T_g), Melting Temperature (T_m) and Decomposition Temperature (T_d) of (Co) polyesters.

(Co)polyester	Diols (and Diacids)	M_n*10^3/g mol^{-1}	T_g/°C	T_m/°C	T_d/°C	Ref
PEF	Ethylene Glycol	18-44	75-80	210-215	389-398	36c,49b,96
PPF	1,3-Propanediol	15-23	50-58	170-180	375-390	36c,49b,120
PBF	1,4-Butanediol	23-26	30-45	167-172	329-388	36c,106a
PBF2	2,3-Butanediol	2-13	71-113	-	276-301	121
PHF	1,6-Hexanediol	13-23	7-28	145	350-390	36c,122
PDPF	2,2-Dimethyl-1,3-Propanediol	15	68	198	408	123
POF	1,8-Octanediol	20-34	-5-22	140-148	375-400	124
PDeF	1,10-Decanediol	36	1	112-116	340-359	125
PDF	1,12-Dodecanediol	25	-	108	340	102,126
PODF	1,18-Octadecanediol	22	-	97	-	126
PDASF	D-Isosorbide	9-25	173-194	-	350[d]	49b
PDAMF	D-Isomannide	14-20	187-191	-	-	127
PDAIF	D-Isoidide	5-21	140-196	-	275[d]	49b
PXIIF	Isoidide-2,5-dimethanol	30	94	250	376[a]; 411[c]	128
PBDMF	1,4-Benzenedimethanol	22	87	-	300[d]; 390[b]	49b
PEF-PPF	Ethylene glycol and Propanediol	14	80	215	398	49b
PEF-PBF	Butanediol, Ethylene Glycol	26-58	39-71	127-163	334-341	112
PBS-PEF	Ethylene Glycol, Succinic Acid	25-57	-	21-172	378-438	129
PBS-PBF	Butanediol, Succinic acid	58-61	-25 to 30	54-159	339-350[a]	113-114
PBA-PBF	Adipic acid, Butanediol	28-57	-44 to 36	30-171	-	115
PET-PEF	Ethylene Glycol, Terephthatic acid	6-16	62-75	198-220	385-408[b]	119
PEF-PLA	Ethylene Glycol, Lactic acid	68-130	25-79	119	232-324[a]	117-118
PBF-PBD	1,4-Butanediol, Diglycolic acid	-	6-35	106-164	366-388[b]	130

[a] Decomposition at 5% weight loss. [b] Maximum degradation temperature. [c] Decomposition temperature at the maximum weight-loss rate. [d] Onset of thermal decompositions.

Other FDCA Based Polymers

FDCA and its derivatives have been used to prepare other polymers or resins,[131] such as polyamides,[132] thermotropic polyesters,[133] photodegraded polyesters,[134] branched furanic polyester resins,[135] linear and cross-linked poly(ester amide),[64,136] epoxy resins[52] and poly(ester urethanes).[131b] For polyamides,[50,71,132a] Gandini *et al.* synthesized and characterized polyamides from FDCA and aromatic diamines.[71] These furanic-aromatic polyamides displayed a regular structure, high molecular weight and good thermal stability. Cureton *et al.* synthesized polyamides from FDCA and *p*-phenylenediamine by direct polycondensation and interfacial polymerization, respectively.[137] It was observed that interfacial polymerization was a more suitable synthesis method in terms of the obtained molecular weight and polydispersity index. As bio-based Kevlar analogs, FDCA based polyamides showed good chemical resistance in most organic solvents, as well as improved solubility. Moreover, these polyamides were fully amorphous polymers with a high T_g (> 180 ^oC) and satisfactory thermal stability (nearly 400 ^oC). The fully amorphous structure was unexpected, since the occurrence of crystallization in other furan polyamides has been observed using aliphatic diamines as the monomer.[126] Therefore, the use of aromatic diamine (*p*-phenylenediamine) might be the reason for the amorphous nature of the polymer due to its more rigid structure, preventing the formation of intermolecular hydrogen bonding. Zhu *et al.* have recently synthesized a series of aromatic furanic polyamides from FDCA and various aromatic diamines by direct polycondensation under optimized conditions. No T_m was observed from DSC analysis, indicating the amorphous structure of these polyamides. In addition, it was suggested that the thermal and mechanical properties of materials varied with different polymer structures.[138] A molecular dynamic simulation test was performed to further analyze FDCA based polyamides. The results for this test showed that compared to nylons, furan polyamides exhibited higher van der Waals cohesive energy densities. Moreover, furan polyamides maintained more rigid planar structures near furan rings. Therefore, FDCA based polyamides showed a higher T_g and comparable mechanical properties than those of nylons, although the overall intermolecular hydrogen bonding in furan polyamides was weaker than that in nylons.[132a] On the other hand, Rastogi *et al.* investigated the effect of the 2,5-furandicarboxamide moiety on the formation of hydrogen bonding in poly(ester amide)s. It was suggested that the relatively weak hydrogen bonding in furan polyamides was due to the presence of oxygen atom in FDCA which functioned as a hydrogen bonding acceptor, forming

the intramolecular hydrogen bonding with the amide hydrogens. Therefore, it prevented the formation of intermolecular hydrogen bonding.[136]

In summary, FDCA based polyesters (PEF and PBF) have been systematically investigated in terms of thermal, mechanical and barrier properties. The rigidity of furan rings was one of the key features to impart the comparable properties of furan based polymers as compared to petroleum-based analogues. However, challenges still exist to synthesize polymers with high molecular weights from FDCA in order to avoid the decarboxylation and color issues. Therefore, the development of an efficient catalyst system with relatively mild reaction condition seems to be necessary for the synthesis of FDCA based polymers. On the other hand, synthesis of copolymers containing FDCA provided opportunities to adjust the thermal and mechanical properties, as well as degradability. Therefore, research studies on the synthesis and characterization of copolymer from FDCA are still needed, particularly utilizing other renewable resources or monomers with extra functionality.

2.4.1.2 Polymers from BHF and Its Derivatives

BHF, a derivative of HMF, has shown potential as an interesting diol in the preparation of polyesters, polyurethanes and thermosetting polymers. Importantly, further Diels-Alder reaction on the furan ring imparted the possibility of preparing functional polymers. Yoshie *et al.* have reported BHF based polyesters with self-healing ability *via* a reversible Diels-Alder reaction between the furan and maleimide groups (**Scheme 2.2**).[139] The T_g of polyesters increased from 1.8 to 9.6 ^oC as the molar ratio of crosslinkers to linear polyesters increased from 1:10 to 1:2. Moreover, the mechanical properties of the polymers could be adjusted by controlling the amounts of crosslinkers. When the ratio of crosslinker to polyester was 1:2, the Young's modulus, ultimate strength and elongation at break of the resulting crosslinked polymers were around 1230 MPa, 19.2 MPa and 101 %, respectively.[39a] The choice of bis-maleimides crosslinkers was a key factor for designing these self-healing polymers. Bis-maleimides with flexible and long segments were beneficial to self-healing properties, while short and rigid crosslinkers reduced the efficiency of self-healing behavior.[139] Interestingly, polymer films with multi-shape memory features could be synthesized by changing the T_g of polymers as mentioned above.[140] BHF has also been exploited to prepare copolymers with 1,4-butanediol and succinic acid. A network was generated after crosslinking the copolymers by the Diels-Alder reaction.

The thermal and mechanical properties of the copolymers were highly associated with the monomer composition and the maleimide/furan ratio in the polymers.[141] Recently, a derivative of BHF was synthesized for the thiol-Michael addition reaction.[142] The use of dimethylphenylphosphine catalyst had several advantages including short reaction times, mild reaction temperature and high yield. As a result, a bio-based furan polymer with relatively high molecular weight (20000 g/mol) was synthesized within 15 mins. The synthesis of a reversible organogel further indicated that these polymers can be a starting point for engineering different materials using the Diels–Alder reaction.[142] On the other hand, Du Prez *et al.* prepared BHF based polyurethane foams with additional surface functionalities through the Diels-Alder reaction.[39b] More than 90 % of the furan groups reacted after 20 h with a nine-fold excess of N-methylmaleimide. The Retro-Diels-Alder reaction was performed by refluxing polyurethane foams in water at 100 ^{o}C for 24 h. However, the reversibility of the Diels-Alder reaction might limit the application of polyurethane foams at high temperature.[39b]

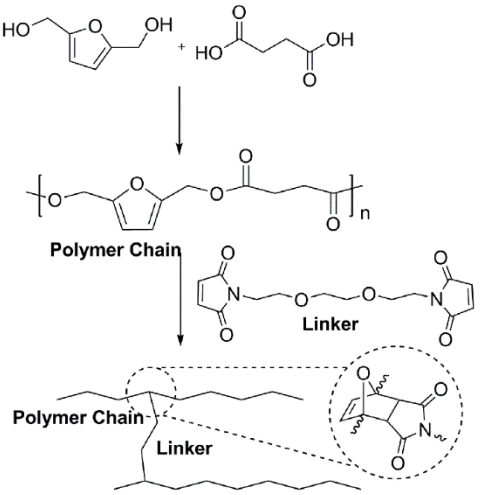

Scheme 2.2 Synthesis of self-healing polyesters

Recently, 2,5-bis[(oxiranylmethoxy)methyl]-furan (BOF) was synthesized as a renewable monomer for epoxy resin. The thermomechanical properties of the resins were evaluated in comparison to those of 2,5-bis[(2-oxiranylmethoxy)methyl]-benzene (BOB).[56a] BOF monomers were liquids of low viscosity. The T_g and storage modulus of BOF-based resins were of higher values than those of BOB-based resins. The rigidity of the furan rings, as well as enhanced hydrogen bonding between the hydroxyl groups generated during the curing process and the oxygen atoms in the furan rings, might have contributed to those results. Furthermore, additional

methylene units between the aromatic rings and the glycidyloxy groups in BOF and BOB monomers decreased the T_g of the resins due to lesser constraint of the aromatic rings.[56a] Recently, the same group of authors prepared fully renewable thermosetting polymers from BOF with 5,5'-methylenedifurfurylamine (DFDA) and 5,5'-ethylidenedifurfirylamine (CH_3DFDA) as amine curing agents. The thermosets showed a T_g value above 60 ^oC. The storage modulus value at room temperature was 3.5 GPa and the thermal stability was up to 272 ^oC (5 wt % loss) under N_2.[56b] More recently, the effects of the furan rings on the thermomechanical properties of BHF based epoxy resins were investigated by molecular simulation.[143] It was suggested that the high packing density from the strong polarity in BOF based resins, rather than enhanced hydrogen bonding mentioned above, reduced the mobility of the polymer chains.

2.4.1.3 Polymers from DFF

Despite growing interest in the preparation of DFF from either HMF or other natural resources,[144] examples of DFF based polymers are relatively rare.[54,145] A crystalline polymer resin was obtained *via* condensation of DFF with urea at 110 ^oC.[146] NMR analysis showed that one aldehyde group of DFF can condense with two urea molecules. The resins were insoluble in water and common organic solvents, but slightly soluble in DMSO and DMF at 45 ^oC. Swelling experiments in toluene showed that the degree of swelling was 12 % after equilibrium, indicating the presence of crosslinking. Schiff based polymers have also been synthesized by polymerization of DFF with aromatic or aliphatic diamines.[147] NMR and mass spectra analysis indicated that the reaction proceeded quickly to form imine bonds. A regular chain structure was confirmed through ^{13}C CP/MAS NMR. In addition, DFF-based porous organic frameworks (DPOF) were prepared by condensation of DFF with aromatic diamines.[145a] These polymers were insoluble in water and common organic solvents. TGA analysis revealed that the thermal stability was up to 300 ^oC under N_2. The geometry of the monomers significantly influenced the crystal and porous morphology of the polymers. Condensation of DFF with nonlinear diamines led to an amorphous structure, while the crystalline structure in DPOF formed using linear diamines. The porous properties of DPOF were analyzed by nitrogen adsorption/desorption, and the pore size distribution was calculated from the non-local density functional theory model. Both micropores and mesopores were present in DPOF. The rigidity and contortion of the molecular structure limited space-efficient packing of polymers in the solid state, leading to the

porous structure. In the case of DPOF prepared from DFF and m-phenylenediamine (DFP), specific surface area determined by the Brunauer-Emmett-Teller (BET) technique and pore volume were 830 m^2/g and 2.10 cm^3/g, respectively. The capacity of adsorption of CO_2 associated with gas storage was 77.0 mg/g.[145a]

2.5 Conclusions

Although a variety of furan based monomers are available, the efficient, simple and inexpensive production of these valuable monomers from renewable resources is desired. Continuous efforts to exploit novel derivatives from HMF are necessary in order to generate new polymers for broader applications, especially in combination with other polymerization methods, such as click, radical and photo polymerization.[148] On the other hand, the advantages of the furan rings in the polymers lie in their ability to improve the mechanical properties and thermal stability. Therefore, the introduction of furan rings into other bio-based polymers seems to be a promising route to adjust the properties of the polymers. Additionally, the incorporation of other functional monomers to synthesize copolymers or the preparation of composites provide the opportunity to tune the thermal and mechanical properties of materials from bio-based HMF and its derivatives.[149] Finally, enzymatic catalysis is worthy of investigation due to the mild reaction conditions, environmental friendliness and high tolerance toward functional groups.[50]

Connecting Statement 1

Chapter 2 described that HMF and its derivatives have been widely used to synthesize polymers and networks. However, current research work has been mainly focusing on the use of 2,5-FDCA to synthesize (co)polyesters. A variety of HMF derivative which can be potentially used to synthesize polymers have been neglected. Particularly, reactions which can occur on the furan rings can provide an opportunity to modify the properties of HMF derivative based polymers.

Chapter 3 investigated the catalyst efficiency and side reactions occurring during the thiol-Michael addition reaction. The catalyst was used to synthesize linear polymers using 2,5-FDA and 1,6-hexanedithiol. The structure of the synthesized polymers was evaluated by NMR and FTIR. The thermal properties of the polymers including thermal transitions and stability were preliminarily investigated using DSC and TGA. The occurrence of the DA reaction was evaluated by the synthesis of an organogel. This chapter is based on an article reproduced from *RSC advances* 2016, **6**, 83466 with permission from the Royal Society of Chemistry. The article was co-authored by Dr. Marie-Josée Dumont and Dr. Alice Cherestes.

Chapter 3: An Efficient Strategy for the Synthesis of 5 hydroxymethylfurfural Derivative Based Poly(β-thioether ester) *via* Thiol-Michael Addition Polymerization

3.1 Abstract

A derivative of 5-hydroxymethylfurfural was synthesized for the thiol-Michael addition reaction. The efficiency of catalysts (base and nucleophiles) and side reactions during the thiol-Michael addition were investigated. Dimethylphenylphosphine efficiently initiated the thiol-Michael addition polymerization for synthesizing bio-based furan polymers. The product poly (β-thioether ester) showed the potential to be functionalized.

3.2 Introduction

The production of polymers from petroleum-based chemicals has caused serious sustainability concerns, thereby stimulating the development of bio-based polymers.[150] 5-hydroxymethylfurfural (5-HMF) is a promising bio-based chemical which can be synthesized from several feedstocks having a rich hexose content.[151] The functional groups of 5-HMF are available for derivatization[152] which renders this platform chemical suitable for the synthesis of fine chemicals, biofuel precursors and monomers used in the synthesis of polymers.[153] Techniques which have been used to synthesize polymers from 5-HMF derivatives include esterification or transesterification, enzymatic polymerization, ring opening polymerization and free radical polymerization.[153d,154] However, these polymerization techniques are often performed under rigorous conditions where high temperature, vacuum and long reaction times are generally needed. Thus, new strategies requiring milder reaction conditions are desired.

The thiol-Michael addition reaction offers high conversion, mild reaction conditions and rapid reaction rate.[155] The applications of thiol-Michael addition reaction range from small molecule synthesis, surface functionalization of materials and polymer modification, to networks formation.[156] However, examples of the synthesis of linear polymers are few,[157] especially involving the use of bio-based monomers. This could be due to side reactions occurring when phosphines and amine catalysts are used.[157g, 158] The presence of side-reactions is an issue when designing polymers through the step-growth polymerization technique since they can prevent the

formation of the desired structure. The side-reactions also influence the molecular weight of linear polymers. Therefore, the elucidation of these side reactions is of importance in order to minimize their occurrence. This chapter first reports on the efficiency of base and nucleophilic catalysts in addition to the potential side reactions occurring by the use of these catalysts. The second section of this chapter focuses on the synthesis and characterization of bio-based furan polymers synthesized by the thiol-Michael addition polymerization. In addition, the incorporation of furan rings through 5-HMF derived monomers in the polymer chain enables the Diels-Alder reaction to occur.[159] It can be used to tune the thermal and mechanical properties of materials. By this reaction, an organogel was synthesized in order to study the feasibility of the Diels-Alder reaction on furan rings.

3.3 Experimental Sections

3.3.1 Materials

5-Hydroxymethylfurfural (HMF, ≥99%), furfural alcohol (≥98%), sodium borohydride powder (≥98%), tetrahydrofuran (THF, anhydrous, ≥99.9%, inhibitor free, and further dried under molecular sieves), triethylamine (TEA, ≥99.5%), acryloyl chloride (97%, contains < 210 ppm MEHQ as stabilizer), 1,8-diazabicycloundec-7-ene (DBU, 98%), dichloromethane (anhydrous, ≥99.8%), 4-dimethylaminopyridine (DMAP, ≥99%), dimethylphenylphosphine (DMPP, ≥99%), 1,6-hexanedithiol (97%), 1-propanethiol (99%), hexylamine (99%), DMSO-d_6 (99.9 atom % D), chloroform-d (99.8 atom % D), TLC plates and silica gel were purchased from Sigma-Aldrich. All reagents were used as received without further purification.

3.3.2 Synthesis of furfural acrylate

Furfural acrylate was prepared by reacting the hydroxyl groups of furfural alcohol (1 eq) with acryloyl chloride (1.5 eq), using triethylamine (1.5 eq) to trap the generated hydrochloric acid.[1] The reaction mixture was stirred for 12 h at room temperature. After removing triethylamine hydrochloride, the solution was concentrated by rotary evaporation. Furfural acrylate was further purified on a silica gel column (ethyl acetate/hexane) to obtain the product. A yield of 80 % was obtained.

^{1}H NMR (400 MHz, $CDCl_3$) δ 7.41 (dd, J = 1.8, 0.8 Hz, 1H), 6.46 – 6.31 (m, 3H), 6.12 (dd, J = 17.3, 10.4 Hz, 1H), 5.82 (dd, J = 10.4, 1.4 Hz, 1H), 5.13 (s, 2H).

^{13}C NMR (101 MHz, $CDCl_3$) δ 165.69, 149.39, 143.26, 131.25, 128.04, 110.71, 110.55, 58.06.

GC-MS (EI): m/z (%) = 152 ([M]$^+$, 44), 134 (5), 123 (3), 107 (35), 97 (11), 81 (100), 55 (47), 41 (6).

3.3.3 General conditions for model reaction

Furfural acrylate (1 eq) and 1-propanethiol (1.1 eq) were dissolved in a THF solution under an air atmosphere. The catalyst (2 mol %) was then added to the solution to initiate the thiol-Michael addition reaction. The conversion and yields of Michael adduct were analyzed by GC-MS.

^{1}H NMR (400 MHz, $CDCl_3$) δ 7.40 (dd, J = 1.8, 0.7 Hz, 1H), 6.45 – 6.26 (m, 2H), 5.07 (s, 2H), 2.79 – 2.71 (m, 2H), 2.64 – 2.57 (m, 2H), 2.50 – 2.44 (m, 2H), 1.63 – 1.53 (m, 2H), 0.96 (t, J = 7.3 Hz, 3H).

^{13}C NMR (101 MHz, $CDCl_3$) δ 171.59, 149.33, 143.26, 110.70, 110.56, 58.18, 34.85, 34.16, 26.79, 22.84, 13.40.

GC-MS (EI): m/z (%) = 228 ([M]+, 3), 152 (19), 129 (14), 105 (5), 103 (9), 89 (8), 81 (100), 61 (7), 53 (2).

3.3.4 Synthesis of 2,5-bis(hydroxymethyl)furan

In a 100 mL round bottom flask, HMF (1 eq) was dissolved in 50 mL of distilled water and kept at 0 ^{o}C in an ice bath. Sodium borohydride (1.5 eq) was slowly added into the flask (within 30 mins).[2] Then, the solution was allowed to react at room temperature, and the reaction was monitored by TLC. After complete reduction, the reaction mixture was neutralized with HCl (2N), and extracted with ethyl acetate (3 x 100 mL). The organic layer was collected and dried with Na_2SO_4. Ethyl acetate was removed by rotary evaporation, and purified by silica gel column chromatography (80% ethyl acetate/hexane) to yield BHF as off-white crystals (96 % yield).

^{1}H NMR (500 MHz, DMSO) δ 6.18 (s, 1H), 5.15 (t, J = 5.7 Hz, 1H), 4.35 (d, J = 5.7 Hz, 2H).

^{13}C NMR (101 MHz, DMSO) δ 154.65, 107.43, 55.73.

GC-MS (EI): m/z (%) = 128 ([M]$^+$, 51), 111 (16), 109 (17), 97 (100), 83 (9), 81 (10), 69 (32), 55 (18), 53 (17), 41 (37).

3.3.5 Synthesis of 2,5-Furan diacrylate

2,5-furan diacrylate (2,5-FDA) was prepared through the reaction of hydroxyl groups of BHF with acryloyl chloride.[152] Triethylamine (2.5 eq) was added to a solution of BHF (1 eq) in THF (100 mL) at 0 ^{o}C under a nitrogen atmosphere. The mixture was stirred at 0 ^{o}C for 15 mins. Acryloyl chloride (2.5 eq) was slowly added to the solution, and the reaction mixture was stirred

for 12 h at room temperature. After the reaction, the solution was filtered to remove triethylamine hydrochloride. The filtrate was concentrated by rotary evaporation. The residue was dissolved in ethyl acetate, and then washed with brine, dried with Na_2SO_4, and concentrated under vacuum to give a yellow oil. The product was further purified on a silica gel column (0-50 % ethyl acetate/hexane) to yield 2,5-furan diacrylate (56 % yield).

^{1}H NMR (400 MHz, $CDCl_3$) δ 6.41 (dd, J = 17.3, 1.4 Hz, 1H), 6.38 (s, 1H), 6.11 (dd, J = 17.3, 10.4 Hz, 1H), 5.82 (dd, J = 10.4, 1.4 Hz, 1H), 5.10 (s, 2H).

^{13}C NMR (101 MHz, $CDCl_3$) δ 166.15, 150.54, 131.93, 128.41, 112.15, 58.56.

GC-MS (EI): m/z (%) = 236 ($[M]^+$, 0.3), 164 (24), 125 (0.8), 123 (1.1), 109 (4), 94 (6), 81 (5), 79 (8), 65 (3), 55 (100).

3.3.6 Synthesis of poly(β-thioether ester)

In a typical procedure, 2,5-FDA (1 eq) was dissolved in THF (0.6 M). The solution was purged with nitrogen for 30 mins to remove oxygen. Thereafter 1,6-hexanedithiol (1 eq) was added *via* a syringe. The reaction mixture was cooled in an ice-bath. Then DMPP (0.005 eq) was slowly added to the mixture to start the polymerization process. The polymerization was conducted at room temperature for 15 mins. Poly (β-thioether ester) was precipitated in cold hexane and recovered by filtration. Finally, the polymer was kept in a vacuum oven at room temperature overnight to obtain a white powder (95 % yield).

^{1}H NMR (400 MHz, $CDCl_3$) δ 6.38 (s, 1H), 5.06 (s, 2H), 2.80 – 2.74 (m, 2H), 2.66 – 2.59 (m, 2H), 2.53 – 2.48 (m, 2H), 1.63 – 1.51 (m, 2H), 1.43 – 1.33 (m, 2H).

^{13}C NMR (101 MHz, $CDCl_3$) δ 171.99, 150.49, 112.13, 58.67, 35.22, 32.54, 29.83, 28.85, 27.31.

3.3.7 Characterization

^{1}H and ^{13}C NMR spectra were obtained on a Bruker AV 400 or Varian/Agilent 500 using deuterated DMSO and $CDCl_3$ as solvents. The chemical shifts are referenced to the solvent residual signals at 2.50 ppm for deuterated DMSO and 7.26 ppm for $CDCl_3$.

The FT-IR spectrometers were recorded on a Thermo Scientific Nicolet iS5 FT-IR spectrometer (Thermo, Madison, WI, USA) using an attenuated total reflectance (ATR) diamond crystal. The spectra were recorded at 64 scans and 8 cm^{-1} resolution in the 4000–400 cm^{-1} range.

The molecular weight distribution was determined using gel permeation chromatography (GPC, Water Breeze) with THF as the mobile phase running at a flow rate of 0.3 mL/min. The GPC was equipped with a guard column, 3 Waters Styragel HR columns, and a differential

refractive index detector (RI 2410). The molecular weights were calibrated using linear narrow polystyrene standards. The molecular weight of the synthesized chemicals was analyzed by gas chromatography coupled with a mass spectrometer (Agilent Technologies, HP 6890N (G1530N), USA). The GC/MS was equipped with a HP-5MS column (30 m × 250 μm × 0.25 μm nominal, Agilent Technologies, 350 °C maximum), and helium gas was used as the carrier gas.[153]

The thermal transitions of poly (β-thioether ester) were determined by DSC (Q100, TA Instruments, Inc., New Castle, DE). The samples were compressed in hermetic aluminum pans and analyzed in duplicate. The heating rate was 10 ºC/min, and the cooling rate was 5 ºC/min. The thermogravimetric analysis (TGA, Q50, TA Instrument, Inc., New Castle, DE) was used to investigate the thermal stability of polymers (powder). The flow rate of N2 was 60 mL/min, and the samples were heated from 20 ºC to 800 ºC.[154]

3.4 Results and Discussions

The effects of three types of catalysts on the reaction rates, conversion, and potential side reactions were investigated using furfural acrylate and 1-propanethiol as the model substrates (**Scheme 3.1**).

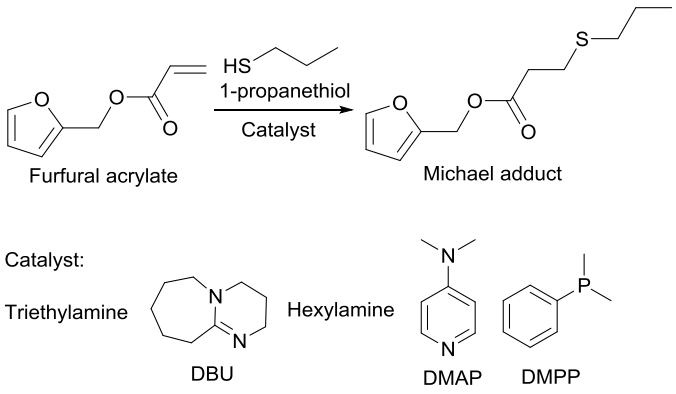

Scheme 3.1 Addition of 1-propanethiol (1.1 eq.) to furfural acrylate (1 eq.) yielding the Michael adduct

For the reaction, base catalysts (triethylamine (TEA) and 1,8-diazabicycloundec-7-ene (DBU)), nitrogen-centered nucleophiles (hexylamine and 4-dimethylamino-pyridine (DMAP)) and a phosphine-centered catalyst (dimethylphenyl-phosphine (DMPP)) were selected (**Scheme 3.1 and Table 3.1**). The structure and molecular weights of furfural acrylate and Michael adduct were confirmed by ^{1}H, ^{13}C NMR and mass spectrometry, respectively (**Figure 3.1 and Figure 3.2**).

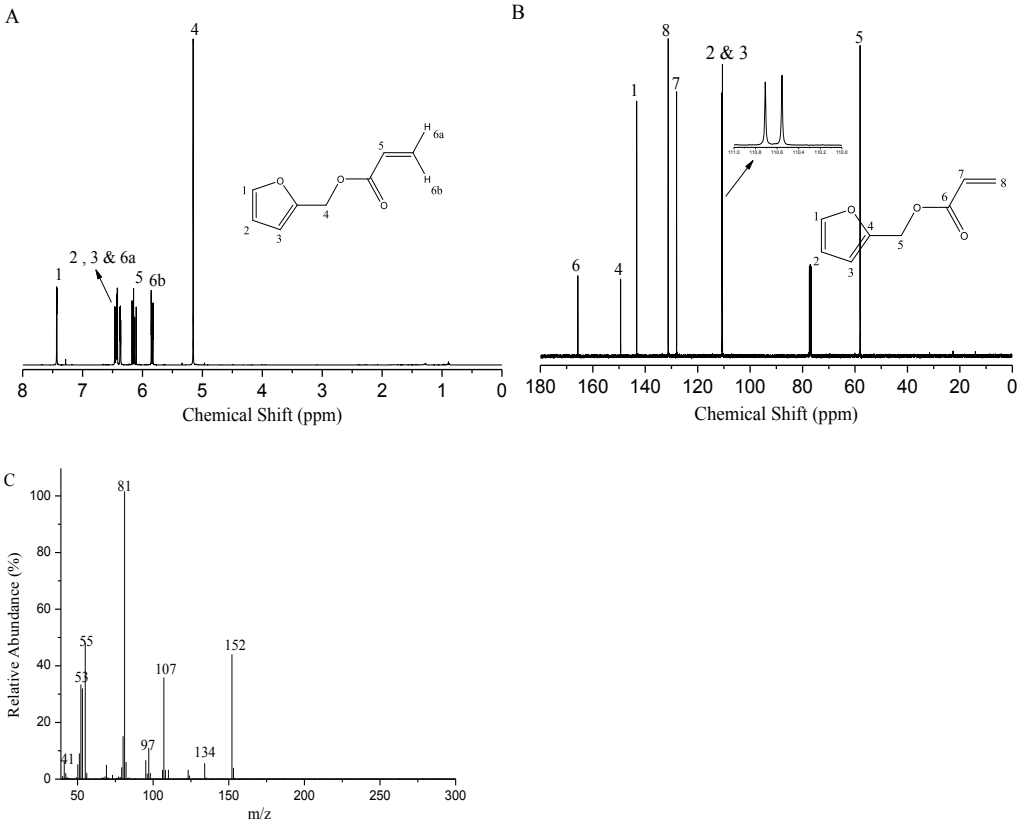

Figure 3.1 ^{1}H (A), ^{13}C NMR (B) and mass spectrometry (C) of furfural acrylate.

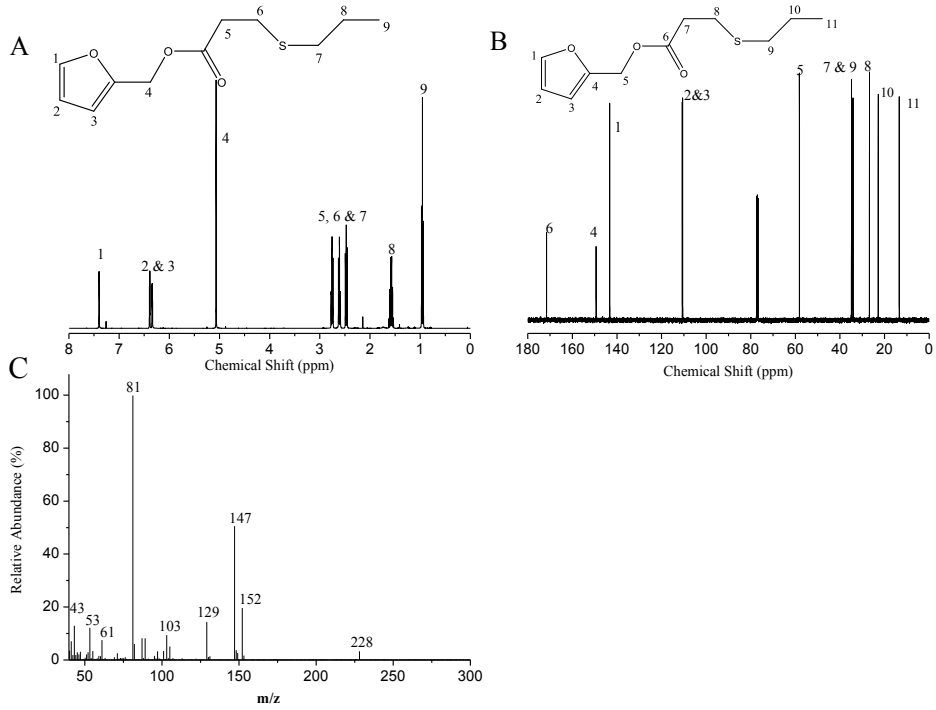

Figure 3.2 ^{1}H (A) and ^{13}C NMR (B) and mass spectrometry (C) of thiol-Michael addition product.

Table 3.1 Thiol-Michael addition catalysed by base, nitrogen-centered and phosphine-centered nucleophiles (2 mol % unless otherwise indicated)

Entry	Catalyst	pK_a[a]	Reaction Time (h)	Conversion (%)
1	TEA	10.8	8	0
2	DBU	11.6	15 mins	>99
3	Hexylamine	10.6	8	>99
4	Hexylamine	10.6	4[b]	>99
5	Hexylamine	10.6	24[c]	67
6	DMAP	9.7	5	44
7	DMPP[d]	6.49	15 mins	>99

General conditions: Furfural acrylate (0.6 mmol), 1-propanethiol (0.66 mmol) and tetrahydrofuran (1 mL) at the room temperature under an air atmosphere. [a] Refers to the *p*Ka of the corresponding conjugates acid in H_2O at 20°C and *p*Ka of 1-propanethiol was 10.2. [b] Hexylamine catalyst loading was 10 mol %. [c] Chloroform was used as the solvent. [d] DMPP catalyst loading was 0.5 mol %.

Table 3.1 shows the general reaction conditions and the effects of catalyst types on the thiol-Michael addition reaction. Typically, the base catalysed thiol-Michael reaction pathway involves the deprotonation of the thiol group to form a thiolate anion, as well as a conjugated acid.[155] Then, the thiolate anion attacks the β-position of α,β-unsaturated carbonyl to yield a carbanion (strong base). The last step involves the abstraction of a proton from a conjugated acid by the carbanion to generate thioether as the product. For TEA, there was no conversion towards the desired Michael adduct (**Table 3.1**, entry 1). This was due to the similar *pKa* of the catalyst and 1-propanethiol. Thus, TEA failed to abstract a proton from 1-propanethiol. DBU, a non-nucleophile strong base, achieved over 99 % conversion after 15 mins, and the yield of the Michael adduct was > 99 % as determined by gas chromatography (GC) (entry 2). These results indicate that the choice of a suitable base catalyst can efficiently initiate the thiol-Michael addition of 1-propanethiol and furfural acrylate. However, it was noticed in previous studies that DBU functioned as a nucleophile as well.[11] Therefore, DBU catalysed thiol-Michael addition is complex as it may involve a basic-nucleophilic hybrid mechanism.[161] The potential mechanism of nucleophile-catalysed thiol-Michael addition is illustrated in **Scheme 3.2A**.[162]

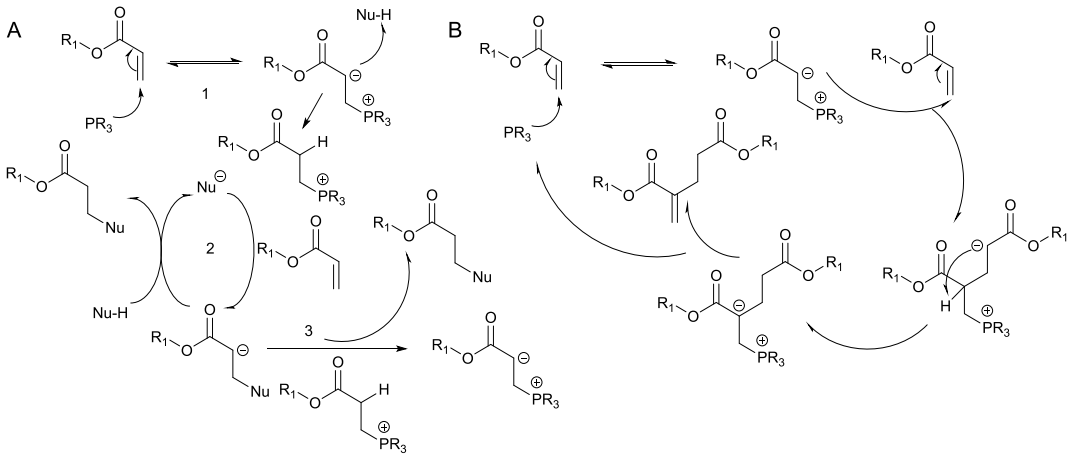

Scheme 3.2 (A) Nucleophile-catalysed mechanism for the thiol-Michael addition reaction, (B) Potential side reaction using DMPP as the catalyst (R_1=C_5H_5O)

The nucleophilic attack of the phosphine- or nitrogen-centered catalyst on the vinyl group generates the intermediate zwitterion. It can then deprotonate the thiol group to yield a thiolate anion. The formed thiolate anion further reacts with the vinyl group to generate the Michael adduct. Finally, the catalyst is recovered. Hexylamine serves as a good nucleophile catalyst for the thiol-Michael addition reaction.[163] The conversion of furfural acrylate was > 99 % when using 2 mol % hexylamine catalyst and a reaction time of 8 h (entry 3) or when using 10 mol % catalyst and a reaction time of 4 h (entry 4). Chan *et al.* reported that the conversion of hexylamine catalysed reaction (0.096 mol %) of hexanethiol and hexyl acrylate was over 99 % after 3 h at room temperature.[161a] Based on Li *et al.*, the choice of the solvent allows the stabilization of the nucleophilic ion.[158] There was 67 % conversion of furfural acrylate after 24 h in chloroform (2 mol %, entry 5). It was suggested that the polarity of the solvent strongly impacted the stabilization of thiolate anions.[158] On the other hand, a by-product was detected by GC analysis when hexylamine was used as the catalyst. As hexylamine concentration increased from 2 mol % to 10 mol %, the yield of the Michael adducts decreased from 98 % to 92 %. The molar mass of the by-product was 253 g/mol, and was identified as the product of Aza-Michael addition between furfural acrylate and hexylamine (**Figure 3.3**).

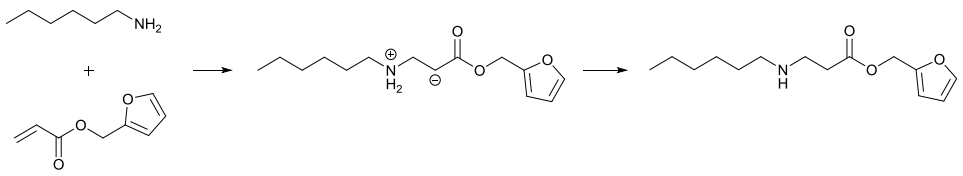

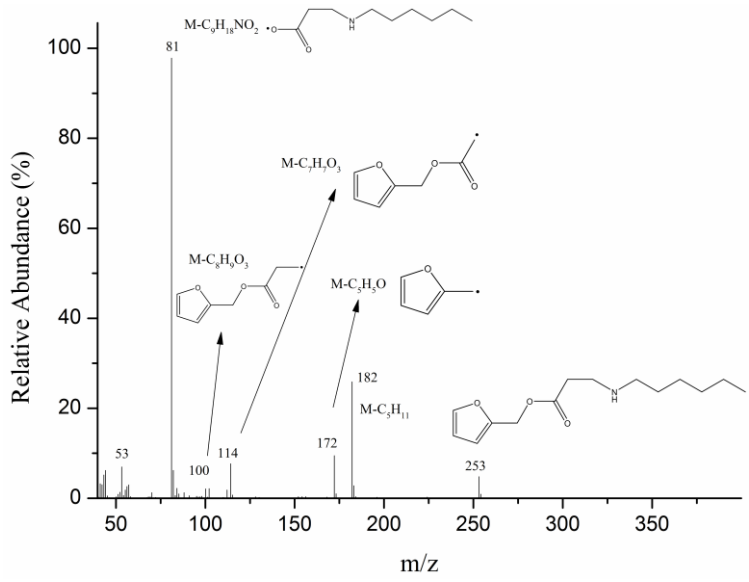

Figure 3.3 Aza-Michael addition and mass spectrometry of side reaction product in hexylamine catalyzed thiol-Michael addition reaction (GC-MS (EI): m/z (%) = 253 ([M]+, 5), 182 (26), 172 (9), 114 (8), 102 (2), 81 (100), 61 (7), 53 (7), 44 (6)).

After the nucleophilic attack of the amine on the vinyl group generating a zwitterion, the proton transfer may have occurred to form the Aza-Michael adduct. Li *et al.* also observed that primary amines were able to react with the vinyl groups, generating stable species.[158] Therefore, the results suggest that the use of hexylamine in a catalytic amount can minimize the side reaction in the thiol-Michael addition reaction, but may compromise the reaction rate. DMAP is another nitrogen-centered nucleophile that showed a relatively slow catalytic activity, as the conversion was 44 % after 5 h reaction (entry 6). Both nucleophilicity and Lewis basicity of DMAP towards *sp*2 carbon centres are weaker than those of DBU,[160] which explains the slow reaction rate. Phosphine catalysts are known to be very reactive for the thiol-Michael addition reaction.[164] Hence, DMPP was investigated. Full conversion towards the expected Michael adduct was observed after 15 mins (entry 7), and the yield of Michael adduct was over 99 %. Although the phosphine catalyst has been reported to give rise to a side reaction in the thiol-Michael addition reaction,[158] the faster reaction rate and the use of a catalytic amount of DMPP (0.5 mol %) are responsible for the quantitative yield in this study. Additionally, in order to exploit the potential side reaction between DMPP and the activated vinyl groups, DMPP (0.1 eq) was mixed with furfural acrylate (1 eq) in THF at room temperature for 6 h. Phosphine catalysed dimerization of furfural acrylate was the main product detected by GC analysis (**Scheme 3.2B**

and **Figure 3.4**). The reaction proceeded slowly in comparison to the thiol-Michael addition reaction. Around 20 % of furfural acrylate was converted after 6h. Similarly, phosphine catalysed head-to-tail dimerization of methyl acrylate has been documented in other studies.[165] In addition, furfural alcohol as a minor product was also observed by GC analysis. The possible pathway is shown in **Scheme 3.3**.

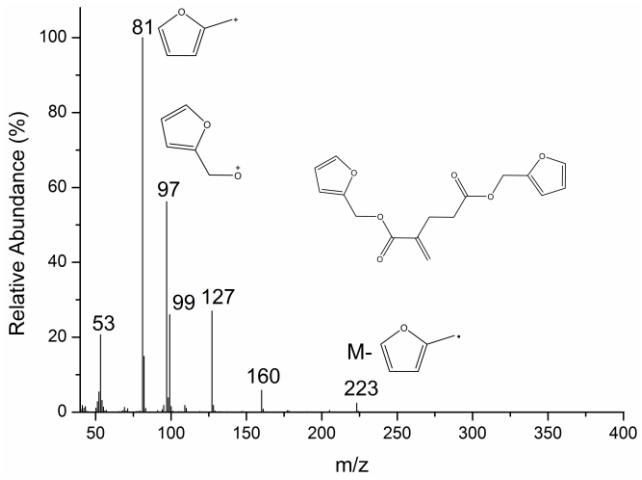

Figure 3.4 Mass spectrometry of phosphine catalyzed reaction of furfural acrylate (GC-MS (EI): m/z (%) = 304 ([M]+, 0.007), 223 (3), 160 (6), 127 (27), 99 (26), 97 (56), 81 (100), 53 (21), 41 (2)).

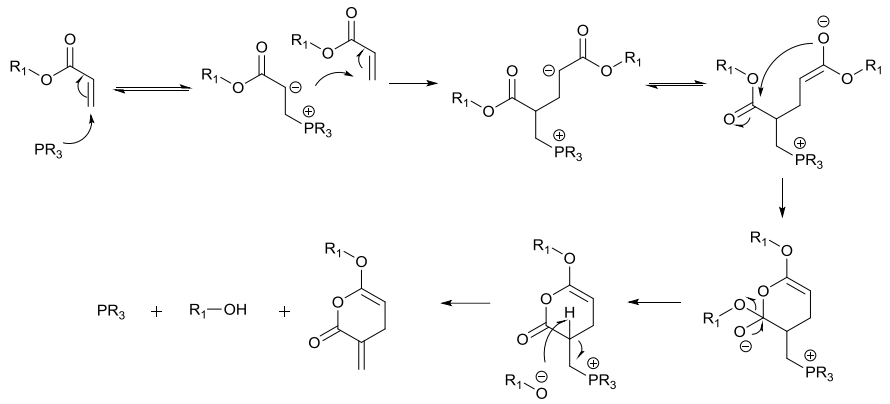

Scheme 3.3 Possible pathway to generate furfural alcohol during phosphine-catalyzed dimerization of furfural acrylate (R_1=C_5H_5O)

Besides the observations mentioned above, the formation of disulfide was observed in the DBU and DMPP catalysed thiol-Michael addition reaction (**Figure 3.5A**). Since the thiol-Michael addition reaction occurred under an air atmosphere, the formation of disulfide might be the result of a base catalysed oxidation of thiols.[166] Therefore, it indicates that the reaction should

be performed under an inert atmosphere. Otherwise, it can influence the structure of polymers synthesized by the thiol-Michael addition polymerization, particularly when the thiol groups are present in excess. In addition, DBU showed significantly higher reactivity toward the formation of disulfide than DMPP under same conditions (**Figure 3.5B**). The presence of disulfide using DMPP is unexpected.[167] DMPP can eliminate the disulfide *via* either preventing the aerial oxidation process or by acting as a reducing agent.[156b, 168] However, the reaction between the disulfide and phosphine catalyst has also been suggested to be a reversible disulfide metathesis process.[169] In summary, these results suggest that DBU and DMPP are efficient catalysts to initiate the thiol-Michael addition reaction. Furthermore, using catalytic amount of DMPP allows the reaction to finish over a short period of time without the occurrence of side reactions. In this study, DMPP was selected to initiate the thiol-Michael addition polymerization of 2,5-furan diacrylate (2,5-FDA) and 1,6-hexanedithiol.

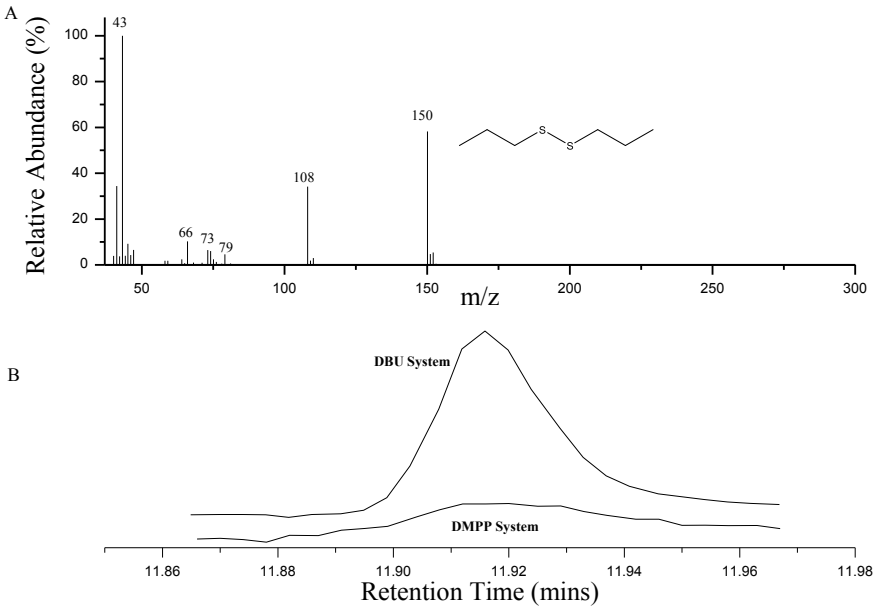

Figure 3.5 (A) Mass spectrometry of disulfide, (B) GC of disulfide in DBU and DMPP catalyzed system

The synthesis of 2,5-FDA from HMF was performed *via* two steps (**Scheme 3.4**). For the first step, an aldehyde group from HMF was efficiently reduced to the hydroxyl group using sodium borohydride (5g, 96 %) to yield BHF (**Figure 3.6**). Water was successfully used as solvent for the reduction reaction under mild conditions,[170] although organic solvents such as methanol, ethanol and THF have been reported in the literature.[158, 171] For the second step, the hydroxyl

groups reacted with acryloyl chloride to generate acrylate groups (2g, 56 %). The structure of 2,5-FDA determined *via* ^{1}H, ^{13}C and HSQC NMR are presented (**Figure 3.7**).

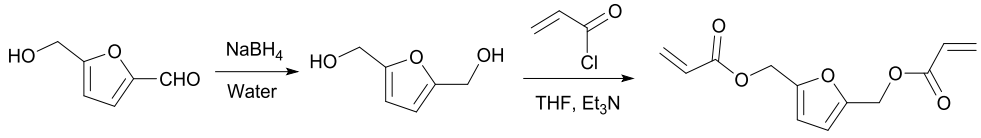

Scheme 3.4 Preparation of 2,5-FDA from HMF *via* two steps

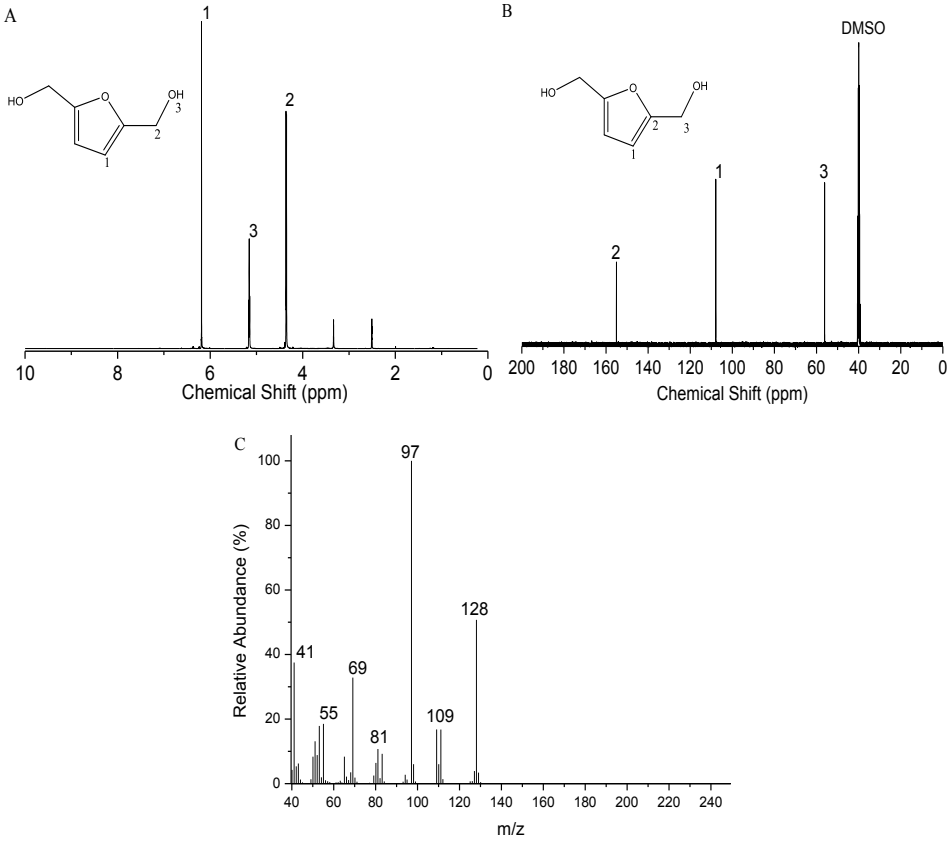

Figure 3.6 ^{1}H NMR (A), ^{13}C NMR (B) and mass spectrometry (C) obtained from BHF

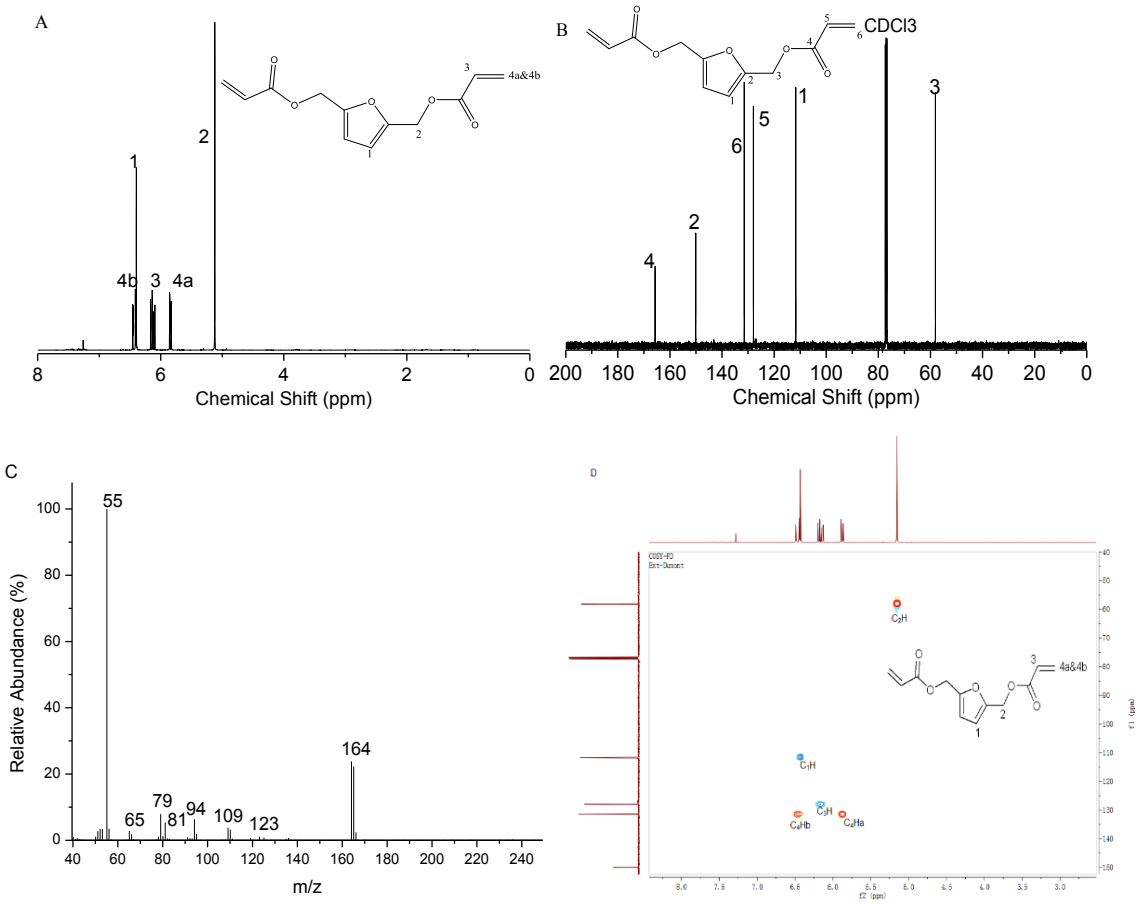

Figure 3.7 ^{1}H NMR (A), ^{13}C NMR (B), mass spectrometry (C) and HSQC (D) of 2,5-FDA

The thiol-Michael addition polymerization of 2,5-FDA and 1,6-hexanethiol (1:1) was initiated *via* DMPP (0.5 mol %) in THF at room temperature under N_2 atmosphere. The polymerization process was monitored by ^{1}H NMR. As expected from the model reaction, the thiol-Michael addition polymerization proceeded quickly as the signals for acrylate groups disappeared within 15 mins (from δ = 6.0 to 5.5 ppm, **Figure 3.8**), and new signals appeared from δ = 3.0 to 2.0 ppm.

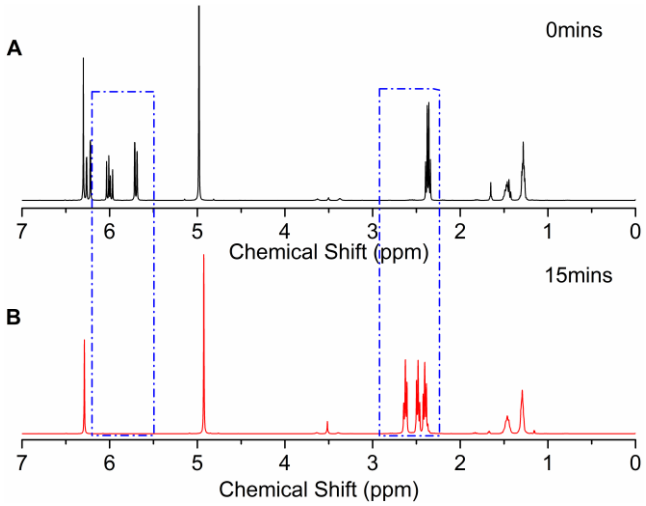

Figure 3.8 ^{1}H NMR spectrum of step-growth polymerization of 2,5-furan diacrylate and 1,6-hexanethiol in THF. (A) 0 mins, (B) 15 mins.

The synthesized polymer (1 g, 95 %) was soluble in common organic solvents, such as THF, chloroform and DMSO, but not soluble in hexane, water or methanol. The molecular weight determined by GPC showed that the number average molecular weight ($\bar{M}_n$) of poly (β-thioether ester) was 20000 g/mol after a 15 mins polymerization reaction (polystyrene as a standard). According to the Carothers equation, the molecular weight of linear polymer can be controlled by introducing one monomer in excess.[172] Moreover, the ends of the polymer chain are capped with the monomer in excess, which provides sites for further functionalization.[157a] Therefore, the polymerization process was performed with different monomer concentrations. As expected, ($\bar{M}_n$) of poly (β-thioether ester) decreased when the stoichiometric ratio of monomers was not equal to one (**Table 3.2 and Figure 3.9**). When the monomers containing acrylate groups were in excess, the molecular weight of polymers decreased more significantly, as compared to when thiol groups were in excess. The results of ATR-FTIR, ^{1}H, ^{13}C and HSQC NMR confirmed the expected structure of poly (β-thioether ester) (**Figure 3.10**).

Table 3.2 GPC Results of poly (β-thioether ester) prepared *via* different stoichiometric conditions

Acrylate:SH	M_n (g/mol)	*PDI*
1.2:1	2600	1.7
1.1:1	9400	1.6
1:1	20000	2.0
1:1.1	12000	1.6
1:1.2	6100	1.8

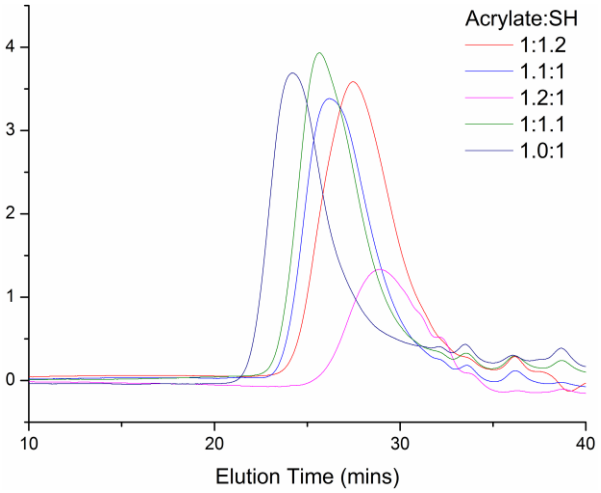

Figure 3.9 GPC Traces of poly (β-thioether ester) synthesized under different stoichiometric conditions

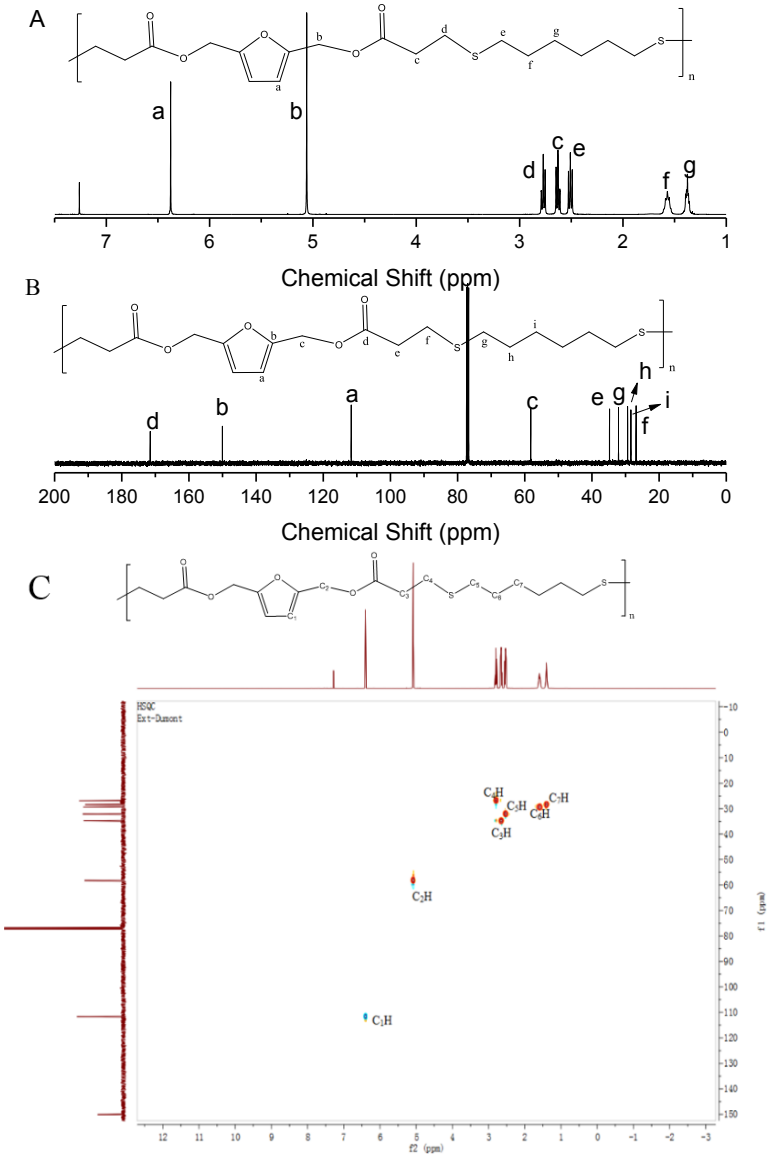

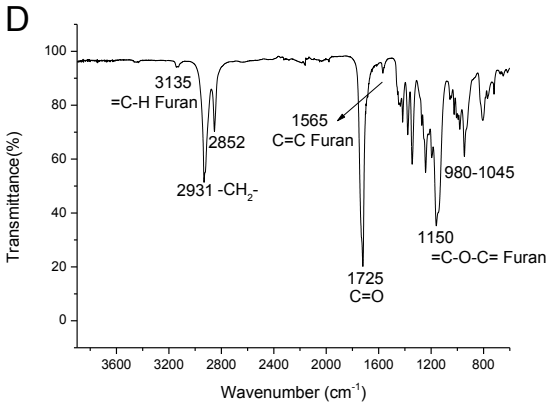

Figure 3.10 ^{1}H NMR (A), ^{13}C NMR (B), HSQC (C) of poly (β-thioether ester) and (D) ATR-FTIR spectra of poly (β-thioether ester)

The thermal transitions of poly (β-thioether ester) were studied by DSC (**Figure 3.11A**). The glass transition temperature (T_g) was -36.9 ºC as determined in the second heating curve. The thermal stability of poly (β-thioether ester) was investigated using TGA under a nitrogen atmosphere (**Figure 3.11B**). The decomposition temperature of the polymer at 5 % weight loss ($T_{5\%}$) was 236 ºC. The maximum degradation rates were observed at 249.1 ºC and 284.5 ºC. The degradation observed at 249.1 ºC was most probably due to the weaker C-S bonds present in the polymer chain.[173]

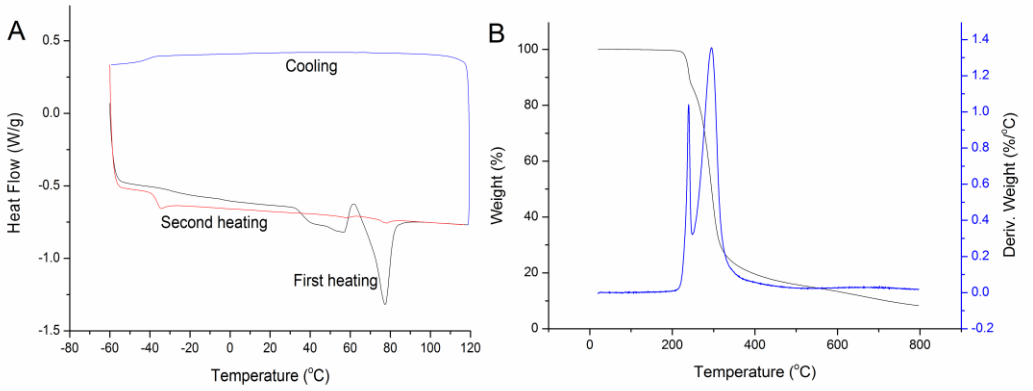

Figure 3.11 DSC curves (A) of poly (β-thioether ester) measured from -60 ºC to 120 ºC at a heating rate of 10 ºC/min, cooling rate of 5 ºC/min; (B) TGA analysis under a nitrogen atmosphere.

An organogel was synthesized in order to observe the Diels-Alder reaction between the furans and maleimides, as shown in **Figure 3.12** and **Scheme 3.5**. Poly (β-thioether ester) was dissolved in chloroform followed by the addition of a bismaleimide cross-linker. The ratio of furan to maleimide was set at 1:1. The polymer solution was gently stirred and transitioned to a gel after

48 h. The material could return to its original form after heating at 140 ºC for 60 mins. The sol-gel process was successfully repeated three times.

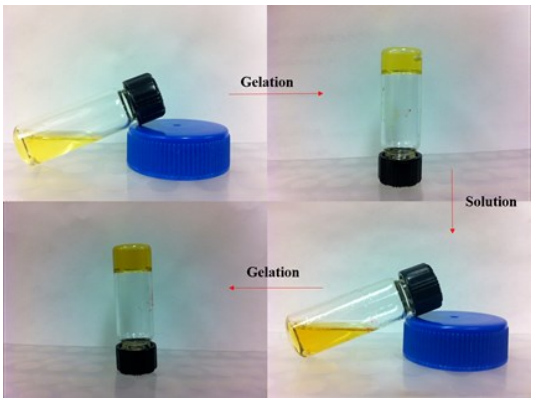

Figure 3.12 Reversible process of gelation-solution.

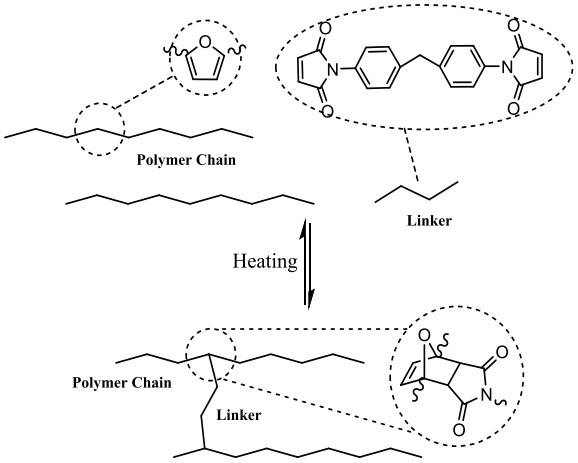

Scheme 3.5 The Diels-Alder equilibrium between furans and maleimides.

3.4 Conclusions

In summary, it was demonstrated that three types of catalyst (base, primary amine and phosphine) were able to initiate the thiol-Michael addition reaction between furfural acrylate and 1-propanethiol. However, there were several side reactions for these catalysts, including the Aza-Michael addition reaction, the formation of disulfide, and the dimerization of furfural acrylate. The use of hexylamine in a catalytic amount could minimize the Aza-Michael addition reaction, but resulted in longer reaction times. The formation of disulfide was eliminated under an inert atmosphere. The dimerization of furfural acrylate was avoidable when using a catalytic amount of DMPP to initiate thiol-Michael addition reaction. As a result, DMPP efficiently catalysed the thiol-Michael addition polymerization to synthesize poly (β-thioether ester) from 5-HMF

derivatives. The use of DMPP had several advantages including short reaction times, mild reaction temperature and high yield. Furthermore, the synthesis of a reversible organogel indicated that these polymers can be a starting point for engineering different materials properties using the Diels-Alder reaction.

Connecting Statement 2

The work in Chapter 3 investigated the catalyst efficiency and side reaction during the thiol-Michael addition reaction. DMPP proved to be an excellent catalyst to initiate the thiol-Michael addition between 2,5-FDA and 1,6-henxanedithiol. The thermal properties of the polymers were preliminarily investigated using DSC and TGA. Multiple melting peaks and two maximum degradation peaks were observed. An organogel was also formed.

Given the high efficiency of the DMPP catalyst, the incorporation of other dithiol monomers to synthesize (co)polymers was investigated. The obtained linear polymer with hydroxyl groups as side groups was evaluated as a hot melt adhesive on wood substrates. Furthermore, the kinetics of DA reaction between furan rings and maleimide was investigated to finely tune the thermal and mechanical properties of linear polymers. NMR was used to confirm the reversibility of the reaction. In addition, multiple melting peaks and two maximum degradation peaks of polymers synthesized from 2,5-FDA and 1,6-hexandithiol were elucidated *via* several techniques. Finally, a thermoplastic elastomer was prepared by the thiol-Michael addition reaction to increase the potential applications of HMF derivative based materials.

All the mentioned points were investigated in Chapter 4. This chapter is based on an article reproduced from *Polymer chemistry*, 2018, DOI: 10.1039/C7PY02052J with permission from the Royal Society of Chemistry.

Chapter 4: Synthesis, Characterization and Potential Applications of 5-Hydroxymethylfurfural Derivative Based Poly (β-thioether ester) Synthesized *via* Thiol-Michael Addition Polymerization

4.1 Abstract

Dimethylphenylphosphine was used to efficiently initiate the thiol-Michael addition polymerization to yield 5-hydroxymethylfurfural (HMF) derivative based poly(β-thioether esters) with relatively high molecular weights (over 10,000 g/mol) under mild conditions. The synthesized linear polymer with hydroxyl groups as side groups could be used as hot melt adhesives. Tests on wood substrates showed an adhesive strength of 1.5 MPa. Additionally, copolymers with various compositions were obtained by adding different ratios of 1,6-hexanedithiol to 1,4-benzenedithiol. ^{1}H NMR analysis revealed that the ratios of these two dithiol monomers present in the copolymers matched well the theoretical ratios. The reversibility of the Diels-Alder reaction between the furan rings and the maleimide groups allowed the poly(β-thioether esters) to be dynamically crosslinked. As the weight ratio of crosslinkers to polymers increased from 1:10 to 1:2, the storage modulus at room temperature was significantly enhanced from 1.5 MPa to 1691 MPa. Additionally, one pot thiol-Michael polymerization to synthesize HMF derivative based thermoplastics elastomers (TPEs) was investigated. The polymerization reaction was completed within 40 mins at room temperature. The maximum elongation at break of TPEs could reach > 450 %. The use of the Diels-Alder reaction to crosslink TPEs provided an efficient approach to improve their mechanical properties. The HMF derivative based polymers synthesized in this study had a wide range of thermal and mechanical properties. These polymers can be easily synthesized at room temperature *via* the combination of thiol-Michael and Diels-Alder reaction.

4.2 Introduction

Hydroxymethylfurfural (HMF) is one of the promising bio-based chemical which has drawn attention since it can be synthesized from various sugar resources.[174] The functional groups of HMF are available for derivatization, which enables this platform chemical to be suitable for the synthesis of fine chemicals, biofuel precursors, and monomers to polymers.[175] Among these applications, the use of HMF derivatives to synthesize polymers has attracted researchers'

attention due to their improved thermal, mechanical and barrier properties, as compared to the petroleum-based polymers.[176] However, current polymerization techniques to synthesize HMF derivative based polymers are often performed under harsh conditions along with high energy input.[176] Therefore, new strategies requiring milder conditions are desired.[177]

The thiol-Michael addition reaction offers several advantages such as high conversion ratio, rapid reaction rate, and mild reaction conditions.[178] Recently, the thiol-Michael adduct has been observed to be thermo-responsive.[178b] This versatile polymerization technique provides polymers with distinct structures as new reactive groups can be included in the polymer chains, and this could broaden the applications of bio-based polymers. To date, very few research groups investigated the synthesis of bio-based polymers through this reaction.[179] In addition, the synthesis of copolymers is an efficient approach to adjust the properties of polymers. However, there is no information available on the synthesis of bio-based copolymers *via* the thiol-Michael addition. Although it has been suggested that the influence of the *pKa* of the thiol group on the reactivity of the reaction could be disregarded when using a strong nucleophile as a catalyst,[178a] Northrop *et al.* recently observed that the reactivity of thiophenol and 1-hexanthiol with N-methyl maleimide was significantly different depending on several factors such as the nature of the catalyst and the solvent used.[180] Therefore, it is necessary to investigate the synthesis of bio-based copolymers *via* the thiol-Michael addition reaction to further enhance their properties.

Despite the high efficiency of the thiol-Michael addition reaction, polymers synthesized *via* this reaction often display very low storage modulus at room temperature due to the flexible thioether linkages. This may prevent them from being implemented in applications where high mechanical and thermal properties are needed.[178a] Although the synthesis of networks improves the thermal and mechanical properties of the polymers, their lack of ability to be reprocessed or recycled may cause other environmental concerns.[181] The presence of furan rings in a polymeric structure is expected to provide reactive sites for the occurrence of Diels-Alder reaction (DA). Because of the reversibility of the DA reaction between the furan rings and the maleimide moieties, materials synthesized through this reaction display interesting properties, such as self-healing, recyclability and reprocessing capacity.[182] Therefore, HMF derivative based polymers synthesized *via* the thiol-Michael addition reaction may also be dynamically crosslinked. This

could potentially improve the thermal and mechanical properties of the materials, and enable the materials to be reprocessed after use.

On the other hand, the presence of flexible thioether linkages in the polymer synthesized *via* thiol-Michael addition reaction could be used for the preparation of thermoplastic elastomers (TPEs).[183] While HMF and its derivatives have been widely utilized in the synthesis of polymers, few information on the synthesis and characterization of TPEs from HMF derivatives are available.[184] TPEs having both thermoplastics and elastomers properties, are generally a series of physically cross-linked polymers which can be prepared *via* several polymerization techniques. One of the advantages of TPEs is their ability to be melt-processed. Currently, research seems to focus on the synthesis of TPEs from renewable resources, and on the development of environmentally friendly synthetic pathways.[185] Additionally, the incorporation of new crosslinks into either the soft or hard segments of TPEs to improve their mechanical properties has been recently investigated.[186] Because of the reversibility of the DA reaction, it is expected that the DA reaction can also be used to improve the mechanical properties of HMF derivative based TPEs without sacrificing the reprocessing ability of TPEs.

Therefore, this chapter reports on the synthesis and characterization of poly(β-thiother ester) from HMF derivative and different dithiol monomers (1,4-benzenedithiol, 1,3-propanedithiol and dithiothreitol). The potential of one of the linear polymers as hot melt adhesive was explored, considering that adhesives with switchable properties have attracted interest.[187] In addition, the synthesis of copoly(β-thiother ester) has been investigated (aromatic dithiol and aliphatic dithiol) to evaluate the efficiency of this reaction for the synthesis of copolymers. The DA reaction using model compounds 2,5-bis(hydroxymethyl)-furan (BHF) and bismaleimide, and retro-DA reaction between the furan rings in the poly(β-thiother ester) and bismaleimide have also been examined. As a result, the use of this reaction to improve the storage modulus of polymers synthesized *via* the thiol-Michael addition reaction was determined. Moreover, the synthesis and characterization of HMF derivative based TPEs synthesized *via* one-pot thiol-Michael addition reaction under room temperature was investigated. The use of the DA reaction to further enhance the mechanical properties of TPEs was evaluated. To the best of the authors' knowledge, this is the first time that HMF derivative based TPEs are being synthesized efficiently under very mild reaction conditions. This study reported herein may broaden the applications of HMF derivatives

for the synthesis of high performance materials. Moreover, the thiol-Michael addition reaction may become a more common polymerization technique for the synthesis of TPEs.

4.3 Experimental

4.3.1 Materials

Hydroxymethylfurfural (HMF, ⩾99%), benzene-1,4-dithiol (⩾99%), 1,3-propanedithiol (⩾99%), sodium borohydride powder (⩾98%), DL-dithiothreitol (⩾98%), tetrahydrofuran (THF, anhydrous, ⩾99.9%, inhibitor free, and further dried under molecular sieves), DMSO-d_6 (99.9 atom % D), chloroform-d (99.8 atom % D), 1,6-hexanedithiol (97%), 1,1'-(Methylenedi-4,1-phenylene)bismaleimide (bismaleimide, 95%), dimethylphenylphosphine (DMPP, ⩾99%), TLC plates and silica gel were purchased from Sigma-Aldrich. All reagents were used as received without further purification. The commercial hot melt glue used was GS264BK (Stanley, New Britain, CT, USA).

4.3.2 General procedure for the synthesis of (co)poly(β-thioether ester) and TPEs

The synthesis of 2,5-furan diacrylate (2,5-FDA) was reported elsewhere.[179b] The procedure for the synthesis of (co)polymers was as follows: 2,5-FDA (1 eq) was dissolved in THF (0.6 M). The solution was purged under a nitrogen stream for 30 mins to remove oxygen. Thereafter, dithiol monomers (1 eq) were added through a syringe. For 1,4-benzene dithiol and dithiothreitol, the monomers were first dissolved in THF in a separated vial and added to the 2,5-FDA solution. The reaction mixture was cooled in an ice-bath. DMPP (0.005 eq) was added to the mixture to start the polymerization process. The reaction was carried out at room temperature for 15 mins. Poly(β-thioether ester) was precipitated in cold hexane and recovered by filtration. Finally, the polymer was kept in a vacuum oven at room temperature overnight to remove the residual solvent. TPEs were synthesized in a similar approach. In a typical procedure, 2,5-FDA (1.3 eq) was dissolved in THF (0.6 M). The solution was purged with nitrogen for 30 mins to remove oxygen. Thereafter, 1,3-propanedithiol (1 eq) was added *via* a syringe. The reaction mixture was cooled in an ice-bath. Then DMPP (0.005 eq) was added to the mixture to start the polymerization process. The reaction was carried out at room temperature for 15 mins. DL-dithiothreitol (0.3 eq) previously dissolved in THF was then added to the solution. The reaction was conducted for another 25 mins. Poly (β-thioether ester) was precipitated in cold hexane and

recovered by filtration. Finally, the polymer was kept in a vacuum oven at room temperature overnight to remove residual solvent.

4.3.3 Diels-Alder reaction and retro Diels–Alder

The model reaction between BHF (0.5 M) and bismaleimides (0.25 M) was chosen to evaluate the DA reaction in $CDCl_3$. BHF and bismaleimides were first dissolved in $CDCl_3$ with the addition of a small amount of DMSO-d_6 to dissolve BHF completely. Then ^1H NMR was recorded at fixed times (0h, 1h, 3h, 8h, 24h and 48h). Furthermore, a ^1H NMR study was conducted to observe the retro-DA reaction. A sample of crosslinked polymer was first added in DMSO-d_6. The solution was subsequently heated at 110 ^oC for 4h. The spectra were frequently recorded (0h, 1h, 3h and 4h).

4.3.4 Film preparation

The poly(β-thioether ester) films were prepared by a solution casting method. A mixture of poly(β-thioether ester) and bismaleimides (polymers/bismaleimides weight ratios of 2:1, 4:1 or 10:1) was dissolved in chloroform. The solution was then poured into a Teflon mold, which was left in a sealed container for 24 h to enable the DA reaction to occur between the furan rings and the maleimide. The residual solvent was completely evaporated in a vacuum oven at 40 ^oC for 24 h. The films were held at room temperature for at least 24 h before analysis.

4.3.5 Diels-Alder reaction to crosslink TPEs

Bismaleimide was used to crosslink 2,5-FDA based TPEs. A typical procedure is described as follows: 2,5-FDA based TPEs (0.5 g) were first dissolved in chloroform (3 mL), then bismaleimide (50 mg) was added. After TPEs and crosslinkers were dissolved completely, the solution was degassed and poured into a Teflon mold and sealed for 24 h to enable the DA reaction to occur. The solvent was completely evaporated in a vacuum oven at 40 ^oC for 24 h. The films were held at room temperature for at least 24 h before analysis.

4.3.6 Swelling test and gel fraction determination

The gel fraction and swelling ratio of the crosslinked polymers were determined by a solvent immersing method.[182k] The samples (W_1) were first submersed in chloroform for 3 days at room temperature. Then, they were taken out to determine the weight of swollen samples (W_2). The insoluble polymer fractions were further dried under vacuum at 60 ^oC for at least 24h to reach a

constant weight (W_3). The tests were conducted in triplicate. The gel fraction and the swelling ratio were calculated according to the following formulas:

$$Gel\ fraction = \frac{W_3}{W_1} \times 100\%$$

$$Swelling\ ratio = \frac{W_2 - W_1}{W_1} \times 100\%$$

4.3.7 Adhesive properties

Adhesion properties were investigated using an Instron Universal Testing Machine (model 4500, Instron corporation, Canton, MA) equipped with a 10 kN load cell and mechanical gripping clamps at a strain rate of 1mm/min at room temperature. Lap joints were made using wood substrates with bond areas of 10 × 20 mm. Around 20 mg of polymer were used to bond the substrates. During heating (at 110 ºC for 10 mins), the joints were mechanically fixed to prevent undesired changes in the bonding area. Then, the samples were pressed at room temperature for 24h and tested. The rebonding process was carried out by clipping the separated two wood substrates together without applying additional polymers, and heating them in the oven at 110 ºC for 10 mins. The samples were also pressed at room temperature for 24h and then tested. Adhesion forces were determined as average values for three measurements.

4.3.8 Characterization

^{1}H and ^{13}C NMR spectra were obtained on a Bruker AV 400 or Varian/Agilent 500 using deuterated DMSO and $CDCl_3$ as solvents. The chemical shifts were referenced to the solvent residual signals at 2.50 ppm for deuterated DMSO and 7.26 ppm for $CDCl_3$. The FTIR spectra were recorded on a Thermo Scientific Nicolet iS5 FTIR spectrometer (Thermo, Madison, WI, USA) using an attenuated total reflectance (ATR) diamond crystal. The spectra were recorded at 32 scans and 8 cm^{-1} resolutions in the 4000–600 cm^{-1} range. The molecular weight distribution was determined using gel permeation chromatography (GPC, Water Breeze). THF was used as the mobile phase and was running at a flow rate of 0.3 mL/min. The GPC was equipped with three Waters Styragel HR columns and a guard column. The GPC was equipped with a differential refractive index detector (RI 2410). The molecular weights were calibrated using linear polystyrene standards having a narrow molecular weight distribution. The thermal transitions of poly(β-thioether ester) were determined by DSC (Q100, TA Instruments, Inc., New Castle, DE). The samples were compressed in aluminum pans. The heating rate was 10 ºC/min,

and the cooling rate was 5 °C/min. Modulated temperature DSC scans (MTDSC) were performed at a heating rate of 1.5 °C/min, with a temperature modulation amplitude of 0.24 °C for a time period of 60 s. Thermogravimetric analysis (TGA, Q50, TA Instrument, Inc., New Castle, DE) was used to investigate the thermal stability of the polymers (powder). The flow rate of N_2 was 60 mL/min, and the samples were heated from 20 °C to 600 °C at a rate of 10 °C/min. Py-GC/MS analysis was performed using a Varian CP-3800 gas chromatograph coupled to a Saturn 2000 ion trap detector interfaced to a CDS Pyroprobe 2000 unit through a valved interface (CDS 1500). A mass of 0.5 ± 0.1 mg of polymer was introduced into a quartz tube plugged with quartz wool, and inserted into the coil probe of the instrument. GC separation was carried out on a fused silica HP-5 MS column (50 m length × 0.2 mm i.d. × 0.33 μm film thickness; J&W Scientific). The pre-selected pyrolysis temperatures were 250 and 300 °C. The dynamic mechanical analyzer (DMA) used for this study was a DMA Q800 (TA instruments, New Castle, DE) equipped with a liquid nitrogen cooling system. The sample dimensions were 10 × 5 × 0.5 mm and were analysed in a tension mode. The tests were performed over a temperature range of -60 to 100 °C at a heating rate of 3 °C/min and a frequency of 1 Hz. Stress-strain tests were also conducted in triplicates using the DMA Q800 at 25 °C by ramping up a force at a rate of 0.5 N min^{-1}. A preload force of 0.01 N was used. The cyclic stress-strain test was performed to evaluate the elasticity of the TPEs. The films were first extended by ramping up a force at a rate of 0.2 N/min to a 150 % strain. After maintaining the strain for 1 min, the films were recovered by ramping down a force at a rate of 0.4 N/min, and then maintained at stress zero for 2 mins. This was marked as one cycle. Three cycles were performed. Polarized optical microscopy (POM) measurements were conducted on a Nikon LEICA L100A polarizing optical microscope. The morphology of the cross-linked films before and after compression molding was observed using a JEOL JSM-7600 TFE scanning electronic microscope (Tokyo, Japan).

4.4 Results and discussions

4.4.1 Composition of poly(β-thioether ester)

To investigate the versatility of this polymerization technique, three commercially available dithiol monomers were used to synthesize poly(β-thioether ester). The chemical structure of these dithiol monomers is illustrated in **Scheme 4.1**.

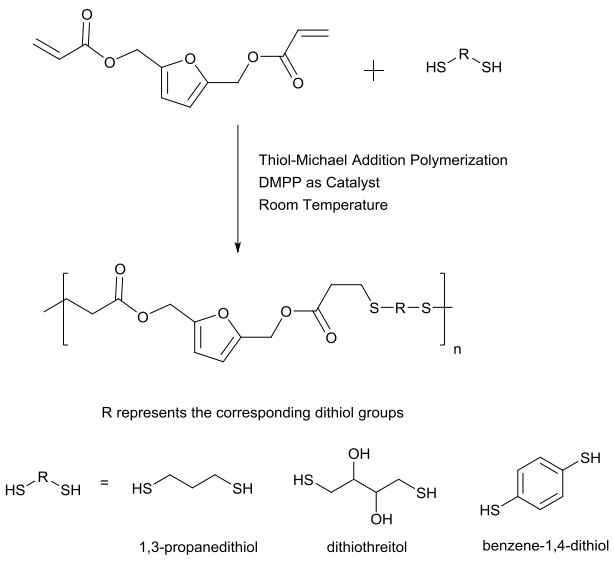

Scheme 4.1 Synthesis of poly(β-thioether ester) from 1,3-propanedithiol (PPF), dithiothreitol (POF) and 1,4-benzene dithiol (PBF).

The polymerization process was monitored by ^{1}H NMR using 1,3-propanedithiol and 2,5-FDA as an example (**Figure 4.1a**). The thiol-Michael addition polymerization occurred quickly as the signals for acrylate groups disappeared within 15 min (from δ = 7.0 to 6.0 ppm), indicating the full conversion of 2,5-FDA. The use of DMPP as a nucleophile catalyst was responsible for the quick polymerization reaction, which was generally faster than the base-catalysed thiol-Michael addition.[179b,183a] DMPP could attack the vinyl groups to generate the intermediate zwitterion, which then deprotonated the thiol groups to yield thiolate anions. The Michael adducts were finally generated by the reaction between thiolate anions and vinyl groups.[178a] The structures of each polymer were confirmed using ^{1}H NMR, ^{13}C NMR and FTIR (**Figure 4.1b, Figures 4.2, 4.3 and 4.4**). For example, the ^{1}H NMR spectrum of poly(β-thioether ester) synthesized from 1,3-propanedithiol and 2,5-FDA is shown in **Figure 4.1b**. Signals (a, b) from δ= 5.0 ppm to 6.5 ppm belonged to the furan protons and methylene protons next to the furan rings ($CDCl_3$). The signals at δ= 2.5 ppm to 3.0 ppm (c, d and e) represented the resonance from the methylene protons between the ester groups and the thioether, and the protons adjacent to the thioether groups, respectively. The peaks at δ =1.7 to 1.9 ppm (f) were attributed to the middle methylene protons from the 1,3-propanedithiol moieties. In addition, two signals were observed at δ = 3.5-3.6 ppm (f) and 4.6-4.8 ppm (g), being assigned to the protons of the hydroxyl groups and the protons next to the hydroxyl groups (**Figure. 4.2a**, POF). The signal from the protons of the benzene rings was observed at δ = 7.2-7.3 ppm (e, **Figure 4.2b**, $CDCl_3$, PBF). The ATR-FTIR

spectra of different poly(β-thioether ester) are presented in **Figure 4.4**. Characteristic bands, including C-H stretching vibrations at 3135 cm^{-1}, the C=C ring stretching vibrations at 1565 cm^{-1} and the ring vibration of the =C-O-C= groups at 1150 cm^{-1}, were assigned to the furan rings. Carbonyl C=O stretching vibrations were observed at around 1730 cm^{-1}. The bands at 2910−2950 and 2850−2860 cm^{-1} were attributed to the asymmetric and symmetric stretching vibrations of the CH_2 groups, respectively. A direct comparison of the FTIR spectra of these polymers showed similar patterns (**Figure 4.4**), except for a broad O-H stretching absorption (3400 cm^{-1}) for POF. However, a careful examination of the spectra in the region of 1700 to 1760 cm-1 showed that the carbonyl C=O stretching vibrations of POF shifted to a lower wavenumber (**Figure 4.1c**). This indicated the presence of interactions between the carbonyl groups and the hydroxyl groups.[183b,188] Furthermore, all polymers synthesized by the thiol-Michael addition reaction had a unimodal distribution, which was illustrated by a typical GPC trace of poly(β-thioether ester) synthesized from 1,3-propanedithiol and 2,5-FDA (**Table 4.1 and Figure 4.1d**). According to the Carothers equation, the molecular weight of linear polymers synthesized *via* step growth polymerization can be controlled by introducing one monomer in excess. Therefore, the polymerization process was performed with different monomer ratios using 1,3-propanedithiol and 2,5-FDA as an example (**Table 4.2**). As expected, the number average molecular weight (M_n) of poly(β-thioether ester) decreased when the stoichiometric ratio of monomers was not equal to one.

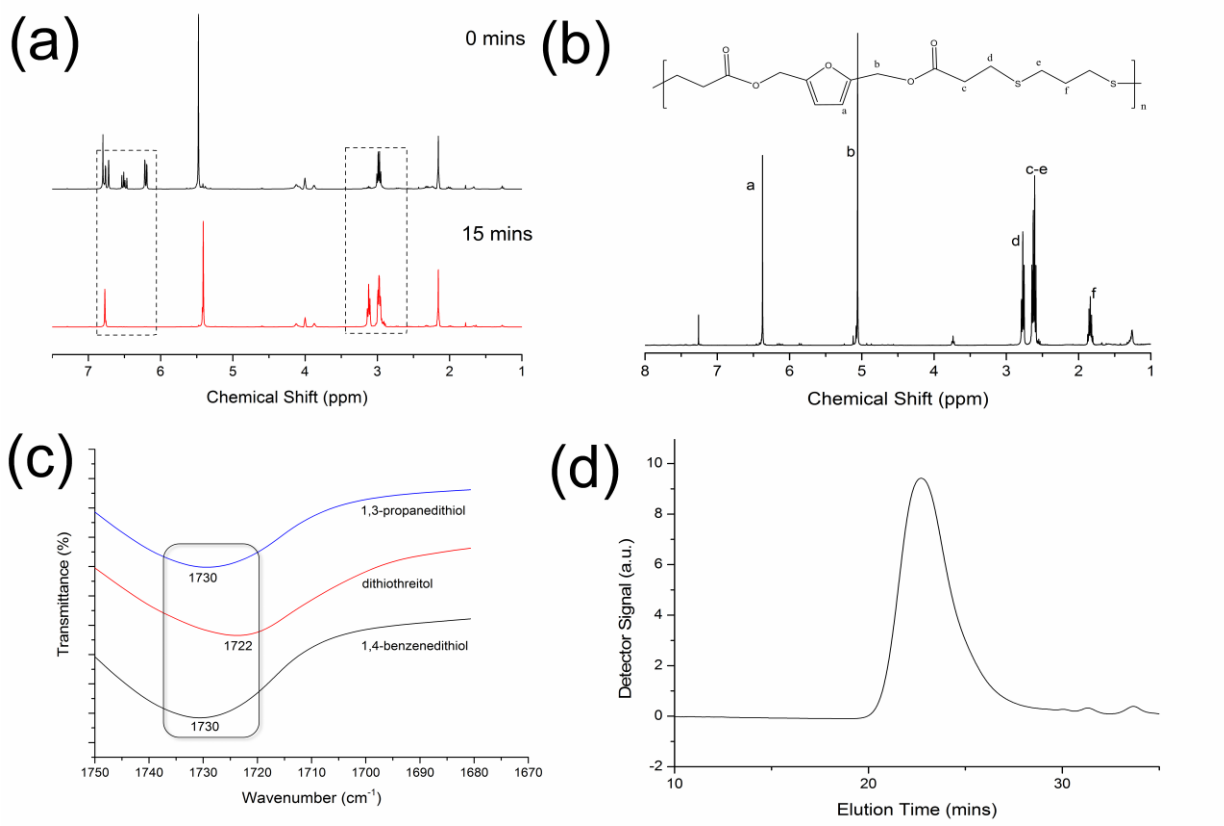

Figure 4.1 a) ^{1}H NMR spectrum of step growth polymerization of 2,5-FDA and 1,3-propanedithiol in THF at 0 min and 15 min, respectively; b) ^{1}H NMR spectrum of poly(β-thioether ester) synthesized from 1,3-propanedithiol (90% yield). c) FTIR spectra in the range of 1760-1700 cm^{-1}; d) A typical GPC trace of poly(β-thioether ester) synthesized from 1,3-propanedithiol and 2,5-FDA.

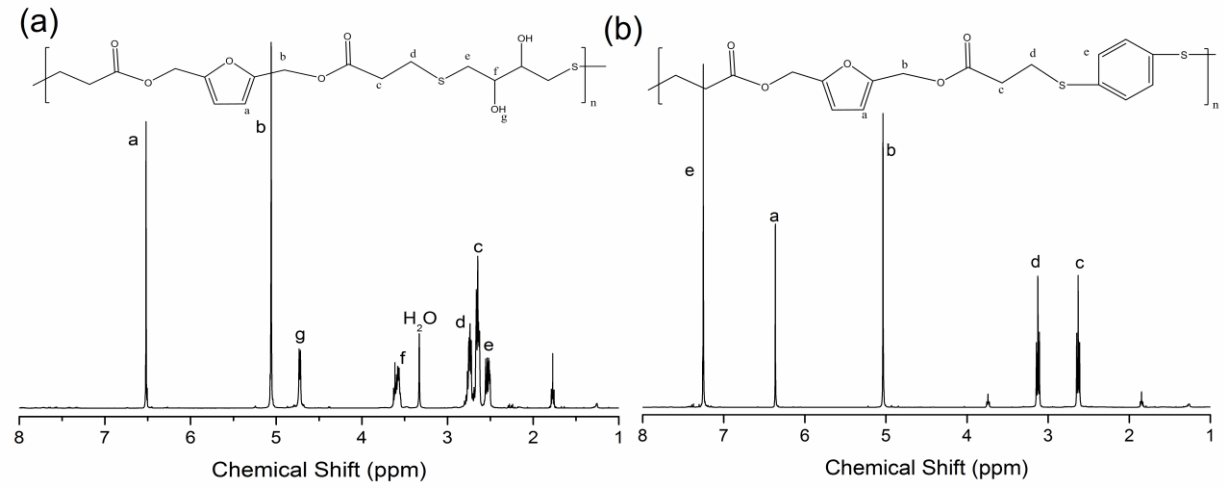

Figure 4.2 ^{1}H NMR spectra of poly(β-thioether ester) synthesized from a) DL-dithiothreitol (92 % yield); b) 1,4-benzenedithiol (90 % yield).

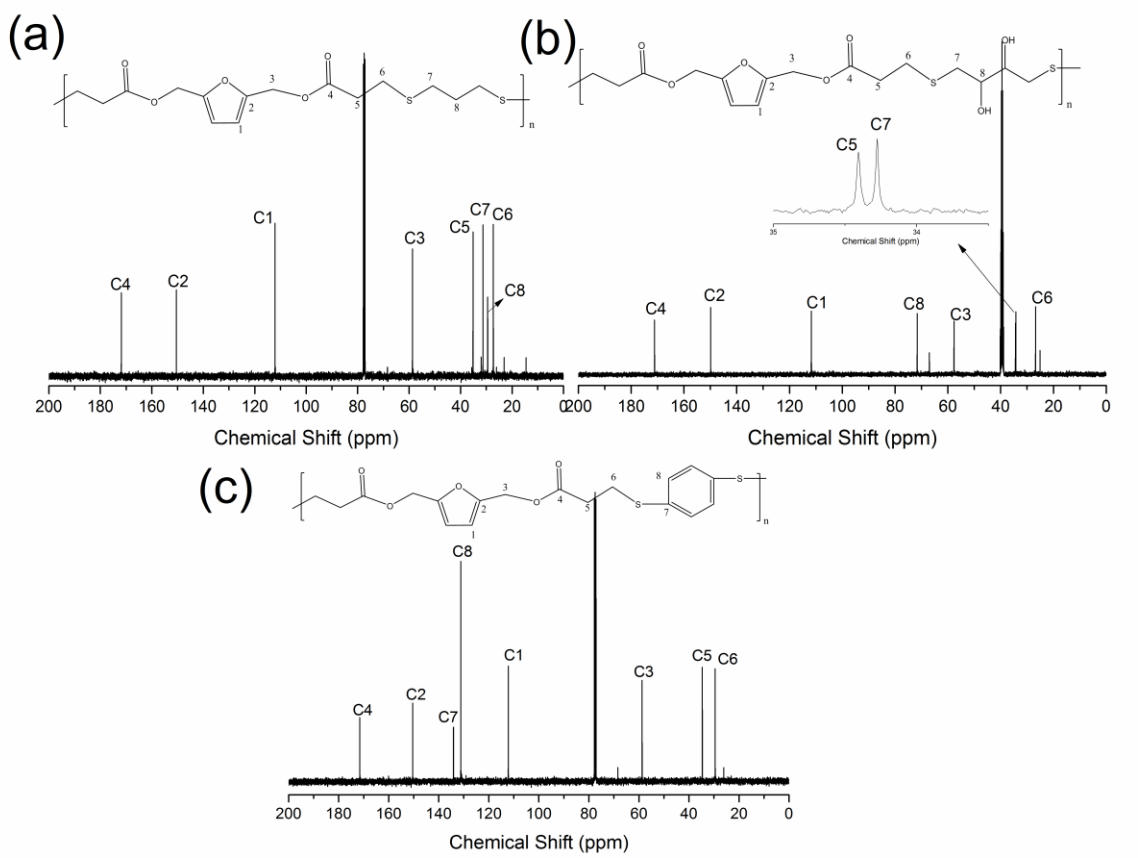

Figure 4.3 ^{13}C NMR spectra of poly(β-thioether ester) synthesized from a) 1,3-propanedithiol; b) dithiothreitol; c) 1,4-benzenedithiol

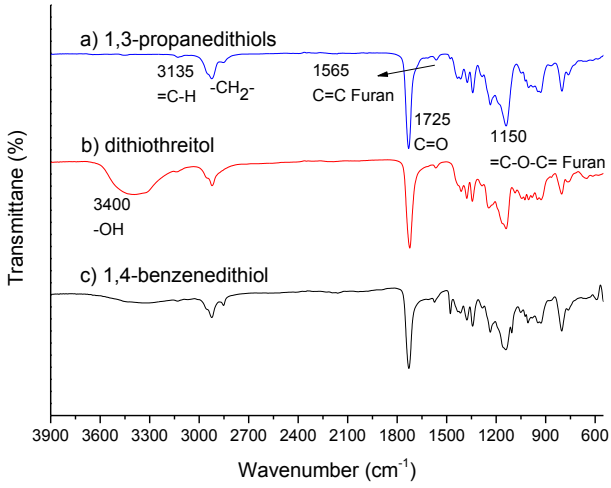

Figure 4.4 FTIR spectra of poly(β-thioether ester) synthesized from a) 1,3-propanedithiol; b) dithiothreitol; c) 1,4-benzenedithiol

Table 4.1 Composition, thermal properties and molecular weights of the synthesized polymers

	GPC		DSC				TGA
			First Heating		Second Heating		
Polymers	Molecular weight (M_n*10^3 g/mol)[a]	PDI	T_g (°C)[b]	T_m (°C)[f]	T_g (°C)	T_m (°C)[d]	$T_{5\%}$(°C)[c], T_{max} (°C)[e]
PHF[j]	19.5	2.0	#	56.1/77.4	-36.9	#	236, 249/285
PPF	21.8	1.7	#	#	-32.3	#	233, 250/298
POF	11.5	1.7	1.4	61.6/66.0	1.4	#	215, 222/259
PBF	17.8	1.9	7.9	64.0/80.6	7.9	#	242, 246/292

[a] Polystyrene as standard. [b] Glass transition temperature. [c] $T_{5\%}$ indicates the 5% weight loss of polymers under a nitrogen atmosphere. [d] Melting temperature. [e] T_{max} indicates the temperature of maximal rate of decompositions. [f] Multiple melting temperature. # = not detected. [j] Polymers synthesized from 1,6-hexanedithiol.[179b]

Table 4.2 GPC results of poly(β-thioether ester) prepared *via* different stoichiometric conditions

Acrylate: Thiols[a]	M_n (g/mol)[b]	PDI
1.2:1	3500	2.8
1.1:1	15000	1.9
1:1	22000	2.0
1:1.1	10000	2.0
1:1.2	2800	2.1

[a] The ratio of 2,5-FDA and 1,3-propanedithiol. [b] Polystyrene as standard.

4.4.2 Thermal properties of poly(β-thioether ester)

The thermal stability of poly(β-thioether ester) was determined by TGA (**Figure 4.5a** and **Table 4.1**). Typically, all the TGA profiles showed a similar two-stage degradation pattern. The decomposition temperature at 5% weight loss of all poly(β-thioether ester) was around 210-240 °C. Around 15 % of the initial weight remained at 600 °C. This degradation behavior was significantly different from other polymers synthesized *via* the thiol-Michael addition reaction. For example, Junkers *et al.* observed only one main degradation stage for poly(β-thioether ester) which occurred between 350 to 400 °C when 1,6-hexanediol diacrylate was used as the monomer.[178c] In order to elucidate the potential mechanism of degradation, Py-GC/MS analysis was performed at 250 °C and 300 °C. The polymer used was poly(β-thioether ester) previously synthesized from 1,6-hexanedithiol and 2,5-FDA (PHF).[179b] It was observed that the first stage of degradation was mainly the result of α-hydrogen bond scission and alkyl-oxygen homolysis due to the presence of 5-methylfurfural as the main degradation product (retention time = 15.79 min, **Figure 4.6a**). Moreover, a small amount of 1,6-hexanedithiol was observed at 22.56 min. As the

pyrolysis temperature increased to 300 ºC, 5-methylfurfural was still present as a degradation product and the amount of 1,6-hexanedithiol increased due to the C-S bond scission (**Figure 4.6b**). These results indicated that the presence of furan rings in the poly(β-thioether ester) led to a different degradation pattern, as compared to poly(β-thioether ester) synthesized from 1,6-hexanediol diacrylate.[178c] Additionally, Loos *et al.* recently investigated the thermal stability of biobased polyesters synthesized from 2,5-bis(hydroxymethyl)-furan (BHF) and various diacid ethyl esters.[177] The $T_{5\%}$ of synthesized polyesters was observed to occur between 250 ºC to 300 ºC. Moreover, two degradation steps were observed, and the T_{max} at the major degradation step was found between 276 ºC to 332 ºC. The thermal stability of poly(β-thioether ester) decreased due to the presence of thioether groups, which might be ascribed to the lower energy value of C-S bond.[189]

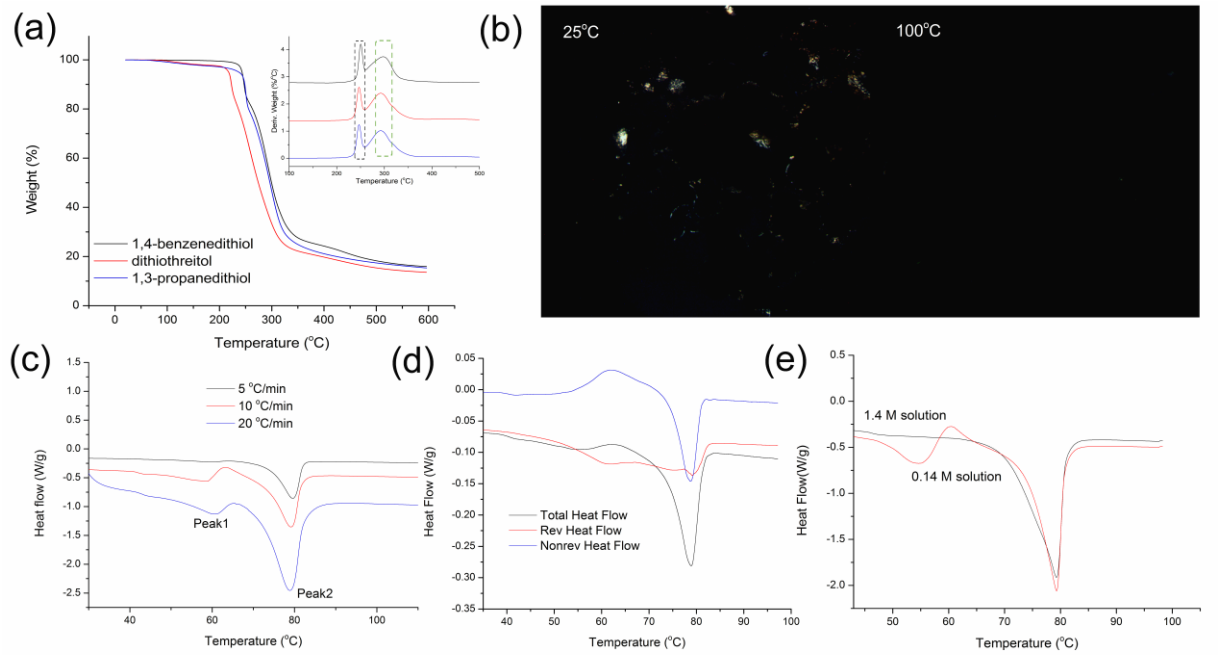

Figure 4.5 a) TGA profiles of poly(β-thioether ester) synthesized from 1,4-benzenedithiol, dithiothreitol and 1,3-propanedithiol; b) POM photographs of PHF samples observed at 25 ºC and 100 ºC, respectively; c) Effect of heating rates on the melting behavior of PHF samples; d) Total, reversing and non-reversing signals obtained by MTDSC of PHF samples; e) Effect of polymer concentration used in the process of precipitation on the thermal transitions of PHF samples.

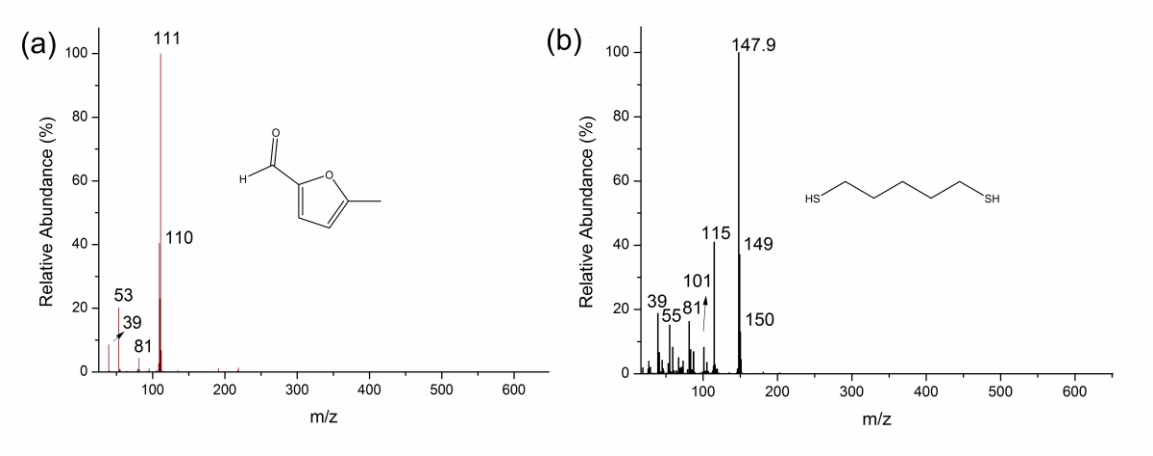

Figure 4.6 a) 5-methylfurfural generated at 250 ºC and b) 1,6-hexanedithiol generated at 300 ºC.

The thermal transitions of poly(β-thioether ester) were investigated by DSC (**Figure 4.7** and **Table 1**). The glass transition temperature (T_g) of PPF slightly increased to -32.3 ºC, as compared to PHF (-36.9 ºC).[179b] As the methylene groups in dithiol monomers decreased from 6 (PHF) to 3 (PPF), the polymer chains are less flexible, leading to an increase in T_g. In addition, the incorporation of benzene rings in the polymer chains significantly improved the T_g to 7.9 ºC, which was consistent with other observations. For example, Munari *et al.* observed that the T_g was improved from -52 ºC to 0 ºC in sulphur-containing polyesters when aliphatic hydrocarbons were substituted with benzene rings.[179] The benzene rings located within the backbone of PBF contributed to an increase in steric hindrance, and hence enhanced the T_g. POF also exhibited a high T_g (1.4 ºC) as compared to aliphatic dithiol monomers. The multiple hydrogen bonds among the OH groups, or between the OH groups and the oxygen atoms of the furan rings, or between the OH groups and the carbonyl groups, might have acted as crosslinking points, leading to the increase in T_g. In addition, multiple melting peaks were observed in the first heating cycle of the synthesized polymers, ranging from 55 ºC to 80 ºC. However, these melting peaks disappeared in the second heating scan for all tested poly(β-thioether ester) due to their poor crystallization ability. It has been hypothesized that the substitution of the oxygen atoms of ether with sulfur (thioether) into the polymer chains increased the flexibility and the mobility of the polymer chains, and therefore enhanced the ability of the polymers to crystallize.[179] However, it was also observed that the crystallization ability of poly(thioether ester-co-ester) decreased as the thioether ester units increased.[190] The presence of multiple melting peaks in the first scan might be due to solvent-induced crystallization during the process of polymer synthesis.[191] POM and

DSC were further used to elucidate the thermal transitions in the first scan, using PHF as an example. PHF was precipitated in hexane and was recovered as a white colored solid, although the T_g value of PHF was around -40 ^oC. The presence of crystals in PHF at room temperature was confirmed *via* POM (**Figure 4.5b**). As the temperature increased to 100 ^oC, the crystals were no longer detected due to the melting process (**Figure 4.5b**). In addition, the effect of heating rates (from 5 ^oC/min to 20 ^oC/min) on the melting behaviour of PHF was tested by DSC (**Figure 4.5c**). The results showed that the relative heights of peak2 and peak1 varied with the increase in heating rate. For slow heating rates (5 ^oC/min), there was enough time for the sample to melt and recrystallize. Therefore, crystals with an increased thermal stability were produced. Modulated temperature DSC (MTDSC) was used to investigate the melting and crystallization behaviour of the polymers. MTDSC scans were performed at 1.5 ^oC/mins. **Figure 4.5d** shows a pronounced exothermic peak in the non-reversing signal curve, indicating the presence of recrystallization process. Hoyle *et al.* and Gall *et al*. also observed multiple melting peaks in the first heating scan of the polymers containing thioether groups.[183a,181d] The endotherms were attributed to the populations of lamella of varying thickness in the polymers. Moreover, the intensity of these melting peaks was enhanced with the increased annealing time.[181d] However, Junkers *et al.* reported only one melting peak when using 1,4-butanedithiol and 1,6-hexanediol diacrylate to poly(β-thioether ester).[178c] These comparisons indicated that this multiple melting behaviour was relevant to the structures of polymers.

In addition, the effect of polymer concentration used during precipitation on the thermal transitions was investigated (**Figure 4.5e**). Two concentrations of PHF solutions were prepared in THF (1.4 M and 0.14 M). Then the solutions were poured into cold hexane. After collecting the white solid, they were further dried in a vacuum oven at 40 ^oC for 12 h to remove the solvent. The result showed that when a high concentration of polymer solution was used (1.4 M), only one melting peak was observed, as compared to two melting peaks for PHF (0.14 M). This result confirmed that the presence of multiple melting peaks in the first PHF scan was mainly due to solvent-induced crystallization. This process was also influenced by the concentration of polymers.

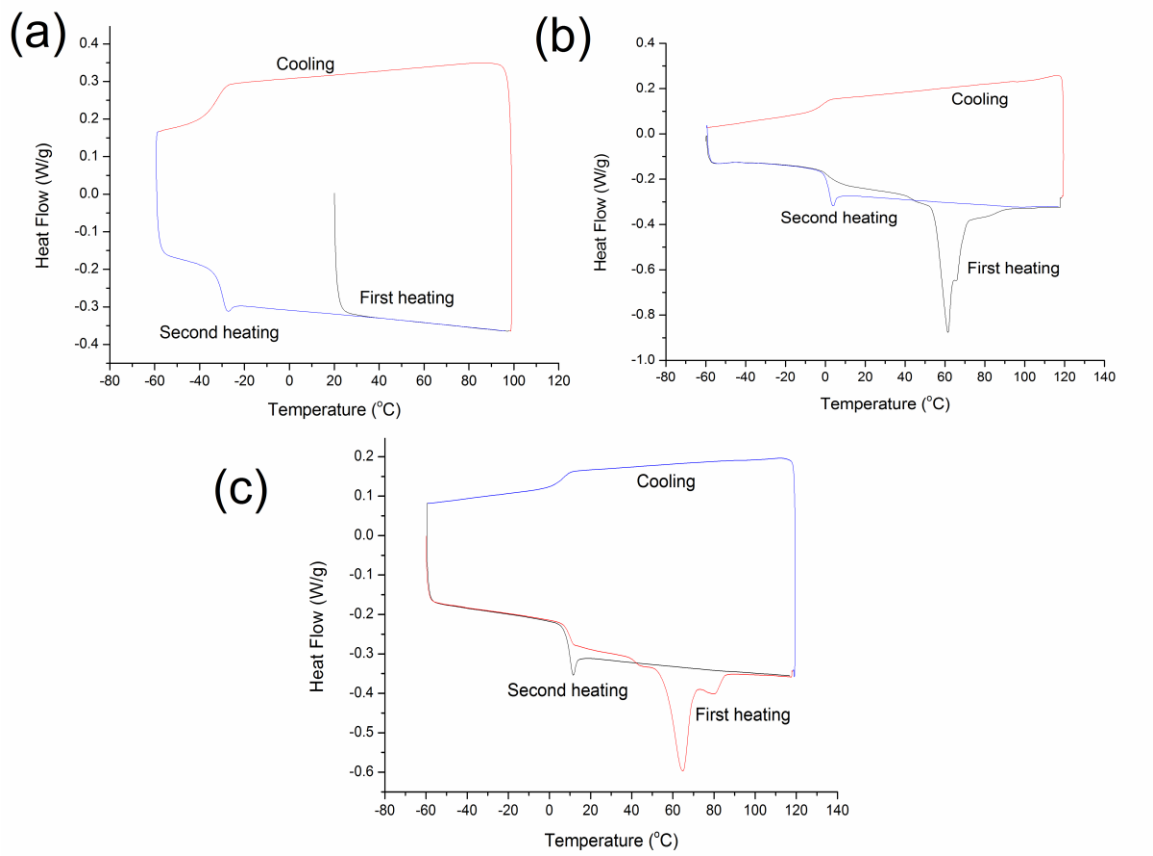

Figure 4.7 DSC curves of poly(β-thioether ester) synthesized from a) 1,3-propanedithiol; b) dithiothreitol; c) 1,4-benzenedithiol measured from -60 to 120 °C at a heating rate of 10 °C/min, a cooling rate of 5 °C/min.

4.4.3 Adhesion properties

Supramolecular polymer adhesives have been recently investigated due to their dynamic, stimuli-responsive nature and non-covalent interactions.[190] Recently, there has been a growing interest to use bio-based polymers as adhesives.[191] Although various applications for the thiol-ene polymerization have been found, such as the synthesis of aerogel, degradable polymeric structures for biomedical and liquid crystal elastomers,[192] there is little information on the potential applications of polymers synthesized *via* thiol-Michael addition.[193] Due to the presence of hydroxyl groups as side chains, it is expected that hydrogen bonding can increase the cohesive forces, as well as the adhesive forces to substrates. Therefore, POF has the potential to be used as hot melt adhesives. The preliminary results of bond strength of lap shear joints between two wood substrates showed that POF exhibited an adhesive strength of 1.5 MPa at room temperature, as compared to 2.1 MPa for the commercial product (Stanley, GS264BK) (**Figure**

4.8). Moreover, the samples showed a good rebonding ability with response to heat due to the linear structure of POF. A cohesive failure mode was observed.

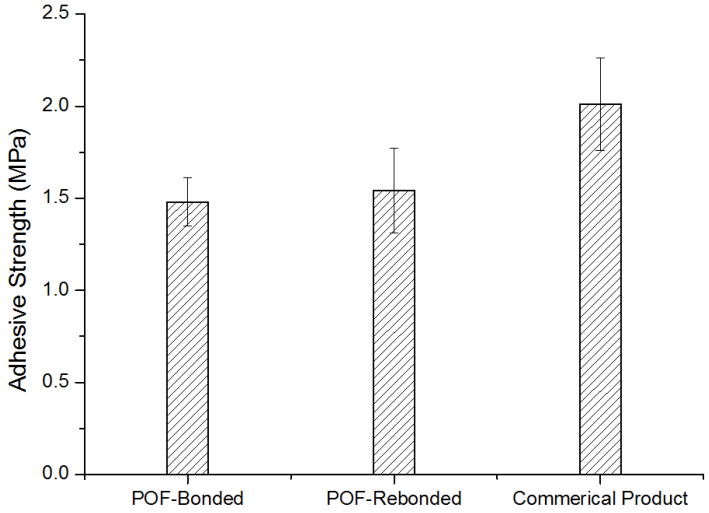

Figure 4.8 Adhesion strength of POF bonded and rebonded compared to commercial product.

4.4.4 Composition and thermal properties of copoly(β-thioether ester)

The synthesis of copoly(β-thioether ester) was performed through the reaction of 2,5-FDA with 1,4-benzenedithiol (BS) and 1,6-hexanedithiol (HS), as shown in **Scheme 4.2**. The polymerization reaction finished within 15 mins at room temperature as indicated by ^{1}H NMR. The obtained copolymers, named as PHF/PBF-*x* (*x* is the molar ratio of HS to BS), were solid at room temperature and the color varied from white to light yellow. The chemical structures and compositions of the polymers were determined by ATR-FTIR and ^{1}H NMR spectra, as shown in **Figure 4.9**.

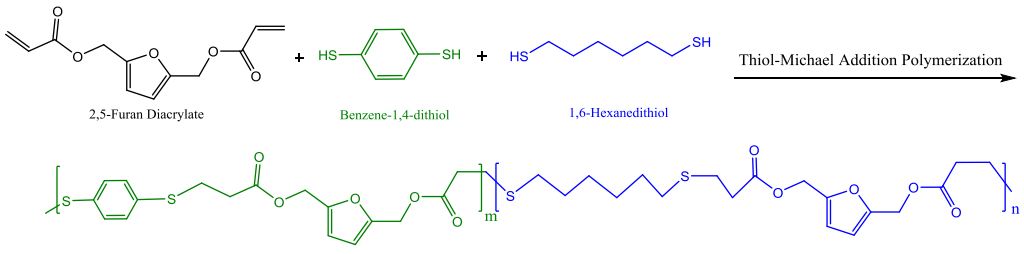

Scheme 4.2 Synthesis of copoly(β-thioether ester) *via* the thiol-Michael addition polymerization

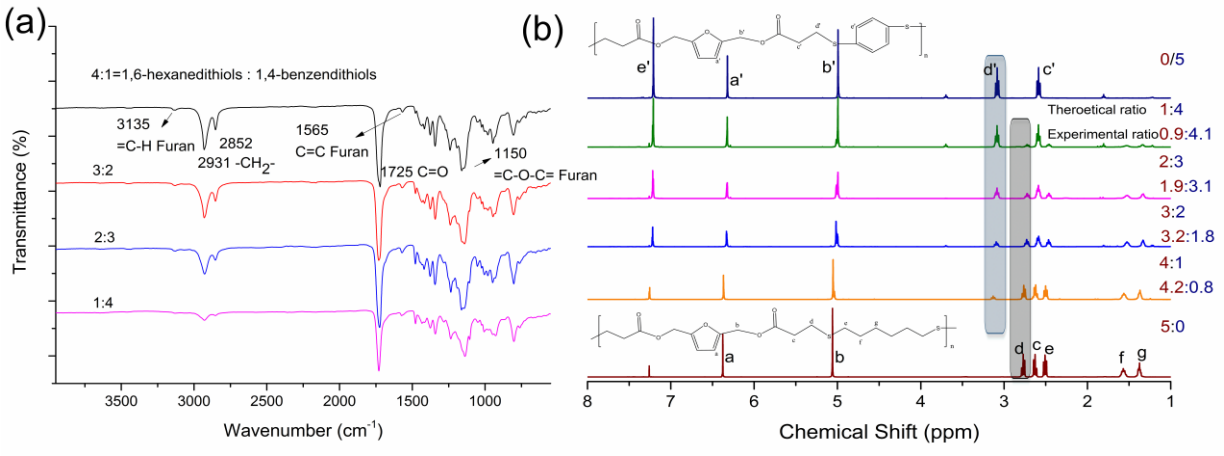

Figure 4.9 a) FTIR spectra of copoly(β-thioether ester); b) ^{1}H NMR of PHF, PBF and P(HF-co-BF) copoly(β-thioether ester) (1:4 for theoretical ratio of PHF to PBF and 0.9:4.1 for experimental ratio).

The ATR-FTIR spectra showed typical characteristic bands of furan based poly(β-thiother ester) (**Figure 4.9a**). As the ratio of 1,6-hexanedithiol to 1,4-benzenedithiol increased, the intensity of -CH_2- signals (2931 and 2852 cm^{-1}) significantly increased. Additionally, nine signals were observed from the ^{1}H NMR spectra of the copolymers (**Figure 4.9b**). The peak at δ=7.25-7.26 ppm (e') was assigned to the protons of the benzene rings. Signals at δ = 6.3-6.4 ppm (a or a') and δ = 5.0-5.1 ppm (b or b') were assigned to the furan protons and methylene protons next to the furan rings, respectively. Signals of methylene protons adjacent to the sulphur group were at δ = 3.1-3.2 ppm (d') in PBF, while the methylene protons adjacent to the sulphur group were at δ = 2.7-2.8 ppm (d) for PHF. Furthermore, the signals of the methylene protons overlapped at δ=2.6-2.7 ppm (c and c'). Peaks at δ= 2.5 ppm (e), 1.5-1.6 ppm (f) and 1.3-1.4 ppm (g) were assigned to the methylene protons of PHF. As the molar ratio of HS to BS decreased, the intensity of the characteristic PHF signal (δ= 2.7-2.8 ppm, d) decreased, while the intensity of the PBF signals (δ=3.1-3.2 ppm, d') increased (highlighted in **Figure 4.9b**).

The composition of PHF/PBF-*x* copolymers was calculated according to the integration area ratio of the characteristic peaks at δ = 2.7-2.8 ppm (d) to δ = 3.1-3.2 ppm (d'), as shown in **Figure 4.9b**. The compositions determined by ^{1}H NMR closely matched the theoretical ones (**Table 4.3** and **Figure 4.9**). These results indicated that while the *pKa* of the thiol groups of BS (6.8) and HS (10.24) were different, DMPP could efficiently initiate the thiol-Michael addition polymerization (thiol-acrylate reaction) due to the formation of a strong base *via* the nucleophilic

attack on a Michael acceptor. This observation was significantly different from the thiol-maleimide reaction, although it has also been classified as one of the thiol-Michael addition reaction. As a result, the composition of copolymers could be adjusted by simply changing the co-monomer feed ratios.

Table 4.3 Composition, thermal properties and molecular weights of synthesized copoly(β-thioether esters)

	^{1}H NMR	GPC		DSC				TGA
				First Heating		Second Heating		
Polymers	**^{1}H NMR HS/BS ratio (mol%)**	**Molecular weight (M_n*10^3 g/mol)[a]**	**PDI**	**T_g (°C)[b]**	**T_m (°C) [f]**	**T_g (°C)**	**T_m (°C) [d]**	**$T_{5\%}$(°C)[c], T_{max} (°C)[e]**
PHF[j]	5/0	19.5	2.0	#	56.1/77.4	-36.9	#	236, 249/285
PHF/PBF-4:1	4.2/0.8	14.7	1.7	-27.1	54.0/69.5	-30.1	#	249, 254/291
PHF/PBF-3:2	3.2/0.8	16.4	1.7	-20.8	47.6	-23.2	#	243, 252/292
PHF/PBF-2:3	1.9/3.1	17.0	1.6	-18.5	49.3/53.7	-16.3	#	236, 247/291
PHF/PBF-1:4	0.9/4.1	13.5	1.8	-6.4	49/56.0/77.5	-5.3	#	236, 246/289
PBF	0/5	17.8	1.9	8.0	64.0/80.6	7.9	#	242, 246/292

[a] Polystyrene as standard. [b] Glass transition temperature. [c] $T_{5\%}$ indicates the 5% weight loss of polymers under a nitrogen atmosphere. [d] Melting temperature. [e] T_{max} indicates the temperature of maximal rate of decompositions. [f] Multiple melting temperature. # = not detected. [j] Polymers synthesized from 1,6-hexanedithiols.[179b]

The copolymers were characterized by DSC for their T_g (**Figure 4.10** and **Table 4.3**). The T_g obtained by DSC measurements varied from -30.1 to -5.3 °C (**Figure 4.10**). The addition of benzene rings decreased the mobility of the polymer chains, and therefore increased the T_g. All DSC profiles showed only one T_g as shown in the second heating cycle (**Figure 4.10**). Multiple melting peaks were observed in the first heating cycle (from 49 to 78 °C), but no melting peak appeared after eliminating the thermal histories. Being consistent with the original poly(β-thiother ester) (PHF and PBF), these copolymers also showed no crystallization under the following conditions: cooling at 5 °C/min, and second heating at 10 °C/min. The thermal stability of the copolymers analysed by TGA showed similar decomposition patterns (**Figure 4.11** and **Table 4.3**). The decomposition temperature for all copolymers at 5% weight loss was around 240 °C.

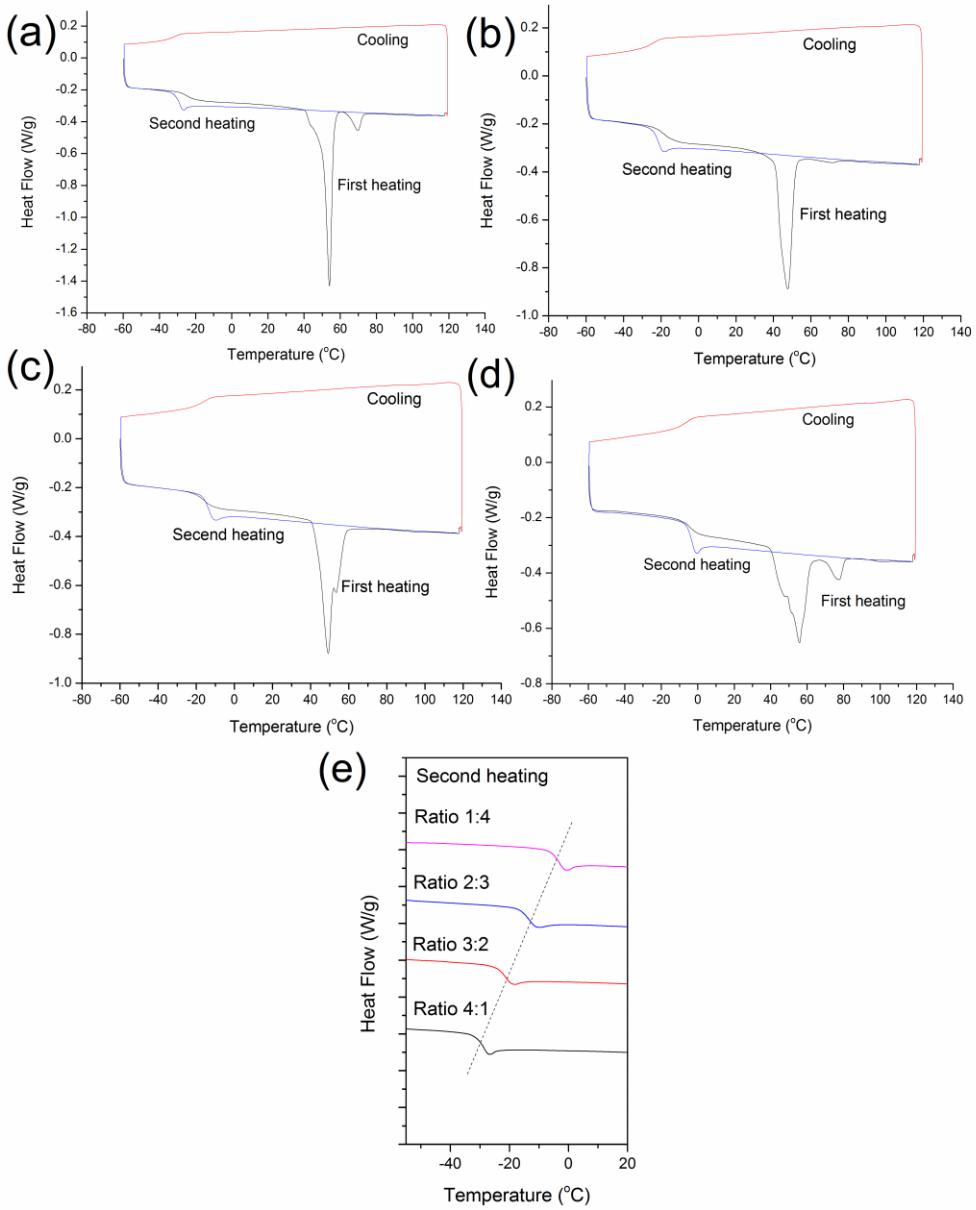

Figure 4.10 (a, b, c and d) DSC curves of copoly(β-thioether ester) with varying monomer ratios; (e) T_g evolution of copoly(β-thioether ester) with varying benzene dithiol monomers. (Ratio 1:4 = the molar ratio of HS to BS)

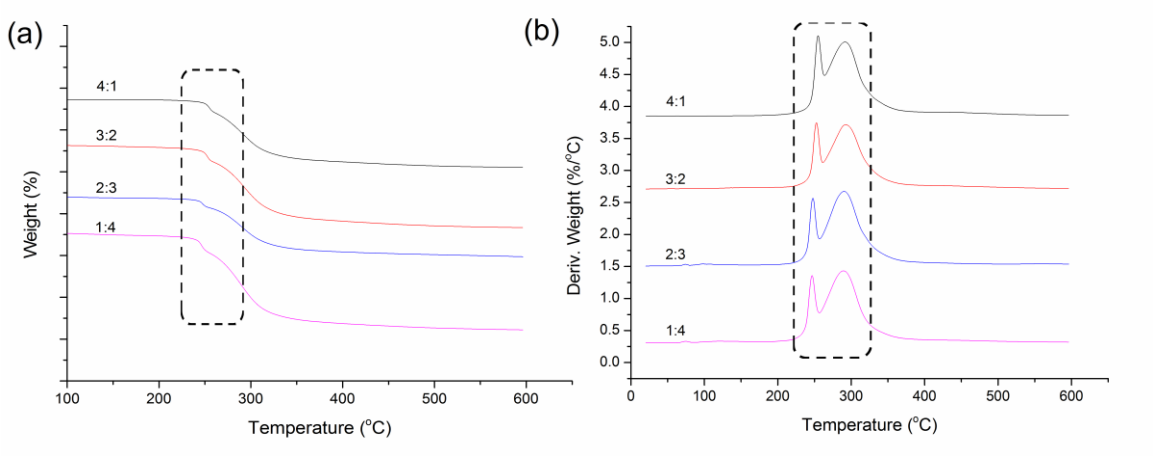

Figure 4.11 TGA curves of copoly(β-thioether ester) with different HS/BS feed ratios

4.4.5 Crosslinking poly(β-thiother ester) with bismaleimide and retro Diels-Alder reaction study

The DA reaction was first investigated in $CDCl_3$ by ^1H NMR using model compounds BHF and bismaleimide (**Figure 4.12**). Due to the poor solubility of BHF in $CDCl_3$, a small amount of DMSO-d_6 was added to dissolve BHF completely. The conversion of the furan rings to DA adduct was calculated according to the integration of the furan proton signals or the maleimide protons signals. It has been suggested that the DA reaction was influenced by several factors, such as the substituents of the furan or the maleimide, the reaction temperature and the solvent, along with the concentration of reactants.[196] The results showed that the DA reaction of BHF and bismaleimide could reach over 55 % conversion at 25 ºC and 84 % conversion at 40 ºC after 48 h in $CDCl_3$. Nguyen *et al.* have also investigated the model DA reaction between BHF and bismaleimide in DMSO-d_6 at varying temperatures and concentrations.[182h] It was observed that the conversion of the furan rings reached 80 % at 20 ºC, and 95 % at 40 ºC after 24 h. Moreover, the increase in the concentration of malemides groups could accelerate the reaction, and increase the conversion as well. While a high conversion of furan rings to DA adduct could be achieved in DMSO, $CHCl_3$ was used to dissolve the polymers since it is easy to evaporate and therefore makes the preparation of the films simpler.

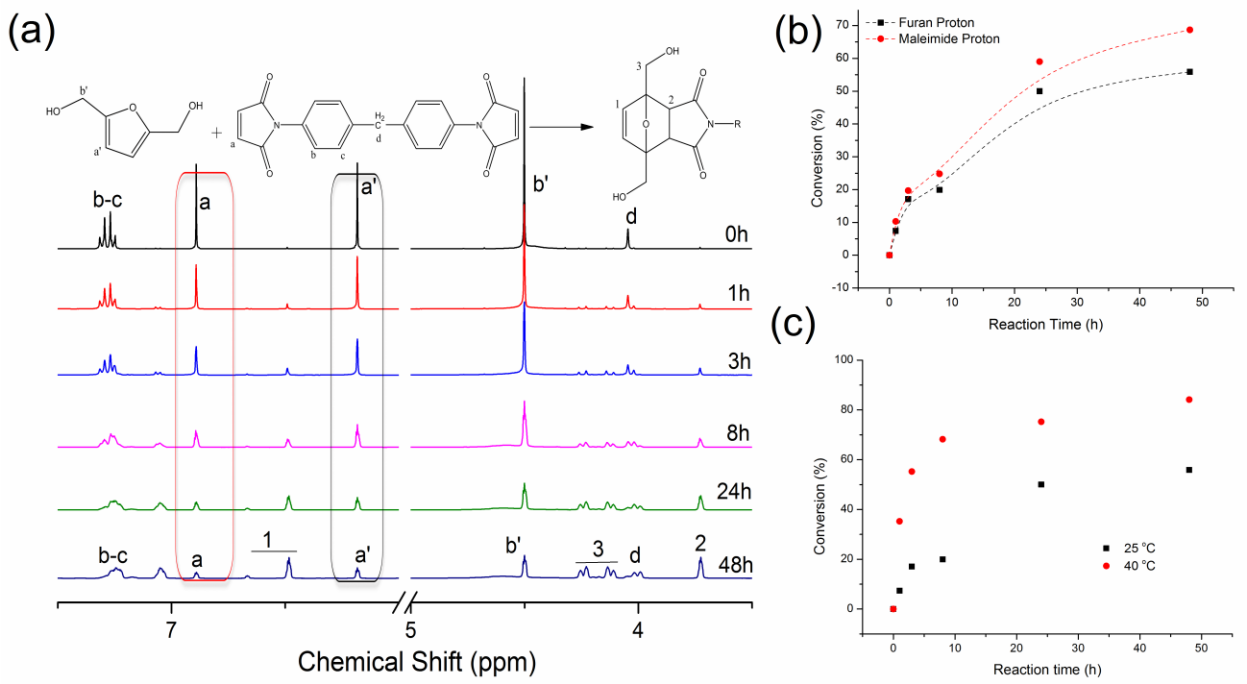

Figure 4.12 a) ^{1}H NMR spectra of DA reaction between BHF and bismaleimide at room temperature (the molar ratio of BHF to bismaleimide=2:1, $CDCl_3$ as solvent with a small amount of DMSO-d_6); b) Furan or maleimide conversion as a function of time; c) Furan conversion versus reaction time at 25 °C and 40 °C, respectively

The crosslinked films were prepared by the DA reaction between bismaleimide (M) and poly(β-thiother ester) (PHF) (**Scheme 4.3**). The weight ratio of polymers to bismaleimide (PHF/M) was set to 10:1, 4:1 and 2:1, respectively. For example, PHF/M 2:1 indicates that the weight ratio of PHF to bismaleimide was 2:1. The gel fractions of crosslinked films were 98.7 % (PHF/M 2:1), 93.1 % (PHF/M 4:1) and 92.5 % (PHF/M 10:1), respectively, indicating the high efficiency of the DA reaction to crosslink PHF. Yoshie *et al.* also observed that the gel fraction of DA crosslinked polyesters synthesized from 2,5-bis(hydroxymethyl)-furan and succinic acid could reach over 97 %. The 3 % loss was due to the presence of partially crosslinked polyesters.[182c] In addition, the swelling ratio of the three crosslinked films was determined after immersion in chloroform. As expected, the swelling ratio of the films was related to the crosslinking ratio, and the values were 127 % for PHF/M 2:1, 211 % for PHF/M 4:1, and 282 % for PHF/M 10:1. **Figure 4.13** shows typical FTIR spectra of the films. As the weight ratio of bismaleimide to polymers increased from 1:10 to 1:2, the intensity of the signal at 1715 cm^{-1} assigned to the carbonyl groups of maleimide significantly increased (**Figure 4.13b**). The signal

at 690 cm^{-1} attributed to the protons of the maleimide ring disappeared, except for the film with high loading of crosslinker (PHF/M 2:1). In fact, the intensity of the peak at 690 cm^{-1} was very small, and the data shown in **Figure 4.13c** were enlarged by 100 times. These results were consistent with other observations,[182c] indicating that most of the maleimide groups could efficiently react with the furan rings in the polymer chains.

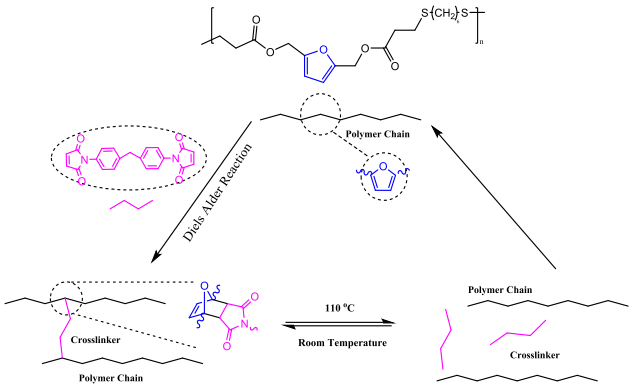

Scheme 4.3 2,5-FDA based poly(β-thioether ester) crosslinked by bismaleimide

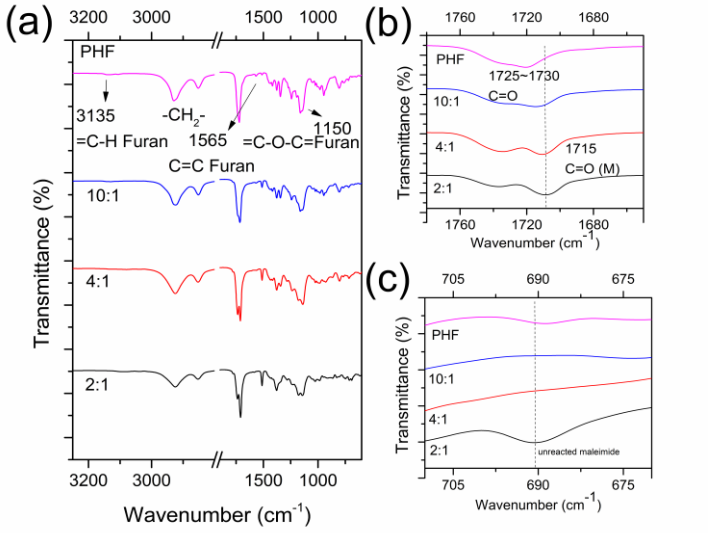

Figure 4.13 a) FTIR of crosslinked poly(β-thioether ester) with different crosslinker ratios; b) carbonyl peak region; b) protons peak region of maleimide (signals * 100).

The polymer network could be de-crosslinked *via* the retro DA reaction when heated (**Scheme 4.3**). The temperature of the retro DA reaction varied depending on the structure of the polymers and the reaction conditions. For example, Tang *et al.* reported that the DA crosslinked networks could dissolve into toluene after heating at 120 °C for 10 mins.[182i] However, it was demonstrated

by Caillol *et al.* that the DA crosslinked networks could be entirely soluble in DMSO after heating at 110 °C for 2h.[182e] Therefore, a thermal treatment was carried out at 110 °C to observe the retro DA reaction. The film (PHF/M 4:1) was chosen for this experiment. The crosslinked poly(β-thiother ester) was first put in DMSO-d_6 for 60 mins. Visually, the film failed to dissolve into DMSO-d_6. Moreover, a ^{1}H NMR spectrum showed no signal of polymer or bismaleimides (**Figure 4.14-0h**). The sample was then heated at 110 °C for 4 h. After 1 h, the network started to partially dissolve into the solvent. After 4 h, a homogeneous solution was observed. ^{1}H NMR was further used to identify the crosslinkers and poly(β-thiother ester) produced after the thermal treatment (**Figure 4.14**-1h, 3h and 4h). The intensity of the signals in the ^{1}H NMR gradually increased with time (1 h to 4 h). After 4 h, the intensity of the signals kept constant, which indicated the end of the retro DA reaction. The characteristic signals of the furan rings in the polymer chains and bismaleimide for a and a' protons were observed at 6.5 and 7.1 ppm, respectively. This confirmed the integrity of the poly(β-thioether ester) backbone and maleimide groups after thermal treatment, allowing the multiple reversibility of the DA reaction.

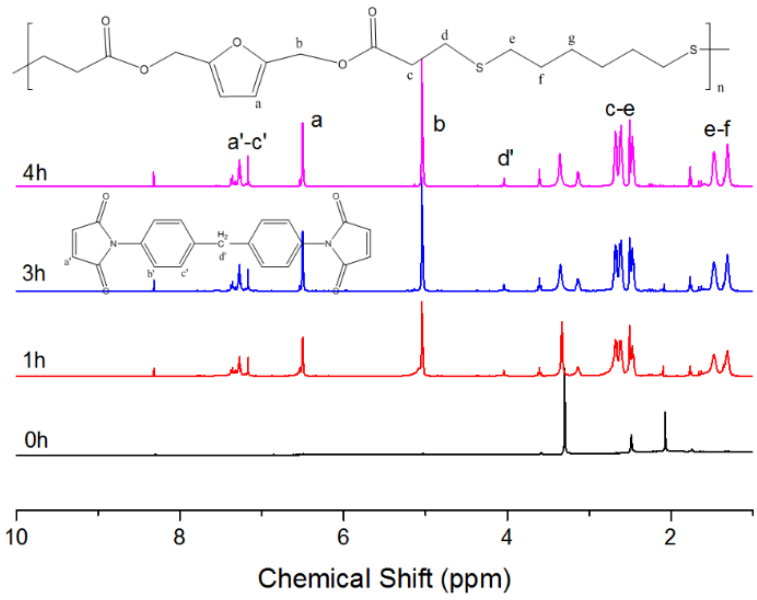

Figure 4.14 ^{1}H NMR spectra recorded at 110 °C in DMSO-d_6 for the retro DA reaction of furan-bearing poly(β-thiother ester) and bismaleimide

4.4.6 Mechanical properties of crosslinked poly(β-thioether ester)

The thermomechanical properties of polymers crosslinked by the DA reaction were evaluated using dynamic mechanical analysis (**Figure 4.15**).

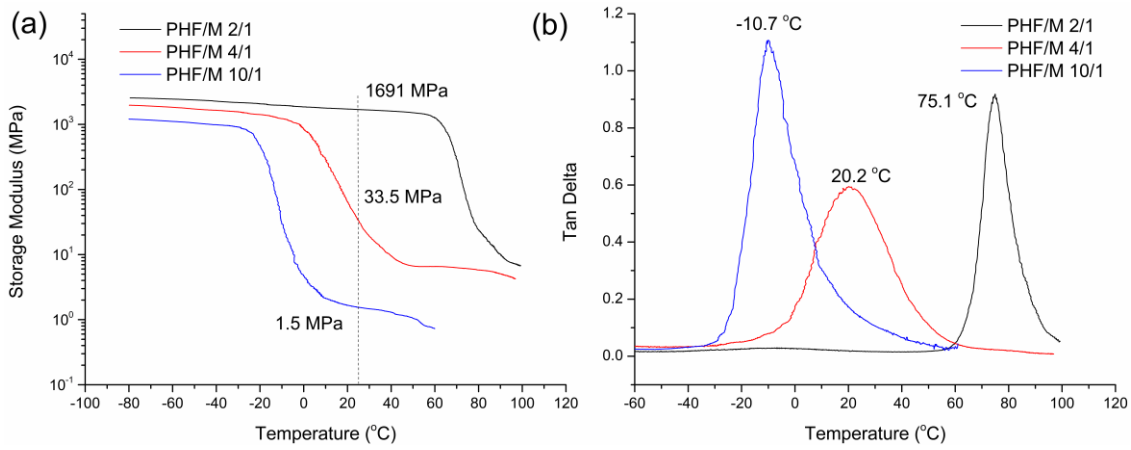

Figure 4.15 Storage modulus (a) and Tan δ (b) of crosslinked poly(β-thioether ester) with different ratios of polymers to crosslinkers

For film PHF/M 10:1, it ruptured at ~60 °C, while films (PHF/M 4:1 and 2:1) could be tested to up to 100 °C. It was observed that the properties could be easily modulated by adjusting the weight ratio of polymers to bismaleimide. The storage modulus (G') of the films at 25 °C significantly increased as the ratio of polymers to bismaleimide increased. For example, the G' of PHF/M 2:1 (1691 MPa) was over 1000 times higher than for PHF/M 10:1 (1.5 MPa). Moreover, it was higher than some networks synthesized *via* thiol-Michael addition polymerization (< 500 MPa).[181] Importantly, the crosslinked poly(β-thioether ester) could be simply reprocessed *via* heating the networks over 110 °C in an organic solvent. These properties can be ascribed to the fact that changes in the ratio of polymer to crosslinker lead to different crosslinking densities. The T_g of crosslinked polymers were -10.7, 20.2 and 75.1 °C, as determined from the maximum peaks of the tan δ curves (**Figure 4.15b**). The T_g of the most crosslinked polymer (PHF/M 2:1) was found to be comparable or even higher than some other networks directly synthesized *via* the thiol-Michael, thiol-ene or thiol-epoxy reaction, but lower than thiol-maleimide networks.[197]

The stress strain curves of crosslinked films at 25 °C are given in **Figure 4.16**. As the ratio of crosslinkers to polymers increased, the Young's modulus increased from 7.9 ± 0.5 MPa (PHF/M

10:1) to 1294 ± 105 MPa (PHF/M 2:1), while sample PHF/M 4:1 showed a similar Young's modulus value (8.5 ± 0.7 MPa) to PHF/M 10:1. The largest elongation at break (%) was observed to be 80 % (PHF/M 4:1). During the preparation of films using chloroform as the solvent (PHF/M 10:1), the crystallization of PHF was observed (**Figure 4.16c**). The presence of these crystals explained the low elongation at break (18 %). However, for the films with higher crosslinking densities, no crystallization of PHF was observed (PHF/M 4:1 and 2:1). These results were consistent with other observations where the DA reaction and the crystallization of polymers was competing processes.[198] When the crosslinking densities were high, the DA reaction was found to suppress the crystallization of PHF. In addition, the crosslinked film (PHF/M 2:1) was remolded by compression and heated to investigate its reprocessing ability. Pieces of the crosslinked film were processed under a pressure of 30 MPa for 15 mins at 140 ^{o}C to produce a new film. The film was further maintained at 80 ^{o}C for 2 hours before slowly cooling to room temperature. **Figure 4.16b** shows typical FTIR signals for uncompressed and compressed films. The tensile test revealed that the Young's modulus of the remolded film was 305 ± 24 MPa. Picchioni *et al.* investigated the mechanical properties of remolded films crosslinked *via* DA reaction.[181j] They suggested that the mechanical properties of remolded films decreased due to the decreased crosslinking density after hot compression. In addition, the film after reprocessing was still uniform as observed by SEM (**Figure 4.17**), although the remolded film showed a relatively rougher surface as compared to the original film.

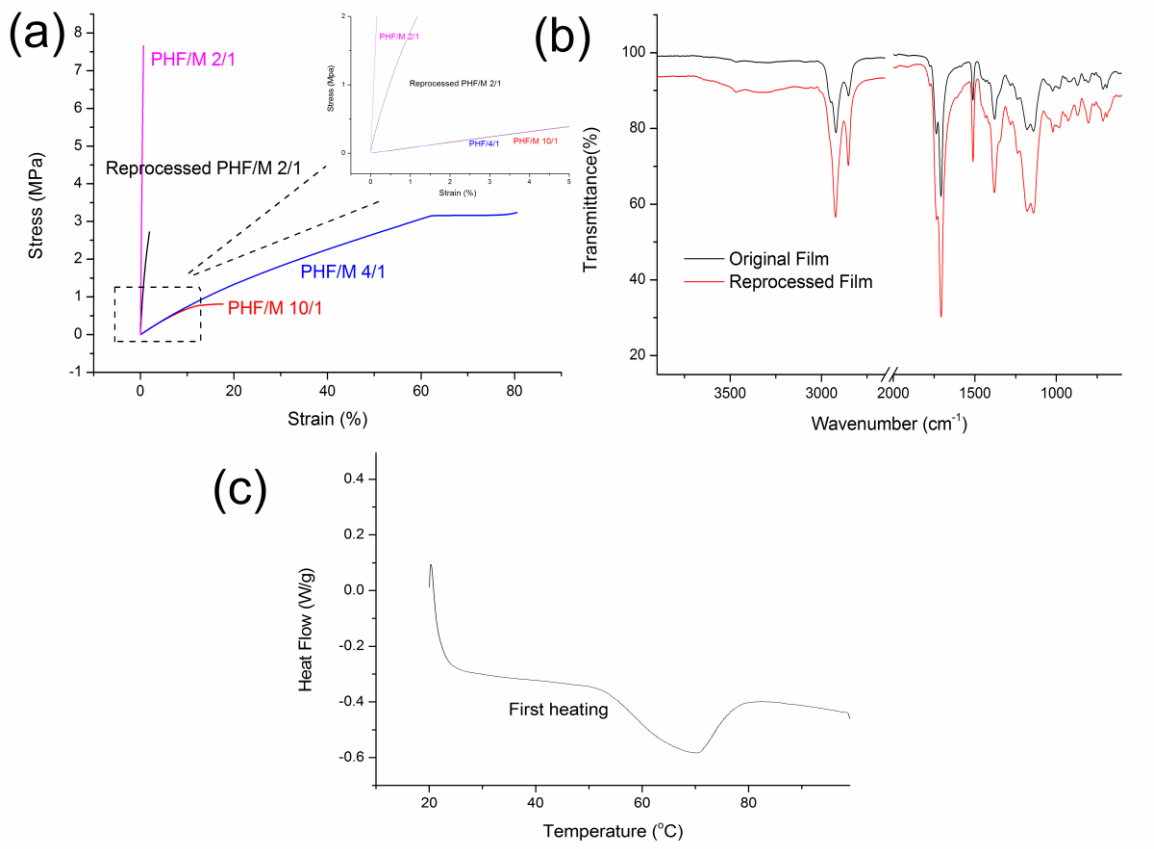

Figure 4.16 a) Strain-stress curves of crosslinked films (PHF/M 2:1) and film after compression molding; b) FTIR of films before and after reprocessing; c) DSC curve of crosslinked polymers (PHF/M 10:1).

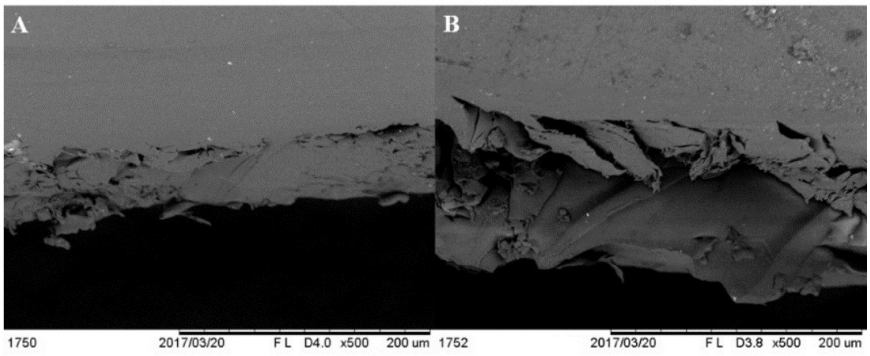

Figure 4.17 SEM observations of film before (A) and after (B) reprocessing.

4.4.7 Synthesis and physical properties of TPEs

Due to the presence of interactions between carbonyl groups and the hydroxyl groups observed in POF (**Figure 4.1c**), it was expected that these interactions might function as physical crosslinking points to provide elasticity to the TPEs. Therefore, HMF derivative based TPEs

were prepared by a two-step thiol-Michael addition reaction (**Figure 4.18a**). At first, the prepolymers were synthesized by reacting 2,5-FDA and 1,3-propanedithiol (1,3-PDT). The molecular weights and the end groups of the prepolymers can be controlled by varying the feeding ratios of the two monomers (**Table 4.2**). Therefore, 1,3-PDT was reacted with an excess of 2,5-FDA to synthesize the acrylate-terminated prepolymers. For example, when the ratio of 2,5-FDA to 1,3-PDT was 1.3 to 1, the molecular weight of the prepolymer determined by GPC was 2500 g/mol. The structure of the synthesized prepolymers was investigated by ^{1}H NMR (**Figure 4.18a**). The signals corresponding to the protons (c', d' and e') of the acrylate groups were observed at δ = 5.5-6.5 ppm, indicating the presence of acrylates end groups. The soft prepolymers were further reacted with DL-dithiothreitol to introduce hydroxyl groups to the copolymers (**Figure 4.18a**). The formation of hydrogen bonds among hydroxyl groups or between hydroxyl groups and ester groups might have provided elasticity to the TPEs. Since the reaction between the prepolymers and DL-dithiothreitol can also be efficiently initiated using DMPP as the catalyst, the TPEs synthesis showed several advantages, such as mild reaction conditions, a short reaction time, and the polymerization which occurred in a one-pot reaction without purification. The structure and composition of the synthesized TPEs were analysed by NMR. Typical ^{1}H and ^{13}C NMR spectra of TPEs are shown in **Figure 4.18b and c**. The ratio of 2,5-FDA to 1,3-PDT to DL-dithiothreitol was 1.3:1:0.3. The molar ratio of total thiols to acrylate groups was kept to 1 to obtain TPEs with high molecular weights. After the second reaction between the prepolymers and DL-dithiothreitol, the signals of the acrylate protons disappeared. A new signal at δ= 3.6-3.8 ppm belonging to the protons next to the hydroxyl groups was observed. All proton signals have been assigned (**Figure 4.18b**). The ^{13}C NMR spectrum of TPEs confirmed the occurrence of the reaction as well. A signal at δ= 70.8 ppm was assigned to the carbon connected to the hydroxyl groups (**Figure 4.18c**). The ATR-FTIR spectra of TPEs are presented in **Figure 4.19**. Characteristic bands, such as C-H stretching vibrations at 3135 cm^{-1} and the ring vibration of the =C-O-C= groups at 1150 cm^{-1}, were assigned to the furan rings. Carbonyl C=O stretching vibrations were observed at around 1730 cm^{-1}. The bands at 2910−2950 and 2850−2860 cm^{-1} were assigned to the asymmetric and symmetric stretching vibrations of the CH_2 groups, respectively. Furthermore, a broad O-H stretching absorption band (3400 cm^{-1}) was observed in all samples. While the presence of interactions between carbonyl groups and the hydroxyl groups leading to the shift of carbonyl stretching vibrations to a lower

wavenumber has been observed in the POF, this observation was not confirmed here probably due to the low intensity of the shifted signal.

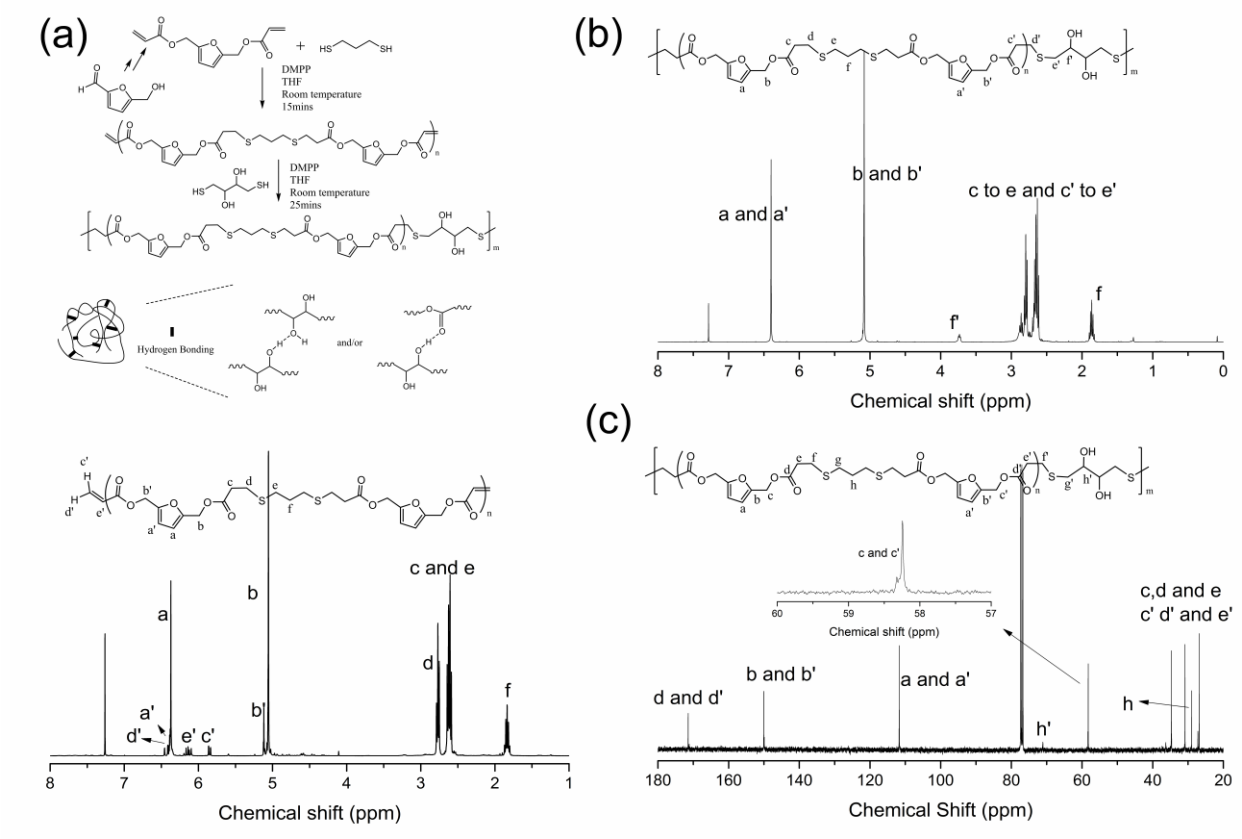

Figure 4.18 a) Synthetic routes of TPEs from HMF derivative and ^{1}H NMR spectrum of prepolymers ending with diacrylates groups; b) ^{1}H and c) ^{13}C NMR spectra of TPEs.

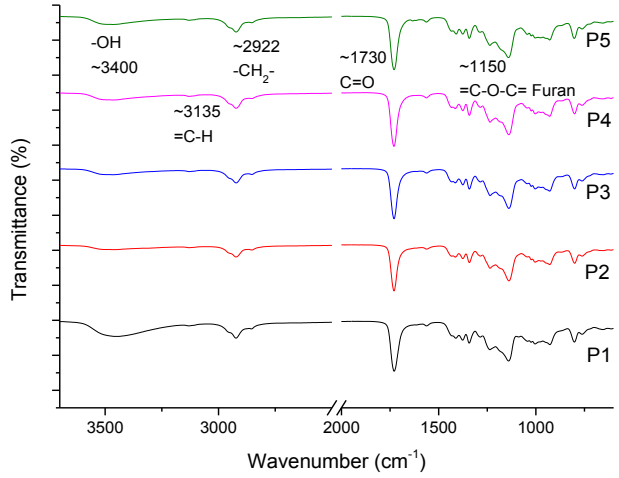

Figure 4.19 FTIR spectra of TPEs synthesized *via* thiol-Michael addition polymerization.

It has been suggested that the ratio of hard segments to soft segments significantly influenced the properties of TPEs. To adjust the composition of the TPEs, two approaches were tested. The first approach involved controlling the molecular weights of the prepolymers by varying the feeding ratio of 2,5-FDA and 1,3-PDT. As shown in **Table 4.4**, P1, P2 and P3 were synthesized using ratios of 2,5-FDA to 1,3-PDT equaling to 1.3 to 1, 1.4 to 1, and 1.5 to 1. Another technique was to increase the hard segment content while keeping the molecular weight of the soft segment content constant. For example, for P4 and P5, the prepolymers were first synthesized using 1.3 eq. of 2,5-FDA and 1 eq. of 1,3-PDT. Then, another 0.5 eq. of DL-dithiothreitol and 0.2 eq. of 2,5-FDA were added to synthesize TPEs (**Table 4.4**). The experimental ratio of 1,3-PDT to DL-dithiothreitol added to TPEs can be calculated according to the integration area ratio of the characteristic peaks at δ = 1.8-1.9 ppm (f) to δ= 3.6-3.8 ppm (f'), which are shown in Table S3. For P1, P2 and P3, the theoretical ratio was close to the experimental one, indicating the efficiency of the thiol-Michael addition reaction to synthesize TPEs. However, for P4 and P5, the addition of DL-dithiothreitol was less effective. For example, the ratio of 1,3-PDT to DL-dithiothreitol varied from 10:7 (theoretical ratio) to 10:6.2 (determined by 1H NMR). This might explain the relatively low molecular weights of the synthesized TPEs, as compared to P1 to P3. The polydispersity index of P4 and P5 was also higher than P1 to P3, indicating the broader distribution of the molecular weights in P4 and P5.

Table 4.4 Polymerization conditions and molecular weights of TPEs

Samples	P/D[a]	P/D[b]	M_n (kg/mol)[c]	PDI	T_g (°C)[d]	$T_{5\%}$(°C)[e], T_{max}(°C)[f]
P1	10/3	10/3.1	20.5	2.0	-22.0	245, 249/282
P2	10/4	10/3.8	19.2	2.1	-20.1	242, 247/280
P3	10/5	10/4.8	16.9	2.0	-19.1	242, 246/277
P4	10/5	10/4.5	13.0	2.3	-22.6	242, 247/280
P5	10/7	10/6.2	13.9	2.6	-16.1	238, 242/277

[a] The feeding molar ratio of 1,3-propanedithiol to dithiothreitol. [b] The molar ratio of 1,3-propanedithiol to dithiothreitol determined *via* ^{1}H NMR spectra. [c] The number average molecular weight and PDI (M_w/M_n) determined by GPC calibrated with polystyrene. [d] Glass transition temperature. [e] $T_{5\%}$ indicates the 5% weight loss of polymers under a nitrogen atmosphere. [f] T_{max} indicates the temperature of maximal rate of decompositions.

4.4.8 Physical properties of TPEs

The thermal transitions, stability, and viscoelastic properties of all TPEs are presented in **Figures 4.20, 4.21 and 4.22**. The DSC results showed that the T_g values of all TPEs determined in the second heating curve were in the range of -25 to -15 ^oC (**Figure 4.20**). No crystallization peak was observed in the cooling curve, probably due to the poor crystallization ability of these furan based TPEs. Furthermore, only one T_g was observed in all DSC profiles. All T_g values were higher than polymers synthesized from 2,5-FDA and 1,3-PDT (-32 ^oC). The presence of hydrogen bonds was believed to decrease the mobility of the polymer chains, and therefore increased the T_g. These behaviours were different from other TPEs synthesized *via* thiol-Michael addition reaction. For example, when using N,N'-methylenebis(acrylamide) as the chain extender, He *et al.* observed that, in addition to one T_g, multiple melting peaks appeared from 35 to 100 ^oC as a result of the dissociation of intermolecular hydrogen bonds.[183b] When using 4,4'-methylenebis(phenylisocyanate) as the chain extender, Hoyle *et al.* observed that there were two T_g corresponding to the hard and soft segments, in addition to the melting peak.[183a] However, when using isophorone diisocyanate or tolylene-2,4-diisocyanate as the chain extender, only one T_g was observed, which was similar to this work. These comparisons show that the structures of the chain extender can significantly influence the thermal transitions of TPEs. All the TGA profiles showed a similar two-stages degradation process (**Figure 4.21**). The decomposition temperature at 5% weight loss of all TPEs was around 230-250 ^oC, indicating their good thermal stability. The degradation temperature of TPEs observed at the second degradation stage was around 275-280 ^oC. DMA was used to evaluate the viscoelastic behaviour of TPEs (**Figure 4.22**). All the TPEs showed similar transitions in both the storage modulus (G') and tan δ as a function of the temperature. The rubbery plateau started at around 0 ^oC for all samples. No significant effect of the soft segments molecular weights and the soft-hard segments ratio on the G' was found. The T_g of all TPEs determined by the DMA were slightly higher than those determined by the DSC.

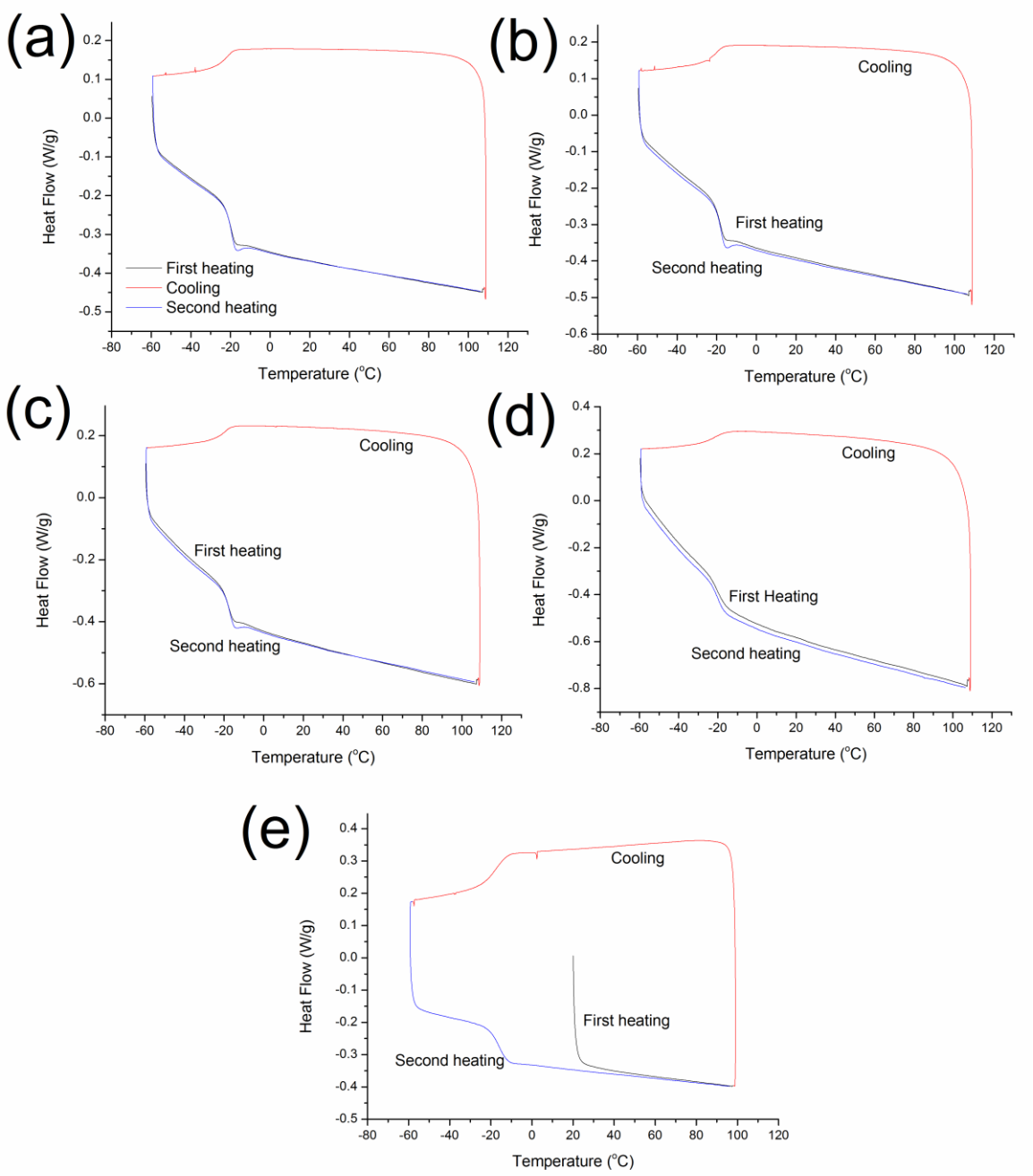

Figure 4.20 DSC curves of TPEs P1 (a), P2 (b), P3 (c), P4 (d) and P5 (e) synthesized from HMF derivative *via* thiol-Michael addition polymerization. Measured at a heating rate of 10 °C/min, a cooling rate of 5 °C/min.

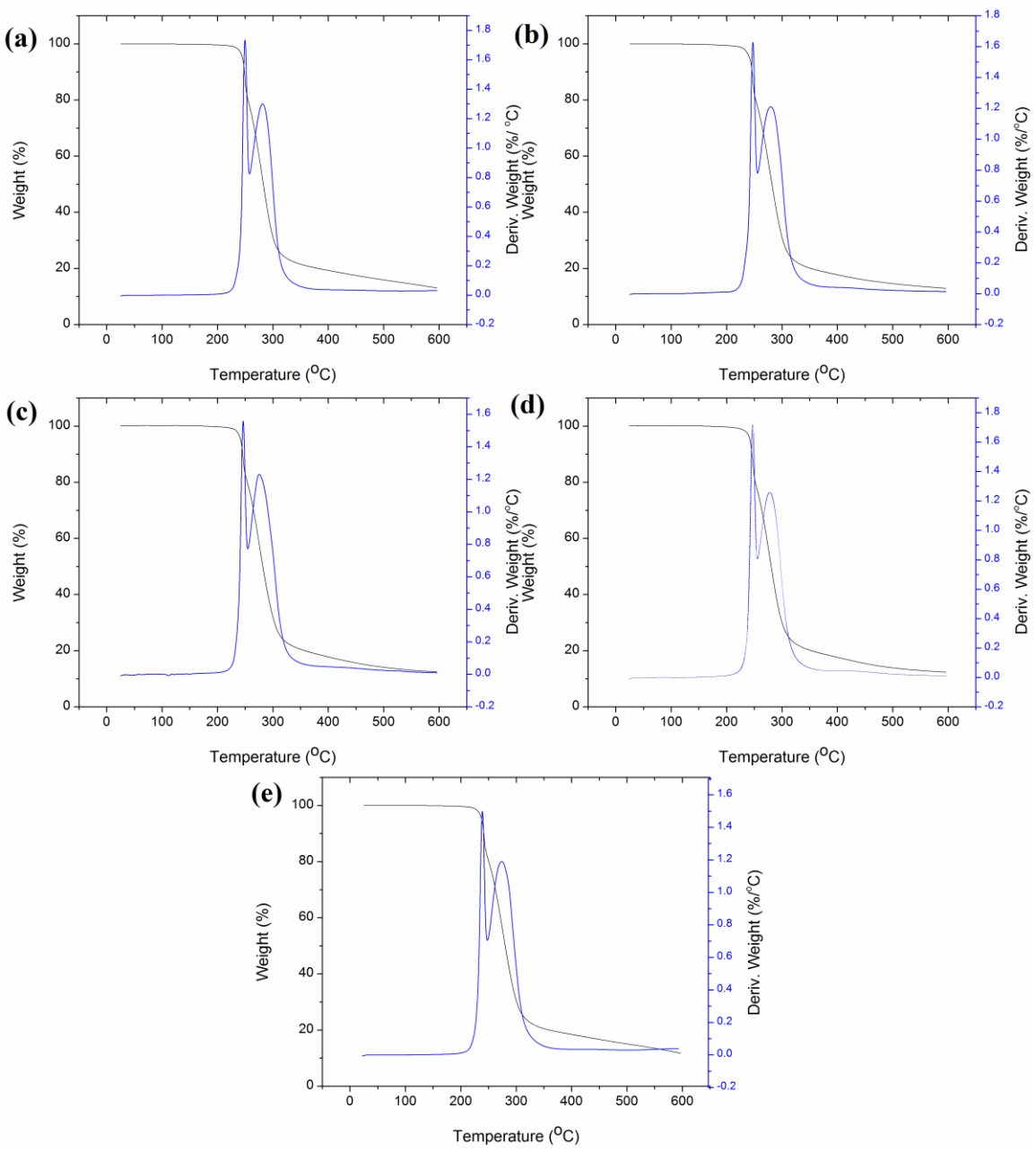

Figure 4.21 TGA curves of TPEs P1 (a), P2 (b), P3 (c), P4 (d), P5 (e).

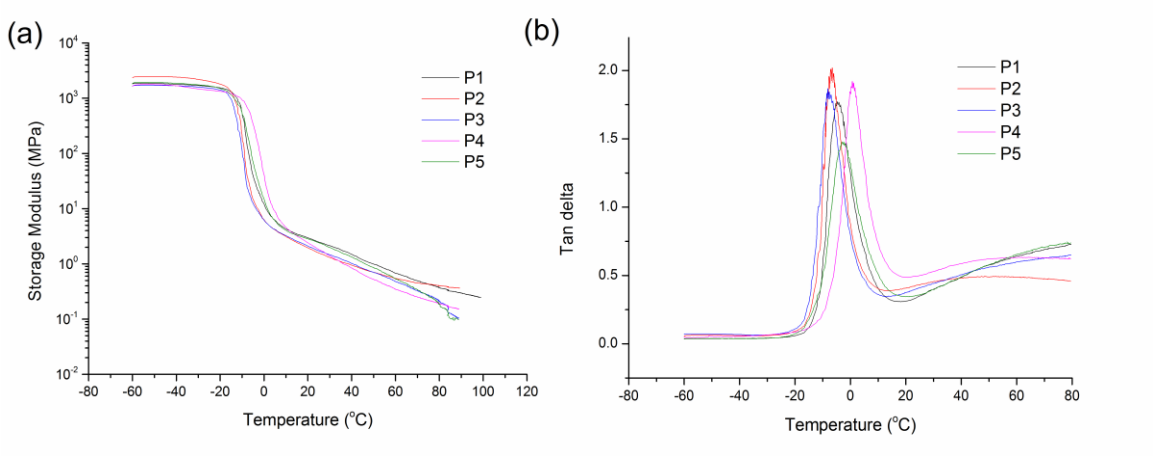

Figure 4.22 DMA curves of TPEs: a) Storage modulus vs. temperature, b) Tan delta as a function of temperature.

The stress-strain curves of P1, P2 and P3 are shown in **Figure 4.23**. At low strains, a linear response was observed in the curve. The mechanical properties of 2,5-FDA based TPEs were similar to other TPEs, such as poly(glycerol sebacates), which have been used in a variety of biomedical applications.[199] The Young's modulus and ultimate tensile strength of P2 were 0.34 ± 0.02 MPa and 0.37 ± 0.04 MPa, respectively. The elongation at break (P3, > 450%) was comparable to some TPEs synthesized from other renewable resources.[200] Since P2 had the maximum ultimate tensile strength value (0.37 ± 0.04 MPa), the elasticity of P2 was determined. For each stress-strain test, P2 was stretched to 150 % strain, and was then maintained for 1 min (**Figure 4.23b**). Between each cycle, the sample was maintained at zero stress for another 2 mins to allow the sample to recover. The recovery was measured by observing the residual strain after the sample was unloaded. A residual strain of 16% was observed after the first cycle. For the second and third cycles, the residual strain values were 5% and 8%, respectively. In addition, the DA reaction between bismaleimide and the furan rings of the TPEs was used to tune the mechanical properties. The sample used was P2. The FTIR results confirmed the occurrence of the DA reaction due to the presence of a signal at 1715 cm^{-1} assigned to the carbonyl groups of maleimide, together with the absence of a signal at 690 cm^{-1} attributed to the protons of the maleimide ring (**Figure 4.24**). The stress-strain curves of DA crosslinked P2 showed that the Young's modulus and ultimate tensile strength were significantly improved to 3.5 ± 0.2 MPa and 2.3 ± 0.1 MPa respectively, as compared to P2 (0.34 ± 0.02 MPa and 0.37 ± 0.04 MPa, respectively) (**Figure 4.23c**). The elongation at break of the DA crosslinked P2 was 109.3 ±

4.7%. These results indicated that the DA reaction was an efficient approach to improve the Young's modulus and the tensile strength of 2,5-FDA based TPEs. The formation of crosslinking points *via* the DA reaction may have a similar behaviour as chain entanglements.[201]

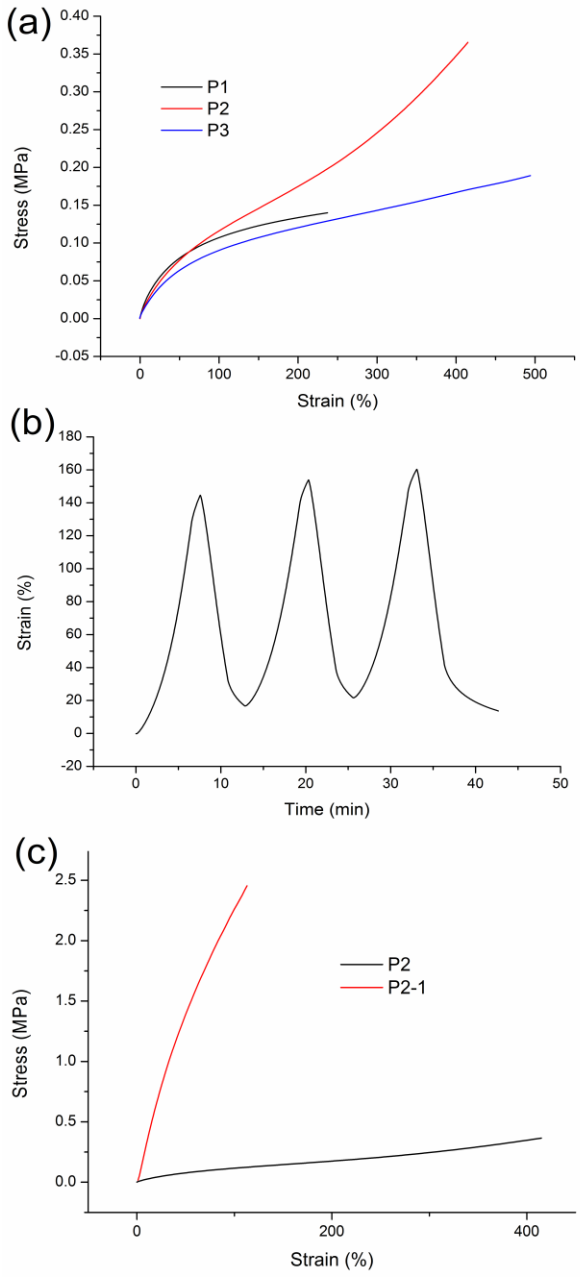

Figure 4.23 Stress–stain curves of TPEs P1, P2 and P3. (b) Strain–time curve of TPEs (P2) with three stress–relaxation cycles at 25 °C. (c) Stress-strain curve of P2 and P2-1 (the weight ratio of P2 to crosslinkers = 10:1).

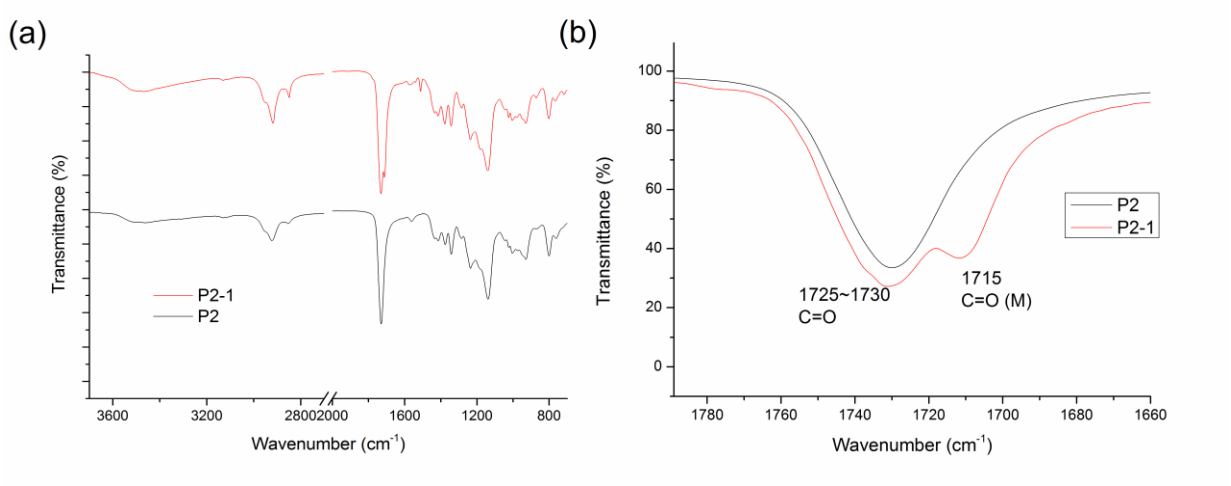

Figure 4.24 a) FTIR of P2 and crosslinked P2-1 *via* Diels-Alder reaction (weight ratio of P2 to crosslinker = 10:1); b) carbonyl peak regions.

4.5 Conclusions

This chapter described the synthesis and characterization of poly(β-thiother ester) *via* the thiol-Michael addition polymerization using DMPP as the catalyst under mild conditions. A variety of dithiol monomers were used to yield a range of linear poly(β-thiother ester) with different physical properties. The number average molecular weights of poly(β-thiother esters) obtained were ranging from 10,000 to 22,000 g/mol. The T_g of poly(β-thiother esters) were greatly improved when adding dithiol monomers with aromatic rings or hydroxyl groups, as compared to the aliphatic dithiol monomers. The obtained linear polymer with hydroxyl groups as side groups could be used as a hot melt adhesive on wood substrates since it had an adhesive strength of 1.5 MPa. The synthesis of copoly(β-thiother esters) was also investigated using two dithiol monomers with different *pKa*. The ^{1}H NMR and DSC results revealed that DMPP could efficiently initiate the thiol-Michael addition polymerization regardless of the *pKa* of the thiols groups due to the formation of a strong base *via* the nucleophilic attack on the Michael acceptor. Additionally, the DA reaction between furan rings and maleimide moieties was exploited to tune the properties of the materials. The mechanical properties of the synthesized films could be significantly enhanced due to the synthesis of DA adducts as crosslinking points in the networks. The synthesis of 2,5-FDA based TPEs using thiol-Michael addition polymerization showed several advantages, such as the occurrence in a one-pot reaction at room temperature and at a short reaction time. The presence of intermolecular hydrogen bonds between hydroxyl groups

and hydroxyl groups, or between hydroxyl groups and ester groups, might have acted as physical crosslinking points, giving the materials elasticity. The maximum elongation at break of TPEs could reach above 450 %. The elasticity of TPEs was observed by subjecting the samples to cycles of loading and unloading at a strain of 150 %. Additionally, the DA reaction also provided an efficient way to improve the mechanical properties of 2,5-FDA based TPEs. These new bio-based furan linear polymers or networks may be used as reversible adhesive, self-healing or recycled materials, and coating applications. Moreover, these results indicated that high performance TPEs with tunable properties might be efficiently synthesized in the future using the thiol-Michael addition *via* the structural design of renewable monomers.

Connecting Statement 3

The work in Chapter 4 investigated the synthesis and characterization of polymers having different structures and properties, the possibility of using the thiol-Michael addition reaction for copolymer synthesis, the adhesive properties of the polymers, and the utilization of the DA and retro-DA reaction to dynamically improve the properties of linear poly (β-thioether ester). Furthermore, TPEs were synthesized by the thiol-Michael addition reaction using 2,5-FDA and two different dithiols.

Although TPEs showed a relatively high elongation at break (> 450%), further improvement in the Young's modulus and tensile strength were desirable. The preliminary results showed that the presence of furan rings in the linear polymers could function as reactive sites to be crosslinked, and the mechanical properties of TPEs were significantly improved. Although covalent bonds were generated in the thermoset elastomers, the reversibility of the DA reaction still allowed the elastomer to be reprocessed.

Therefore, it was hypothesized that a thermoset elastomer could be synthesized *via* the combination of the thiol-Michael addition and DA reaction. The ratio of polymers to crosslinkers was used to adjust the thermal and mechanical properties of the elastomers. In addition, due to the high efficiency of DMPP to catalyze the thiol-Michael addition to copolymers, the compositions and the properties of elastomers were therefore adjustable.

The synthesis and characterization of 2,5-FDA based thermoset elastomers were investigated in Chapter 5. Furthermore, this chapter is based on the manuscript submitted for publication with Dr. Marie-Josée Dumont.

Chapter 5: Reprocessable 5-hydroxymethylfurfural Derivative-based Thermoset Elastomers Synthesized through the Thiol-Michael and Diels-Alder Reactions

5.1 Abstract

The combination of the thiol-Michael addition reaction and the Diels-Alder reaction (DA) was exploited to synthesize thermoset elastomers from 5-hydroxymethylfurfural derivative. The first step involved the synthesis of linear poly(β-thioether ester) *via* the thiol-Michael addition polymerization of 2,5-furan diacrylate (2,5-FDA) and 1,3-propanedithiol. Then, the DA reaction between the furan rings and the maleimide groups allowed the linear polymers to be dynamically crosslinked to reprocessable elastomers. When the weight ratio of polymers to crosslinker was 5:1, the Young's modulus, ultimate strength, and elongation at break were 4.3±0.6 MPa, 5.7±1.1 MPa, and 205.3±20.1%, respectively. Moreover, a high elastic recovery (98.9%) and low residual strain (0.7%) were observed after the third cycle during the cyclic tensile test. Additionally, the structures, properties and functionality of elastomers were varied *via* the synthesis of linear copoly(β-thioether ester) using DL-dithiothreitol or poly (ethylene glycol) diacrylate as comonomers. Furthermore, the mechanical properties of the elastomers were adjusted by the incorporation of 1,6-hexanedithiol or 1,4-butanediol diacrylate as comonomers. The reprocessability of elastomers was demonstrated by heating the crosslinked film in dimethylformamide solution to a new film. The advantages of these 2,5-FDA based elastomers include the easy synthesis process and mild reaction conditions, the good elasticity, and their reprocessability.

5.2 Introduction

Renewable 5-hydroxymethylfurfural (HMF) has been regarded as a promising chemical due to its potential to be derivatized, enabling this platform chemical to be suitable for the synthesis of biofuel precursors, fine chemicals and monomers to polymers.[202] In the area of polymers synthesis, current research mainly focuses on using 2,5-furandicarboxylic acid to (co)polymers and thermoset networks.[203] The information on the utilization of other HMF derivatives is less available, particularly to synthesize high performance materials.[204]

The thiol-Michael addition reaction offers several advantages such as rapid reaction rate, high conversion ratio, and mild reaction conditions.[205] There are a variety of applications including networks and hydrogel synthesis, monomers derivatization, and polymer modification.[206] Currently, a great deal of research has been focusing on the improvement of the properties of materials containing thioether groups, such as the synthesis of networks using monomers with rigid structures, the oxidation of thioether to sulfone groups, and the preparation of hybrid materials.[207] Elastomers have been synthesized by the thiol-Michael addition reaction as well through the flexible thioether groups in the polymeric chains.[208] For example, Ware *et al*. designed a liquid crystalline elastomer *via* the thiol-Michael addition reaction using a liquid crystal monomer with diacrylate groups and a dithiol monomer.[208a] However, the lack of reprocessability and the impossibility to recycle these networks caused environmental concerns.[209] He *et al.* and Hoyle *et al.* reported the synthesis of thermoplastic elastomers using the thiol-Michael addition reaction. Although these elastomers had potentials to be melt-reprocessed, their relatively poor solvent resistance and unsatisfactory elasticity limited their applications.[208d, 208e] Recently, the introduction of dynamic covalent bonds into polymer networks has been widely evaluated as a powerful approach towards design materials with high performance, without losing the reprocessing and recycling ability.[210] Among them, networks synthesized *via* the Diels-Alder (DA) reaction have been investigated, and the ability of networks to be reprocessed or recycled was observed.[211]

However, most of the research investigated the DA reaction involving furan rings as the end groups or as side chains.[212] Little information is available to directly synthesize polymers incorporating furan rings in the main polymer chains, and then evaluate the use of the DA reaction to crosslink linear polymers enabling the materials to be recycled or reprocessed.[210, 211, 213] Recently, the synthesis of HMF derivative based linear poly(β-thioether ester) *via* the thiol-Michael addition reaction has been reported.[210] Due to the presence of furan rings in the polymeric chains, the DA reaction occurred to crosslink linear polymers to networks.[214] However, networks exhibited a relatively low elongation at break (less than 80%) due to the crystallization of poly(β-thioether ester) synthesized from HMF derivative and 1,6-hexanedithiol. Given the high efficiency of the thiol-Michael addition, it is hypothesized that reprocessable elastomers

with tunable structures, properties and functionalities can be synthesized *via* the thiol-Michael and DA reaction through varying the structures of (co)monomers.

This chapter reports on the synthesis and the characterization of HMF derivative (2,5-FDA) based elastomers by using the DA reaction to crosslink linear polymers synthesized using the thiol-Michael addition. Additionally, hydroxyl or ether groups were incorporated in the elastomers to increase the functionalities of the elastomers using DL-ditihothreitol or polyethylene glycol diacrylate as comonomers. The mechanical properties of the elastomers varied when using 1,4-butanediol diacrylate or 1,6-hexanedithiol as comonomers. The reversibility of the DA reaction between the linear polymers and the maleimide crosslinker was confirmed by ^{1}H NMR analysis, which enabled the elastomers to be reprocessed. Due to the simple synthesis, mild reaction conditions, and easy incorporation of other functionalities, this strategy using two well-known "click reactions" may be widely used to synthesize HMF derivative based reprocessable elastomers.

5.3 Experimental Sections

5.3.1 Materials

Hydroxymethylfurfural (HMF, ⩾99%), 1,6-hexanedithiol (97%), 1,3-propanedithiol (⩾99%), 1,1'-(methylenedi-4,1-phenylene)bismaleimide (bismaleimide, 95%), DL-dithiothreitol (⩾98%), 1,4-butanediol diacrylate (90%), poly(ethylene glycol) diacrylate (M_n=700), triethylamine (TEA, ⩾99.5%), tetrahydrofuran (THF, anhydrous, ⩾99.9%, inhibitor free, and further dried under molecular sieves), *N*-phenylmaleimide (97%), acryloyl chloride (97%, contains <210 ppm MEHQ as stabilizer), dichloromethane (anhydrous, ⩾99.8%), dimethylphenylphosphine (DMPP, ⩾99%), DMSO-d_6 (99.9 atom % D), chloroform-d (99.8 atom % D), thin layer chromatography (TLC) plates, and silica gel were purchased from Sigma-Aldrich. All reagents were used as received without further purification.

5.3.2 General procedure for the synthesis of poly(β-thioether ester) and copolymers

The synthesis of 2,5-FDA from HMF and poly(β-thioether ester) (PPF) from 2,5-FDA and 1,3-propanedithiol *via* the thiol-Michael addition reaction was reported elsewhere.[210, 214] The synthesis of copolymers was performed in a similar approach. In a typical experiment, 2,5-FDA

(0.95 eq) was dissolved in THF (0.6 M). The comonomer (1,4-butanediol diacrylate) were then added (0.5 eq). The solution was purged under a nitrogen stream for 30 mins to remove the oxygen. 1,3-propanedithiol (1 eq) was then added through a syringe. The reaction mixture was cooled in an ice-bath. DMPP (0.005 eq) was added to start the polymerization process. The reaction was performed at room temperature for 30 mins. The copolymers were then precipitated in cold hexane and recovered by filtration. Finally, the copolymers were kept in a vacuum oven at room temperature overnight to remove the residual solvent.

5.3.3 Diels-Alder reaction and retro Diels–Alder

The model reaction between PPF (100 mg) and *N*-phenylmaleimide (20 mg) was chosen to evaluate the DA reaction in $CDCl_3$ (1.5 mL) at 40 ºC. ^1H NMR was recorded at fixed times to monitor the DA reaction. Furthermore, a ^1H NMR study was conducted to observe the retro-DA reaction. A sample of crosslinked polymer was first added in DMSO-d_6. The solution was subsequently heated at 130 ºC for 4h. The spectra were frequently recorded.

5.3.4 Film preparation and reprocessing of films

The elastomers were prepared by a solution casting method in chloroform. A mixture of polymers (150 mg) and bismaleimide (polymers/bismaleimide weight ratios of 5:1, 10:1, and 20:1) was first dissolved in chloroform (2.5 mL). The solution was then transferred into a Teflon mold, which was sealed for 24 h. The residual solvent was evaporated under atmospheric conditions, and then completely evaporated in a vacuum oven at 40 ºC for 48 h. This was performed to increase the conversion of furan ring to cyclohexene in the polymers. The films were held at room temperature for at least 24 h before analysis. The reprocessing of crosslinked films was performed as follows: 150 mg of films were dissolved in dimethylformamide (2 mL) and heated to 130 ºC for 2h. The films were further prepared by solution casting. The residual solvent was evaporated at a temperature of 80 ºC for 24 h, and then at 100 ºC for 24 h. Finally, the films were kept at 40 ºC for another 48 h before analysis.

5.3.5 Swelling test and gel fraction determination

The gel fraction and swelling ratio of the crosslinked polymers were determined by solvent immersing method.[215] The samples (W_1) were first submersed in chloroform for 3 days at room temperature. Then, the weight of the swollen samples (W_2) was determined. The insoluble

polymer fractions were dried in a vacuum oven at 60 ºC for at least 24h to obtain a constant weight (W_3). The swelling ratio and the gel fraction were calculated according to equation 1 and equation 2. The experiments were performed in triplicate.

$$Gel\ fraction = \frac{W_3}{W_1} \times 100\% \qquad \text{eq. 1}$$

$$Swelling\ ratio = \frac{W_2 - W_1}{W_1} \times 100 \qquad \text{eq. 2}$$

5.3.6 Characterization

^{1}H and ^{13}C NMR spectra were obtained on a Bruker AV 400 using DMSO-d_6 and $CDCl_3$ as solvents. The chemical shifts were referenced to the solvent residual signals at 2.50 ppm for deuterated DMSO and 7.26 ppm for $CDCl_3$. FTIR spectra were recorded on a Thermo Scientific Nicolet iS5 FTIR spectrometer (Thermo, Madison, WI, USA) using an attenuated total reflectance (ATR) diamond crystal. The spectra were recorded in duplicate at 32 scans and 4 cm^{-1} resolutions in the range of 4000–600 cm^{-1}. The molecular weight distribution was determined using gel permeation chromatography (GPC, Water Breeze) using THF as the mobile phase. The flow rate was set to 0.3 mL/min. The molecular weights were calibrated using linear polystyrene standards having a narrow molecular weight distribution. The thermal transitions of the polymers were evaluated by DSC in duplicate (Q100, TA Instruments, Inc., New Castle, DE). The samples were compressed in hermetic aluminum pans. Thermogravimetric analysis (TGA, Q50, TA Instrument, Inc., New Castle, DE) was used to investigate the thermal stability of the polymers (powder). The flow rate of N_2 was 60 mL/min, and the samples were heated from 20 ºC to 600 ºC at a rate of 10 ºC/min. The heating rate and cooling rate were 10 ºC/min. The dynamic mechanical analyzer (DMA) used was a DMA Q800 (TA instruments, New Castle, DE) equipped with a liquid nitrogen cooling system. The experiments were carried out in a tension mode with a temperature range of -60 to 100 °C at a heating rate of 3 ºC/min and a frequency of 1 Hz. Stress-strain tests were also conducted in triplicates using the DMA Q800 at 25 °C by ramping up a force at a rate of 1 N/min. A preload force of 0.01 N was used. The cyclic tensile test was performed to evaluate the elasticity of the elastomers. The films were first extended by ramping up a force at a rate of 0.2 N/min to a target force (0.8 N). Then the force was

immediately reversed by ramping down a force at the same rate to 0 N. This was marked as one cycle, and three cycles were performed.

5.4 Results and Discussion

5.4.1 DA reaction of poly(β-thioether ester) and N-phenylmaleimide

The DA reaction is affected by several factors, such as the reactants concentration, the reaction temperature, the solvent type, and the substituents of the furan or the maleimide.[204b, 216] Here, the DA reaction was investigated in $CDCl_3$ by ^1H NMR using PPF and *N*-phenylmaleimide as a model reaction (**Figure 5.1a**). The reaction was performed at 40 ^oC. The weight ratio of PPF to *N*-phenylmaleimide was 5:1. During the DA reaction from 0 h to 48 h, the intensity of the proton peak at 6.85 ppm ascribed to maleimide proton (c) decreased (**Figure 5.1b**). New peaks at 6.53 ppm (a'), 4.88 ppm (b'), 4.63 ppm (b') and 3.69 ppm (c') attributed to the characteristic peaks of the DA adduct were observed. The intensities of these new peaks gradually increased. The conversion of maleimide to DA adduct was calculated based on the integration of maleimide proton (c) and oxanorbornene proton signals (a'). The results showed that the conversion of maleimide to DA adduct could reach over 70 % at 40 ^oC in $CDCl_3$ (**Figure 5.1c**).

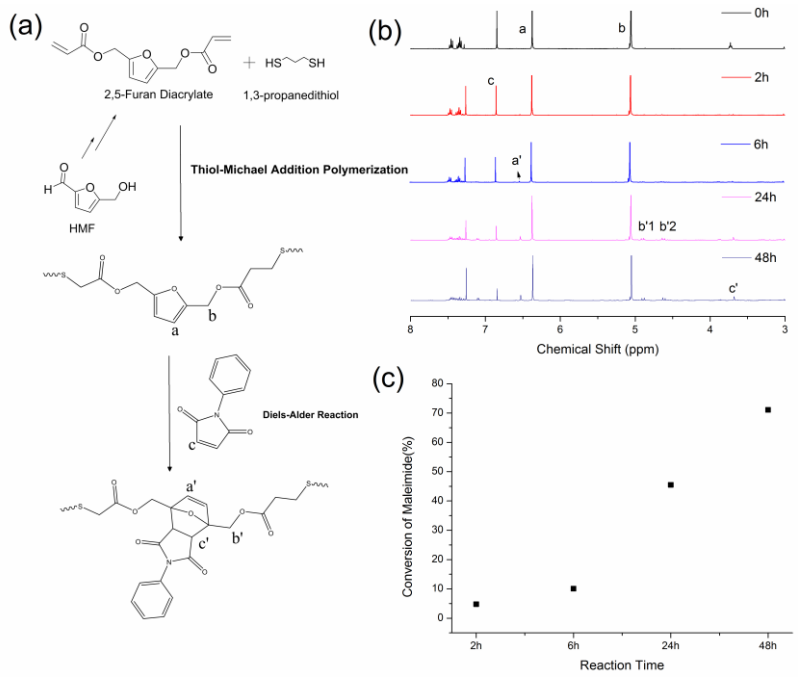

Figure 5.1 a) Schematic diagram of the model reaction between PPF and *N*-phenylmaleimide; b) ^{1}H NMR spectra of DA reaction between PPF and *N*-phenylmaleimide at 40 ^{o}C (the weight ratio of PPF to *N*-phenylmaleimide = 5:1, $CDCl_3$ as solvent); c) Conversion of maleimide to DA adduct versus reaction time.

5.4.2 Crosslinking PPF *via* DA reaction to elastomers

The elastomers were prepared by dynamically crosslinking PPF with bismaleimide *via* the DA reaction (**Figure 5.2a**). The weight ratio of PPF to bismaleimide (PPF/M) was chosen to be 20:1, 10:1, and 5:1, respectively. The gel fractions of the crosslinked films were 93.3±1.2 % (PPF/M 5:1), 91.5±1.5 % (PPF/M 10:1), and 89.9±1.3% (PPF/M 20:1), respectively, indicating the formation of highly crosslinked network. Oh *et al.* have synthesized the films *via* the DA reaction between methacrylate copolymers having maleimide pendants and various polyfurans. They investigated the gel fractions of films as well, and over 90% of gel fractions were observed, indicating the high efficiency of the DA reaction to crosslink polymers to networks.[217] In addition, Li *et al.* suggested that the gel fractions of networks crosslinked *via* DA reaction were influenced by the bismaleimide/furan ratio.[215] Similar to our observations, they observed that the gel fractions increased with the increase in the bismalemide/furan ratio. Furthermore, the swelling ratios of crosslinked films were evaluated after immersion in chloroform. It was observed that the swelling ratios of the films were 152±22% (PPF/M 5:1), 211±31% (PPF/M 10:1) and 312±25 % (PPF/M 20:1), respectively. Caillol *et al.* investigated the swelling ratios of networks synthesized *via* crosslinking copolyethers of propylene oxide (PO) and furfuryl glycidyl ether with bismaleimide. The swelling ratios were in the range of 26-138 %.[218] Barrau *et al.* observed that when the DA reaction occurred between poly(ethyl methacrylate-co-furfuryl methacrylate) and bismaleimide, the highest swelling ratio of the network could reach 1100 %.[219] Moreover, the swelling ratio increased with the decrease in the crosslinking ratio. These comparisons indicated that the swelling ratios of films crosslinked *via* the DA reaction were influenced by the bismaleimide/furan ratio. As the amount of crosslinker increased, the crosslinking densities increased, leading to a decrease in the distance between two neighbouring crosslinks. Moreover, the structures of polymers may also have influenced the swelling ratio.

The FTIR spectra showed that the intensity of the signal at 1715 cm^{-1} attributed to the carbonyl groups of maleimide increased with the increase in the ratio of crosslinker to PPF

(**Figure 5.2b**), whereas the imide peak near 700 cm^{-1} was weak (**Figure 5.2c**). These results indicated that most of the maleimide groups reacted with the furan rings in PPF to form a network. Yoshie *et al.* also investigated the use of the DA reaction to crosslink polyesters. The DA reaction was almost completed after several hours. The presence of small amounts of maleimide groups was due to the equilibrium between furan and maleimide groups.[213]

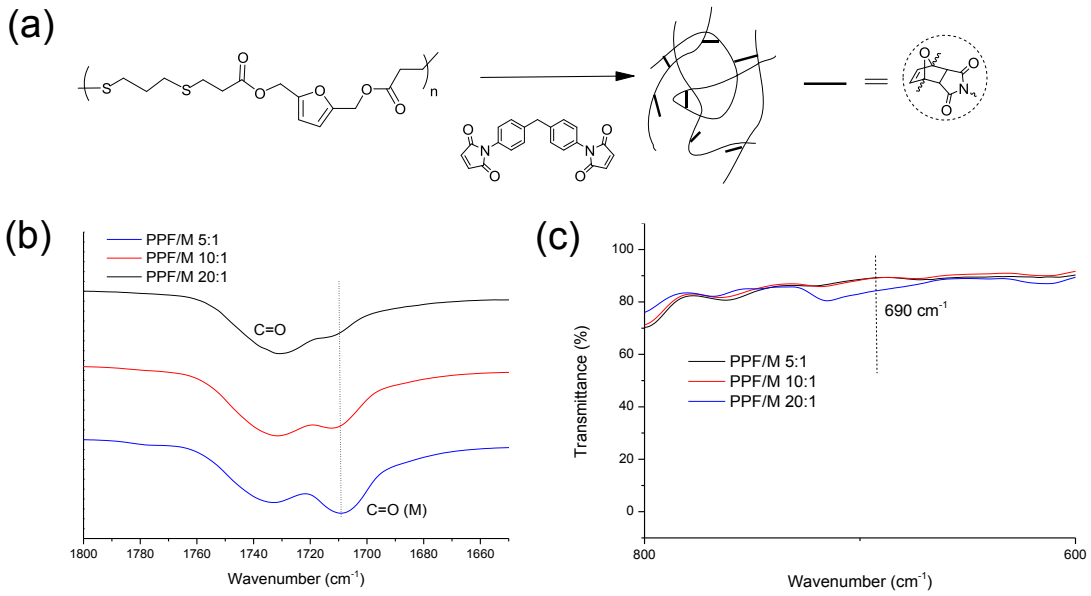

Figure 5.2 (a) Schematic diagram of crosslinking PPF *via* the DA reaction to elastomers; (b) FTIR of carbonyl peak region; (c) imide peak region.

5.4.3 Mechanical properties of crosslinked poly (β-thioether ester)

The viscoelastic properties of crosslinked PPF were determined using a DMA (**Figure 5.3**). The results showed that the storage modulus (G') of the films at 25 °C increased when the amounts of bismaleimide increased. For example, the G' of PPF/M 5:1 was 50.9 MPa, as compared to 1.5 MPa (PPF/M 10:1), and 0.8 MPa (PPF/M 20:1) (**Figure 5.3a**). In addition, the T_g of crosslinked films determined from the maximum peaks in the tan δ curves increased as well. When the ratio of polymers to crosslinker was 5:1, the T_g was enhanced from -32.3 °C (PPF) to 27.7 °C (**Figure 5.3b**). For PPF/M 10: 1 and PPF/M 20:1, the T_g values were similar (-12.5 °C and -12.6 °C, respectively).

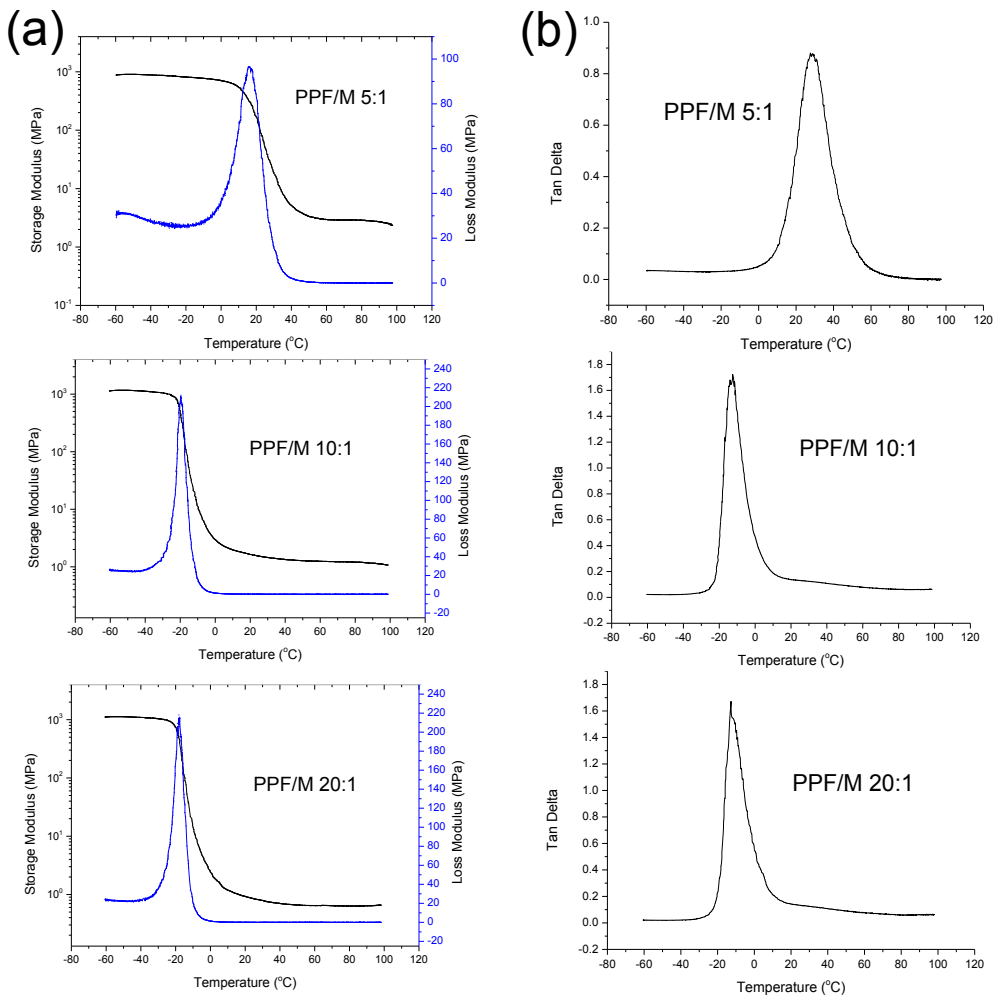

Figure 5.3 (a) Storage modulus and loss modulus of crosslinked films; (b) Tan δ of different crosslinked films.

The stress-strain behavior of the elastomers was evaluated at 25 °C and shown in **Figure 5.4 and Table 5.1**. It was observed that as the weight ratio of PPF/M changed from 20:1 to 5:1, the Young's modulus was gradually increased from 1.1±0.2 MPa to 4.3±0.6 MPa (**Figure 5.4a**). Moreover, the ultimate strength was enhanced from 1.3±0.1 MPa to 5.7±1.1 MPa. The elongation at break values ranged from 150-270 %. These results indicated that the Young's modulus and ultimate strength of the elastomers synthesized *via* thiol-Michael and DA reaction could be improved by increasing the amount of crosslinker. Tang *et al.* synthesized plant oil-derived fatty polymers having furan rings as the side groups. The Young's modulus and the ultimate strength of the elastomers crosslinked *via* the DA reaction were also enhanced with the increase in the crosslinking densities.[220] Additionally, cyclic tensile tests were carried out to

examine the elastic recovery and residual strain using elastomers with the highest crosslinking density (**PPF/M 5:1, Figure 5.4b**). It was observed that the residual strain after the first cycle (9.2 %) significantly decreased to 0.5 % (after the second cycle) and 0.7 % (after the third cycle). The elastic recovery was calculated to be 85.9 % (the first cycle), 99.2 % (the second cycle) and 98.9 % (the third cycle). These results demonstrated that elastomers synthesized *via* thiol-Michael and DA reaction exhibited excellent elastic properties.

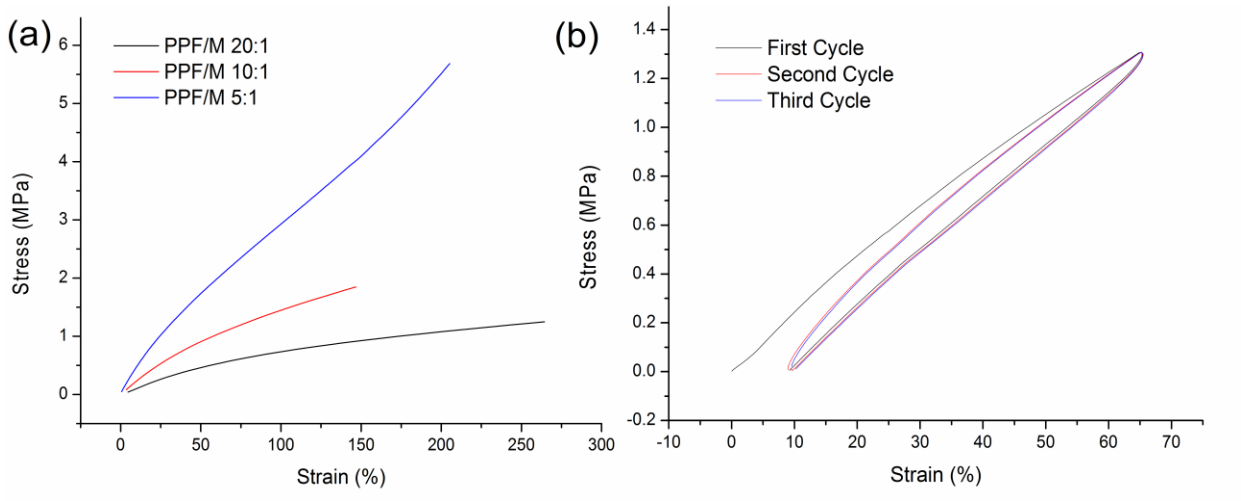

Figure 5.4 (a) Typical tensile tests of films from PPF crosslinked by Diels-Alder reaction; (b) A typical cyclic test of PPF/M 5:1.

Table 5.1 Mechanical properties of PPF/M crosslinked with different amounts of crosslinker

Sample	E^a (MPa)	σ^b (MPa)	ε^c (%)
PPF/M 20:1	1.1±0.2	1.3±0.1	264.4±18.5
PPF/M 10:1	2.2±0.3	1.8±0.2	146.8±11.2
PPF/M 5:1	4.3±0.6	5.7±1.1	205.3±20.1

[a] Young's modulus; [b] Tensile strength; [c] Elongation at break;

5.4.4 Incorporation of hydroxyl groups or poly(ethylene glycol) into elastomers

The DL-dithiothreitol (5 or 15 mol%) was used as a comonomer to synthesize polymers having hydroxyl groups, which could potentially be used as the reactive sites for the functionalization (**Figure 5.5a**). ^{1}H NMR spectra confirmed the successful synthesis of copolymers due to the presence of signals of PPF and the proton (a', 3.71 ppm) from DL-dithiothreitol (**Figure 5.5a**). The mole percentage of DL-dithiothreitol present in the synthesized

copolymers was calculated according to the integration area of the peaks at 3.71 ppm (a') and at 6.38 ppm (a). The compositions determined by ^{1}H NMR closely matched the theoretical ones (4.4 and 13.4 mol%). FTIR analysis showed that the broad signal at 3400 cm^{-1} attributed to OH stretching absorption increased as the concentration of DL-dithiothreitol increased (**Figure 5.6a**). The number average molecular weights were 33000 g/mol and 22000 g/mol, respectively (**Figure 5.5b**). Furthermore, the T_g of POF15%-PPF (-24.3 ^{o}C) determined by DSC was slightly higher than POF5%-PPF (-26.2 ^{o}C) (**Figure 5.6b and c**), but both were higher than PPF (-32.3 ^{o}C).[214] A typical TGA analysis of POF15%-PPF showed a two-stage degradation pattern (246.7 ^{o}C and 273.4 ^{o}C) (**Figure 5.5c**) corresponding to the α-hydrogen bond scission, alkyl oxygen homolysis, and C-S bond scission, which was analysed *via* pyrolysis-gas chromatography-mass spectrometry.[214] The decomposition temperature at 5% weight loss was 243 ^{o}C. Moreover, around 18 % of the initial weight remained at 600 ^{o}C.

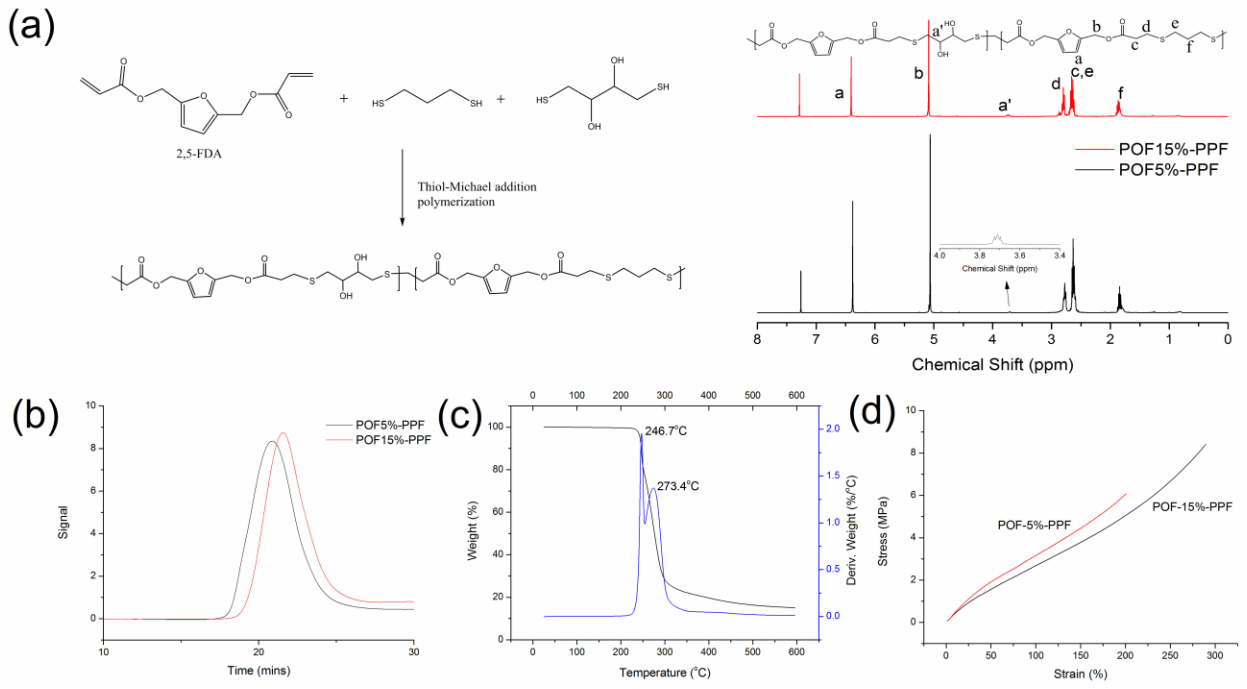

Figure 5.5 (a) Schematic diagram of the synthesis of copolymers from 2,5-FDA, DL-dithiothreitol and 1,3-propanedithiol, ^{1}H NMR, and (b) GPC analysis of copolymers (POF15%-PPF and POF5%-PPF); (c) TGA of POF15%-PPF; (d) Tensile tests of films from POF-PPF copolymers crosslinked by DA reaction.

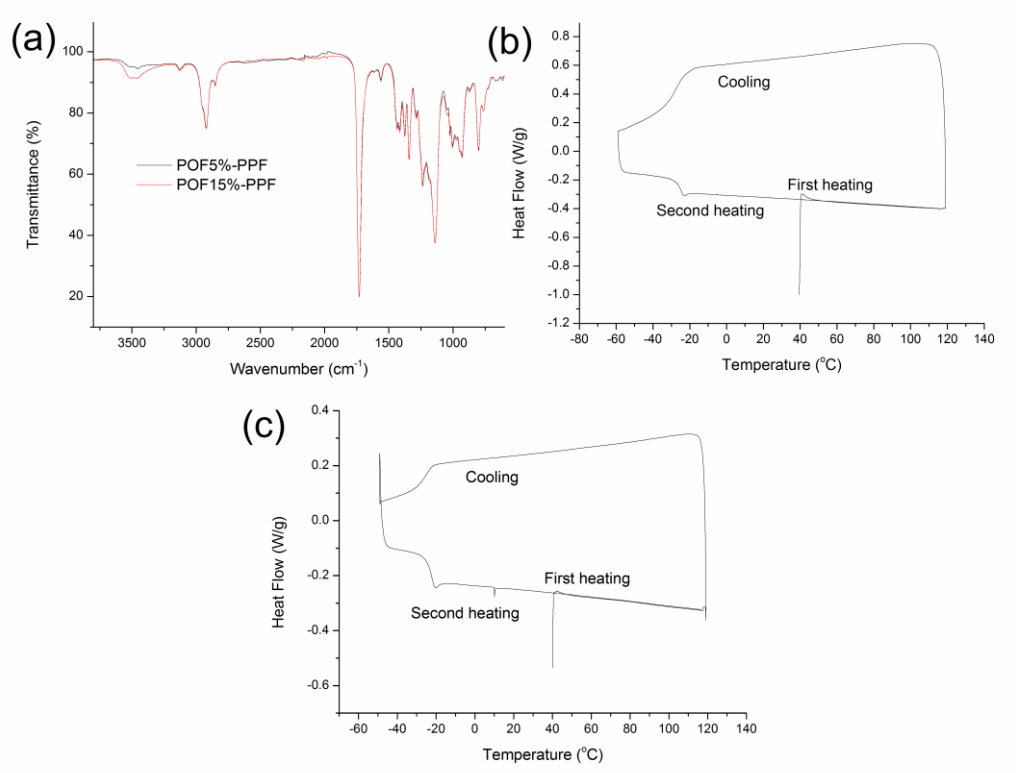

Figure 5.6 (a) FTIR of copolymers POF5%-PPF and POF15%-PPF; DSC of copolymers of POF5%-PPF (b) and POF15%-PPF (c) (Measured at heating rate of 10 °C/min, cooling rate of 10 °C/min).

The copolymers were then crosslinked to elastomers *via* the DA reaction using bismaleimide as the crosslinker. The weight ratio of copolymer to crosslinker was chosen to be 5 to 1. Using crosslinked POF15%-PPF as an example, the DA reaction between copolymer and crosslinker occurred as shown by the FTIR spectra (**Figure 5.7a and b**). Additionally, the T_g of crosslinked POF15%-PPF determined by DMA analysis revealed that it was significantly improved from -24.3 °C to 38.8 °C (**Figure 5.7c and d**). The gel fractions and swelling ratios of crosslinked film (POF15%-PPF) were 91.3±1.1 %, and 205±28 %, respectively. The stress-strain tests of two crosslinked copolymers are shown in **Table 5.2 and Figure 5.5d**. The crosslinked POF15%-PPF exhibited a higher elongation at break (289.4±27.2%) and ultimate strength (8.4±0.8 MPa), but a lower Youngs's modulus (4.0±0.3 MPa), as compared to POF5%-PPF (**Figure 5.5d**). The presence of hydroxyl groups in the elastomer as dynamic bonds can dissipate the energy during elongation.[221] Therefore, copolymers with high hydroxyl group concentration after crosslinking possessed enhanced mechanical properties in terms of elongation at break and ultimate strength.

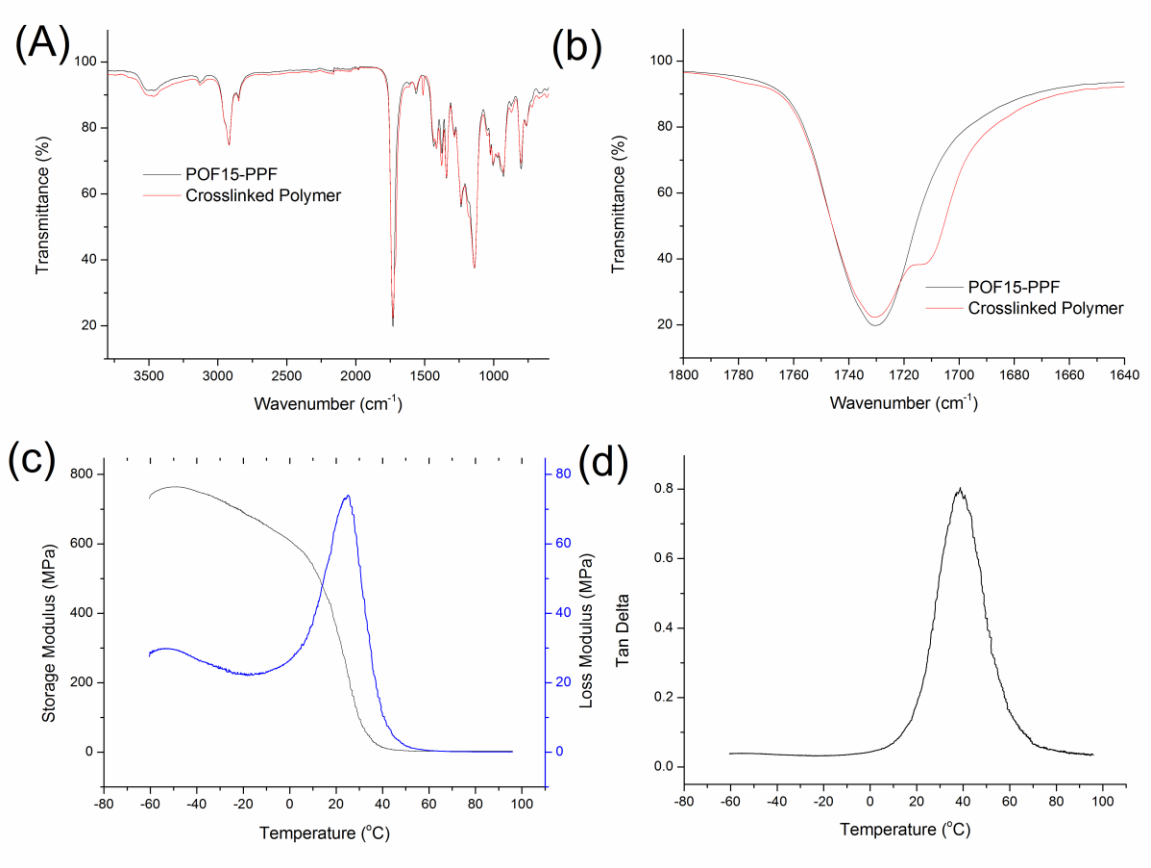

Figure 5.7 (a) FTIR of POF15%-PPF and crosslinked polymer; (b) FTIR of carbonyl peak region; (c) Storage and loss modulus of crosslinked POF15%-PPF (weight ratio of polymer to crosslinker = 5 :1); (d) Tan delta of crosslinked POF15%-PPF.

Table 5.2 Mechanical properties of crosslinked POF5%-PPF and POF15%-PPF

Sample	E^a (MPa)	σ^b (MPa)	ε^c (%)
POF5%-PPF	5.0±0.8	6.1±0.5	200.7±20.1%
POF15%-PPF	4.0±0.3	8.4±0.8	289.4±27.2%

[a] Young's modulus; [b] Tensile strength; [c] Elongation at break;

PEG has been widely used in the synthesis of elastomers or hydrogels due to its biocompatibility, non-toxicity, and biodegradability.[222,223] Therefore, PEG diacrylate (M_n=700 g/mol) was used as a comonomer (5% and 15% mol%) to synthesize elastomers. The structures of copolymers were characterized by ^{1}H NMR (**Figure 5.8a**) and FTIR (**Figure 5.9a**). The mole percentage of PEG in the copolymers was calculated according to the integration area of the

peaks at 4.23 ppm (c') and 5.12 ppm (b), and the results were 5.1 mol% and 13.4 mol%, respectively. These results indicated that PEG was efficiently incorporated in elastomers. The number average molecular weights of PEG5%-PPF and PEG15%-PPF determined by GPC were 25000 g/mol and 17000 g/mol. Due to the flexibility of PEG polymeric chains, the T_g of PEG15%-PPF decreased to -40.2 ^oC, as compared to -33.5 ^oC of PEG5%-PPF (**Figure 5.9b and c**). The T_g of both copolymers was lower than PPF (-32.3 ^oC). Furthermore, TGA analysis of PEG15%-PPF showed a two-stage degradation pattern (251.8 ^oC and 285.1 ^oC, **Figure 5.9d**). The decomposition temperature at 5% weight loss was 248.8 ^oC.

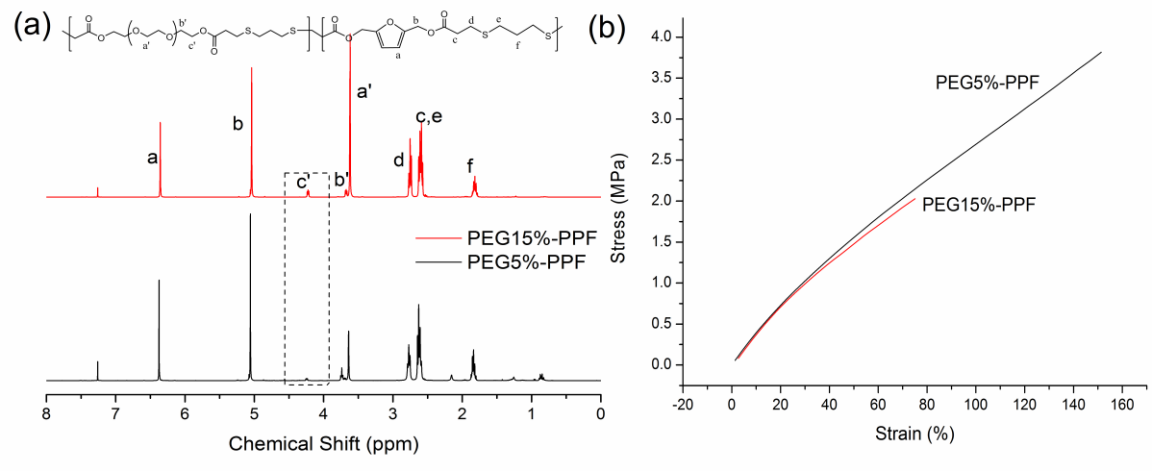

Figure 5.8 (a) ^1H NMR of PEG5%-PPF and PEG15%-PPF; (b) Tensile tests of elastomers prepared from PEG5%-PPF and PEG15%-PPF crosslinked by DA reaction.

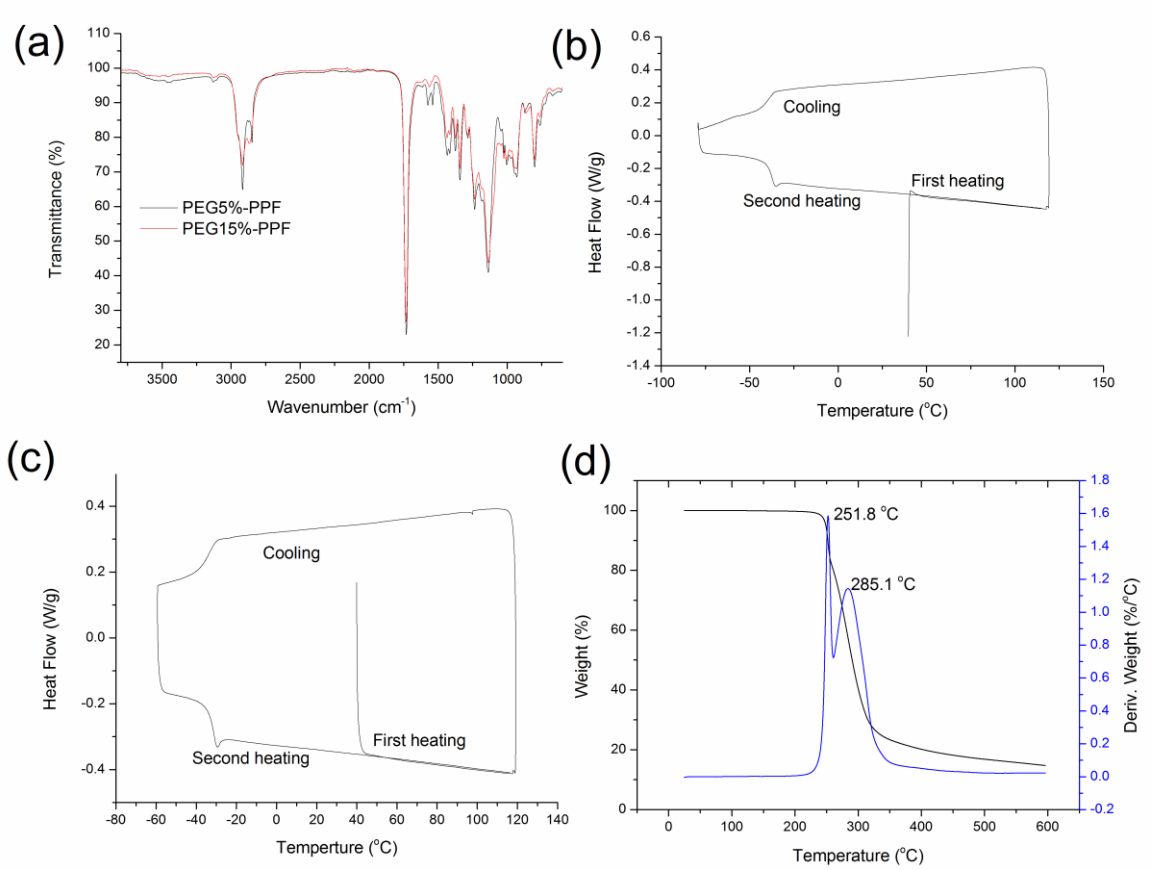

Figure 5.9 (a) FTIR spectra of PEG5%-PPF and PEG15-PPF; (b) DSC of PEG5%-PPF; (c) DSC of PEG15%-PPF; (d) TGA of PEG15%-PPF.

Similarly, the weight ratio of copolymers to crosslinker was 5 to 1 to synthesize elastomers. Typical FTIR spectra of PEG15%-PPF and crosslinked polymers showed the occurrence of the DA reaction (**Figure 5.10a and b**). The T_g of crosslinked PEG15%-PPF determined by DMA was 18.4 °C (**Figure 5.10c and d**). The gel fraction and swelling ratio of PEG15%-PPF were 96.3±1.2 % and 221±28%, respectively. The results of stress-strain tests are shown in **Figure 5.8b** and **Table 5.3**. PEG5%-PPF exhibited a better elongation at break (151.4±13.5 %), ultimate strength (3.8±0.5 MPa), and Young's modulus (3.8±0.3 MPa), as compared to 75.0±8.2% (elongation at break), 2.0±0.3 MPa (ultimate strength), and 2.7±0.3 MPa (Young's modulus) for PEG15%-PPF (**Table 5.3**). This might due to the relatively low molecular weights of PEG15%-PPF as compared to PEG5%-PPF.

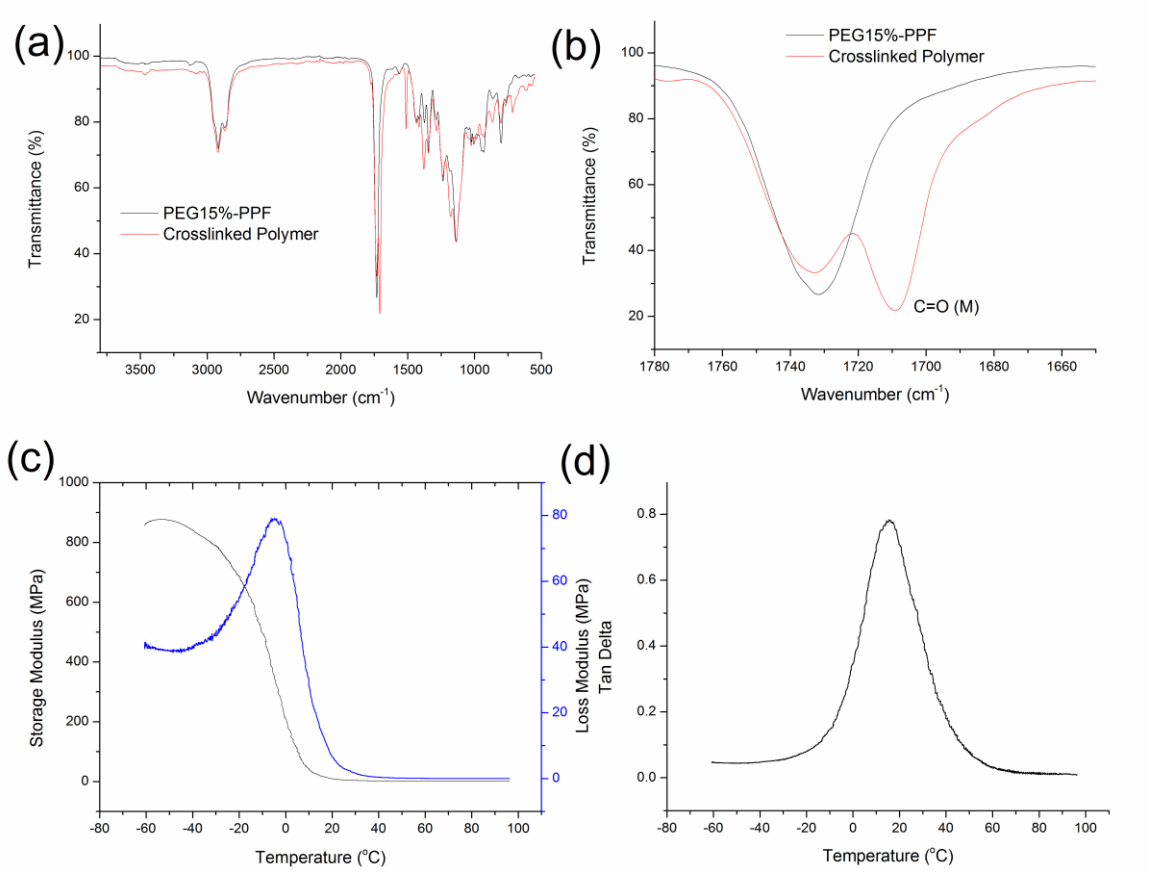

Figure 5.10 (a) FTIR of PEG15%-PPF and crosslinked polymer; (b) FTIR of carbonyl peak region; (c) Storage and loss modulus of crosslinked PEG15%-PPF (weight ratio of polymer to crosslinker = 5 :1); (d) Tan delta of crosslinked PEG15%-PPF.

Table 5.3 Mechanical properties of crosslinked PEG5%-PPF and PEG15%-PPF

Sample	E^a (MPa)	σ^b (MPa)	ε^c (%)
PEG5%-PPF	3.8±0.3	3.8±0.5	151.4±13.5%
PEG15%-PPF	4.0±0.3	2.0±0.3	75.0±8.2%

[a] Young's modulus; [b] Tensile strength; [c] Elongation at break;

5.4.5 Tuning the mechanical properties of elastomers

Although the mechanical properties of HMF derivative based elastomers can be adjusted depending on the weight ratio of polymers to crosslinker, a further increase in the concentration of crosslinker could lead to the increase in the T_g of network. Therefore, the elongation at break

of the networks might decrease. Instead of varying the ratio of polymers to crosslinker, it was hypothesized that the mechanical properties could be adjusted by incorporating more flexible polymeric chains. 1,4-butanediol diacrylate (BD) and 1,6-hexanedithiol (HDT) were used, respectively, as comonomers in the synthesis of elastomers. The molar percentage of the comonomers was 15 %. The number average molecular weights of the two copolymers were 23000 g/mol (PBD15%-PPF) and 24000 g/mol (PHF15%-PPF), respectively. The structures of two copolymers were analysed *via* ^{1}H NMR and FTIR (**Figure 5.11a and b**). The compositions of BD or HDT in the copolymers were calculated to be 14.5 % and 14.1 %, respectively, indicating the incorporation of these comonomers to the polymeric structure. The thermal properties of PBD15%-PPF and PHF15%-PPF were evaluated by DSC and TGA (**Figure 5.11c and d**). The T_g values of PBD15%-PPF and PHF15%-PPF were -33.0 ^{o}C and -32.5 ^{o}C, respectively, which were lower that the T_g of PPF. The polymers were thermally stable to up to 250 ^{o}C. After crosslinking *via* the DA reaction, the T_g values were enhanced to 17.7 ^{o}C (PBD15%-PPF) and 28.8 ^{o}C (PHF15%-PPF) as determined by DMA (**Figure 5.12a and b**). The FTIR analysis confirmed the occurrence of the DA reaction (**Figure 5.12c**). The gel fraction and swelling ratio of PBD15%-PPF were 95.3±2.4% and 211±15%, respectively, as compared to 94.8±3.1% and 155±12% for PHF15%-PPF, indicating the formation of highly crosslinked networks. The stress-strain tensile tests showed that the elongation at break values of the elastomers were improved to 237.2±22.3 % (PBD15%-PPF) and 279.5±29.6 % (PHF15%-PPF) as compared to 205.3±20.1 % for PPF/M 5:1 (**Figure 5.13**). Although the ultimate strength of PBD15%-PPF decreased to 4.2±0.5 MPa, it was enhanced to 6.9±0.8 MPa for PHF15%-PPF, as compared to 5.7±1.1 MPa for PPF/M 5:1. These results indicated that the mechanical properties of 2,5-FDA based elastomers could be varied *via* the incorporation of 1,4-butanediol diacrylate or 1,6-hexanedithiol as comonomers.

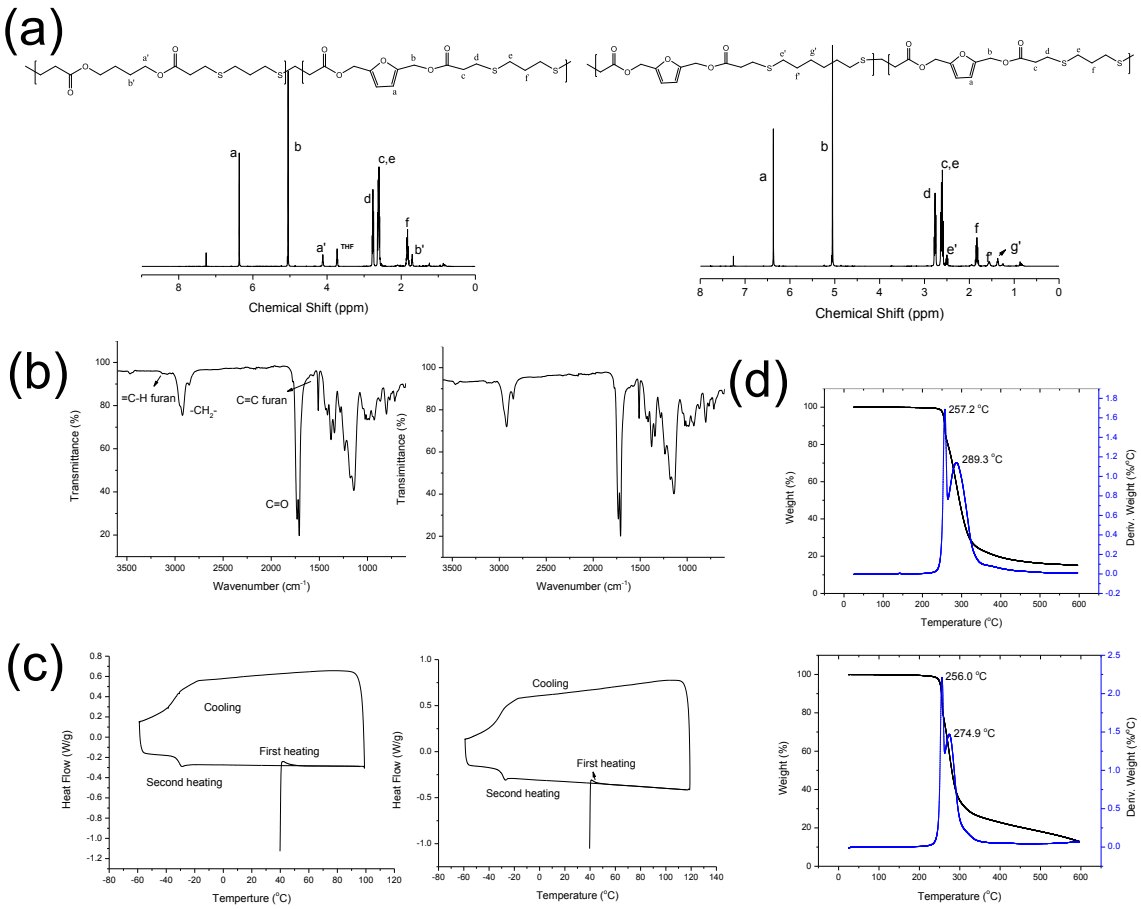

Figure 5.11 (a) ^{1}H NMR of PBD15%-PPF and PHF15%-PPF; (b) FTIR spectra of PBD15%-PPF and PHF15%-PPF; (c) DSC of PBD15%-PPF and PHF15%-PPF; (d) TGA of PBD15%-PPF and PHF15%-PPF.

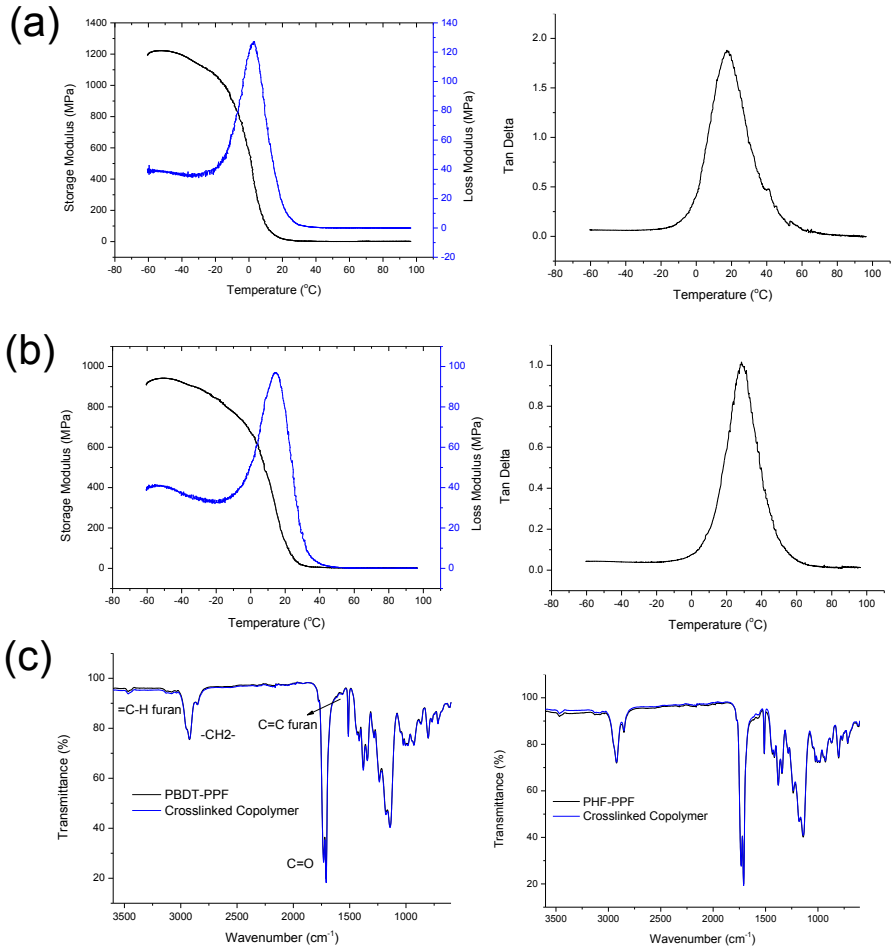

Figure 5.12 (a) Storage modulus and tan delta of PBD15%-PPF; (b) Storage modulus and tan delta of PHF15%-PPF; (c) FTIR of PBD15%-PPF and PHF15%-PPF, as well as their crosslinked copolymers.

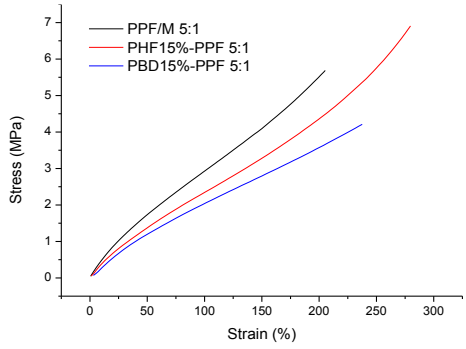

Figure 5.13 Tensile tests of crosslinked PPF/M 5:1, PHF15%-PPF 5:1 and PBD15%-PPF 5:1.

5.4.6 Reprocessing of elastomers

The retro-DA reaction was investigated by ^{1}H NMR in DMSO-d_6. Pieces of the crosslinked film (PPF/M 5:1) were added in DMSO-d_6 for 1h. Visually, the film was insoluble in DMSO-d_6 due to the crosslinked network. ^{1}H NMR was taken as 0h (**Figure 5.14a-0h**). Since the retro-DA is a thermo-responsive reaction, the crosslinked polymer network can be soluble in the solution after heating. As a result, the proton signal of the dissolved polymer and crosslinker was observed using ^{1}H NMR. The DMSO-d_6 solution was heated to 130 ^{o}C to observe the retro-DA reaction. After 1h of reaction, the characteristic signals of the furan rings in the polymer chain and bismaleimide were observed at 6.51 ppm (furan proton) and 7.18 ppm (maleimide proton), respectively, indicating the occurrence of the retro-DA reaction (**Figure 5.14a-1h**). The structure of the crosslinker and polymer was further confirmed *via* COSY spectra (**Figure 5.15**). After 2h of reaction, a homogeneous solution was observed. The intensity of the signals observed at 2h in ^{1}H NMR almost kept constant as compared to the signals observed at 4h, indicating the end of the retro-DA reaction. Similar results were observed by Barrau *et al*., and the insoluble crosslinked copolymers were soluble in chlorobenzene after heating at 130 ^{o}C.[219]

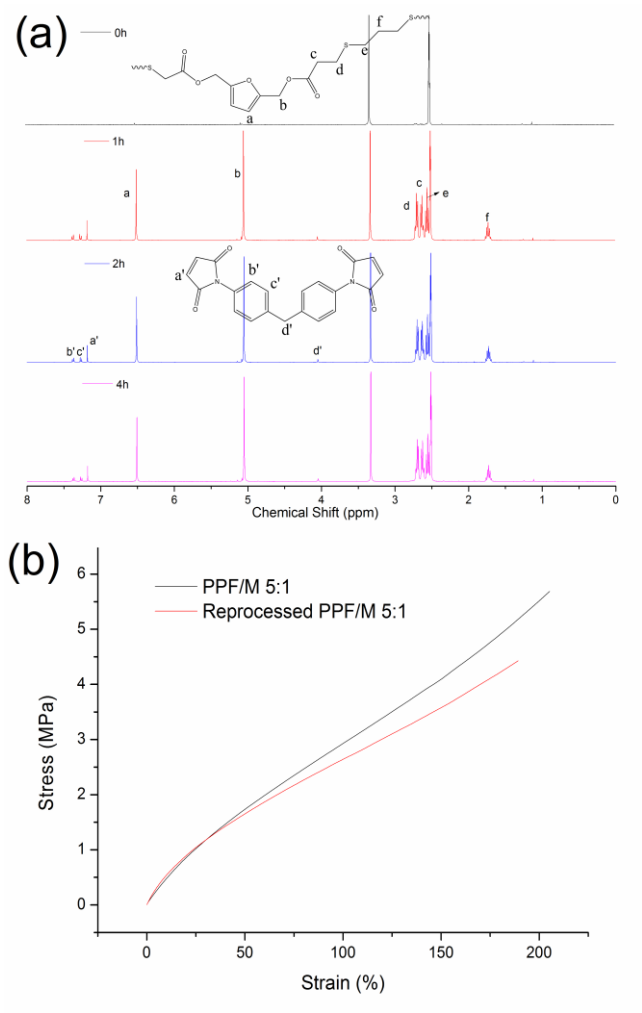

Figure 5.14 (a) ^{1}H NMR spectra recorded at 130 ^{o}C in DMSO-d_6 for the retro-DA reaction of crosslinked PPF/M 5:1; (b) Stress-strain test of PPF/M 5:1 and reprocessed PPF/M 5:1.

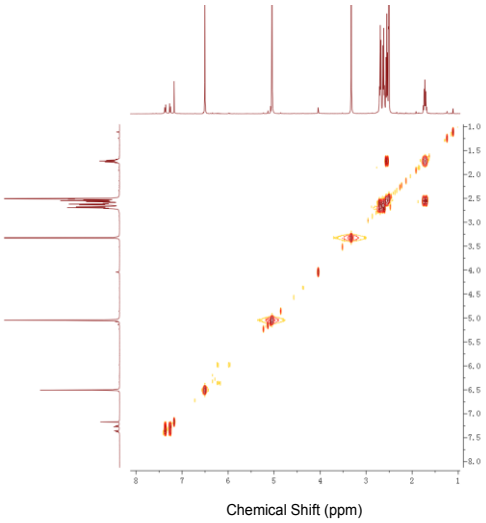

Figure 5.15 COSY spectra of products generated after the retro-DA reaction of crosslinked PPF/M 5:1.

Pieces of the crosslinked films (PPF/M 5:1) were added in DMF. Then the solution was heated to 130 ^{o}C for 2h. After 2h heating, a homogenous solution was formed due to the occurrence of the retro-DA reaction to linear polymers. A new film was then prepared by a solution casting method. **Figure 5.16** showed the typical FTIR spectra for PPF/M 5:1 and reprocessed PPF/5:1. A similar spectrum was observed indicating the reversibility of the DA reaction which occurred during the reprocessing step. The tensile test analysis revealed that the mechanical properties of the reprocessed elastomers were similar to the original elastomers, despite the slight decrease in elongation at break (189.3±15.2 %) and ultimate strength (4.4±0.5 MPa) (**Figure 5.14b**). Tang *et al.* also observed the different mechanical properties of initial films and remolded films. It might be due to the different processing method, leading to slightly different crosslinking densities.[211a, 220]

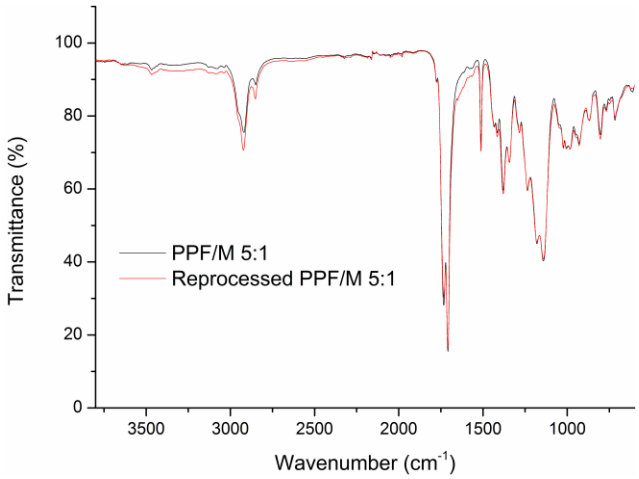

Figure 5.16 FTIR of crosslinked films before and after reprocessing.

5.5 Conclusions

This chapter described the synthesis and characterization of elastomers synthesized from 2,5-FDA. The effects of crosslinker concentration on the mechanical properties showed that the Young's modulus and ultimate strength of 2,5-FDA based elastomers could be improved by increasing the weight ratio of crosslinker to polymers. Cyclic tensile tests of PPF/M 5:1 demonstrated its good elasticity in terms of low residual strain (0.7 % after the third cycle) and high elastic recovery (98.9 % after the third cycle). Furthermore, functional groups (hydroxyl groups) or PEG were incorporated in the structure of the elastomers as determined *via* ^{1}H NMR. The elongation at break and ultimate strength values were 289.4±27.2% and 8.4±0.8 MPa for POF15%-PPF, probably due to the presence of hydroxyl groups which dissipated the energy. Additionally, the mechanical properties of 2,5-FDA based elastomers, particularly the elongation at break, were well adjusted *via* the incorporation of flexible polymeric chains (PBD15%-PPF and PHF15%-PPF). The tensile tests showed that the elongation at break values were improved to 279.5±29.6 % for PHF15%-PPF, as compared to 205.3±20.1 % of PPF/M 5:1. Finally, the reprocessing of elastomers was evaluated *via* heating the crosslinked elastomer (PPF/M 5:1) in solution at 130 ^{o}C. Due to the reversibility of the DA reaction, a new elastomer with comparable mechanical properties was prepared. The combination of thiol-Michael and DA reactions to synthesize HMF derivative based elastomers showed several advantages, such as mild reaction conditions, easily adjustable structures and properties, and reprocessable properties.

Connecting Statement 4

The work in Chapter 5 investigated the synthesis and characterization of reprocessable elastomers using the combination of the thiol-Michael addition and the DA reaction. Functionalities were incorporated in the elastomers structure *via* the synthesis of linear copolymers by the thiol-Michael addition reaction. Moreover, the mechanical properties of thermoset elastomers varied when 1,6-hexanedithiol or 1,4-butanediol diacrylate were used as comonomers. These 2,5-FDA based thermoset elastomers showed several interesting properties, such as high elastic recovery and reprocessability.

Recently, PLA has been found in a variety of applications due to its low toxicity, biocompatibility, and biodegradability. One interesting field of application is the use PLA as hard segments to synthesize triblock copolymers, which behaved as thermoplastic elastomers (TPEs). Although a large number of soft segments have been investigated, no information is available regarding the use of poly(β-thioether ester) as the soft segments in the synthesis of PLA based TPEs. Given the presence of flexible thioether groups in the polymers, it was expected that poly(β-thioether ester) could also be used as soft segments to provide ductility to PLA based TPEs.

Hence, the synthesis and characterization of 2,5-FDA based TPEs using PLA as hard ends were investigated in Chapter 6. This chapter is based on an accepted manuscript with Dr. Marie-Josée Dumont in *Macromolecular chemistry and physics*.

Chapter 6: 5-Hydroxymethylfurfural Derivative Based Thermoplastic Elastomers Synthesized *via* Thiol-Michael Addition Reaction Utilizing Poly(lactic acid) as Hard End Blocks

6.1 Abstract

5-hydroxymethylfurfural derivative based thermoplastic elastomers (TPEs) were efficiently synthesized *via* a two-step thiol-Michael addition reaction using polylactide (PLA) as the hard segments in a one-pot reaction under mild conditions. The first step involved the synthesis of prepolymers having thiol groups as end groups. The macromolecular coupling reaction which occurred between the prepolymers and the PLA having acrylate-end groups was demonstrated *via* ^{1}H NMR and GPC. Additionally, by varying the ratio of 1,3-propanedithiol and 2,5-furan diacrylate, TPEs with soft segments having different molecular weights were synthesized, and then characterized. The cyclic tensile tests demonstrated the elasticity of the synthesized TPEs. Furthermore, the Diels-Alder reaction was used to dynamically crosslink the soft segments in the TPEs, leading to the increased mechanical properties in terms of Young's modulus and tensile strength.

6.2 Introduction

Renewable resources have been widely utilized for biofuels production, fine chemicals synthesis, and polymers synthesis.[224] 5-hydroxymethylfurfural (HMF) has shown its potential to be a versatile platform chemical.[225] Despite various polymers synthesized from HMF and its derivatives, 2,5-furan dicarboxylic acid based (co)polyesters seems to be the most promising one.[226] Due to the multiple functional groups of HMF available for derivatization, it is of interest to investigate the synthesis of new polymers from HMF and its derivative.[225a, 227]

Thermoplastic elastomers (TPEs) are physically cross-linked polymers which can be prepared *via* several polymerization techniques.[228] Research efforts have been made on the utilization of renewable resources to synthesize degradable TPEs.[229] Due to the renewability, non-toxicity, biodegradability, and tunable crystallization behavior, polylactic acid (PLA), a bacterial biodegradable polyester, has been studied as hard blocks in the synthesis of TPEs.[230] It has been suggested that the properties of soft middle segments could influence the performance of PLA based TPEs.[231] Therefore, various polymers with flexible polymeric chains have been evaluated

as soft segments in PLA based TPEs.[232] Recently, it has been shown that HMF derivative based poly(β-thioether ester) with tunable structures and properties could be efficiently synthesized *via* the thiol-Michael addition polymerization.[233] The presence of thioether groups could be used as soft segments in TPEs.[234] However, no information is available on the synthesis of PLA based TPEs using soft segments with thioether groups. Additionally, due to the presence of furan rings in the soft segments, HMF derivative based TPEs could be dynamically crosslinked by the Diels-Alder (DA) reaction to improve the mechanical properties without losing other properties of TPEs.

Hence, this chapter reports the synthesis and characterization of HMF derivative based TPEs using PLA as the hard blocks. The first step was to synthesize HMF derivative (2,5-FDA) based prepolymers with thiol end groups. The TPEs were then synthesized by a coupling reaction between the prepolymers and the PLA having acrylate end groups. The structural, physical, and mechanical properties of the synthesized TPEs were investigated by NMR, FTIR, DSC, TGA, and tensile tests. Furthermore, the effect of the DA reaction on the mechanical properties of TPEs was investigated. To the best of the authors' knowledge, this is the first study reporting the synthesis of PLA based TPEs using soft segments with thioether groups in a one-pot reaction under mild conditions. Moreover, the use of HMF derivative enabled the properties of TPEs to be adjusted.

6.3 Experimental Sections

6.3.1 Materials

Hydroxymethylfurfural (HMF, ≥99%), 1,3-propanedithiol (≥99%), triethylamine (TEA, ≥ 99.5%), tetrahydrofuran (THF, anhydrous, ≥99.9%, inhibitor free, and further dried under molecular sieves), N-phenylmaleimide (97%), acryloyl chloride (97%, contains<210 ppm MEHQ as stabilizer), dimethylphenylphosphine (DMPP, ≥ 99%), 1,1’-(methylenedi-4,1-phenylene)bismaleimide (bismaleimide, 95%), DMSO-d_6 (99.9 atom % D), chloroform-d (99.8 atom % D), poly(L-lactide), acrylate terminated (M_n 5,500, PDI ≤ 1.2), thin layer chromatography (TLC) plates and silica gel were purchased from Sigma-Aldrich. All reagents were used as received without further purification.

6.3.2 General procedure for the synthesis of TPEs

The synthesis of 2,5-furan diacrylate (2,5-FDA) was reported elsewhere.[227] A typical procedure for the synthesis of TPEs is described as follows: 2,5-FDA (1 eq) was dissolved in chloroform (0.6 M). The solution was purged under a nitrogen stream for 30 mins to remove the oxygen. Thereafter, 1,3-propanedithiol (1.1 eq) was added through a syringe. The reaction mixture was cooled in an ice-bath. DMPP (0.005 eq) was added to start the polymerization process. The reaction was performed at room temperature for 30 mins. Then, PLA with acrylate groups as end groups was dissolved in chloroform (0.1 eq) and added to the reaction. The reaction was carried out for another 30 mins. TPEs were then precipitated in cold hexane and recovered by filtration. Finally, TPEs were kept in a vacuum oven at 40 ^{o}C overnight to remove the residual solvent.

6.3.3 Film preparation and Diels-Alder reaction to tune the properties of TPEs

The TPEs films were prepared by solution casting in chloroform. TPEs (150 mg) were first dissolved in chloroform (2.5 mL) at 40 ^{o}C for 12h. The solution was then transferred into a Teflon mold, which was loosely covered for 24h to allow the solvent to evaporate. The residual solvent was removed in a vacuum oven at 40 ^{o}C for 48 h. For the TPE films crosslinked by Diels-Alder (DA) reaction, the procedure is described as follows: the polymer was first dissolved in chloroform at 40 ^{o}C for 12h. Bismaleimide was then added. After being transferred into a Teflon mold, the solution was kept for 24h at atmospheric conditions to evaporate the solvent. The residual solvent was completely removed in a vacuum oven at 40 ^{o}C for 48 h. This process was expected to increase the conversion of the furan rings to the DA adduct in the polymer. The films were held at room temperature for at least 24 h before analysis.

6.3.4 Characterization

^{1}H and ^{13}C NMR spectra were obtained on a Bruker AV 400 using DMSO-d_6 and $CDCl_3$ as solvents. The chemical shifts were referenced to the solvent residual signals at 2.50 ppm for deuterated DMSO and 7.26 ppm for $CDCl_3$. FTIR spectra were recorded in duplicate on a Thermo Scientific Nicolet iS5 FTIR spectrometer (Thermo, Madison, WI, USA) using an attenuated total reflectance (ATR) diamond crystal. The spectra were recorded at 32 scans and 4 cm^{-1} resolution in the range of 4000–600 cm^{-1}. The molecular weight distribution was determined by gel permeation chromatography (GPC, Water Breeze) using THF as the mobile

phase. The flow rate was set to 0.3 mL/min. The molecular weights were calibrated using linear polystyrene standards having a narrow molecular weight distribution. The thermal transitions of polymers were evaluated in duplicate by DSC (Q100, TA Instruments, Inc., New Castle, DE). The samples were compressed in aluminum pans. The heating rate and cooling rate were 10 ^{o}C/min. Thermogravimetric analysis (TGA, Q50, TA Instrument, Inc., New Castle, DE) was used to investigate the thermal stability of the polymers (powder). The flow rate of N_2 was 60 mL/min, and the samples were heated from 20 ^{o}C to 600 ^{o}C at a rate of 10 ^{o}C/min. Stress-strain tests were conducted in triplicates using a DMA Q800 (TA instruments, New Castle, DE) at 25 °C by ramping up a force at a rate of 1 N/min. A preload force of 0.01 N was used. A cyclic tensile test was performed to evaluate the elasticity of the elastomer. The films were first extended by ramping up a force at a rate of 0.2 N/min to a target force (1 N). Then the force was immediately reversed by ramping down at the same rate to 0 N. This was marked as one cycle, and three cycles were performed.

6.3.5 Calculation of crystallnity and elastic recovery

The percentage of crystallinity (X_c) of the PLA in the TPEs films was calculated based on the following equation:

$$X_c(\%) = [(\Delta H_m - \Delta H_c)/(\Delta H_{m'} \times x_{PLA})] \times 100$$

Where ΔH_m is the enthalpy of fusion, ΔH_c is the enthalpy of crystallization and the $\Delta H_{m'}$ is the melting enthalpy of 100% pure crystalline PLA (93 J/g).[230] x_{PLA} is the weight percentage of PLA in the TPEs determined by ^{1}H NMR.

The elastic recovery (ER) was measured by the step cyclic tensile tests. The following equation was used:

$$ER = 100\ [\varepsilon_{max} - \varepsilon(0, \varepsilon_{max})]/\varepsilon_{max}$$

Where ε_{max} is the maximum strain and $\varepsilon(0, \varepsilon_{max})$ is the strain in the cycle at zero stress after the maximums strain.

6.4 Results and Discussion

6.3.1 Synthesis and Characterization of Poly(β-thioether ester) and TPEs

2,5-FDA based TPEs were synthesized by a two-step thiol-Michael addition reaction, as shown in **Figure 6.1A**. The first step was to synthesize a prepolymer with thiol end groups. Then the prepolymer reacted with PLA having acrylate groups as end groups to generate triblock copolymers. Dimethylphenylphosphine (DMPP) has been observed to efficiently initiate the thiol-Michael reaction in THF.[227] However, PLA was partially soluble in THF, which prevented the synthesis of TPEs occurring in a one-pot reaction system. Hence, chloroform was used to solubilize PLA. ^{1}H NMR spectra showed that the acrylate groups proton signals of 2,5-FDA disappeared within 15 mins, indicating the full conversion of 2,5-FDA (**Figure 6.1B and 1C**). These results revealed that the thiol-Michael addition polymerization catalysed by DMPP could be quickly performed in chloroform as well.

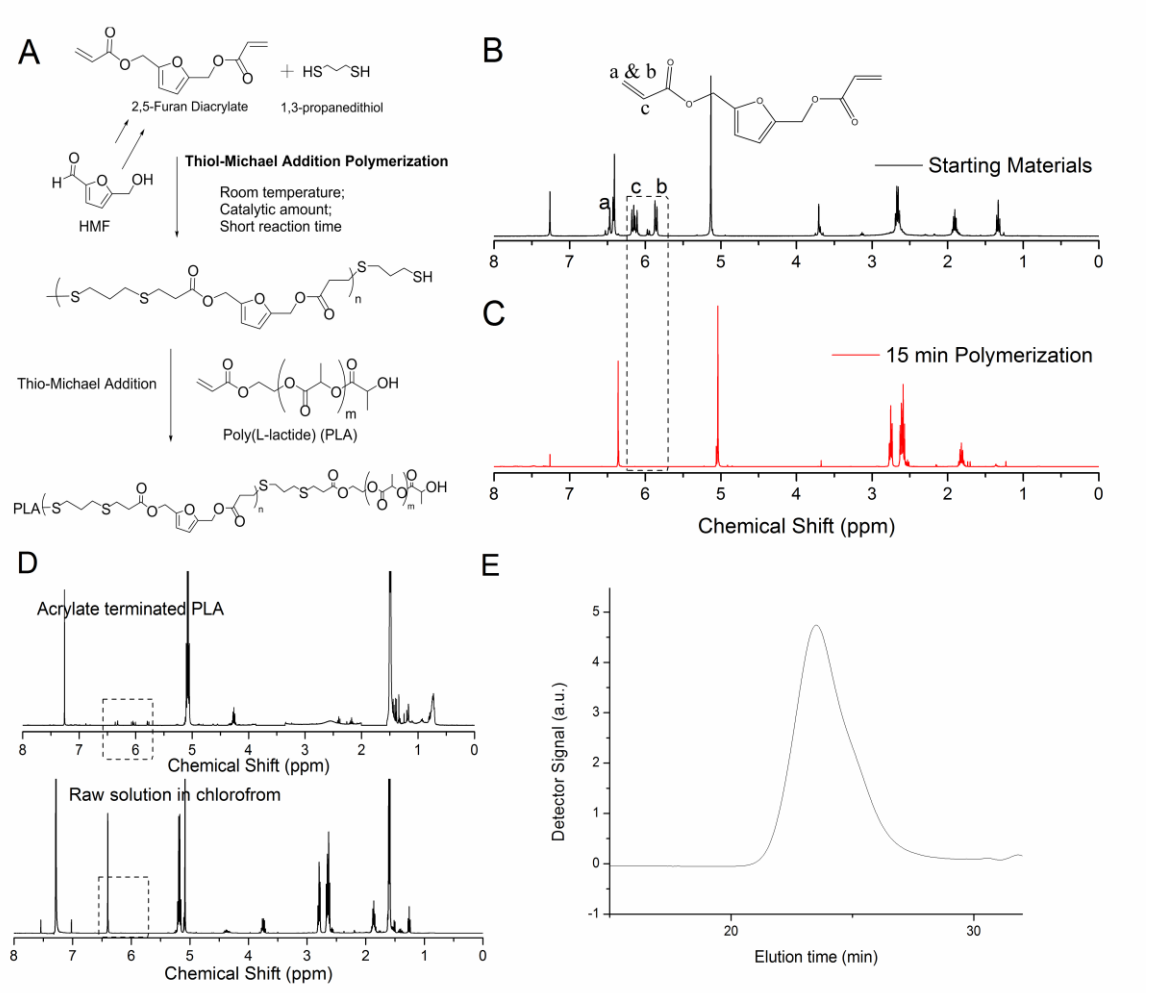

Figure 6.1 (A) Scheme to synthesize 2,5-FDA based TPEs from HMF; ^{1}H NMR spectra of step growth polymerization of 2,5-FDA and 1,3-propanedithiol in chloroform-d. (B) 0 min; (C) 15 min; (D) ^{1}H NMR of the macromolecular coupling between prepolymers and PLA with acrylate end groups in raw solution (chloroform); (E) GPC of PLA-PPF1.1-PLA.

Then, a prepolymer with thiol end groups was synthesized using a ratio of 1,3-propanedithiol to 2,5-FDA equalling to 1.1 to 1, which was represented by PPF1.1. The presence of thiol groups in the raw solution after the thiol-Michael addition polymerization was analysed by ^{1}H, ^{13}C NMR and HSQC (**Figure 6.2**). The proton signals corresponding to the thiol groups and the protons next to thiol groups were observed at 1.34 ppm (h') and 1.87 ppm (f') (**Figure 6.2A**). Moreover, carbon signals assigned to the carbon next to the thiol groups at the end of the prepolymer were observed at 23.47 ppm (g') (**Figure 6.2B and 1C**). These results revealed the successful synthesis of prepolymers having thiols end groups.

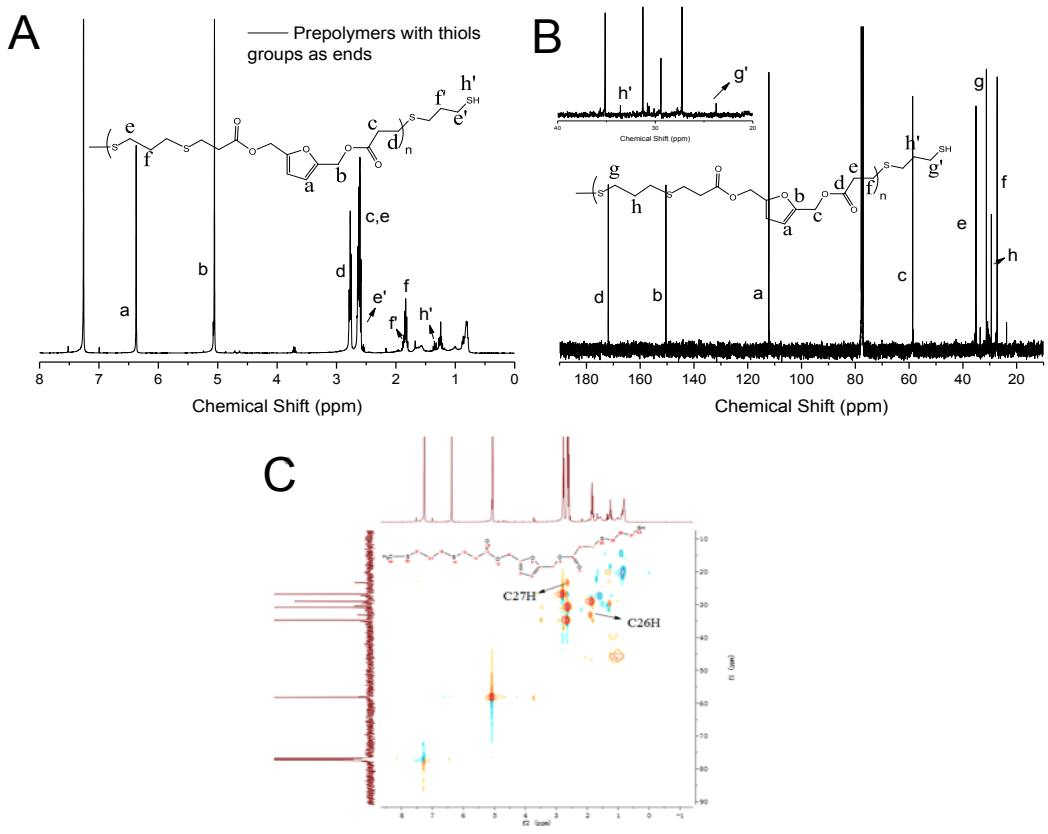

Figure 6.2 (A) ^{1}H NMR spectrum of prepolymers ended with thiol groups; (B) ^{13}C NMR of prepolymers; (C) HSQC of prepolymers.

Additionally, the macromolecular coupling between the prepolymers and PLA with acrylate end groups by the thiol-Michael addition reaction was investigated in chloroform (**Figure 6.1A**). The number average molecular weight of PLA with acrylate end groups was 5500 g/mol. First, a ^{1}H NMR spectrum of the raw solution showed that the proton signals of the acrylate groups disappeared after adding PLA to the prepolymer solution for 30 mins (PLA-PPF1.1-PLA indicating triblock copolymers with PPF1.1 as the soft segments, **Figure 6.1D**). Furthermore, a unimodal distribution of the synthesized polymers was observed by GPC analysis, and the number average molecular weight was 17000 g/mol (**Figure 6.1E**). These results indicated the high efficiency of DMPP to catalyse the coupling reaction between the thiol and the acrylate groups of the polymers.

The TPEs were then precipitated in cold hexane, and the structure was confirmed by ^{1}H, ^{13}C (**Figure 6.3A and B**), COSY, and HSQC NMR analyses (**Figure 6.4**). Furthermore, soft segments with higher molecular weights were synthesized to investigate their effects on the mechanical properties of TPEs. The ratios of 1,3-propanedithiol and 2,5-FDA were set to 1.05 to 1 (PLA-PPF1.05-PLA) and 1.02 to 1 (PLA-PPF1.02-PLA), respectively. The molecular weights of the soft segments increased as the ratio of 1,3-propanedithiol and 2,5-FDA decreased from 1.05:1 to 1.02:1. As shown in **Figure 6.3C**, the molecular weights of TPEs increased from 28000 g/mol to 36000 g/mol. The structure of the synthesized TPEs analysed by ^{1}H NMR and FTIR are shown in **Figure 6.3D and E**. The ratio of the signal intensity at 5.15 ppm (proton next to methyl groups of PLA) to the signal at 5.06 ppm (methylene groups next to the furan rings) decreased, indicating a decrease in the mass percentage of PLA in TPEs (**Figure 6.3D**). Additionally, the characteristic bands of PLA were observed, including stretching vibration of $-CH_2-$ at 2996 cm^{-1} and 2952 cm^{-1}, and C=O stretching vibration at 1755 cm^{-1} (**Figure 6.3 E, F and Figure 6.5**).

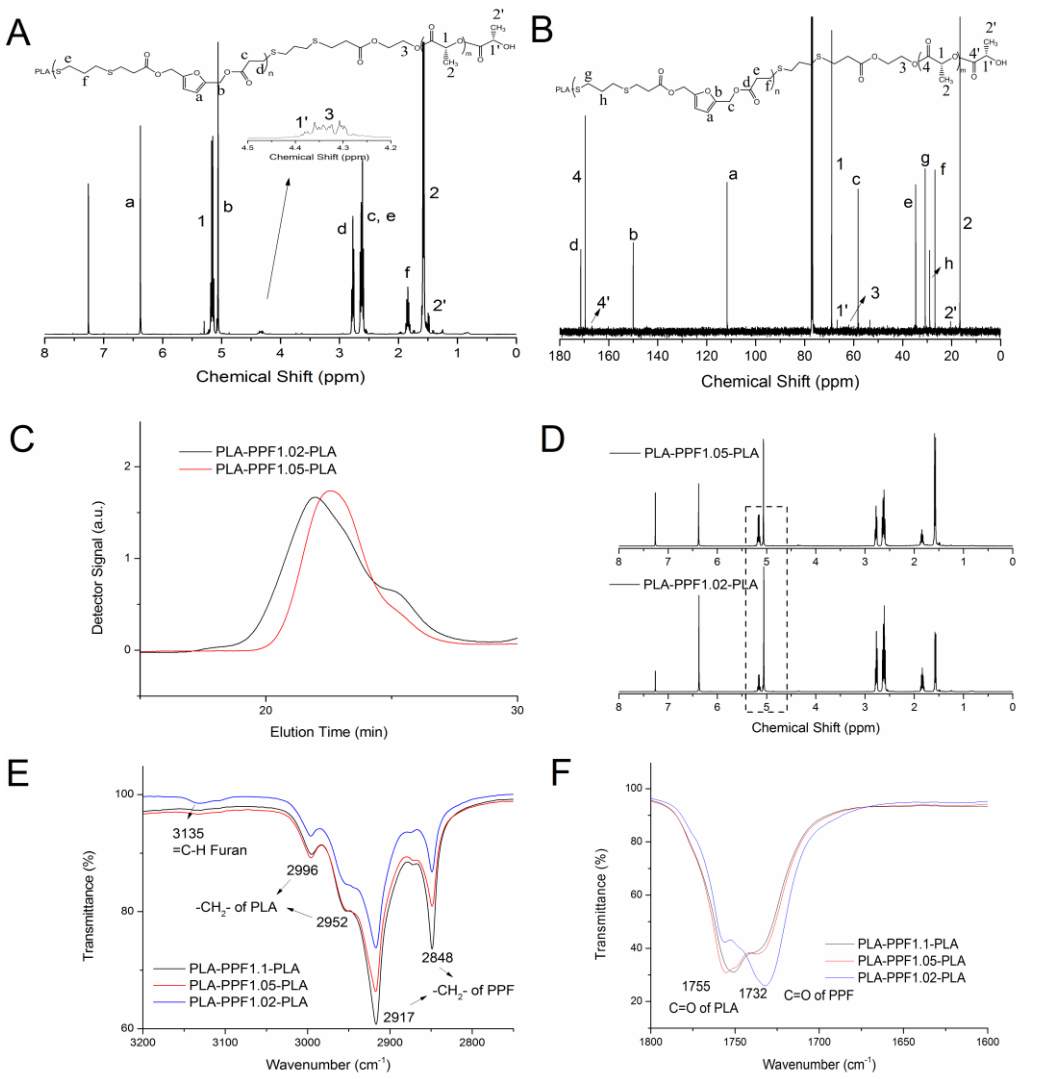

Figure 6.3 ^{1}H (A) and ^{13}C NMR (B) of PLA-PPF1.1-PLA; (C) GPC analysis of PLA-PPF-PLA with different soft segments; (D) ^{1}H NMR of PLA-PPF1.05-PLA and PLA-PPF1.02-PLA; (E) $-CH_2-$ regions; (F) carbonyl regions.

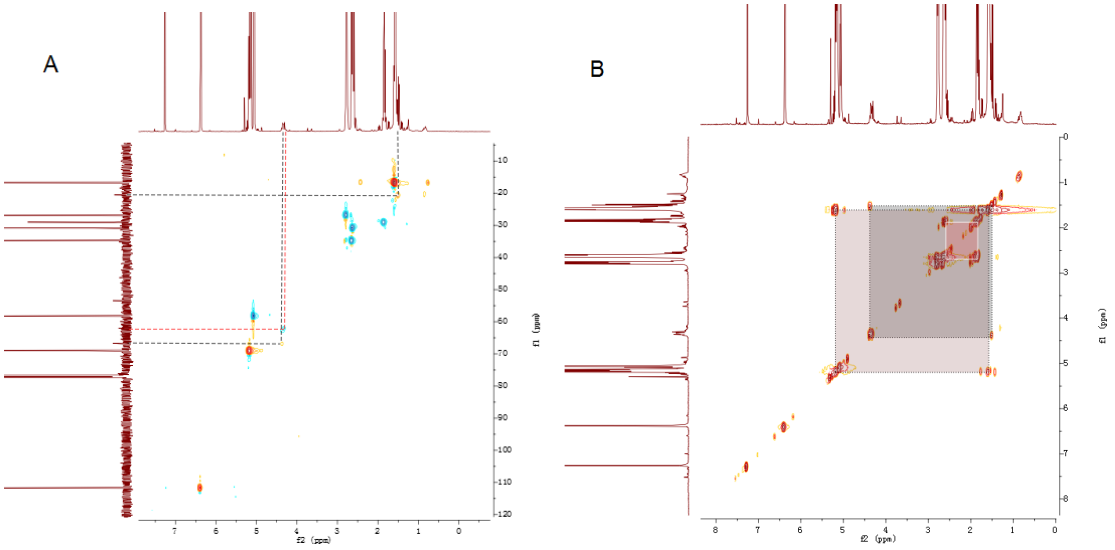

Figure 6.4 (A) HSQC and (B) COSY of TPEs.

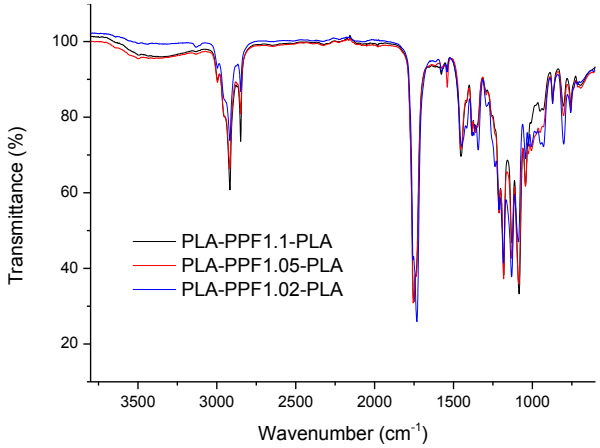

Figure 6.5 FTIR of PLA-PPF-PLA.

6.3.2 Thermal and Mechanical Properties of TPEs

DSC was used to evaluate the thermal transitions of the TPEs (**Figure 6.6**). A summary of the thermal transitions and the second heating curves are shown in **Table 6.1 and Figure 6.7A**, respectively. Two glass transition temperatures (T_g) for each synthesized TPE were observed, corresponding to the soft segment and the PLA segment in the TPEs. For example, the T_g of the soft segment in PLA-PPF1.1-PLA was -28.5 ºC, while the T_g of PLA segment was 37.7 ºC. Furthermore, the crystallization peaks were observed in the cooling step and the second heating curve. The cold crystallization temperature of PLA-PPF1.1-PLA was 89.2 ºC, which was higher

than the melt crystallization temperature (77.0 ºC). As the molecular weight of the soft segments increased, the melt crystallization temperature observed in the second heating curve slightly increased from 77.0 ºC to 79.8 ºC. Moreover, the ΔH_m was significantly increased from 10.0 J/g (PLA-PPF1.02-PLA) to 34.1 J/g (PLA-PPF1.1-PLA), indicating the presence of more crystallites in the TPEs. This could be explained by the different mass percentage of PLA in the TPEs. When the molecular weight of the soft segments in the TPEs increased, the mass percentage of PLA decreased from 67.9% (PLA-PPF1.1-PLA) to 27.8% (PLA-PPF1.02-PLA), as determined by ^{1}H NMR. The thermal stability of the synthesized TPEs was evaluated by TGA (**Figure 6.7B and 6.8**). The temperature at 5% weight loss for the TPEs was around 209-240 ºC (**Table 6.1**). Moreover, the maximum decomposition temperatures of PLA-PPF1.05-PLA were observed to be 225.9 ºC, 252.9 ºC and 285.1 ºC, respectively. The first two decomposition steps were the results of the decomposition of the soft segments, corresponding to the first stage of the α-hydrogen bond scission and alkyl-oxygen homolyses, as well as the second stage of C-S bond scission.[233]The decomposition step at 285.1 ºC was due to the degradation of the PLA segment.[235] However, for PLA-PPF1.02-PLA, only two decomposition stages were observed. This was probably due to the relatively low mass percentage of PLA present in TPEs (27.8%).

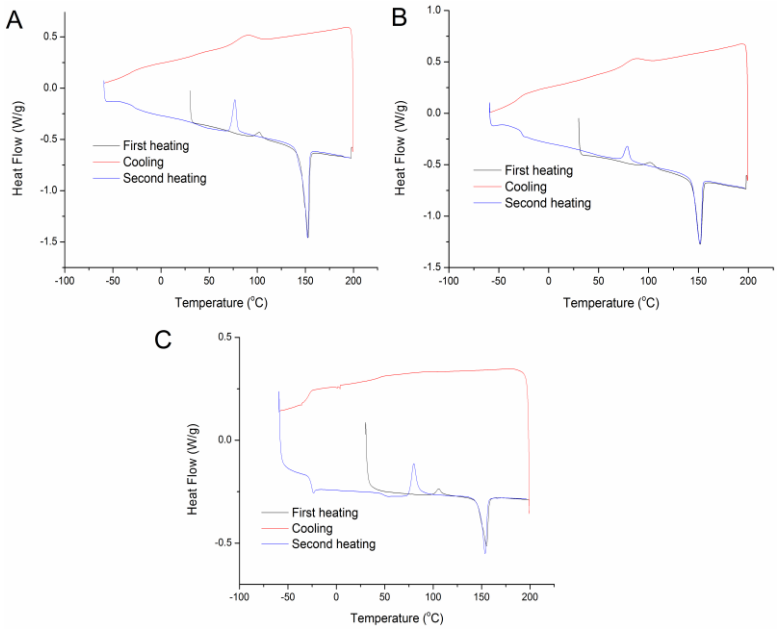

Figure 6.6 DSC curves of PLA-PPF1.1-PLA (A), PLA-PPF1.05-PLA (B) and PLA-PPF1.05-PLA (C). (Measured at heating rate of 10 ºC/min, cooling rate of 10 ºC/min)

Table 6.1 Thermal transitions and stability of synthesized PLA-PPF-PLA

Samples	TGA[b]		DSC[a]										
			First heating			Cooling			Second heating				
	$T_{5\%}$ (°C)	T_{max} (°C)	T_c(°C)	T_m (°C)	ΔH_m (J/g)	T_g (°C)	T_c (°C)	ΔH_c (J/g)	T_g (°C)	T_{cc} (°C)	ΔH_{cc} (J/g)	T_m (°C)	ΔH_m (J/g)
PLA-PPF1.1-PLA	233.8	233.3/ 269.8/ 301.4	102.4	152.8	34.4	-31.5/34.1	89.2	9.9	-28.5/37.7	77.0	9.6	152.2	34.1
PLA-PPF1.05-PLA	209.6	225.9/ 252.9/ 285.1	101.9	151.6	27.3	-27.5/39.9	85.9	8.1	-27.1/35.8	78.9	5.2	151.7	25.8
PLA-PPF1.02-PLA	238.1	239.7/ 283.1	105.9	155.1	10.7	-35.5/44.7	94.3	1.0	-25.4/47.6	79.8	6.8	153.5	10.0

[a] T_g = glass transition temperature, T_m = melting temperature, ΔH = enthalpy of transitions, T_c = crystallization temperature, T_{cc} =cold crystallization temperature upon heating. [b] $T_{5\%}$ = temperature where 5% mass loss, T_{max}= the maximum degradation rate.

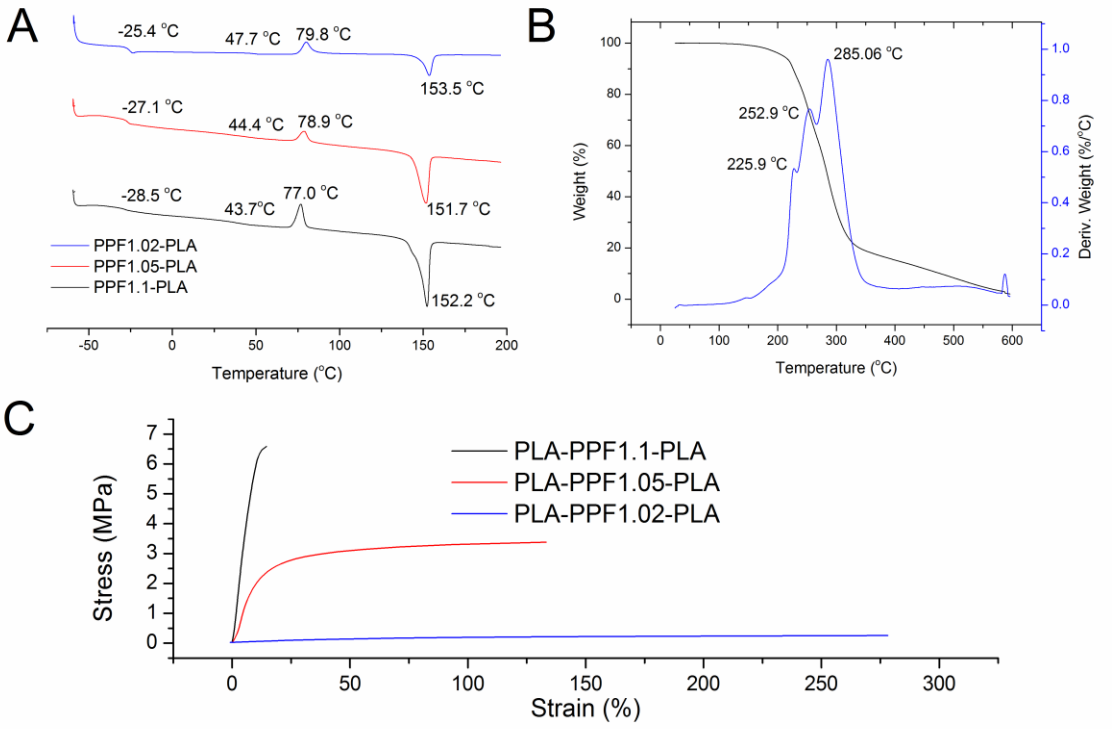

Figure 6.7 (A) DSC curves of PLA-PPF-PLA; (B) TGA curves of PLA-PPF-PLA and (C) Tensile tests of PLA-PPF-PLA.

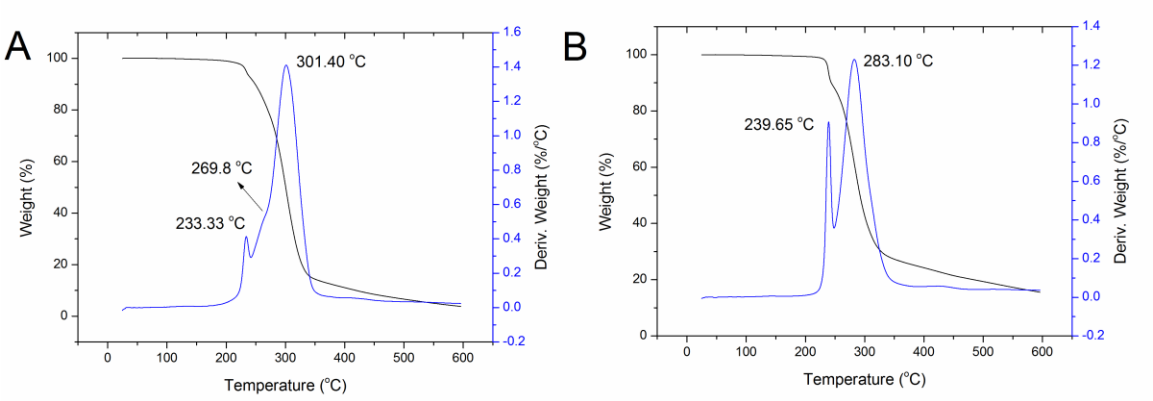

Figure 6.8 TGA curves of PLA-PPF1.1-PLA (A) and PLA-PPF1.02-PLA (B).

DMA was used to evaluate the viscoelastic behavior of elastomers (**Figure 6.9**). The storage modulus significantly decreased in the temperature regions of -35 ~ -10 °C and 40 ~ 60 °C, corresponding to the glass transition of soft segments and PLA segments, respectively. In addition, when the temperature was lower than 40 °C, the storage modulus of PLA-PPF1.1-PLA was obviously higher than the other two samples. This was consistent with other observation that increasing the mass percentage of PLA segments in the TPEs led to an enhancement of storage modulus.

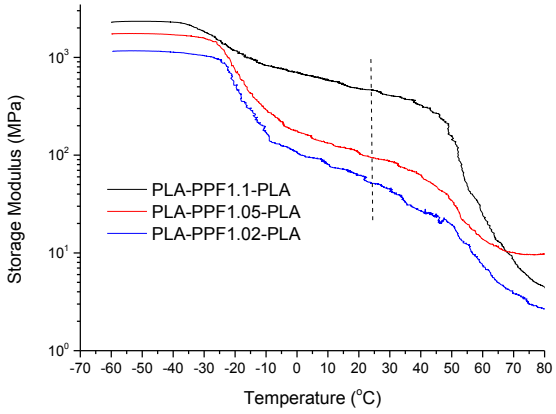

Figure 6.9 Representative DMA curves of storage modulus versus temperature for PLF-PPF-PLA.

The films used for the determination of the mechanical properties were prepared by solution casting. Several factors, such as the type of solvent used, the evaporation rate, and concentration of polymer, can influence the crystallization of PLA during the solution casting process.[236] Here, the effect of the solvent used (dichloromethane or chloroform) was investigated using PLA-PPF1.1-PLA. Similar to the behavior of pure PLA,[237] the crystallinity percentage of TPEs in

dichloromethane was higher (41.2%) than in chloroform (21.6%) (**Figure 6.10**). Due to the brittleness of the films obtained in dichloromethane, chloroform was chosen for the film preparation. The mechanical properties of three TPEs were determined by tensile tests (**Figure 6.7C and Table 6.2**). A linear response was observed for the three samples at low strain. As the molecular weight of the soft segments increased, the Young's modulus and the tensile strength decreased from 45.6 MPa (PLA-PPF1.1-PLA) to 0.3 MPa (PLA-PPF1.05-PLA), and from 6.6 MPa to 0.4 MPa, respectively. However, the elongation at break was increased from 14.5% to 277.8%. In addition, cyclic tests for PLA-PPF-1.05-PLA were performed to evaluate the elasticity of TPEs (**Figure 6.11**). It was observed that the residual strain for the first cycle was 2.4%, as compared to 0.7% (second cycle), and 0.6 % (third cycle). Moreover, the elastic recovery was increased from 70.2 % (first cycle) to 93.4 % (third cycle). It has been suggested that the mechanical properties of PLA based TPEs were highly dependent on several factors, such as the composition of TPEs and the crystalline structure of PLA blocks.[231] Although only the effect of the molecular weight of soft segments on the mechanical properties was investigated, the observed mechanical behavior of PLA-PPF-PLA could be the result of microphase separation, due to the presence of two T_g values as observed by DSC analysis. PLA segments acted as physical crosslinks to provide the strength, while the PPF soft segments were responsible for the ductility. In addition, the presence of residual strain for PLA based TPEs has been suggested to be the results of either crystals orientation or "slippage" effect.[232b]

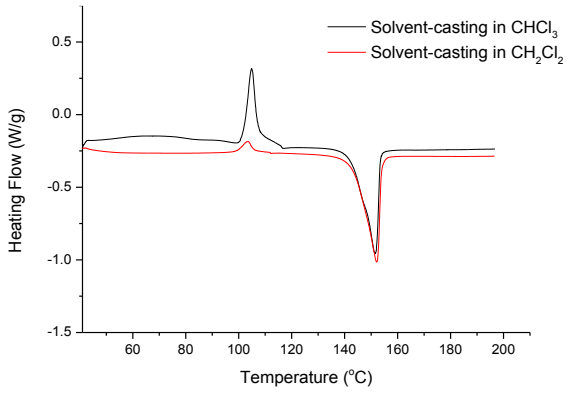

Figure 6.10 The comparison of thermal transitions of two films prepared *via* CH_2Cl_2 and $CHCl_3$, respectively.

Table 6.2 Tensile properties of solvent-casting PLA-PPF-PLA

Samples	Young's modulus (MPa)	Tensile strength (MPa)	Elongation at break (%)
PLA-PPF1.1-PLA	45.6±3.2	6.6±1.2	14.5±2.5
PLA-PPF1.05-PLA	16.7±2.9	3.4±0.5	133.1±10.9
PLA-PPF1.02-PLA	0.3±0.1	0.4±0.1	277.8±25.7

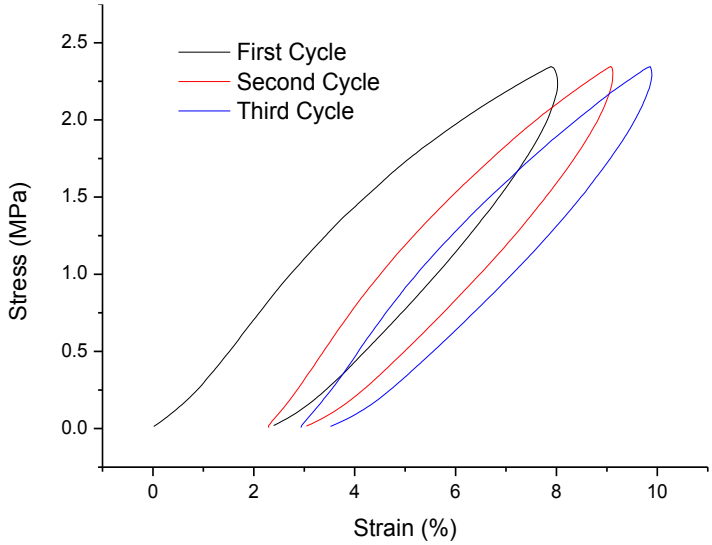

Figure 6.11 Cyclic tests of PLA-PPF1.05-PLA (Strains < 10%).

6.3.3 Diels-Alder reaction of furan rings in the TPEs

The DA reaction has been widely used to tune the properties of polymers, modify the films to increase the functionality, and synthesize self-healing materials.[238] Due to the presence of furan rings in the soft segments of TPEs, it was hypothesized that the DA reaction between the furan rings and the maleimides groups could be utilized to modify the synthesized TPEs. PLA-PPF1.02-PLA was used as model, and the DA reaction was investigated to tune the mechanical properties of TPEs. The DA crosslinked films were prepared by mixing the polymer solution and bismaleimide. The weight ratio of TPEs to crosslinkers was 10:1. After curing at 40 ^{o}C for 48h, the FTIR and mechanical properties of the crosslinked films were determined (**Figure 6.12 and Figure 6.13**). A new peak at 1715 cm^{-1}, assigned to the carbonyl groups of maleimide, appeared (**Figure 6.12A**), while the signal at 690 cm^{-1} attributed to the protons of the maleimide ring disappeared (**Figure 6.12B**). These results indicated that most of the maleimide groups had efficiently reacted with the furan rings in the TPEs. The stress-strain curves of DA crosslinked

TPEs showed that the Young's modulus and ultimate tensile strength were significantly improved to 5.5 MPa and 3.3 MPa, respectively, despite the decrease in elongation at break (112.7%) (**Figure 6.12C**). These results indicated that the mechanical properties of PLA-PPF-PLA could be efficiently improved in terms of Young's modulus and tensile strength, due to the ability of the DA reaction to form new crosslinking points.[239]

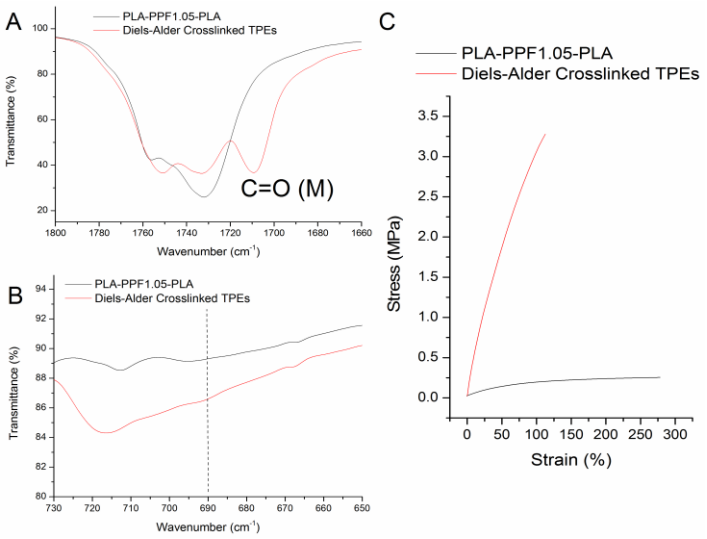

Figure 6.12 (A) Carbonyl region of PLA-PPF1.02-PLA and DA crosslinked films; (B) protons peak region of maleimide; (C) Stress-strain tensile tests of PLA-PPF1.05-PLA and crosslinked films.

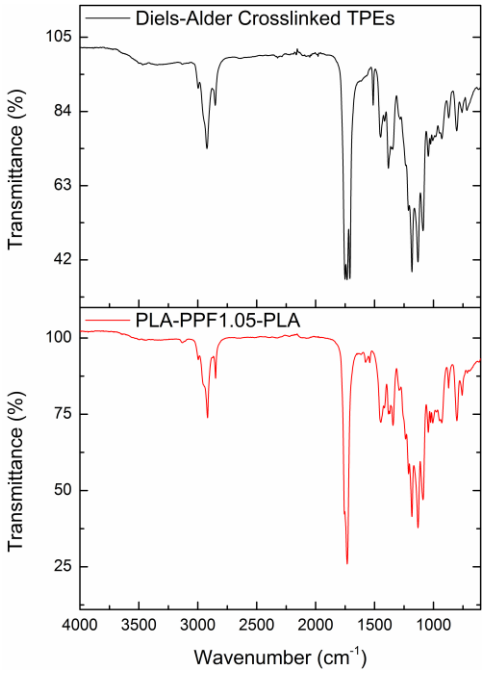

Figure 6.13 FTIR of PLA-PPF1.02-PLA and DA crosslinked TPEs.

6.5 Conclusion

HMF derivative based TPEs were synthesized using the thiol-Michael addition reaction in a one-pot system under mild conditions. Chloroform was used as solvent to initiate the thiol-Michael addition reaction using DMPP as catalyst. The macromolecular coupling between the thiols and the acrylate groups of the polymers could be achieved under the same conditions. The molecular weights of the middle soft segments were adjustable depending on the ratio of the two monomers. Therefore, TPEs with different molecular weights were prepared, leading to TPEs films with varied thermal and mechanical properties. DSC analysis revealed two T_g, indicating the presence of microphase separation. Similar to pure PLA, PLA in the TPEs crystallized during the solvent casting process in chloroform, which was important for the mechanical properties of TPEs films. TGA analysis showed that all the TPEs were thermally stable to at least 210 ^oC. The presence of furan rings in the soft segments could function as reactive sites to be dynamically crosslinked *via* the DA reaction. As a result, the tensile strength of PLA-PPF1.02-PLA could be significantly improved from 0.4 MPa to 3.3 MPa (crosslinked PLA-PPF1.02-PLA). Although the mechanical properties of the synthesized HMF derivative based TPEs were not comparable to some of other renewable TPEs, the presence of furan rings, available for properties adjustment, might broaden their applications. Moreover, the compositions and properties of the soft segments could be adjusted by the copolymerization of different monomers to yield a variety of TPEs.[233]

Chapter 7: General Conclusions and Recommendations

7.1 General conclusions and summary

This thesis investigated the synthesis and characterization of HMF derivative based polymers and networks. In order to obtain the expected structures of linear polymers with relatively high molecular weight, the catalyst effect on the conversion and side reactions occurring during the thiol-Michael addition reaction was investigated using a model reaction. The elucidation of this effect and side reactions is beneficial for the synthesis of linear polymers. Although the presence of side reactions for DBU and DMPP has been observed, such as the formation of disulfide and the dimerization of furfural acrylate, it was avoidable when using a catalytic amount of catalyst under an inert atmosphere. As a result, DMPP efficiently catalyzed the thiol-Michael addition polymerization to synthesize poly(β-thioether ester) from 2,5-FDA. In addition, the occurrence of the DA reaction between the furan rings and bismaleimide was observed due to the formation of an organogel (**Chapter 3**).

To tune the structures and properties of 2,5-FDA based polymers, (co)polymers were synthesized. The ^{1}H NMR and DSC results revealed that DMPP efficiently initiated the thiol-Michael addition polymerization regardless of the *pKa* of the thiols groups due to the formation of a strong base *via* the nucleophilic attack on the Michael acceptor. Furthermore, the obtained linear polymer with hydroxyl groups as side groups were used as a hot melt adhesive on wood substrates. The results showed that the polymers had an adhesive strength of 1.5 MPa. For the polymers synthesized from 2,5-FDA and 1,6-hexanedithiol, multiple melting peaks were observed in the first scan during the DSC analysis. It was demonstrated due to the solvent-induced crystallization during the process of polymer synthesis. Furthermore, the observed two-stage degradation of 2,5-FDA based poly(β-thioether ester) was the result of α-hydrogen bond scission and alkyl-oxygen homolysis at low temperature, as well as the C-S bond scission at high temperature. To improve the mechanical properties of linear polymers, the DA reaction was used to dynamically crosslink the linear polymers to networks. The kinetic of the DA and retro-DA reactions were investigated in detail. The results showed that the DA reaction between BHF and bismaleimide could reach over 84% conversion at 40 ^{o}C after 48 h. Moreover, the polymer network could be de-crosslinked *via* the retro DA reaction when it was heated to 110 ^{o}C for 2h. As the weight ratio of crosslinkers to polymers increased from 1:10 to 1:2, the storage modulus

at room temperature was significantly enhanced from 1.5 MPa to 1691 MPa. These results indicated that the DA reaction was an efficient way to increase the mechanical properties of 2,5-FDA based polymers without losing the reprocessability. Finally, TPEs were synthesized *via* the thiol-Michael addition reaction in a one-pot system. The elasticity of TPEs was observed, and the maximum elongation at break of TPEs could reach > 450 % (**Chapter 4**).

By the combination of the thiol-Michael addition and the DA reaction, thermoset elastomers were synthesized (**Chapter 5**). The choice of 1,3-propanedithiol as monomers was important due to its decreased ability to crystallize, as compared to the networks synthesized from 1,6-hexanedithiol. When the weight ratio of polymer to crosslinker was 5:1, the Young's modulus, ultimate strength, and elongation at break were 4.3±0.6 MPa, 5.7±1.1 MPa, and 205.3±20.1%, respectively. Moreover, a high elastic recovery (98.9%) and low residual strain (0.7%) were observed after the third cycle during the cyclic tensile test. The structure, properties and functionality of elastomers were varied by the synthesis of linear copoly(β-thioether ester) due to the high efficiency of the thiol-Michael addition observed in the synthesis of copolymer (**Chapter 4**). Finally, the reprocessability of thermoset elastomers was demonstrated *via* heating the crosslinked films in dimethylformamide solution to a new film. The tensile test analysis revealed that the mechanical properties of the reprocessed elastomers were similar to the original elastomers, despite the slight decrease in elongation at break (189.3±15.2 %) and ultimate strength (4.4±0.5 MPa).

The last chapter (**Chapter 6**) investigated the synthesis and characterization of PLA based TPEs using the soft segments synthesized from 2,5-FDA. Chloroform was a good solvent to dissolve PLA and allowed the occurrence of the thiol-Michael addition as determined by ^{1}H NMR. Moreover, the macromolecular coupling between thiol and acrylate groups was observed using DMPP as the catalyst. As a result, the triblock copolymers were synthesized as TPEs. TPEs with different molecular weights were also prepared, leading to TPEs films with varied thermal and mechanical properties. DSC analysis revealed two T_g, indicating the presence of microphase separation. The cyclic tensile tests demonstrated the elasticity of the synthesized TPEs. The furan rings in the soft segments were dynamically crosslinked *via* DA reaction. As a result, the tensile strength of TPEs was significantly improved from 0.4 MPa to 3.3 MPa (crosslinked TPEs).

7.2 Contributions to knowledge

HMF, an important renewable platform chemical, has been widely investigated. However, in addition to 2,5-FDCA, information on the use of other HMF derivative to synthesize high-performance materials is less available. This work has demonstrated the use of a HMF derivative (2,5-FDA) to synthesize polymers and networks, which contributed to the knowledge in the following aspects:

1. a) Side reactions were observed for the thiol-Michael addition reaction when a model reaction between furfural acrylate and 1-propanethiol was performed, including the Aza-Michael addition reaction, the formation of disulfide, and the dimerization of furfural acrylate. The use of hexylamine in a catalytic amount minimized the Aza-Michael addition reaction, but resulted in a longer reaction time. The formation of disulfide was eliminated under an inert atmosphere. The dimerization of furfural acrylate was avoidable when using a catalytic amount of DMPP to initiate the thiol-Michael addition reaction. This contribution may enable the thiol-Michael addition to be widely used in the synthesis of polymers. b) Due to the high nucleophilicity of DMPP, it was shown that thiol-Michael addition was an efficient reaction to synthesize copolymers (2,5-FDA, 1,6-hexanedithiol and 1,4-benzenedithiol), regardless of the *pKa* of dithiol monomers. Moreover, polymers having functional groups, such as hydroxyl groups, were synthesized.

2. The thiol-Michael addition reaction can be used to synthesize 2,5-FDA based linear polymers. The DA and retro-DA reaction occurred between the furan rings in the polymeric chains and bismaleimide, which was confirmed by NMR. This provided an efficient approach to improve the thermal and mechanical properties of the materials synthesized *via* the thiol-Michael addition reaction, as compared to other reported methods, such as the oxidation of thioether groups to sulfone groups and the synthesis of hybrid materials.[240]

3. The flexible thioether groups were shown to be suitable in the synthesis of elastomers. a) *Via* the use of hydrogen bondings as crosslinking points, a thermoplastic elastomer was synthesized under mild reaction conditions when 2,5-FDA, 1,3-propanedithiol, and dithiothreitol were used. b) Due to the occurrence of the DA reaction between the furan rings and bismaleimide, a thermoset elastomer was synthesized via the combination of the thiol-Michael and the DA reactions. The advantages of these 2,5-FDA based thermoset elastomers include easy

synthesis process, facile incorporation of other functionalities, mild reaction conditions, good elasticity, and reprocessability.

4. The potential use of 2,5-FDA based linear polymers as hot melt adhesive was determined. It is expected that the adhesive properties can be further improved *via* the copolymerization of other monomers.

5. a) It was demonstrated that the presence of multiple melting peaks shown in the first scan during DSC analysis for poly(β-thioether ester) synthesized from 2,5-FDA and 1,6-hexanedithiol was due to solvent-induced crystallization during the process of polymer synthesis. Moreover, this process was influenced by the concentration of polymers. This contribution may be used to explain similar thermal properties observed in other polyesters.[241] b) TGA analysis showed that there was a two-stage degradation pattern for poly(β-thioether ester). Py-GC-MS revealed that the first stage of degradation was mainly the result of α-hydrogen bond scission and alkyl-oxygen homolysis, while the second stage was mainly due to a C-S bond scission. The contribution indicated that the presence of furan rings in poly(β-thioether ester) led to a different degradation pattern, as compared to poly(β-thioether ester) synthesized from 1,6-hexanediol diacrylate.[3]

6. When DMPP was used as a catylyst, the thiol-Michael addition reaction between 2,5-FDA and 1,3-propanedithiol was initiated in various organic solvents, such as THF and chloroform. Furthermore, the macromolecular coupling between the thiol and acrylate groups of polymers was demonstrated by NMR and GPC. As a result, the synthesis of TPEs by the thiol-Michael addition reaction in a one-pot system under mild reaction conditions was performed. The presence of furan rings in the soft segments enabled the TPEs to be modified.

7.3 Recommendations for future research

Based on the work performed in this thesis, certain avenues for further advances in this line of research are proposed:

1. Solvent-free reaction has been suggested to be an environmentally friendly approach to synthesize polymers and networks. Thiol-ene reactions have been investigated under solvent free conditions.[243] Therefore, the development of catalysts which could initiate the thiol-Michael addition reaction under similar conditions could further improve the sustainability of the reaction. One potential development is to design a photo-responsive catalyst.

2. The use of 2,5-FDA based polymers with hydroxyl groups as the side chains could be used as a hot melt adhesive. Recently, supramolecular polymer adhesives have been investigated due to their dynamic, stimuli-responsive nature and non-covalent interaction.[244] Therefore, the incorporation of other supramolecular interaction, such as ureido-pyrimidinone into 2,5-FDA based polymers, could further improve the adhesive properties without compromising their heat responsive properties.

3. Generally, PUs are synthesized by the reaction between isocyanate and polyols. The structures and properties of PU are tunable depending on the structures of the polyols and diisocyanates. So far, most of polyols are synthesized from petroleum. Therefore, polyols could be synthesized from 2,5-FDA based polymers and be used in the synthesis of PUs. The thermal and mechanical properties of PU networks were adjustable by tuning the structures of polyols. Moreover, due to the presence of furan rings in the PU networks, the DA reaction could be used to modify the surface of networks and broaden their potential applications.

4. The synthesis of networks is of interest since it increases both the mechanical and thermal properties of polymers. Recently, the preparation of hybrid materials has been examined to improve the properties of networks containing thioether groups.[240a] Therefore, the thiol-Michael addition reaction and photoinitiated radical polymerization can be combined to synthesize 2,5-FDA based networks. The first step would involve the synthesis of prepolymers with acrylate groups. The molecular weight of the prepolymers could be varied by changing the ratio of diacrylate to dithiol. Then, polymers having acrylate groups as ends could be crosslinked *via*

radical polymerization. As a result, a network with tunable properties could be synthesized from 2,5-FDA.

5. It has been observed that the strcutures of crosslinker significantly influnenced the properties of networks synthesized *via* DA reaction.[245] Hence, the effect of the structures of crosslinker on the thermal and mechanical properies of reprocessable thermoset elastomers is worthy of being investigated. In addition, in order to broaden the potential applications of reprocessable thermoset elastomers, a further improvement in their properties needs to be evaluated. The potential aspects include the addition of fillers (nanocellulose, carbon nanotube and graphene), the modification of hydroxyl groups with antibacterial peptides, and the incorporation of other functional comonomers. Furthermore, 3D printing can be also used to produce reprocessable elastomers with varied 3D structures.

List of References

1. a) C. Voirin, S. Caillol, N. V. Sadavarte, B. V. Tawade, B. Boutevin and P. P. Wadgaonkar, *Polym. Chem.*, 2014, **5**, 3142-3162; b)F. Fenouillot, A. Rousseau, G. Colomines, R. Saint-Loup and J. P. Pascault, *Prog. Polym. Sci.* , 2010, **35**, 578-622; c)Y. Xia and R. C. Larock, *Green Chemistry*, 2010, **12**, 1893-1909; d) P. A. Wilbon, F. Chu and C. Tang, *Macromol. Rapid Commun.* , 2013, **34**, 8-37; e)M. Fache, E. Darroman, V. Besse, R. Auvergne, S. Caillol and B. Boutevin, *Green Chemistry*, 2014, **16**, 1987-1998; f)C. Moreau, M. N. Belgacem and A. Gandini, *Top. Catal.* , 2004, **27**, 11-30; g) M. N. Belgacem and A. Gandini, *Monomers, polymers and composites from renewable resources*, Elsevier, 2011; h)L. Montero de Espinosa and M. A. R. Meier, *Eur. Polym. J.* , 2011, **47**, 837-852; i) A. Gandini, *Green Chemistry*, 2011, **13**, 1061-1083.

2. a) R.-J. van Putten, J. C. van der Waal, E. De Jong, C. B. Rasrendra, H. J. Heeres and J. G. de Vries, *Chem. Rev.* , 2013, **113**, 1499-1597; b)A. A. Rosatella, S. P. Simeonov, R. F. M. Frade and C. A. M. Afonso, *Green Chemistry*, 2011, **13**, 754-793; c)E. Capuano and V. Fogliano, *LWT - Food Science and Technology*, 2011, **44**, 793-810; d)F. Koopman, N. Wierckx, J. H. de Winde and H. J. Ruijssenaars, *Proceedings of the National Academy of Sciences*, 2010, **107**, 4919-4924.

3. a) T. Wang, M. W. Nolte and B. H. Shanks, *Green Chemistry*, 2014, **16**, 548-572; b)I. Agirrezabal-Telleria, I. Gandarias and P. Arias, *Catal. Today* 2014, **234**, 42-58; c)S. Dutta, S. De and B. Saha, *Biomass Bioenergy* 2013, **55**, 355-369; d)A. Corma, S. Iborra and A. Velty, *Chem. Rev.* , 2007, **107**, 2411-2502; e)X. Tong, Y. Ma and Y. Li, *Appl. Catal., A* 2010, **385**, 1-13; f)J. N. Chheda, G. W. Huber and J. A. Dumesic, *Angew. Chem. Int. Ed.* , 2007, **46**, 7164-7183; g)M. J. Climent, A. Corma and S. Iborra, *Green chemistry*, 2011, **13**, 520-540; h)R. Karinen, K. Vilonen and M. Niemelä, *ChemSusChem*, 2011, **4**, 1002-1016.

4. a) S. P. Teong, G. Yi and Y. Zhang, *Green Chemistry*, 2014, **16**, 2015-2026; b)A. Mukherjee, M.-J. Dumont and V. Raghavan, *Biomass Bioenergy* 2015, **72**, 143-183.

5. a) M. E. Zakrzewska, E. Bogel-Łukasik and R. Bogel-Łukasik, *Chem. Rev.* , 2010, **111**, 397-417; b)T. Ståhlberg, W. Fu, J. M. Woodley and A. Riisager, *ChemSusChem*, 2011, **4**, 451-458; c)B. Saha and M. M. Abu-Omar, *Green Chemistry*, 2014, **16**, 24-38; d)S. Roy Goswami,

M.-J. Dumont and V. Raghavan, *Industrial & Engineering Chemistry Research*, 2016, **55**, 4473-4481.

6. a) L. Hu, G. Zhao, W. Hao, X. Tang, Y. Sun, L. Lin and S. Liu, *RSC Adv.*, 2012, **2**, 11184-11206; b)S. Dutta, S. De and B. Saha, *ChemPlusChem*, 2012, **77**, 259-272.

7. J. Lewkowski, *Arkivoc* 2001, **2**,17.

8. a) A. S. Amarasekara, *Renewable Polymers: Synthesis, Processing, and Technology*, 2011, 381-428; b)A. Gandini and M. N. Belgacem, *Prog. Polym. Sci.* , 1997, **22**, 1203-1379; c)A. Gandini, *Polym. Chem.*, 2010, **1**, 245-251; d)A. Gandini, *Macromolecules*, 2008, **41**, 9491-9504.

9. M. l. Besson, P. Gallezot and C. Pinel, *Chem. Rev.* , 2013, **114**, 1827-1870.

10. a) S. K. Burgess, J. E. Leisen, B. E. Kraftschik, C. R. Mubarak, R. M. Kriegel and W. J. Koros, *Macromolecules*, 2014, **47**, 1383-1391; b)G. Z. Papageorgiou, V. Tsanaktsis and D. N. Bikiaris, *PCCP* 2014, **16**, 7946-7958; c)E. de Jong, M. Dam, L. Sipos and G. Gruter, *Biobased monomers, polymers, and materials*, 2012, **1105**, 1-13; d)S. K. Burgess, O. Karvan, J. Johnson, R. M. Kriegel and W. J. Koros, *Polymer*, 2014, **55**, 4748-4756; e)V. Tsanaktsis, D. G. Papageorgiou, S. Exarhopoulos, D. N. Bikiaris and G. Z. Papageorgiou, *Crystal Growth & Design*, 2015, **15**, 5505-5512; f)Y. Mao, R. M. Kriegel and D. G. Bucknall, *Polymer*, 2016, **102**, 308-314; g)L. Martino, N. Guigo, J. G. van Berkel, J. J. Kolstad and N. Sbirrazzuoli, *Macromol. Mater. Eng.* , 2016, **301**, 586-596; h)A. Codou, M. Moncel, J. G. van Berkel, N. Guigo and N. Sbirrazzuoli, *PCCP* 2016, **18**, 16647-16658; i)T. Dimitriadis, D. N. Bikiaris, G. Z. Papageorgiou and G. Floudas, *Macromol. Chem. Phys.* , 2016, **217**, 2056-2062; j)M. Lomelí-Rodríguez, M. Martín-Molina, M. Jiménez-Pardo, Z. Nasim-Afzal, S. I. Cauët, T. E. Davies, M. Rivera-Toledo and J. A. Lopez-Sanchez, *J. Polym. Sci., Part A: Polym. Chem.* , 2016, **54**, 2876-2887; k)Z. Terzopoulou, V. Tsanaktsis, M. Nerantzaki, D. S. Achilias, T. Vaimakis, G. Z. Papageorgiou and D. N. Bikiaris, *J. Anal. Appl. Pyrolysis* 2016, **117**, 162-175.

11. A. F. Sousa, C. Vilela, A. C. Fonseca, M. Matos, C. S. R. Freire, G.-J. M. Gruter, J. F. J. Coelho and A. J. D. Silvestre, *Polym. Chem.*, 2015, **6**, 5961-5983.

12. a) Y. Jiang, D. Maniar, A. J. J. Woortman, G. O. R. Alberda van Ekenstein and K. Loos, *Biomacromolecules*, 2015, **16**, 3674-3685; b)J. Carlos Morales-Huerta, A. Martínez de Ilarduya

and S. Muñoz-Guerra, *Polymer*, 2016, **87**, 148-158; c)N. Yoshida, N. Kasuya, N. Haga and K. Fukuda, *Polym. J.* , 2008, **40**, 1164-1169; d)A. F. Sousa, A. C. Fonseca, A. C. Serra, C. S. R. Freire, A. J. D. Silvestre and J. F. J. Coelho, *Polym. Chem.*, 2016, **7**, 1049-1058.

13. B. D. Mather, K. Viswanathan, K. M. Miller and T. E. Long, *Prog. Polym. Sci.* , 2006, **31**, 487-531.

14. a) D. P. Nair, M. Podgórski, S. Chatani, T. Gong, W. Xi, C. R. Fenoli and C. N. Bowman, *Chem. Mater.* , 2014, 26, 724-744; b)J. W. Chan, B. Yu, C. E. Hoyle and A. B. Lowe, *Polymer*, 2009, 50, 3158-3168; c)J. Xu and C. Boyer, *Macromolecules*, 2015, 48, 520-529; d)A. H. Soeriyadi, G.-Z. Li, S. Slavin, M. W. Jones, C. M. Amos, C. R. Becer, M. R. Whittaker, D. M. Haddleton, C. Boyer and T. P. Davis, *Polym. Chem*., 2011, 2, 815-822.

15. J. D. Flores, N. J. Treat, A. W. York and C. L. McCormick, *Polym. Chem.*, 2011, **2**, 1976-1985.

16. a) J. Shin, H. Matsushima, J. W. Chan and C. E. Hoyle, *Macromolecules*, 2009, **42**, 3294-3301; b)J. Vandenbergh, M. Peeters, T. Kretschmer, P. Wagner and T. Junkers, *Polymer*, 2014, **55**, 3525-3532; c)J. Vandenbergh, G. Ramakers, L. van Lokeren, G. van Assche and T. Junkers, *RSC Adv.*, 2015, **5**, 81920-81932; d)J. Vandenbergh, K. Ranieri and T. Junkers, *Macromol. Chem. Phys.* , 2012, **213**, 2611-2617; e)K. Dan and S. Ghosh, *Polym. Chem.*, 2014, **5**, 3901-3909; f)N. Zaquen, B. Wenn, K. Ranieri, J. Vandenbergh and T. Junkers, *J. Polym. Sci., Part A: Polym. Chem.* , 2014, **52**, 178-187; g)A. C. Pauly and F. di Lena, *Polymer*, 2015, **72**, 378-381.

17. G.-Z. Li, R. K. Randev, A. H. Soeriyadi, G. Rees, C. Boyer, Z. Tong, T. P. Davis, C. R. Becer and D. M. Haddleton, *Polym. Chem.*, 2010, **1**, 1196-1204.

18. J. M. Sarapas and G. N. Tew, *Angew. Chem. Int. Ed.* , 2016, **55**, 15860-15863.

19. a)V. A. Ganesh, A. Baji and S. Ramakrishna, *RSC Adv.*, 2014, **4**, 53352-53364; b)R. Kakuchi and P. Theato, *Polym. Chem.*, 2014, **5**, 2320-2325; c)J. M. Frechet, *Science-AAAS-Weekly Paper Edition-including Guide to Scientific Information*, 1994, **263**, 1710-1714; d)M. A. Gauthier, M. I. Gibson and H.-A. Klok, *Angew. Chem. Int. Ed.* , 2009, **48**, 48-58; e)P. Theato and H.-A. Klok, *Functional polymers by post-polymerization modification: concepts, guidelines and applications*, John Wiley & Sons, 2013.

20. a)Z. Terzopoulou, V. Tsanaktsis, D. N. Bikiaris, S. Exarhopoulos, D. G. Papageorgiou and G. Z. Papageorgiou, *RSC Adv.*, 2016, **6**, 84003-84015; b)S. Hong, K.-D. Min, B.-U. Nam and O. O. Park, *Green Chemistry*, 2016, **18**, 5142-5150; c)J. Wang, X. Liu, Y. Zhang, F. Liu and J. Zhu, *Polymer*, 2016, **103**, 1-8.

21. A. Kausar, S. Zulfiqar and M. I. Sarwar, *Polymer Reviews*, 2014, **54**, 185-267.

22. a)A. B. Lowe and C. N. Bowman, *Thiol-X Chemistries in Polymer and Materials Science*, Royal Society of Chemistry, 2013; b)A. Brandle and A. Khan, *Polym. Chem.*, 2012, **3**, 3224-3227; c)S. Binder, I. Gadwal, A. Bielmann and A. Khan, *J. Polym. Sci., Part A: Polym. Chem.* , 2014, **52**, 2040-2046; d)H. Lin, J. Ou, Z. Liu, H. Wang, J. Dong and H. Zou, *Anal. Chem.* , 2015, **87**, 3476-3483; e)M. C. Stuparu and A. Khan, *J. Polym. Sci., Part A: Polym. Chem.* , 2016, **54**, 3057-3070; f)J. A. Carioscia, J. W. Stansbury and C. N. Bowman, *Polymer*, 2007, **48**, 1526-1532; g)R. M. Hensarling, S. B. Rahane, A. P. LeBlanc, B. J. Sparks, E. M. White, J. Locklin and D. L. Patton, *Polym. Chem.*, 2011, **2**, 88-90.

23. T. S. Kristufek, S. L. Kristufek, L. A. Link, A. C. Weems, S. Khan, S.-M. Lim, A. T. Lonnecker, J. E. Raymond, D. J. Maitland and K. L. Wooley, *Polym. Chem.*, 2016, **7**, 2639-2644.

24. G. Yang, S. L. Kristufek, L. A. Link, K. L. Wooley and M. L. Robertson, *Macromolecules*, 2015, **48**, 8418-8427.

25. a) M. O. Saed, A. H. Torbati, D. P. Nair and C. M. Yakacki, *Journal of visualized experiments: JoVE*, 2016; b)M. Claudino, X. Zhang, M. D. Alim, M. Podgórski and C. N. Bowman, *Macromolecules*, 2016, **49**, 8061-8074; c)X. Zhang, W. Xi, C. Wang, M. Podgórski and C. N. Bowman, *ACS Macro Lett.*, 2016, **5**, 229-233; d)W. Xi, M. Krieger, C. J. Kloxin and C. N. Bowman, *Chem. Commun.* , 2013, **49**, 4504-4506; e)S. Auty, University of Liverpool, 2014; f)W. Xi, UNIVERSITY OF COLORADO AT BOULDER, 2015.

26. M. Moreno, I. Armentano, E. Fortunati, S. Mattioli, L. Torre, G. Lligadas, J. C. Ronda, M. Galià and V. Cádiz, *Eur. Polym. J.* , 2016, **79**, 109-120.

27. a)C. Voirin, S. Caillol, N. V. Sadavarte, B. V. Tawade, B. Boutevin and P. P. Wadgaonkar, *Polym. Chem.*, 2014, **5**, 3142-3162; b)F. Fenouillot, A. Rousseau, G. Colomines, R. Saint-Loup and J. P. Pascault, *Prog. Polym. Sci.* , 2010, **35**, 578-622; c)Y. Xia and R. C. Larock, *Green Chemistry*, 2010, **12**, 1893-1909; d)P. A. Wilbon, F. Chu and C. Tang, *Macromol. Rapid*

Commun. , 2013, **34**, 8-37; e)M. Fache, E. Darroman, V. Besse, R. Auvergne, S. Caillol and B. Boutevin, *Green Chemistry*, 2014, **16**, 1987-1998; f)C. Moreau, M. N. Belgacem and A. Gandini, *Top. Catal.* , 2004, **27**, 11-30; g)M. N. Belgacem and A. Gandini, *Monomers, polymers and composites from renewable resources*, Elsevier, 2011; h)L. Montero de Espinosa and M. A. R. Meier, *Eur. Polym. J.* , 2011, **47**, 837-852; i)A. Gandini, *Green Chemistry*, 2011, **13**, 1061-1083.

28. a)R.-J. van Putten, J. C. van der Waal, E. De Jong, C. B. Rasrendra, H. J. Heeres and J. G. de Vries, *Chem. Rev.* , 2013, **113**, 1499-1597; b)A. A. Rosatella, S. P. Simeonov, R. F. M. Frade and C. A. M. Afonso, *Green Chemistry*, 2011, **13**, 754-793; c)E. Capuano and V. Fogliano, *LWT - Food Science and Technology*, 2011, **44**, 793-810; d)F. Koopman, N. Wierckx, J. H. de Winde and H. J. Ruijssenaars, *Proceedings of the National Academy of Sciences*, 2010, **107**, 4919-4924.

29. a)T. Wang, M. W. Nolte and B. H. Shanks, *Green Chemistry*, 2014, **16**, 548-572; b)I. Agirrezabal-Telleria, I. Gandarias and P. Arias, *Catal. Today* 2014, **234**, 42-58; c)S. Dutta, S. De and B. Saha, *Biomass Bioenergy* 2013, **55**, 355-369; d)A. Corma, S. Iborra and A. Velty, *Chem. Rev.* , 2007, **107**, 2411-2502; e)X. Tong, Y. Ma and Y. Li, *Appl. Catal., A* 2010, **385**, 1-13; f)J. N. Chheda, G. W. Huber and J. A. Dumesic, *Angew. Chem. Int. Ed.* , 2007, **46**, 7164-7183; g)M. J. Climent, A. Corma and S. Iborra, *Green chemistry*, 2011, **13**, 520-540; h)R. Karinen, K. Vilonen and M. Niemelä, *ChemSusChem*, 2011, **4**, 1002-1016.

30. a)S. P. Teong, G. Yi and Y. Zhang, *Green Chemistry*, 2014, **16**, 2015-2026; b)A. Mukherjee, M.-J. Dumont and V. Raghavan, *Biomass Bioenergy* 2015, **72**, 143-183.

31. a)M. E. Zakrzewska, E. Bogel-Łukasik and R. Bogel-Łukasik, *Chem. Rev.* , 2010, **111**, 397-417; b)T. Ståhlberg, W. Fu, J. M. Woodley and A. Riisager, *ChemSusChem*, 2011, **4**, 451-458; c)B. Saha and M. M. Abu-Omar, *Green Chemistry*, 2014, **16**, 24-38; d)S. Roy Goswami, M.-J. Dumont and V. Raghavan, *Industrial & Engineering Chemistry Research*, 2016, **55**, 4473-4481.

32. a)L. Hu, G. Zhao, W. Hao, X. Tang, Y. Sun, L. Lin and S. Liu, *RSC Adv.*, 2012, **2**, 11184-11206; b)S. Dutta, S. De and B. Saha, *ChemPlusChem*, 2012, **77**, 259-272.

33. J. Lewkowski, Arkivoc, 2001. **2**, 17-54

34. a)A. S. Amarasekara, *Renewable Polymers: Synthesis, Processing, and Technology*, 2011, 381-428; b)A. Gandini and M. N. Belgacem, *Prog. Polym. Sci.* , 1997, **22**, 1203-1379; c)A. Gandini, *Polym. Chem.*, 2010, **1**, 245-251; d)A. Gandini, *Macromolecules*, 2008, **41**, 9491-9504.

35. M. l. Besson, P. Gallezot and C. Pinel, *Chem. Rev.* , 2013, **114**, 1827-1870.

36. a)S. K. Burgess, J. E. Leisen, B. E. Kraftschik, C. R. Mubarak, R. M. Kriegel and W. J. Koros, *Macromolecules*, 2014, **47**, 1383-1391; b)G. Z. Papageorgiou, V. Tsanaktsis and D. N. Bikiaris, *PCCP* 2014, **16**, 7946-7958; c)E. de Jong, M. Dam, L. Sipos and G. Gruter, *Biobased monomers, polymers, and materials*, 2012, **1105**, 1-13; d)S. K. Burgess, O. Karvan, J. Johnson, R. M. Kriegel and W. J. Koros, *Polymer*, 2014, **55**, 4748-4756; e)V. Tsanaktsis, D. G. Papageorgiou, S. Exarhopoulos, D. N. Bikiaris and G. Z. Papageorgiou, *Crystal Growth & Design*, 2015, **15**, 5505-5512; f)Y. Mao, R. M. Kriegel and D. G. Bucknall, *Polymer*, 2016, **102**, 308-314; g)L. Martino, N. Guigo, J. G. van Berkel, J. J. Kolstad and N. Sbirrazzuoli, *Macromol. Mater. Eng.* , 2016, **301**, 586-596; h)A. Codou, M. Moncel, J. G. van Berkel, N. Guigo and N. Sbirrazzuoli, *PCCP* 2016, **18**, 16647-16658; i)T. Dimitriadis, D. N. Bikiaris, G. Z. Papageorgiou and G. Floudas, *Macromol. Chem. Phys.* , 2016, **217**, 2056-2062; j)M. Lomelí-Rodríguez, M. Martín-Molina, M. Jiménez-Pardo, Z. Nasim-Afzal, S. I. Cauët, T. E. Davies, M. Rivera-Toledo and J. A. Lopez-Sanchez, *J. Polym. Sci., Part A: Polym. Chem.* , 2016, **54**, 2876-2887; k)Z. Terzopoulou, V. Tsanaktsis, M. Nerantzaki, D. S. Achilias, T. Vaimakis, G. Z. Papageorgiou and D. N. Bikiaris, *J. Anal. Appl. Pyrolysis* 2016, **117**, 162-175.

37. J. Zhang, J. Li, Y. Tang, L. Lin and M. Long, *Carbohydr. Polym.* , 2015, **130**, 420-428.

38. a)A. F. Sousa, C. Vilela, A. C. Fonseca, M. Matos, C. S. R. Freire, G.-J. M. Gruter, J. F. J. Coelho and A. J. D. Silvestre, *Polym. Chem.*, 2015, **6**, 5961-5983; b)G. Z. Papageorgiou, D. G. Papageorgiou, Z. Terzopoulou and D. N. Bikiaris, *Eur. Polym. J.* , 2016, **83**, 202-229.

39. a)C. Zeng, H. Seino, J. Ren, K. Hatanaka and N. Yoshie, *Macromolecules*, 2013, **46**, 1794-1802; b)L.-T. T. Nguyen, J. Devroede, K. Plasschaert, L. Jonckheere, N. Haucourt and F. E. Du Prez, *Polym. Chem.*, 2013, **4**, 1546-1556; c)A. Gandini, T. M. Lacerda, A. J. Carvalho and E. Trovatti, *Chemical reviews*, 2015, **116**, 1637-1669

40. Y. Jiang and K. Loos, *Polymers*, 2016, **8**, 243.

41. H. Ait Rass, N. Essayem and M. Besson, *ChemSusChem*, 2015, **8**, 1206-1217.

42. Y. Y. Gorbanev, S. Kegnæs and A. Riisager, *Catal. Lett.* , 2011, **141**, 1752-1760.

43. N. Mei, B. Liu, J. Zheng, K. Lv, D. Tang and Z. Zhang, *Catalysis Science & Technology*, 2015, **5**, 3194-3202.

44. G. Yi, S. P. Teong and Y. Zhang, *Green Chemistry*, 2016, **18**, 979-983.

45. a)J. Cai, H. Ma, J. Zhang, Q. Song, Z. Du, Y. Huang and J. Xu, *Chemistry – A European Journal*, 2013, **19**, 14215-14223; b)B. N. Zope, S. E. Davis and R. J. Davis, *Top. Catal.* , 2012, **55**, 24-32; c)N. K. Gupta, S. Nishimura, A. Takagaki and K. Ebitani, *Green Chemistry*, 2011, **13**, 824-827; d)O. Casanova, S. Iborra and A. Corma, *ChemSusChem*, 2009, **2**, 1138-1144.

46. a)W. P. Dijkman, D. E. Groothuis and M. W. Fraaije, *Angew. Chem. Int. Ed.* , 2014, **53**, 6515-6518; b)F. Koopman, N. Wierckx, J. H. de Winde and H. J. Ruijssenaars, *Bioresour. Technol.* , 2010, **101**, 6291-6296.

47. a)J. A. S. Coelho, A. F. Trindade, V. Andre, M. Teresa Duarte, L. F. Veiros and C. A. M. Afonso, *Org. Biomol. Chem.* , 2014, **12**, 9324-9328; b)J. Lewkowski, *Pol. J. Chem.* , 2001, **75**, 1943-1946.

48. a)F. Menegazzo, T. Fantinel, M. Signoretto, F. Pinna and M. Manzoli, *J. Catal.* , 2014, **319**, 61-70; b)F. Menegazzo, M. Signoretto, D. Marchese, F. Pinna and M. Manzoli, *J. Catal.* , 2015, **326**, 1-8; c)O. Casanova, S. Iborra and A. Corma, *J. Catal.* , 2009, **265**, 109-116.

49. a)D. van Es, S. Marinkovic, X. Oduber and B. Estrine, *J. Surfactants Deterg.* , 2013, **16**, 147-154; b)M. Gomes, A. Gandini, A. J. D. Silvestre and B. Reis, *J. Polym. Sci., Part A: Polym. Chem.* , 2011, **49**, 3759-3768.

50. J. W. Chan, F. Nederberg, B. Rajagopalan, S. R. Williams and M. W. COBB, *PCT patent*, WO 2013149180 A1, 2013.

51. a)S. Nielek and T. Lesiak, *J. Prakt. Chem.*, 1988, **330**, 825-829; b)S. Boufi, M. N. Belgacem, J. Quillerou and A. Gandini, *Macromolecules*, 1993, **26**, 6706-6717.

52. J. Deng, X. Liu, C. Li, Y. Jiang and J. Zhu, *RSC Adv.*, 2015, **5**, 15930-15939.

53. N. R. Jang, H.-R. Kim, C. T. Hou and B. S. Kim, *Polym. Adv. Technol.* , 2013, **24**, 814-818.

54. P. D. Bloom and P. Venkitasubramanian, U.S. Patents, US20090018300 A1, 2008.

55. L. Cottier, G. Descotes and Y. Soro, *Synth. Commun.* , 2003, **33**, 4285-4295.

56. a)F. Hu, J. J. La Scala, J. M. Sadler and G. R. Palmese, *Macromolecules*, 2014, **47**, 3332-3342; b)F. Hu, S. K. Yadav, J. J. La Scala, J. M. Sadler and G. R. Palmese, *Macromol. Chem. Phys.* , 2015, **216**, 1441-1446.

57. a)G. Tarrago, C. Marzin, O. Najimi and V. Pellegrin, *The Journal of Organic Chemistry*, 1990, **55**, 420-425; b)S. Jeol, US 20140135449 A1, 2012.

58. O. Rau, W. Kern and G. Spiteller, *Liebigs Ann. Chem.* , 1984, **1984**, 1504-1512.

59. F. K. Thomas Haas, Martina Ortelt, Jan Christoph Pfeffer, Michael Rimbach, and M. V. Thomas Tacke, Patents, DE1224305 B, 2012.

60. N.-T. Le, A. Byun, Y. Han, K.-I. Lee and H. Kim, *Green and Sustainable Chemistry*, 2015, **5**, 115.

61. A. Viallet and A. Gandini, *J. Photochem. Photobiol., A* 1990, **54**, 129-130.

62. P. Bauchat, N. Le Bras, L. Rigal and A. Foucaud, *Tetrahedron*, 1994, **50**, 7815-7826.

63. W. J. Li and S. X. Qiu, *J. Heterocycl. Chem.* , 2010, **47**, 1340-1343.

64. C. H. R. M. Wilsens, N. J. M. Wullems, E. Gubbels, Y. Yao, S. Rastogi and B. A. J. Noordover, *Polym. Chem.*, 2015, **6**, 2707-2716.

65. a)J. P. Weyrauch, A. S. K. Hashmi, A. Schuster, T. Hengst, S. Schetter, A. Littmann, M. Rudolph, M. Hamzic, J. Visus and F. Rominger, *Chemistry-A European Journal*, 2010, **16**, 956-963; b)L. Racané, V. Tralić-Kulenović, S. Kraljević Pavelić, I. Ratkaj, P. Peixoto, R. Nhili, S. Depauw, M.-P. Hildebrand, M.-H. David-Cordonnier, K. Pavelić and G. Karminski-Zamola, *J. Med. Chem.* , 2010, **53**, 2418-2432.

66. M. Abid, M. Aden Ali, J. Bernard, S. Abid, E. Fleury and R. Gharbi, *Polymer Science Series B*, 2014, **56**, 290-297.

67. a)C. N. D. Neumann, W. D. Bulach, M. Rehahn and R. Klein, *Macromol. Rapid Commun.* , 2011, **32**, 1373-1378; b)H. Wang, Y. Wang, T. Deng, C. Chen, Y. Zhu and X. Hou, *Catal. Commun.* , 2015, **59**, 127-130; c)D. Chundury and H. H. Szmant, *Industrial & Engineering Chemistry Product Research and Development*, 1981, **20**, 158-163; d)O. Casanova, S. Iborra and A. Corma, *J. Catal.* , 2010, **275**, 236-242.

68. C. Larousse, L. Rigal and A. Gaset, *Journal of Chemical Technology & Biotechnology*, 1992, **53**, 111-116.

69. F. Y. R. Wen, X. Dong, Y. Miao, P. Zhou, Z. Lin, J. Zheng, H. Wang, L. Huang, D. Qing, Patents, CN 1456556 A, 2003.

70. M. Sander, T. Jarrosson, S.-C. Chuang, S. I. Khan and Y. Rubin, *The Journal of Organic Chemistry*, 2007, **72**, 2724-2731.

71. A. Mitiakoudis and A. Gandini, *Macromolecules*, 1991, **24**, 830-835.

72. Z. Mou, S. Feng and E. Y. X. Chen, *Polym. Chem.*, 2016, **7**, 1593-1602.

73. Z. Xu, P. Yan, K. Liu, L. Wan, W. Xu, H. Li, X. Liu and Z. C. Zhang, *ChemSusChem*, 2016, **9**, 1255-1258.

74. N. Yoshida, N. Kasuya, N. Haga and K. Fukuda, *Polym. J.* , 2008, **40**, 1164-1169.

75. A. Baliani, G. J. Bueno, M. L. Stewart, V. Yardley, R. Brun, M. P. Barrett and I. H. Gilbert, *J. Med. Chem.* , 2005, **48**, 5570-5579.

76. K. Mitsukura, Y. Sato, T. Yoshida and T. Nagasawa, *Biotechnol. Lett* 2004, **26**, 1643-1648.

77. Z. Zhang, B. Liu, K. Lv, J. Sun and K. Deng, *Green Chemistry*, 2014, **16**, 2762-2770.

78. G. Papadogianakis, L. Maat and R. A. Sheldon, *J. Chem. Soc., Chem. Commun.* , 1994, 2659-2660.

79. B. Mallesham, P. Sudarsanam, G. Raju and B. M. Reddy, *Green Chemistry*, 2013, **15**, 478-489.

80. J.-N. Tan, M. Ahmar and Y. Queneau, *RSC Adv.*, 2013, **3**, 17649-17653.

81. M. Balakrishnan, E. R. Sacia and A. T. Bell, *Green Chemistry*, 2012, **14**, 1626-1634.

82. H. N. C. Wong, K. S. Yeung and Z. Yang, In Comprehensive Heterocyclic Chemistry III; Elsevier: Oxford, 2008, pp 407-496.

83. F. W. Lichtenthaler, A. Brust and E. Cuny, *Green Chemistry*, 2001, **3**, 201-209.

84. Z. Du, J. Ma, F. Wang, J. Liu and J. Xu, *Green Chemistry*, 2011, **13**, 554-557.

85. D. W. Rackemann and W. O. Doherty, *Biofuels, Bioprod. Biorefin.* , 2011, **5**, 198-214.

86. a)A. J. Sanborn and P. D. Bloom, US Patents, US 20060128843 A1, 2008.; b)J. G. De Vries, P. H. Phua, I. V. M. Cabrera and H. J. Heeres, Patents, EP 2576506 A1, 2011.

87. T. Buntara, S. Noel, P. H. Phua, I. Melián-Cabrera, J. G. de Vries and H. J. Heeres, *Angew. Chem. Int. Ed.* , 2011, **50**, 7083-7087.

88. J. Tuteja, H. Choudhary, S. Nishimura and K. Ebitani, *ChemSusChem*, 2014, **7**, 96-100.

89. D.L. Guy. US Patents, US 2763644 A, 1956.

90. A. Gandini, *Prog. Polym. Sci.* , 2013, **38**, 1-29.

91. V. Froidevaux, M. Borne, E. Laborbe, R. Auvergne, A. Gandini and B. Boutevin, *RSC Adv.*, 2015, **5**, 37742-37754.

92. a)D. Pfister, G. Storti, F. Tancini, L. I. Costa and M. Morbidelli, *Macromol. Chem. Phys.* , 2015, **216**, 2141-2146; b)J. C. Morales-Huerta, A. Martínez de Ilarduya and S. Muñoz-Guerra, *ACS Sustainable Chemistry & Engineering*, 2016, **4**, 4965-4973; c)Y. Kanetaka, S. Yamazaki and K. Kimura, *Macromolecules*, 2016, **49**, 1252-1258.

93. M. Vannini, P. Marchese, A. Celli and C. Lorenzetti, *Green Chemistry*, 2015, **17**, 4162-4166.

94. D. G. Papageorgiou, N. Guigo, V. Tsanaktsis, S. Exarhopoulos, D. N. Bikiaris, N. Sbirrazzuoli and G. Z. Papageorgiou, *Industrial & Engineering Chemistry Research*, 2016, **55**, 5315-5326.

95. V. Tsanaktsis, Z. Terzopoulou, M. Nerantzaki, G. Z. Papageorgiou and D. N. Bikiaris, *Mater. Lett.* , 2016, **178**, 64-67.

96. A. Gandini, A. J. Silvestre, C. P. Neto, A. F. Sousa and M. Gomes, *J. Polym. Sci., Part A: Polym. Chem.* , 2009, **47**, 295-298.

97. M. Jiang, Q. Liu, Q. Zhang, C. Ye and G. Zhou, *J. Polym. Sci., Part A: Polym. Chem.* , 2012, **50**, 1026-1036.

98. J. Carlos Morales-Huerta, A. Martínez de Ilarduya and S. Muñoz-Guerra, *Polymer*, 2016, **87**, 148-158.

99. R. J. I. Knoop, W. Vogelzang, J. van Haveren and D. S. van Es, *J. Polym. Sci., Part A: Polym. Chem.* , 2013, **51**, 4191-4199.

100. J. G. van Berkel, N. Guigo, J. J. Kolstad, L. Sipos, B. Wang, M. A. Dam and N. Sbirrazzuoli, *Macromol. Mater. Eng.* , 2015, **300**, 466-474.

101. A. Codou, N. Guigo, J. van Berkel, E. de Jong and N. Sbirrazzuoli, *Macromol. Chem. Phys.* , 2014, **215**, 2065-2074.

102. V. Tsanaktsis, E. Vouvoudi, G. Z. Papageorgiou, D. G. Papageorgiou, K. Chrissafis and D. N. Bikiaris, *J. Anal. Appl. Pyrolysis* 2015, **112**, 369-378.

103. Z. Terzopoulou, V. Tsanaktsis, M. Nerantzaki, G. Z. Papageorgiou and D. N. Bikiaris, *Polym. Degrad. Stab.* , 2016, **132**, 127-136.

104. a)S. K. Burgess, R. M. Kriegel and W. J. Koros, *Macromolecules*, 2015, **48**, 2184-2193; b)S. K. Burgess, D. S. Mikkilineni, B. Y. Daniel, D. J. Kim, C. R. Mubarak, R. M. Kriegel and W. J. Koros, *Polymer*, 2014, **55**, 6861-6869; c)S. K. Burgess, D. S. Mikkilineni, B. Y. Daniel, D. J. Kim, C. R. Mubarak, R. M. Kriegel and W. J. Koros, *Polymer*, 2014, **55**, 6870-6882; d)S. K. Burgess, G. B. Wenz, R. M. Kriegel and W. J. Koros, *Polymer*, 2016, **98**, 305-310.

105. L. Sipos and M. L. Olson, US Patents, US 9073886 B2, 2011.

106. a)J. Ma, X. Yu, J. Xu and Y. Pang, *Polymer*, 2012, **53**, 4145-4151; b)S. Thiyagarajan, W. Vogelzang, R. J. I. Knoop, A. E. Frissen, J. van Haveren and D. S. van Es, *Green Chemistry*, 2014, **16**, 1957-1966.

107. J. Zhu, J. Cai, W. Xie, P.-H. Chen, M. Gazzano, M. Scandola and R. A. Gross, *Macromolecules*, 2013, **46**, 796-804.

108. B. Wu, Y. Xu, Z. Bu, L. Wu, B.-G. Li and P. Dubois, *Polymer*, 2014, **55**, 3648-3655.

109. G. Z. Papageorgiou, V. Tsanaktsis, D. G. Papageorgiou, S. Exarhopoulos, M. Papageorgiou and D. N. Bikiaris, *Polymer*, 2014, **55**, 3846-3858.

110. Z. Wang, T. Lan and J. Zhu, *Biotechnol. Biofuels* 2013, **6**, 1-11.

111. a)Z. Terzopoulou, V. Tsanaktsis, D. N. Bikiaris, S. Exarhopoulos, D. G. Papageorgiou and G. Z. Papageorgiou, *RSC Adv.*, 2016, **6**, 84003-84015; b)S. Hong, K.-D. Min, B.-U. Nam and O. O. Park, *Green Chemistry*, 2016, DOI: 10.1039/C6GC01060A; c)A. F. Sousa, J. F. J. Coelho and A. J. D. Silvestre, *Polymer*, 2016, **98**, 129-135; d)J. Wang, X. Liu, Y. Zhang, F. Liu and J. Zhu, *Polymer*, 2016, **103**, 1-8.

112. J. Ma, Y. Pang, M. Wang, J. Xu, H. Ma and X. Nie, *Journal of Materials Chemistry*, 2012, **22**, 3457-3461.

113. L. Wu, R. Mincheva, Y. Xu, J.-M. Raquez and P. Dubois, *Biomacromolecules*, 2012, **13**, 2973-2981.

114. N. Jacquel, R. Saint-Loup, J.-P. Pascault, A. Rousseau and F. Fenouillot, *Polymer*, 2015, **59**, 234-242.

115. W. Zhou, X. Wang, B. Yang, Y. Xu, W. Zhang, Y. Zhang and J. Ji, *Polym. Degrad. Stab.* , 2013, **98**, 2177-2183.

116. L. T. Lim, R. Auras and M. Rubino, *Prog. Polym. Sci.* , 2008, **33**, 820-852.

117. M. Matos, A. F. Sousa, A. C. Fonseca, C. S. R. Freire, J. F. J. Coelho and A. J. D. Silvestre, *Macromol. Chem. Phys.* , 2014, **215**, 2175-2184.

118. H. Wu, B. Wen, H. Zhou, J. Zhou, Z. Yu, L. Cui, T. Huang and F. Cao, *Polymer Degradation and Stability*, 2015, **121**, 100-104

119. A. F. Sousa, M. Matos, C. S. R. Freire, A. J. D. Silvestre and J. F. J. Coelho, *Polymer*, 2013, **54**, 513-519.

120. G. Z. Papageorgiou, D. G. Papageorgiou, V. Tsanaktsis and D. N. Bikiaris, *Polymer*, 2015, **62**, 28-38.

121. E. Gubbels, L. Jasinska‐Walc and C. Koning, *J. Polym. Sci., Part A: Polym. Chem.* , 2013, **51**, 890-898.

122. G. Z. Papageorgiou, V. Tsanaktsis, D. G. Papageorgiou, K. Chrissafis, S. Exarhopoulos and D. N. Bikiaris, *Eur. Polym. J.* , 2015, **67**, 383-396.

123. V. Tsanaktsis, Z. Terzopoulou, S. Exarhopoulos, D. N. Bikiaris, D. S. Achilias, D. G. Papageorgiou and G. Z. Papageorgiou, *Polym. Chem.*, 2015, **6**, 8284-8296.

124. G. Z. Papageorgiou, N. Guigo, V. Tsanaktsis, D. G. Papageorgiou, S. Exarhopoulos, N. Sbirrazzuoli and D. N. Bikiaris, *Eur. Polym. J.* , 2015, **68**, 115-127.

125. V. Tsanaktsis, D. N. Bikiaris, N. Guigo, S. Exarhopoulos, D. G. Papageorgiou, N. Sbirrazzuoli and G. Z. Papageorgiou, *RSC Adv.*, 2015, **5**, 74592-74604.

126. U. Fehrenbacher, O. Grosshardt, K. Kowollik, B. Tübke, N. Dingenouts and M. Wilhelm, *Chem. Ing. Tech.* , 2009, **81**, 1829-1835.

127. R. Storbeck and M. Ballauff, *Polymer*, 1993, **34**, 5003-5006.

128. J. Wu, P. Eduard, S. Thiyagarajan, B. A. J. Noordover, D. S. van Es and C. E. Koning, *ChemSusChem*, 2015, **8**, 67-72.

129. Z. Yu, J. Zhou, F. Cao, B. Wen, X. Zhu and P. Wei, *J. Appl. Polym. Sci.* , 2013, **130**, 1415-1420.

130. M. Soccio, M. Costa, N. Lotti, M. Gazzano, V. Siracusa, E. Salatelli, P. Manaresi and A. Munari, *Eur. Polym. J.* , 2016, **81**, 397-412.

131. a)A. F. Sousa, A. C. Fonseca, A. C. Serra, C. S. R. Freire, A. J. D. Silvestre and J. F. J. Coelho, *Polym. Chem.*, 2016, **7**, 1049-1058.; b)E. Gubbels, L. Jasinska-Walc, B. A. J. Noordover and C. E. Koning, *Eur. Polym. J.* , 2013, **49**, 3188-3198.

132. a)I.-C. Yeh, B. C. Rinderspacher, J. W. Andzelm, L. T. Cureton and J. La Scala, *Polymer*, 2014, **55**, 166-174; b)Y. K. Endah, S. H. Han, J. H. Kim, N.-K. Kim, W. N. Kim, H.-S. Lee and H. Lee, *J. Appl. Polym. Sci.* , 2016, DOI: 10.1002/app.43391.

133. a)C. H. Wilsens, J. M. Verhoeven, B. A. Noordover, M. R. Hansen, D. Auhl and S. Rastogi, *Macromolecules*, 2014, **47**, 3306-3316; b)C. H. R. M. Wilsens, B. A. J. Noordover and S. Rastogi, *Polymer*, 2014, **55**, 2432-2439.

134. S. Rajendran, R. Raghunathan, I. Hevus, R. Krishnan, A. Ugrinov, M. P. Sibi, D. C. Webster and J. Sivaguru, *Angew. Chem. Int. Ed.* , 2015, **54**, 1159-1163.

135. A. S. Amarasekara, A. Razzaq and P. Bonham, *ISRN Polymer Science*, 2013, **2013**, 4.

136. C. H. R. M. Wilsens, Y. S. Deshmukh, B. A. J. Noordover and S. Rastogi, *Macromolecules*, 2014, **47**, 6196-6206.

137. L. T. Cureton and J. J. La Scala, DTIC Document, No. ARL-TR-6828, 2014.

138. K. Luo, Y. Wang, J. Yu, J. Zhu and Z. Hu, RSC Adv., 2016, **6**, 87013-87020.

139. C. Zeng, H. Seino, J. Ren, K. Hatanaka and N. Yoshie, *Polymer*, 2013, **54**, 5351-5357.

140. C. Zeng, H. Seino, J. Ren and N. Yoshie, *ACS Appl. Mat. Interfaces* 2014, **6**, 2753-2758.

141. T. Ikezaki, R. Matsuoka, K. Hatanaka and N. Yoshie, *J. Polym. Sci., Part A: Polym. Chem.* , 2014, **52**, 216-222.

142. D. Zhang, M.-J. Dumont and A. Cherestes, *RSC Adv.*, 2016, **6**, 83466-83470.

143. K. Li, N. Huo, X. Liu, J. Cheng and J. Zhang, *RSC Adv.*, 2016, **6**, 769-777.

144. a)S. Roy Goswami, M.-J. Dumont and V. Raghavan, *Starch - Stärke*, 2016, 68, 274-286; b)A. Takagaki, M. Takahashi, S. Nishimura and K. Ebitani, *ACS Catalysis*, 2011, **1**, 1562-1565; c)J. Nie, J. Xie and H. Liu, *J. Catal.* , 2013, **301**, 83-91.

145. a)J. Ma, M. Wang, Z. Du, C. Chen, J. Gao and J. Xu, *Polym. Chem.*, 2012, **3**, 2346-2349; b)Z. Hui and A. Gandini, *Eur. Polym. J.* , 1992, **28**, 1461-1469; c)C. Méalares and A. Gandini, *Polym. Int.* , 1996, **40**, 33-39.

146. A. S. Amarasekara, D. Green and L. D. Williams, *Eur. Polym. J.* , 2009, **45**, 595-598.

147. T. Xiang, X. Liu, P. Yi, M. Guo, Y. Chen, C. Wesdemiotis, J. Xu and Y. Pang, *Polym. Int.* , 2013, **62**, 1517-1523.

148. a)I. K. Varma, A.-C. Albertsson, R. Rajkhowa and R. K. Srivastava, *Prog. Polym. Sci.* , 2005, **30**, 949-981; b)R. A. Gross, M. Ganesh and W. Lu, *Trends Biotechnol.* , 2010, **28**, 435-443.

149. a)Y. Jiang, A. J. J. Woortman, G. O. R. Alberda van Ekenstein and K. Loos, *Polym. Chem.*, 2015, **6**, 5198-5211; b)Á. Cruz-Izquierdo, L. A. van den Broek, J. L. Serra, M. J. Llama and C. G. Boeriu, *Pure Appl. Chem.* , 2015, **87**, 59-69; c)Y. Jiang, D. Maniar, A. J. J. Woortman and K. Loos, *RSC Adv.*, 2016, **6**, 67941-67953.

150. A. Gandini, T. M. Lacerda, A. J. F. Carvalho and E. Trovatti, *Chem. Rev.* , 2016, **116**, 1637-1669.

151. a) R.-J. van Putten, J. C. van der Waal, E. De Jong, C. B. Rasrendra, H. J. Heeres and J. G. de Vries, *Chem. Rev.* , 2013, **113**, 1499-1597; b)A. A. Rosatella, S. P. Simeonov, R. F. M. Frade and C. A. M. Afonso, *Green Chem.*, 2011, **13**, 754-793; c)A. S. Amarasekara, in *Renewable Polymers*, John Wiley & Sons, Inc., 2011, DOI: 10.1002/9781118217689.

152. a) J. Chen, K. Li, L. Chen, R. Liu, X. Huang and D. Ye, *Green Chem.*, 2014, **16**, 2490-2499; b)Y. J. Pagán-Torres, T. Wang, J. M. R. Gallo, B. H. Shanks and J. A. Dumesic, *ACS Catal.*, 2012, **2**, 930-934; c)Y. Su, H. M. Brown, X. Huang, X.-d. Zhou, J. E. Amonette and Z. C. Zhang, *Appl. Catal., A* 2009, **361**, 117-122; d)J.-A. Chun, J.-W. Lee, Y.-B. Yi, S.-S. Hong and C.-H. Chung, *Starch - Stärke*, 2010, **62**, 326-330.

153. a) L. Hu, G. Zhao, W. Hao, X. Tang, Y. Sun, L. Lin and S. Liu, *RSC Adv.*, 2012, **2**, 11184-11206; b)S. Dutta, S. De and B. Saha, *ChemPlusChem*, 2012, **77**, 259-272; c)A. Gandini, *Polym. Chem.*, 2010, **1**, 245-251; d)Y. Jiang, D. Maniar, A. J. J. Woortman, G. O. R. Alberda van Ekenstein and K. Loos, *Biomacromolecules*, 2015, **16**, 3674-3685.

154. a) J. Carlos Morales-Huerta, A. Martínez de Ilarduya and S. Muñoz-Guerra, *Polymer*, 2016, **87**, 148-158; b)N. Yoshida, N. Kasuya, N. Haga and K. Fukuda, *Polym. J*, 2008, **40**, 1164-

1169; c)A. F. Sousa, C. Vilela, A. C. Fonseca, M. Matos, C. S. R. Freire, G.-J. M. Gruter, J. F. J. Coelho and A. J. D. Silvestre, *Polym. Chem.*, 2015, **6**, 5961-5983.

155. B. D. Mather, K. Viswanathan, K. M. Miller and T. E. Long, *Prog. Polym. Sci.* , 2006, **31**, 487-531.

156. a) D. P. Nair, M. Podgórski, S. Chatani, T. Gong, W. Xi, C. R. Fenoli and C. N. Bowman, *Chem. Mater.* , 2014, **26**, 724-744; b)J. W. Chan, B. Yu, C. E. Hoyle and A. B. Lowe, *Polymer*, 2009, **50**, 3158-3168. c)J. Xu and C. Boyer, *Macromolecules*, 2015, 48, 520-529; d)A. H. Soeriyadi, G.-Z. Li, S. Slavin, M. W. Jones, C. M. Amos, C. R. Becer, M. R. Whittaker, D. M. Haddleton, C. Boyer and T. P. Davis, *Polym. Chem.*, 2011, 2, 815-822.

157. a) J. Shin, H. Matsushima, J. W. Chan and C. E. Hoyle, *Macromolecules*, 2009, **42**, 3294-3301; b)J. Vandenbergh, K. Ranieri and T. Junkers, *Macromol. Chem. Phys.* , 2012, **213**, 2611-2617; c)K. Dan and S. Ghosh, *Polym. Chem.*, 2014, **5**, 3901-3909; d)K. Dan and S. Ghosh, *Angew. Chem. Int. Ed.* , 2013, **52**, 7300-7305; e)N. Zaquen, B. Wenn, K. Ranieri, J. Vandenbergh and T. Junkers, *J. Polym. Sci., Part A: Polym. Chem.* , 2014, **52**, 178-187; f)J. Vandenbergh, M. Peeters, T. Kretschmer, P. Wagner and T. Junkers, *Polymer*, 2014, **55**, 3525-3532; g)J. Vandenbergh, G. Ramakers, L. van Lokeren, G. van Assche and T. Junkers, *RSC Adv.*, 2015, **5**, 81920-81932; h)A. C. Pauly and F. di Lena, *Polymer*, 2015, **72**, 378-381; i) S. Tomasi, R. Bizzarri, R. Solaro and E. Chiellini, *J. Bioact. Compat. Polym.*, 2002, **17**, 3-21; j) C. Xiao, J. Ding, L. Ma, C. Yang, X. Zhuang and X. Chen, *Polym. Chem.*, 2015, **6**, 738-747.

158. G.-Z. Li, R. K. Randev, A. H. Soeriyadi, G. Rees, C. Boyer, Z. Tong, T. P. Davis, C. R. Becer and D. M. Haddleton, *Polym. Chem.*, 2010, **1**, 1196-1204.

159. C. Zeng, H. Seino, J. Ren, K. Hatanaka and N. Yoshie, *Macromolecules*, 2013, **46**, 1794-1802.

160. M. Baidya and H. Mayr, *Chem. Commun.* , 2008, DOI: 10.1039/B801811A, 1792-1794.

161. a) J. W. Chan, C. E. Hoyle, A. B. Lowe and M. Bowman, *Macromolecules*, 2010, **43**, 6381-6388; b)W. Xi, C. Wang, C. J. Kloxin and C. N. Bowman, *ACS Macro Lett.*, 2012, **1**, 811-814.

162. a) C. Gimbert, M. Lumbierres, C. Marchi, M. Moreno-Mañas, R. M. Sebastián and A. Vallribera, *Tetrahedron*, 2005, **61**, 8598-8605; b)C. Gimbert, A. Vallribera, J. A. Gladysz and M. Jurisch, *Tetrahedron Lett.* , 2010, **51**, 4662-4665.

163. J. W. Chan, H. Wei, H. Zhou and C. E. Hoyle, *Eur. Polym. J.* , 2009, **45**, 2717-2725.

164. B. S. Sumerlin and A. P. Vogt, *Macromolecules*, 2010, **43**, 1-13.

165. a) R. Tello-Aburto, A. N. Lucero and S. Rogelj, *Tetrahedron Lett.* , 2014, **55**, 6266-6268; b)Y. Feng and J. K. Coward, *J. Med. Chem.* , 2006, **49**, 770-788.

166. a)A. L. Kieran, S. I. Pascu, T. Jarrosson, M. J. Gunter and J. K. M. Sanders, *Chem. Commun.* , 2005, DOI: 10.1039/B418811J, 1842-1844; b)S. Diemer, M. Kristensen, B. Rasmussen, S. Beeren and M. Pittelkow, *Int. J. Mol. Sci.* , 2015, **16**, 21858; c)E. Q. Rosenthal, J. E. Puskas and C. Wesdemiotis, *Biomacromolecules*, 2012, **13**, 154-164.

167. T. Zhao, Y. Zheng, J. Poly and W. Wang, *Nat Commun*, 2013, **4**, 1873.

168. J. W. Chan, B. Yu, C. E. Hoyle and A. B. Lowe, *Chem. Commun.* , 2008, DOI: 10.1039/B813438C, 4959-4961.

169. R. Caraballo, M. Rahm, P. Vongvilai, T. Brinck and O. Ramstrom, *Chem. Commun.* , 2008, DOI: 10.1039/B815710C, 6603-6605.

170. S. De, T. Kumar, A. Bohre, L. R. Singh and B. Saha, *Bioorg. Med. Chem.*, 2015, **23**, 791-796.

171. a)B. Saha, C. M. Bohn and M. M. Abu-Omar, *ChemSusChem*, 2014, **7**, 3095-3101; b)E. R. Sacia, M. Balakrishnan and A. T. Bell, *J. Catal.* , 2014, **313**, 70-79.

172. W. H. Carothers, G. L. Dorough and F. J. v. Natta, *J. Am. Chem. Soc.* , 1932, **54**, 761-772.

173. a) J. Zhang, C. Pang and G. Wu, *RSC Adv.*, 2016, **6**, 11848-11854; b)N. Lotti, V. Siracusa, L. Finelli, P. Marchese and A. Munari, *Eur. Polym. J.* , 2006, **42**, 3374-3382.

174. a) A. Mukherjee, M.-J. Dumont and V. Raghavan, *Biomass Bioenergy*, 2015, **72**, 143; b) F. H. Isikgor and C. R. Becer, *Polym. Chem*., 2015, **6**, 4497; c) J. A. Galbis, M. d. G. García-Martín, M. V. de Paz and E. Galbis, *Chem. Rev.,* 2016, **116**, 1600; d) C. Lai, M. Tu, C. Xia, Z.

Shi, S. Sun, Q. Yong and S. Yu, *Energy Fuels*, 2017, **31**, 12317; e) C. Lai, S. Tang, B. Yang, Z. Gao, X. Li and Q. Yong, *Bioresour. Technol*., 2017, **244**, 92.

175. a) A. A. Rosatella, S. P. Simeonov, R. F. Frade and C. A. Afonso, *Green Chem*., 2011, **13**, 754; b) R.-J. van Putten, J. C. van der Waal, E. De Jong, C. B. Rasrendra, H. J. Heeres and J. G. de Vries, *Chem. Rev*., 2013, **113**, 1499.

176. a) D. Zhang and M.-J. Dumont, *J. Polym. Sci., Part A: Polym. Chem.*, 2017, **55**, 11559; b) A. F. Sousa, C. Vilela, A. C. Fonseca, M. Matos, C. S. R. Freire, G.-J. M. Gruter, J. F. J. Coelho and A. J. D. Silvestre, *Polym. Chem.*, 2015, **6**, 5961; c) A. Gandini, T. M. Lacerda, A. J. F. Car valho and E. Trovatti, *Chem. Rev*, 2016, **116**, 1637.

177. Y. Jiang, A. J. J. Woortman, G. O. R. Alberda van Ekenstein, D. M. Petrović and K. Loos, *Biomacromolecules*, 2014, **15**, 2482.

178. a) D. P. Nair, M. Podgórski, S. Chatani, T. Gong, W. Xi, C. R. Fenoli and C. N. Bowman, *Chem. Mater.*, 2014, **26**, 724; b) B. Zhang, Z. A. Digby, J. A. Flum, P. Chakma, J. M. Saul, J. L. Sparks and D. Konkolewicz, *Macromolecules*, 2016, **49**, 6871; c) J. Vandenbergh, K. Ranieri and T. Junkers, *Macromol. Chem. Phys*., 2012, **213**, 2611.

179. a) A. C. Pauly and F. di Lena, *Polymer*, 2015, **72**, 378; b) D. Zhang, M.-J. Dumont and A. Cherestes, *RSC Adv*., 2016, **6**, 83466.

180. B. H. Northrop, S. H. Frayne and U. Choudhary, *Polym. Chem*., 2015, **6**, 3415.

181. a) J. W. Chan, H. Wei, H. Zhou and C. E. Hoyle, *Eur. Polym. J*., 2009, **45**, 2717; b) W. Xi, H. Peng, A. Aguirre-Soto, C. J. Kloxin, J. W. Stansbury and C. N. Bowman, *Macromolecules,* 2014, **47**, 6159; c) M. Podgórski, C. Wang, Y. Yuan, D. Konetski, I. Smalyukh and C. N. Bowman, *Chem. Mater*., 2016, **28**, 5102.

182. a) A. Gandini, *Prog. Polym. Sci*., 2013, **38**, 1; b) A. Duval, H. Lange, M. Lawoko and C. Crestini, *Green Chem*., 2015, **17**, 4991; c) C. Zeng, H. Seino, J. Ren, K. Hatanaka and N. Yoshie, *Macromolecules*, 2013, **46**, 1794; d) S. Motoki, T. Nakano, Y. Tokiwa, K. Saruwatari, I. Tomita and T. Iwamura, *Polymer*, 2016, **101**, 98; e) K. Roos, E. Dolci, S. Carlotti and S. Caillol, *Polym. Chem*., 2016, **7**, 1612; f) A. Duval, G. Couture, S. Caillol and L. Averous, *ACS Sustainable Chem. Eng.,* 2017, **5**, 1199; g) G. Zhang, Q. Zhao, L. Yang, W. Zou, X. Xi and T. Xie, *ACS*

Macro Lett., 2016, **5**, 805; h) L.-T. T. Nguyen, J. Devroede, K. Plasschaert, L. Jonckheere, N. Haucourt and F. E. Du Prez, *Polym. Chem.*, 2013, **4**, 1546.

183. a) J. Shin, H. Matsushima, J. W. Chan, C. E. Hoyle, *Macromolecules*, 2009, **42**, 3294; b) H. Li, S. Thanneeru, L. Jin, C. J. Guild, J. He, *Polym. Chem.*, 2016, **7**, 4824.

184. S. Boufi, A. Gandini, M. N. Belgacem, *Polymer*, 1995, **36**, 1689.

185. a) Z. Wang, L. Yuan, N. M. Trenor, L. Vlaminck, S. Billiet, A. Sarkar, F. E. Du Prez, M. Stefik, C. Tang, *Green Chem.,* 2015, **17**, 3806-3818; b) J. Shin, Y. Lee, W. B. Tolman, M. A. Hillmyer, *Biomacromolecules*, 2012, **13**, 3833; c) Y. Chen, A. M. Kushner, G. A. Williams, Z. Guan, *Nat Chem*, 2012, **4**, 467; d) E. McMullin, H. T. Rebar, P. T. Mather, *Macromolecules*, 2016, **49**, 3769; e) F. Liu, J. Zhang, J. Wang, X. Liu, R. Zhang, G. Hu, H. Na, J. Zhu, *J. Mater. Chem. A*, 2015, **3**, 13637; f) X. Zhang, Z. Tang, B. Guo, L. Zhang, *ACS Appl. Mat. Interfaces,* 2016, **8**, 32520.

186. a) S. Yoshida, H. Ejima, N. Yoshie, *Adv. Funct. Mater*., 2017, **27**, 1701670; b) H.-Y. Mi, X. Jing, B. S. Hagerty, G. Chen, A. Huang, L.-S. Turng, *Mater. Des.*, 2017, **127**, 106; c) J. Liu, S. Wang, Z. Tang, J. Huang, B. Guo, G. Huang, *Macromolecules*, 2016, **49**, 8593; d) M. Hayashi, S. Matsushima, A. Noro, Y. Matsushita, *Macromolecules*, 2015, **48**, 421.

187. C. Heinzmann, S. Coulibaly, A. Roulin, G. L. Fiore and C. Weder, *ACS Appl. Mater. Interfaces*, 2014, **6**, 4713.

188. T. K. Kwei, *J. Polym. Sci., Polym. Lett. Ed.*, 1984, **22**, 307.

189. a) V. Vittoria, R. H. Olley and D. C. Bassett, *Colloid. Polym. Sci.,* 1989, **267**, 661; b) K. Tashiro, Y. Ueno, A. Yoshioka and M. Kobayashi, *Macromolecules*, 2001, **34**, 310.

190. a) C. Heinzmann, C. Weder and L. M. de Espinosa, *Chem. Soc. Rev*., 2016, **45**, 342; b) M. T. Northen, C. Greiner, E. Arzt and K. L. Turner, *Adv. Mater.*, 2008, **20**, 3905.

191. C. L. Jenkins, H. M. Siebert and J. J. Wilker, *Macromolecules*, 2017, **50**, 561.

192. a) B. T. Michal, W. A. Brenn, B. N. Nguyen, L. S. McCorkle, M. A. B. Meador and S. J. Rowan, *Chem. Mater*., 2016, **28**, 2341-2347; b) T. H. Ware, Z. P. Perry, C. M. Middleton, S. T.

Iacono and T. J. White, *ACS Macro Lett*., 2015, **4**, 942-946; c) A. B. Lowe, *Polym. Chem*., 2010, **1**, 17-36.

193. a) H. Kim, J. M. Boothby, S. Ramachandran, C. D. Lee and T. H. Ware, *Macromolecules*, 2017, **50**, 4267-4275; b) C. O. Bounds, J. Upadhyay, N. Totaro, S. Thakuri, L. Garber, M. Vincent, Z. Huang, M. Hupert and J. A. Pojman, *ACS Appl. Mat. Interfaces*, 2013, **5**, 1643-1655; c) C. Xiao, J. Ding, L. Ma, C. Yang, X. Zhuang and X. Chen, *Polym. Chem*., 2015, **6**, 738-747; d) L. He, D. Szopinski, Y. Wu, G. A. Luinstra and P. Theato, *ACS Macro Lett.*, 2015, **4**, 673-678.

194. N. Lotti, V. Siracusa, L. Finelli, P. Marchese and A. Munari, *Eur. Polym. J*., 2006, **42**, 3374.

195. a) M. Soccio, N. Lotti, M. Gazzano, M. Govoni, E. Giordano and A. Munari, *React. Funct. Polym.*, 2012, **72**, 856.

196. a) V. Froidevaux, M. Borne, E. Laborbe, R. Auvergne, A. Gandini and B. Boutevin, *RSC Adv.*, 2015, **5**, 37742; b) D. C. Rideout and R. Breslow, *J. Am. Chem. Soc.,* 1980, **102**, 7816; c) P. A. Pratama, A. M. Peterson and G. R. Palmese, *Polym. Chem.*, 2013, **4**, 5000; d) R. W. Foster, L. Benhamou, M. J. Porter, D. K. Bučar, H. C. Hailes, C. J. Tame and T. D. Sheppard, *Chem. Eur. J.*, 2015, **21**, 6107; e) R. C. Boutelle and B. H. Northrop, *J. Org. Chem*., 2011, **76**, 7994.

197. S. Parker, R. Reit, H. Abitz, G. Ellson, K. Yang, B. Lund and W. E. Voit, *Macromol. Rapid Commun*., 2016, **37**, 1027-1032.

198. X. Kuang, G. Liu, L. Zheng, C. Li and D. Wang, *Polymer*, 2015, **65**, 202-209.

199. R. Rai, M. Tallawi, A. Grigore, A. R. Boccaccini, *Prog. Polym. Sci*. 2012, **37**, 1051.

200. a) D. Tang, C. W. Macosko, M. A. Hillmyer, *Polym. Chem*. 2014, **5**, 3231; b) S. Liu, X. Zhang, M. Li, X. Ren, Y. Tao, *J. Polym. Sci., Part A: Polym. Chem*. 2017, **55**, 349; c) C. Zhou, Z. Wei, X. Lei, Y. Li, *RSC Adv*., 2016, **6**, 63508.

201. Z. Wang, L. Yuan, N. M. Trenor, L. Vlaminck, S. Billiet, A. Sarkar, F. E. Du Prez, M. Stefik and C. Tang, *Green Chem.*, 2015, **17**, 3806-3818

202. a)A. A. Rosatella, S. P. Simeonov, R. F. Frade and C. A. Afonso, *Green Chemistry*, 2011, **13**, 754-793; b)D. Zhang and M.-J. Dumont, *J. Polym. Sci., Part A: Polym. Chem.* , 2017, **55**,

1478-1492; c)J. A. Galbis, M. d. G. García-Martín, M. V. de Paz and E. Galbis, *Chem. Rev.* , 2016, **116**, 1600-1636; d)R.-J. van Putten, J. C. van der Waal, E. De Jong, C. B. Rasrendra, H. J. Heeres and J. G. de Vries, *Chem. Rev.* , 2013, **113**, 1499-1597; e)C. Lai, M. Tu, C. Xia, Z. Shi, S. Sun, Q. Yong and S. Yu, *Energy & Fuels*, 2017, **31**, 12317-12326; f)C. Lai, S. Tang, B. Yang, Z. Gao, X. Li and Q. Yong, *Bioresour. Technol.* , 2017, **244**, 92-99.

203. a)A. F. Sousa, C. Vilela, A. C. Fonseca, M. Matos, C. S. R. Freire, G.-J. M. Gruter, J. F. J. Coelho and A. J. D. Silvestre, *Polym. Chem.*, 2015, **6**, 5961-5983; b)A. F. Sousa, A. C. Fonseca, A. C. Serra, C. S. R. Freire, A. J. D. Silvestre and J. F. J. Coelho, *Polym. Chem.*, 2016, **7**, 1049-1058.

204. a)D. Zhang, M.-J. Dumont and A. Cherestes, *RSC Adv.*, 2016, **6**, 83466-83470; b)L.-T. T. Nguyen, J. Devroede, K. Plasschaert, L. Jonckheere, N. Haucourt and F. E. Du Prez, *Polym. Chem.*, 2013, **4**, 1546-1556; c)F. Hu, J. J. La Scala, J. M. Sadler and G. R. Palmese, *Macromolecules*, 2014, **47**, 3332-3342; d)J. Ma, M. Wang, Z. Du, C. Chen, J. Gao and J. Xu, *Polym. Chem.*, 2012, **3**, 2346-2349; e)Y. Jiang, A. J. J. Woortman, G. O. R. Alberda van Ekenstein, D. M. Petrović and K. Loos, *Biomacromolecules*, 2014, **15**, 2482-2493.

205. D. P. Nair, M. Podgórski, S. Chatani, T. Gong, W. Xi, C. R. Fenoli and C. N. Bowman, *Chem. Mater.* , 2014, **26**, 724-744.

206. a)M. Podgórski, S. Chatani and C. N. Bowman, *Macromol. Rapid Commun.* , 2014, **35**, 1497-1502; b)M. O. Saed, A. H. Torbati, D. P. Nair and C. M. Yakacki, *Journal of visualized experiments: JoVE*, 2016; c)M. Moreno, I. Armentano, E. Fortunati, S. Mattioli, L. Torre, G. Lligadas, J. C. Ronda, M. Galià and V. Cádiz, *Eur. Polym. J.* , 2016, **79**, 109-120; d)P. Buono, A. Duval, L. Averous and Y. Habibi, *ChemSusChem*, 2017, **10**, 984-992; e)K. Dan and S. Ghosh, *Angew. Chem. Int. Ed.* , 2013, **52**, 7300-7305; f)L. He, D. Szopinski, Y. Wu, G. A. Luinstra and P. Theato, *ACS Macro Lett.*, 2015, **4**, 673-678.

207. a)D. P. Nair, N. B. Cramer, J. C. Gaipa, M. K. McBride, E. M. Matherly, R. R. McLeod, R. Shandas and C. N. Bowman, *Adv. Funct. Mater.* , 2012, **22**, 1502-1510; b)M. Podgórski, C. Wang, Y. Yuan, D. Konetski, I. Smalyukh and C. N. Bowman, *Chem. Mater.* , 2016, **28**, 5102-

5109; c)S. Parker, R. Reit, H. Abitz, G. Ellson, K. Yang, B. Lund and W. E. Voit, *Macromol. Rapid Commun.* , 2016, **37**, 1027-1032.

208. a)H. Kim, J. M. Boothby, S. Ramachandran, C. D. Lee and T. H. Ware, *Macromolecules*, 2017, **50**, 4267-4275; b)T. H. Ware, Z. P. Perry, C. M. Middleton, S. T. Iacono and T. J. White, *ACS Macro Lett.*, 2015, **4**, 942-946; c)C. Yakacki, M. Saed, D. Nair, T. Gong, S. Reed and C. Bowman, *RSC Adv.*, 2015, **5**, 18997-19001; d)J. Shin, H. Matsushima, J. W. Chan and C. E. Hoyle, *Macromolecules*, 2009, **42**, 3294-3301; e)H. Li, S. Thanneeru, L. Jin, C. J. Guild and J. He, *Polym. Chem.*, 2016, **7**, 4824-4832.

209. W. Amass, A. Amass and B. Tighe, *Polym. Int.* , 1998, **47**, 89-144.

210. a)W. Denissen, J. M. Winne and F. E. Du Prez, *Chemical Science*, 2016, **7**, 30-38; b)R. Martin, A. Rekondo, A. Ruiz de Luzuriaga, G. Cabanero, H. J. Grande and I. Odriozola, *Journal of Materials Chemistry A*, 2014, **2**, 5710-5715; c)K. Yu, P. Taynton, W. Zhang, M. L. Dunn and H. J. Qi, *RSC Adv.*, 2014, **4**, 10108-10117; d)B. Zhang, P. Zhang, H. Zhang, C. Yan, Z. Zheng, B. Wu and Y. Yu, *Macromol. Rapid Commun.* , 2017, **38**, https://doi.org/10.1002/marc.201700110.

211. a)L. M. Polgar, M. van Duin, A. A. Broekhuis and F. Picchioni, *Macromolecules*, 2015, **48**, 7096-7105; b)P. Berto, S. Grelier and F. Peruch, *Macromol. Rapid Commun.* , 2017, **38**, https://doi.org/10.1002/marc.201700475.

212. a)E. Trovatti, T. M. Lacerda, A. J. F. Carvalho and A. Gandini, *Adv. Mater.* , 2015, **27**, 2242-2245; b)A. Gandini, *Prog. Polym. Sci.* , 2013, **38**, 1-29.

213. C. Zeng, H. Seino, J. Ren, K. Hatanaka and N. Yoshie, *Macromolecules*, 2013, **46**, 1794-1802.

214. D. Zhang, M.-J. Dumont, Polym. Chem. 2018, DOI: 10.1039/C7PY02052J.

215. A. Wang, H. Niu, Z. He and Y. Li, *Polym. Chem.*, 2017, **8**, 4494-4502.

216. V. Froidevaux, M. Borne, E. Laborbe, R. Auvergne, A. Gandini and B. Boutevin, *RSC Adv.*, 2015, **5**, 37742-37754.

217. S. Jung and J. K. Oh, *Materials Today Communications*, 2017, **13**, 241-247.

218. K. Roos, E. Dolci, S. Carlotti and S. Caillol, *Polym. Chem.*, 2016, **7**, 1612-1622.

219. A. Laquièvre, S. Barrau, D. Fournier, G. Stoclet, P. Woisel and J.-M. Lefebvre, *Polymer*, 2017, **117**, 342-353.

220. L. Yuan, Z. Wang, M. S. Ganewatta, M. A. Rahman, M. E. Lamm and C. Tang, *Soft Matter*, 2017, **13**, 1306-1313.

221. M. Hayashi, S. Matsushima, A. Noro and Y. Matsushita, *Macromolecules*, 2015, **48**, 421-431.

222. a)Z. Gao, J. Peng, T. Zhong, J. Sun, X. Wang and C. Yue, *Carbohydr. Polym.* , 2012, **87**, 2068-2075; b)C.-C. Lin and K. S. Anseth, *Pharm. Res.* , 2009, **26**, 631-643.

223. X. Hu, H. Kang, Y. Li, M. Li, R. Wang, R. Xu, H. Qiao and L. Zhang, *Polym. Chem.*, 2015, **6**, 8112-8123.

224. a) A. Gandini, T. M. Lacerda, A. J. F. Carvalho, E. Trovatti, *Chem. Rev.* **2016**, *116*, 1637; b) F. H. Isikgor, C. R. Becer, *Polym. Chem.* **2015**, *6*, 4497; c) C. Lai, M. Tu, C. Xia, Z. Shi, S. Sun, Q. Yong, S. Yu, *Energy Fuels* **2017**, *31*, 12317.

225. D. Zhang, M.-J. Dumont, *J. Polym. Sci., Part A: Polym. Chem.* **2017**, *55*, 1478.

226. a) R.-J. van Putten, J. C. van der Waal, E. De Jong, C. B. Rasrendra, H. J. Heeres, J. G. de Vries, *Chem. Rev.* **2013**, *113*, 1499; b) A. F. Sousa, C. Vilela, A. C. Fonseca, M. Matos, C. S. R. Freire, G.-J. M. Gruter, J. F. J. Coelho, A. J. D. Silvestre, *Polym. Chem.* **2015**, *6*, 5961.

227. D. Zhang, M.-J. Dumont, A. Cherestes, *RSC Adv.* **2016**, *6*, 83466.

228. a) K. Satoh, D.-H. Lee, K. Nagai, M. Kamigaito, *Macromol. Rapid Commun.* **2014**, *35*, 161. b) S. H. M. Söntjens, R. A. E. Renken, G. M. L. van Gemert, T. A. P. Engels, A. W. Bosman, H. M. Janssen, L. E. Govaert, F. P. T. Baaijens, *Macromolecules* **2008**, *41*, 5703.

229. Z. Wang, L. Yuan, C. Tang, *Acc. Chem. Res.* **2017**, *50*, 1762.

230. D. Cohn, A. Hotovely Salomon, *Biomaterials* **2005**, *26*, 2297.

231. Y. Huang, P. Pan, G. Shan, Y. Bao, *RSC Adv.* **2014**, *4*, 47965.

232. a) M. A. Hillmyer, W. B. Tolman, *Acc. Chem. Res.* **2014**, *47*, 2390; b) E. M. Frick, A. S. Zalusky, M. A. Hillmyer, *Biomacromolecules* **2003**, *4*, 216; c) C. L. Wanamaker, L. E. O'Leary, N. A. Lynd, M. A. Hillmyer, W. B. Tolman, *Biomacromolecules* **2007**, *8*, 3634; d) D. K. Schneiderman, E. M. Hill, M. T. Martello, M. A. Hillmyer, *Polym. Chem.* **2015**, *6*, 3641.

233. D. Zhang, M.-J. Dumont, *Polym. Chem.* **2018**, *9*, 743.

234. a) H. Li, S. Thanneeru, L. Jin, C. J. Guild, J. He, *Polym. Chem.* **2016**, *7*, 4824; b) J. Shin, H. Matsushima, J. W. Chan, C. E. Hoyle, *Macromolecules* **2009**, *42*, 3294.

235. M. Yang, Y. Lin, *J Test Eval*, **2009**, 37, 1.

236. Y. Koide, H. Ikake, Y. Muroga, S. Shimizu, *Polym. J.* **2012**, *45*, 645.

237. Y. Byun, S. Whiteside, R. Thomas, M. Dharman, J. Hughes, Y. T. Kim, *J. Appl. Polym. Sci.* **2012**, *124*, 3577.

238. a) C. Zeng, H. Seino, J. Ren, K. Hatanaka, N. Yoshie, *Macromolecules* **2013**, *46*, 1794; b) A. Duval, G. Couture, S. Caillol, L. Averous, *ACS Sustainable Chem. Eng.* **2017**, *5*, 1199; c) A. Nasresfahani, P. M. Zelisko, *Polym. Chem.* **2017**, *8*, 2942; d) O. I. Kalaoglu-Altan, A. Kirac-Aydin, B. Sumer Bolu, R. Sanyal, A. Sanyal, *Bioconjugate Chem.* **2017**, *28*, 2420.

239. Z. Wang, L. Yuan, N. M. Trenor, L. Vlaminck, S. Billiet, A. Sarkar, F. E. Du Prez, M. Stefik, C. Tang, *Green Chem.* **2015**, *17*, 3806.

240. a) D. P. Nair, N. B. Cramer, J. C. Gaipa, M. K. McBride, E. M. Matherly, R. R. McLeod, R. Shandas and C. N. Bowman, Adv. Funct. Mater., 2012, 22, 1502-1510; b) M. Podgórski, C. Wang, Y. Yuan, D. Konetski, I. Smalyukh and C. N. Bowman, Chem. Mater., 2016, 28, 5102-

5109; c) S. Parker, R. Reit, H. Abitz, G. Ellson, K. Yang, B. Lund and W. E. Voit, Macromol. Rapid Commun., 2016, 37, 1027-1032.

241. Y. Jiang, A. J. J. Woortman, G. O. R. Alberda van Ekenstein, D. M. Petrović and K. Loos, Biomacromolecules, 2014, 15, 2482-2493.

242. J. Vandenbergh, K. Ranieri and T. Junkers, Macromol. Chem. Phys., 2012, 213, 2611-2617.

243. Y. Feng, H. Liang, Z. Yang, T. Yuan, Y. Luo, P. Li, Z. Yang and C. Zhang, ACS Sustainable Chemistry & Engineering, 2017, 5, 7365-7373.

244. C. Heinzmann, C. Weder and L. M. de Espinosa, Chem. Soc. Rev., 2016, 45, 342-358.

245. C. Zeng, H. Seino, J. Ren, K. Hatanaka and N. Yoshie, Polymer, 2013, 54, 5351-5357.